MODELLING OF THE MIXING CHARACTERISTICS AND FLOTATION KINETICS OF THE COLLECTION ZONE IN FLOTATION COLUMNS

By:

Peter John Temple Mills
B.Sc. Eng. (Chemical), University of Cape Town

A thesis submitted to the University of Cape Town in fulfillment of the requirements for the degree of Doctor of Philosophy.

Department of Chemical Engineering
University of Cape Town
August 1992

SYNOPSIS

Column flotation has gained worldwide acceptance in the minerals processing industry in the past decade. This has been due the operating characteristics of flotation columns which can produce improved grades and recoveries over conventional cells. Added to this, flotation columns are both simple to operate and generally less expensive than the equivalent requirement of conventional cells. Flotation columns are able to produce improved results due to a deep washed froth phase and a quiescent pulp phase in which the pulp interacts countercurrently with the air bubbles. Models describing the behaviour of particles in both of these phases have been developed over the past decade. The present study focusses specifically on the pulp phase and models presently used to describe the pulp zone hydrodynamics and kinetics are evaluated and improved.

The hydrodynamics of the pulp or collection zone are evaluated using data obtained from three residence time distribution (RTD) studies performed on two pilot columns (5.4cm and 5.8cm diameter) and an industrial column (120cm diameter). Sodium chloride liquid tracers as well as radioactively labelled solid and liquid tracers were used in the RTD studies. In the study performed on a pilot column using the salt tracer the degree of mixing was found to increase both with increasing gas rate at constant bubble size and decreasing bubble size at a constant gas rate. This increase in mixing is attributed to the increase in the number of bubbles and the subsequent increase in the tracer-bubble interactions. By extrapolating this result to industrial columns it is clear that flotation columns, which have smaller and substantially more bubbles, will be more mixed than bubble columns.

The solution of the axial dispersion model for closed-closed boundary conditions and the tanks-in-series model were fitted to the RTD data. The axial dispersion model and tanks-in-series models were found to be equally applicable in pilot columns (less than 10cm diameter) due to the small deviation from plug flow. For flotation columns of intermediate diameters viz. 10cm < diameter < 180cm the axial dispersion model provided the best fit of the experimental data. For flotation columns with diameters greater than 180cm the limitations of the axial dispersion model are exceeded and

a single stirred tank generally provides the best description of the particle hydrodynamics. However the assumption that all industrial columns are single stirred tanks can lead to unnecessary overdesign for columns with diameters less than 180cm.

The solid dispersion coefficient was found to be on average a factor of 1.25 larger than the liquid dispersion coefficient in the industrial column RTD studies. It is proposed that ultra-fine particles have a similar degree of mixing as the liquid due to the fact that they follow the liquid streamlines around a bubble rather than intercepting the bubble itself. However as particles get larger they begin to intercept with the bubbles thus leading to a greater dispersion as observed in the present study. It is shown that the difference in solid and liquid dispersion coefficients would not substantially affect scale-up predictions

In order to study the kinetics of the collection zone a novel method was developed whereby labelled hydrophobic tracer samples were pulsed into the feed stream of two pilot columns (5.4cm and 5.8cm diameter) and an industrial column (120cm diameter) and the recovery of tracer to the concentrate was measured. Pure chalcopyrite and radioactively labelled pure pyrite samples were used as tracers. A shallow froth bed was utilised in order to ensure that only the kinetics of the collection zone were being measured. The method was found to give highly reproducible results. Modelling of the recovery vs. time data indicates that the axial dispersion model combined with first order kinetics produces an excellent fit of almost all the recovery vs. time data. This result shows that the axial dispersion model combined with first order kinetics provides an accurate description of the collection zone hydrodynamics and kinetics in flotation columns with diameters less than 180cm.

The collection zone rate constants determined in the industrial column kinetic study were found to be a factor of about 4 less than the rate constants determined using an identical tracer at the same operating conditions in the pilot column study. This difference is partly attributed to the fact that the industrial column could have been operating above the carrying capacity limits of the froth. However it is also suggested that industrial column rate constants are a factor of between 2.5 and 4 smaller than pilot column rate constants.

The method described above to determine collection zone kinetics was used in a study on a pilot column to evaluate the effect of gas flow rate, bubble size and particle size on the collection zone rate constant. Parameters of the particle collection model developed by Finch and Dobby (1990) were also calculated for each of the operating conditions. The final recovery and rate constant increased with increasing gas flow rate for the range investigated. It is proposed that a maximum rate constant and final recovery will usually occur at a gas rate of about 3.0cm/s. Above this value the gas flow will begin to approach slugging and the recovery and rate will level off. The collection efficiency as well as the induction times remained constant with the change in gas rate. Increasing the bubble diameter in the kinetics study resulted in a sharp decrease the rate constant and optimum recovery occurred between bubble diameters of 1 and 2mm. Flotation columns are usually operated at bubble sizes between 1 and 2mm and the present work shows that this is the range for optimum final recovery. Further reductions in bubble size serve only to improve the rate of recovery. The effect of particle size on the final recovery and rate constants followed the same trend as in previous studies. The optimum particle size range for the final recovery of pyrite was found to be between 50 and 90μm. The rate constants as well as the collection efficiencies had an optimum for particles of about 90μm in size. The induction time was found to decrease with increasing particle size. It is expected that for particle sizes larger than the maximum size used in the testwork the induction time would begin to increase.

For each of the operating conditions investigated the particle collection model of Finch and Dobby (1990) was found to fit the experimentally determined rate constants well. The model can therefore be used with confidence in the prediction of collection zone kinetics in laboratory flotation columns. The injection of hydrophobic tracers into a flotation column has been found to provide an accurate estimate of collection zone kinetics. This method could used in future testwork to evaluate in more detail collection zone kinetics in industrial columns, to determine the kinetics of other flotation systems and to investigate froth zone behaviour.

ACKNOWLEDGEMENTS

I would like to express my sincere thanks to my supervisor, Prof. Cyril T. O'Connor for his enthusiasm, assistance and guidance in this study.

The support of the following organisations is gratefully acknowledged:

The Anglo American Corporation of South Africa (AAC) for allowing me to do this project and funding the research.

The Foundation for Research and Development (FRD) for the award of a postgraduate bursary and a special merit award entailing an overseas trip to a conference in Canada.

The University of Cape Town for a research associateship award and a doctoral travel bursary.

The Freegold South division of AAC for allowing me to perform testwork on the President Steyn flotation column.

Olifantsrivier Rekenaars vir die gebruik van 'n rekenaar.

The help of the following people is also acknowledged:

Dr. B.K. Loveday as my mentor at AAC for his advice and assistance.

Prof. J.B. Yianatos for his valuable advice and for allowing me to use his residence time distribution data.

Mr. Schalk Smith and his colleagues at the Atomic Energy Corporation of South Africa for their untiring efforts in the performance of the radioactive tracer testwork.

Mr. Ashli Breed and Mr. John Worsley for their assistance in the performance of the residence time distribution tests.

Mrs. Dee Bradshaw, Mr. Martin Harris, Dr. Paul Stonestreet, Mr. Jeremy Tucker, Mr. Sean von Holt and other colleagues in the Minerals Processing Group for their interest and advice.

The staff of the mechanical and electronic workshops who provided and maintained equipment and facilities used in this thesis.

Mr. Miles van Niekerk for being a great business partner and friend.

Finally to my friends, Annemarie, Hester, Julie, Peggy, Philip and Stephan for their support.

CERTIFICATION BY SUPERVISOR

During the course of this study, the following papers have been published:

Journals:

Mills P.J.T and O'Connor C.T. "The modelling of liquid and solids mixing in a flotation column", *Minerals Engineering*, 3(6) (1990) 567-576.

O'Connor C.T. and Mills P.J.T. "The effect of temperature on the pulp and froth phases in the flotation of pyrite", *Minerals Engineering*, 3(6) (1990) 615-624.

Mills P.J.T. and O'Connor C.T. "The use of the axial dispersion model to describe mixing in a flotation column", *Minerals Engineering*, 5(8) (1992) 939-944.

Conference Proceedings:

Mills P.J.T., Yianatos J.B. and O'Connor C.T. "The mixing characteristics of solid and liquid phases in a flotation column", Minerals Engineering '92, Vancouver, Canada, 14-16 April 1992, (*Minerals Engineering*, in press).

In terms of Paragraph GP 8 of "General Rules for the degree of Ph.D.", I, Prof. C.T. O'Connor, as supervisor of the candidate, P.J.T. Mills, certify that I approve of the incorporation in this thesis of material that has been published.

Signed by candidate
Signature Removed

Professor C.T. O'Connor
Department of Chemical Engineering
University of Cape Town
Private Bag
Rondebosch, 7700

TABLE OF CONTENTS

CHAPTER 1: INTRODUCTION

CHAPTER 2: EXPERIMENTAL DETAILS

CHAPTER 3: RESULTS

CHAPTER 4: DISCUSSION

LIST OF APPENDICES

LIST OF FIGURES

LIST OF TABLES

NOMENCLATURE

A	Cross sectional area (m^2, cm^2)
C_a	Carrying capacity ($g/min/cm^2$)
c, C	Concentration
d	Diameter (m, μm, mm)
d_{80}	80% sample passing given diameter (μm)
D	Dispersion coefficient (m^2/s)
E	Dimensionless concentration ($E = C/C_0$)
e	Degree of entrainment
E	Efficiency
F	True recovery by flotation
g	Gravity (m^2/s)
G	Grade
h_{crit}	Critical thickness of film rupture (mm)
j	Superficial velocity (cm/s)
j_g^*	Superficial gas velocity at standard conditions (cm/s)
j_{gmax}	Value of j_g at the onset of turbulence (cm/s)
j_b	Superficial bias velocity (cm/s)
j_f	Superficial feed velocity (cm/s)
k	First order rate constant (min^{-1})
k_c	Collection zone rate constant (min^{-1})
k_{fc}	Overall rate constant (min^{-1})
k_f	Fast floating rate constant (min^{-1})
k_s	Slow floating rate constant (min^{-1})
K_1	Fractional monolayer bubble loading
K	Constant
l	Primary length parameter (m)
L	Collection zone length (m)
M_c	Concentrate solids rate per unit cross sectional area
N_p	Vessel dispersion number ($N_p = D/uL$)
N	Number of tanks-in-series
n	Constant
n_θ	Fraction of particles that collide between the front stagnation point and some angle θ
P	Pressure (kPa)
P_m	Specific energy dissipation rate

q	Constant
Q	Volumetric flow rate (cm^3/s)
R	Flotation recovery
R_c	Collection zone recovery
R_f	Froth zone recovery
R_I	Infinite time recovery
Re	Reynolds number ($Re = \rho du/\mu$)
S	Feed percent solids (%)
Sk	Stokes Number
t	Time (min)
t_s	Particle sliding time
t_i	Induction time
u	Interstitial velocity (cm/s)
u_l	Interstitial liquid velocity (cm/s)
u_p	Particle terminal velocity (cm/s)
u_p^*	Dimensionless particle terminal velocity ($u_p^* = u_p/U_b$)
U_b	Terminal rise velocity of a bubble (cm/s)
U_{sg}	Slip velocity between gas and bubble (cm/s)
U_{sp}	Slip velocity between particle and water (cm/s)
v_θ	Particle sliding velocity (cm/s)
W	Water recovery
x	Dimensionless length ($x = Z/L$)
X	Number of flotation units

Greek Letters

ϵ	Holdup (%)
θ	Angle or dimensionless time ($\theta = t/\tau$)
θ_c	Angle of closest approach for fluid streamlines
θ_m	Maximum angle of contact between sliding particle and bubble
θ'	Angle θ when $t_s = t_i$
ρ	Density (g/cm^3)
σ	Variance
μ	Viscosity (P)
τ	Mean residence time (min)
ξ_s	Surface vorticity

General Subscripts

b	Bubble
c	Column
C	Collision
Cg	Gravitational collision
Ci	Interceptional collision
D	Detachment
f, F	Feed
fc	Overall
g	Gas
K	Collection
l	Liquid
p	Particle
sl	Slurry
t	Tailings

LIST OF ABBREVIATIONS

RTD	Residence time distribution
ADM	Axial dispersion model
T-I-S	Tanks-in-series model
US	USBM-type sparger
FC	Filter cloth sparger

CHAPTER 1

INTRODUCTION

An inherent limitation of flotation in conventional cells is the recovery of hydrophilic particles by mechanical entrainment in the water reporting to the froth. Flotation columns effectively overcome this limitation in two ways. Firstly a deep froth is produced in order to allow the hydrophilic particles to drain back into the pulp while retaining the hydrophobic particles. Secondly the draining of hydrophilic particles is facilitated by a flow of clean water down through the froth. The column differs from conventional mechanical flotation units both in design and operating philosophy and this has been a reason for its slow acceptance by the mineral industry. Boutin and Wheeler (1967) developed the concept in the 1960's, but only since 1981 has the column begun to obtain widespread acceptance (Finch and Dobby, 1990). Columns are utilised on an ever increasing scale in Canada, Australia and the United States. In South Africa the flotation column is beginning to gain acceptance in the mining industry. Due to the low capital and running costs of a flotation column and the recoveries and corresponding grades which can be obtained it is likely that the column will be utilised more extensively by the industry in future years. The column is particularly attractive for applications involving multiple cleaning stages and can upgrade in a single stage compared with several stages of mechanical cells. This results in simpler more controllable circuits.

Methods for flotation column scale-up have developed with the increased use of the column (Finch and Dobby, 1990). Modelling of the column is less empirical than the scale-up methods used for conventional flotation cells. The quiescent pulp phase allows the use of traditional chemical engineering models to describe the mixing characteristics and kinetics. These models have been used successfully in column scale-up (Espinosa-Gomez et al., 1989). Modelling of the kinetics and mixing characteristics in the flotation column are continually improving with the increased interest in this process (Xu and Finch, 1991b and Mular and Musara, 1991).

This chapter begins by outlining the design and operation of flotation columns. The various constituents of a flotation column as well as the effect of the operating conditions on column performance are described within this outline. Yianatos (1989) and Finch and Dobby (1990) review column design and operation extensively and as this is not the main focus of this study these aspects are only briefly outlined below. The following two sections discuss the focus of the present study viz. the modelling of the mixing characteristics and kinetics of the pulp zone in flotation columns. Thereafter a typical scale-up procedure for the design of a column cell is described. The final section of this chapter presents the objectives of this research.

1. COLUMN DESIGN AND OPERATION

As depicted in Figure 1.1, a column cell consists of two basic regions viz. the collection (or pulp zone) and the cleaning zone (or froth zone). The feed slurry enters the collection zone about one-third of the way from the top and the feed particles descend counter-current against a large assemblage of rising gas bubbles generated by a sparger at the base of the column. The particles collide with the bubbles and the hydrophobic particles attach to the bubbles and are transported into the cleaning zone. The hydrophilic particles and partially hydrophobic particles which do not attach to bubbles are transported down the column and are removed from the bottom. Baffles are installed in some columns especially large diameter columns in order to reduce the effective column diameter.

In the cleaning zone, wash water is added near (or at) the top of the froth. The flow rate is set to provide a net downward liquid flow in the column, called a positive bias. In practice, this means that the tails water flow rate is higher than the feed water flow rate. This positive bias cleans the froth of entrained particles and also stabilizes the froth, promoting the formation of a deep froth (0.5 to 2m).

The overall performance of a column is affected by the behaviour of both the collection zone and the cleaning zone. This behaviour is in turn affected by a number of variables (reagent dosage, gas and liquid flow

rates, bubble size, feed particle size, froth depth etc.) some of which are under the control of the operator. In the next two sections, the behaviour of the collection zone and cleaning zone are examined, together with the variables that affect them.

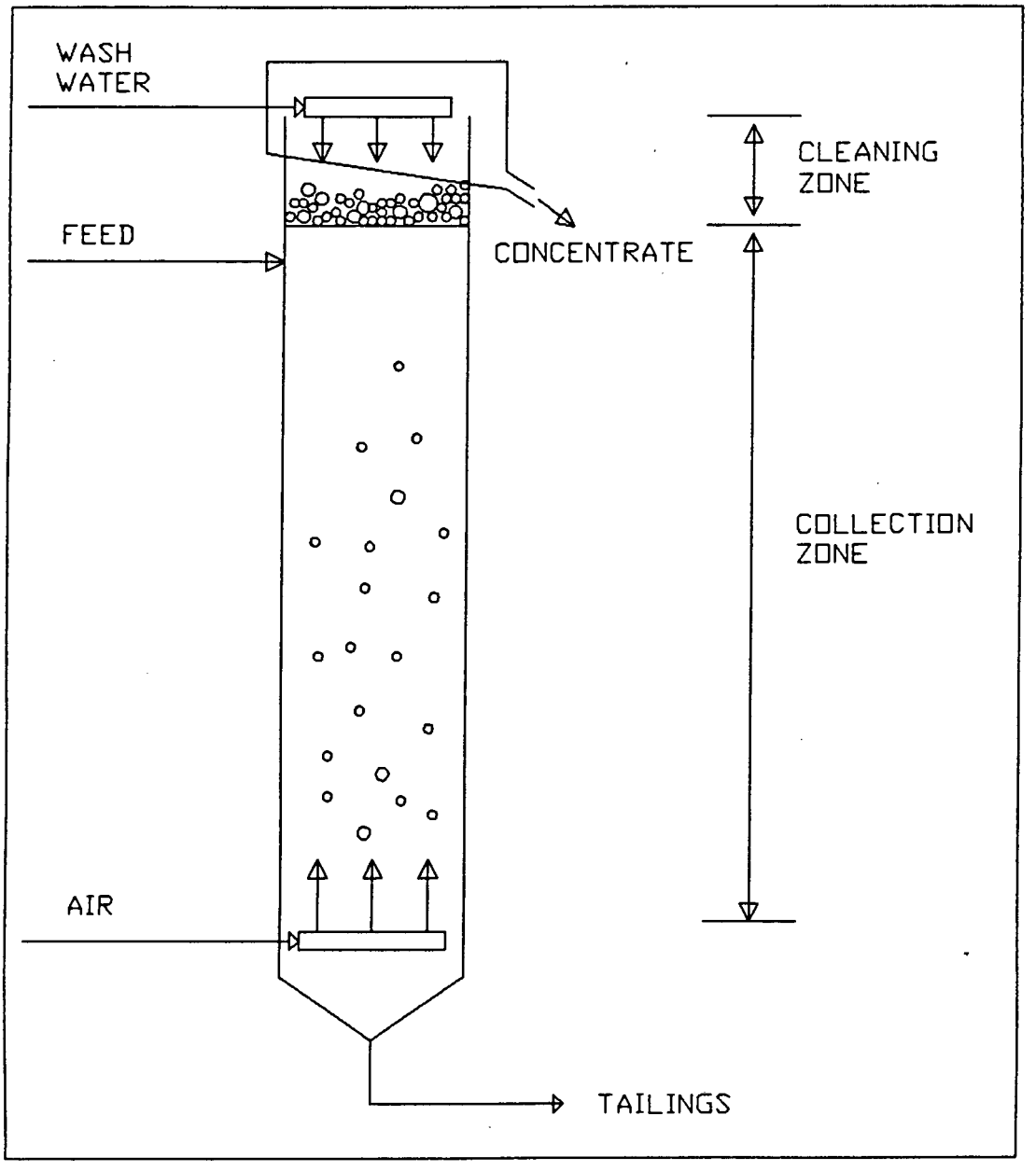

Figure 1.1: Schematic Diagram of a Column Cell

1.1 COLLECTION ZONE

1.1.1 GAS HOLDUP AND FLOW REGIMES

When gas is introduced into a column containing a flotation pulp, it displaces a certain volume of slurry. The volumetric fraction displaced is known as the gas holdup, ϵ_g. The gas holdup is an important variable in that it gives an indication of the hydrodynamic condition of the collection zone. Gas holdup can be experimentally determined by static head measurements (see Figure 1.2) (Finch and Dobby, 1990).

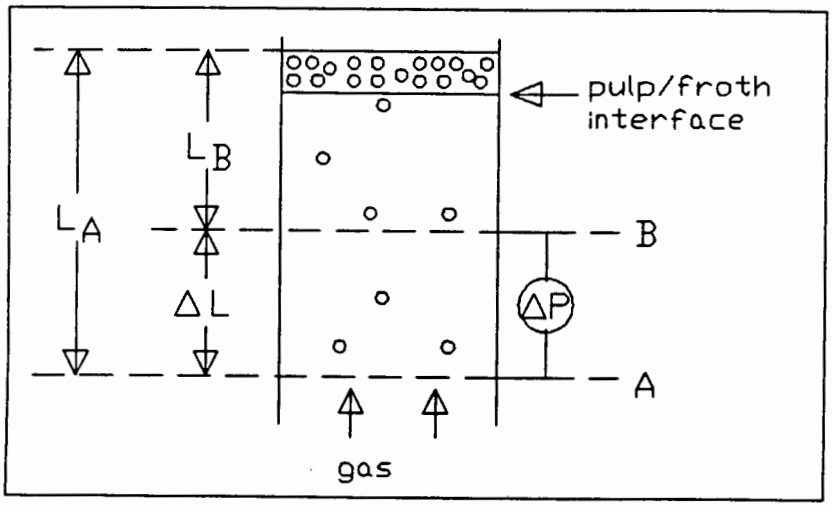

Figure 1.2: Pressure Reading Points to determine Gas Holdup

The pressure above atmospheric at A and B, ignoring frictional losses and the density of the gas, is given by

$$P_A = \rho_{sl}\, g\, L_A\, (1 - \epsilon_{gA}) \qquad (1.1)$$

and $$P_B = \rho_{sl}\, g\, L_B\, (1 - \epsilon_{gB}) \qquad (1.2)$$

where ϵ_{gA} and ϵ_{gB} are the average gas holdup above A and B respectively. The above equations give the following expression for pressure difference, ΔP:

$$\Delta P = \rho_{sl}\, g\, \Delta L\, (1 - \epsilon_g) \qquad (1.3)$$

where ϵ_g is the average holdup between A and B. Rearranging (1.3) gives

$$\epsilon_g = 1 - \Delta P/(\rho_{sl}\, g\, \Delta L) \qquad (1.4)$$

A useful way of defining gas and liquid flow rates in a column is by expressing them as volumetric flow rate per unit cross-section. This is called superficial velocity. Superficial velocities facilitate comparisons with columns of different cross-sections. For the gas, the superficial gas rate is given by the equation

$$j_g = Q_g/A_c \qquad (1.5)$$

where A_c is the cross-sectional area of the column and Q_g is the volumetric gas rate. j_g represents the superficial gas rate at a specific point in the column where the volumetric rate is Q_g. To determine the average gas rate, reference must be made to standard conditions. The following relationship may be used to estimate the average j_g (Yianatos, 1989):

$$j_{g(ave)} = \frac{P_c\, j_g^*\, \ln (P_t/P_c)}{P_t - P_c} \qquad (1.6)$$

In this equation, j_g^* is the superficial gas (air) rate at atmospheric conditions, P_t is the pressure (absolute) at the bottom of the column and P_c is the pressure at the concentrate overflow. For a tall industrial column of 12m the value of $j_{g(ave)}$ will differ considerably from j_g^* because of the large head of slurry. For a laboratory scale column with a 1.0 to 2.0m head, $j_{g(ave)} \approx 0.95 j_g^*$, so j_g^* is usually an adequate estimate.

The relationship between gas holdup, ϵ_g, and the superficial gas rate, j_g, is used to define the flow regime in the collection zone. Figure 1.3 shows a general relationship between gas holdup and gas rate (Finch and Dobby, 1990). As j_g increases, ϵ_g increases. The linear section of the relationship represents a flow condition that is characterized by a homogeneous distribution of bubbles of fairly uniform size rising at a uniform rate. This is called the "bubbly flow regime", which is the

desirable flow condition in which to operate a column. As j_g increases, the gas holdup eventually becomes unstable and the flow is characterized by rapidly rising bubbles, which displace water and small bubbles downward. This is called the "churn-turbulent region" and is undesirable because the unstable slugging flow of the gas is not conducive to particle collection.

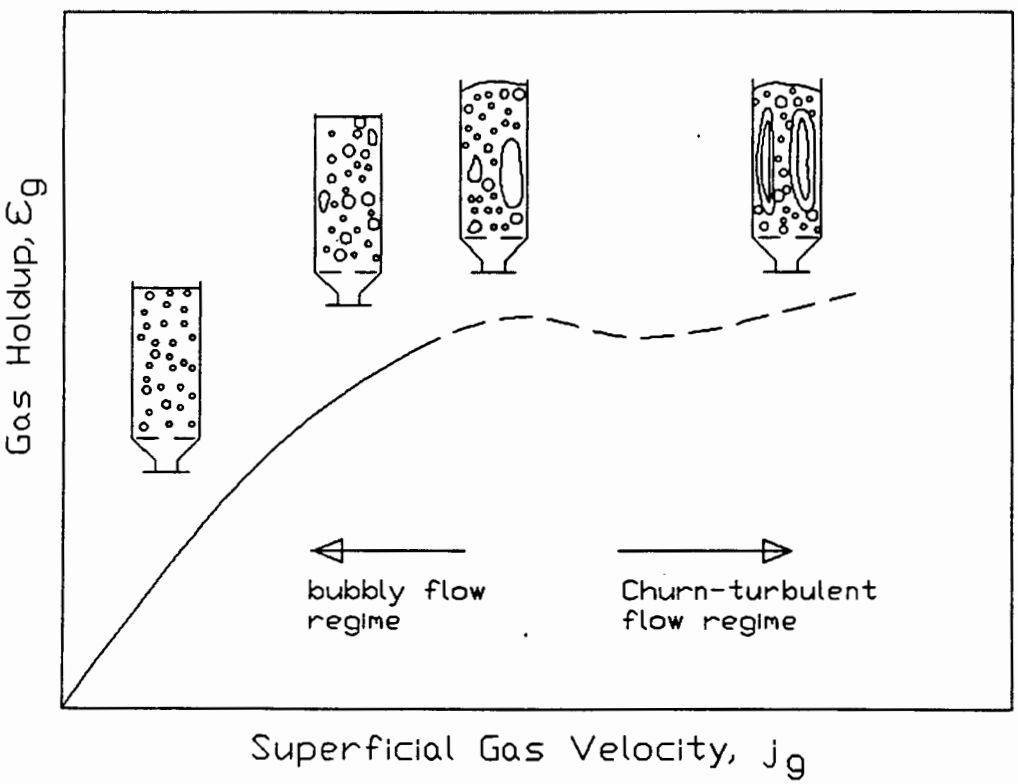

Figure 1.3: Relationship between Gas Holdup and Gas Rate (after Finch and Dobby, 1990)

1.1.2 EFFECT OF VARIOUS PARAMETERS ON COLLECTION ZONE BEHAVIOUR

In order to operate a column in the desired bubbly flow regime, it is important to know the influence various parameters have on this aspect of collection zone operation. It is also important to operate the column at conditions which will ensure an optimum rate of collection of particles. This section deals specifically with the former and the latter is discussed in detail in Chapter 1 Sec. 3.3.

The range of gas rates is restricted by an upper limit. This upper limit, j_{gmax}, is defined as the value of j_g corresponding to the onset of turbulence. Industrial experience has shown that an excess of gas causes grade and recovery losses due to the gas flow entering the turbulent regime, while very low gas rates also cause severe recovery losses (Coffin and Misczak, 1982 and Clingan and Macgregor, 1987). In normal column operation the superficial liquid rate, j_l, is counter-current to the bubbles. Increasing the liquid rate for a given j_g will increase the gas holdup because of a decrease in bubble rise velocity. This means that j_{gmax} will be lower if the liquid rate is increased while all the other factors are kept constant (Finch and Dobby, 1990). The addition of a frother reduces the bubble size and increases the gas holdup for a given j_g because of the reduced bubble rise velocity. Therefore j_{gmax} will again be lower. Above a certain level of frother dosage, however, the bubble size change becomes very small and gas holdup is therefore unaffected.

1.1.3 BUBBLE GENERATION

The nature of the generation of air bubbles in the column cell is a factor which distinguishes column cells from other flotation equipment and which is also of fundamental importance in determining collection zone behaviour. The bubbles are generated by the use of spargers, of which there are two main types.

1.1.3.1 Internal Porous Spargers

An internal sparger is one in which bubble generation occurs in the pulp zone itself. The spargers are made of porous materials such as ceramic or fritted glass with pore sizes up to 300μm or steel sieve plates into which holes (of more or less equal sizes) have been drilled. Other types are made of perforated rubber or filter cloth wrapped around piping into which holes are drilled. The pressurized gas passes into the pulp through the pores and this causes the formation of the bubbles.

The bubble size that is generated using this type of sparger is a function of the gas flow rate, the sparger material and the frother content of the

pulp. The bubble diameter usually increases with increasing gas rate: it has been reported that it is proportional to j_g^n, where n can be approximated as 0.25 (Dobby and Finch, 1986b). Sparger material has a small effect on bubble size, although the filter cloth tends to give the largest bubbles (Finch and Dobby, 1990). Frother concentration in the pulp will affect the bubble size produced from internal spargers.

1.1.3.2 External Spargers

An external sparger is one in which the gas bubbles are generated by contacting the gas with a separate water stream outside of the column. The combined stream is then fed into the column. This is the basis for a number of designs, including the U.S. Bureau of Mines sparger design. In this design, pressurised air and water streams are mixed in a contact chamber and the resulting mixture is injected into the column through small orifices (typically 1mm diameter) (Ynchausti et al., 1988). Factors which affect bubble size in this instance are air and water pressure and flow rate, number of orifices and orifice size, and frother concentration (Finch and Dobby, 1990). The control over bubble size is largely independent of the feed pulp. External spargers generally have the ability to produce both smaller and more uniform bubbles than internal spargers.

1.2 CLEANING ZONE

Conventional (sub-aeration) cells suffer from the problem of entrainment of unwanted materials in the froth phase which adversely affects the cleaning action. Generally, it is the fine hydrophilic particles that are entrained but all particles, both hydrophilic and hydrophobic, can be entrained. Entrainment is inherent in conventional flotation because water recovery to the froth cannot be avoided.

1.2.1 ENTRAINMENT IN FLOTATION CELLS

Entrainment occurs when particles enter the froth phase suspended in the water occupying the spaces between the bubbles (Warren, 1985). The finer

the particle, the more likely it is to remain suspended and thus to be recovered in the concentrate by entrainment rather than by true flotation. This recovery by entrainment is a problem in flotation because it is non-selective. The nature of entrainment has been the subject of numerous studies. Jowett (1966) states that recovery of the non-floatable gangue mineral occurs by a mass transfer process initiated by water currents. Warren (1985) has investigated the contributions of true flotation and recovery by entrainment in various flotation systems. He has shown that overall flotation recovery, R_t, obeys the relationship:

$$R_t = F_t + e_t W \qquad (1.7)$$

where F_t is the true recovery by flotation, e_t is the degree of entrainment and W is the feed water recovery. It would seem logical from this equation that if the feed water recovery to the froth could be eliminated, then recovery by entrainment could be avoided. This is exactly the method by which a column cell operates. The froth phase of a column differs fundamentally from a conventional cell because of the net downward flow of water in the column. This downward flow is known as the positive bias and is determined by the following equation:

$$j_b = j_t - j_f \qquad (1.8)$$

where j_b is the superficial bias rate, j_t is the superficial tailings rate and j_f is the superficial feed rate. The positive bias is maintained by the addition of wash water at the top of the froth. The wash water flowing through the froth eliminates entrainment and enhances froth stability, promoting the formation of a deep froth bed.

1.2.2 EFFECT OF VARIABLES ON FROTH BEHAVIOUR

In order to minimize feed water recovery and to obtain the best possible cleaning action, it is important to know the effects of various parameters on the froth zone behaviour.

1.2.2.1 Effect of Gas Rate

Increasing the gas rate results in an increase in the amount of feed water in the froth. This is detrimental to the cleaning action. It is even possible that, at a high enough gas rate, sufficient water will be entrained into the froth to bring about a condition of negative bias. Clearly there is an upper limit to the value of j_g both in terms of efficient cleaning and in maintaining the desirable bubbly flow regime in the pulp zone.

1.2.2.2 Effect of Frother Dosage

Increasing the frother dosage will reduce the bubble size. This means that for a given pulp/froth interface area, there will be a greater number of bubbles crossing the interface per unit time and consequently more water is entrained. The frother dosage will thus also affect the upper limit of j_g for the onset of negative bias in the froth zone. The frother does serve to create a stable bubble bed.

1.2.2.3 Effect of Wash Water Rate

It has been shown that, as long as the wash water rate is sufficient to maintain a positive j_b value, the cleaning action is relatively insensitive to the actual value of j_b, provided excessively high bias rates are avoided (Yianatos, 1989). Tracer studies showed that, as j_b was increased from 0.1cm/s to 0.3cm/s, the concentration of feed water at the top of the froth zone was reduced from 8% to 5%. However, if the j_b value was increased further to 0.5cm/s, the situation was reversed and the feed water concentration became 47% at the top of the froth. A large bias rate increases mixing by altering the plug flow regime of the froth to a heterogeneous behaviour in which severe channeling and recirculation occur. Sprinkler design is also an important factor in minimizing channeling and mixing. The design should be such as to avoid a jetting behaviour for the whole range of water rates that is likely to be used.

1.2.2.4 Effect of Froth Depth

A study of column flotation froths by Yianatos et al. (1988a) found firstly that entrainment is effectively eliminated in column froths and secondly that rejection of entrained material does not take place throughout the froth, but rather very close to the pulp/froth interface. Typical froth depths in plant operation are 0.5 to 1.5m and there is little effect over this range (Yianatos, 1989). There are cases where froth depth affects cleaning action. For example, when particles differing in hydrophobicity need to be separated, the froth depth has a bearing on selectivity. Yianatos et al. (1988a) showed that in the selective flotation of Mo from a Mo/Cu/Fe/Si ore, a froth depth of over 1.0m was required for the selective recovery of Mo.

1.2.3 FROTH CARRYING CAPACITY

If the feed rate to a column cell is increased, the concentrate recovery rate will increase to a certain point, after which it will level off, even though the feed rate continues to increase. This occurs because, at a given superficial gas rate and bubble loading, there is a certain limiting mass rate of solids that can be accommodated in the froth.

The practical measure of the maximum carrying rate for a given set of conditions is called the carrying capacity. A semi-theoretical expression which relates carrying capacity, C_a, to particle size and gas rate is the following (Finch and Dobby, 1990):

$$C_a = K_1 \rho_p d_p [j_g^{(1-q)}] \qquad (1.9)$$

where K_1 is the fractional monolayer bubble loading and q is a constant. Studies on laboratory and pilot scale columns have revealed that C_a is independent of air rate and the value of q can be taken as 1 for j_g in the range 1.5 to 3.0cm/s (Finch and Dobby, 1990). Empirical relationships have also been used. One such relationship is as follows (Espinosa-Gomez et al., 1988):

$$C_a = 0.068\ d_{80}\ \rho_p\ (g/min/cm^2) \qquad (1.10)$$

Because it is an empirical model it only applies within the range of variables tested. In this case, the upper limit on the value of d_p is 40μm. For design and scale-up purposes, the values for C_a are best determined experimentally as the carrying capacity correlations do not provide accurate predictions. The carrying capacity is determined by measuring the concentrate solids rate as a function of the feed solids rate for a given column set-up and operating conditions.

A new parameter, C_l, lip loading capacity based on the concentrate slurry production per unit lip length, accounts for the geometry of the column (Amelunxen, 1990). This parameter simply incorporates the physical constraints of concentrate removal in an industrial column. A particle appearing at the top of the froth not only hinders the surfacing of other particles, but also, because of the long horizontal distance that it has to travel to the overflow, has a high probability of drop back into the froth zone. Using a zinc database on column operation (column sizes examined were from 0.3 to 3m), C_l was correlated to column diameter:

$$C_l = 900\ d_c^{0.3} \quad \text{(g of slurry/cm/min)} \qquad (1.11)$$

1.3 TYPICAL FLOTATION COLUMN OPERATING CONDITIONS

The preceding sections have outlined the operation of the various constituents of a flotation column and given a summary of column operation. Table 1.1 illustrates the typical range of operating conditions of flotation columns.

Parameter	Value
Superficial Gas Rate	0.5-0.3cm/s
Superficial Tailings Rate	0.5-2cm/s
Superficial Wash Water Rate	0.3-0.8cm/s
Superficial Bias Rate	0.1-0.3cm/s
Froth Depth	0.5-1.5m
Average Bubble Size	0.8-2.0mm
Height/Diameter Ratio	>10/1

Table 1.1: Typical Flotation Column Operating Conditions

2. MODELLING OF THE MIXING CHARACTERISTICS OF THE COLLECTION ZONE

An understanding of the dynamics of the particles in the collection zone of a flotation column is essential for the scale-up of a flotation column. This section begins by presenting models which can be used to describe the mixing characteristics of the collection zone. Following this the experimental approach to analysing collection zone mixing, viz. residence time distribution studies (RTD), is discussed and previous RTD studies performed on both bubble and flotation columns are reviewed. The particular aspects of the modelling of collection zone hydrodynamics which are addressed in the present study are summarized at the end of this section.

2.1 MODELS USED TO DESCRIBE THE DEGREE OF MIXING IN THE COLLECTION ZONE

The collection zone is relatively quiescent and can be well described using existing chemical engineering models. The degree of mixing in the collection zone ranges from virtual plug flow in laboratory columns to almost completely mixed flow in industrial columns. Models used to predict collection zone recovery involve the assumption of first order kinetics

and combine the rate constant, the mixing parameter and the residence time to predict recovery. For the extreme systems of plug flow and completely mixed transport a mixing parameter is not required. The recovery for a system exhibiting plug flow transport having a first order rate constant k and a retention time t, is given by

$$R_c = 1 - \exp(-k\ t) \qquad (1.12)$$

and for a system exhibiting perfect mixing with a mean residence time τ

$$R_c = 1 - (1 + k\ \tau)^{-1} \qquad (1.13)$$

The degree of mixing in the collection zone is usually between the above two flow conditions. Following work by Rice et al. (1974) the mixing in the collection zone of the flotation column has generally been modelled, as in bubble columns, using the axial dispersion model (Finch and Dobby, 1990). It has been suggested that the tanks-in-series model may also be appropriate (Goodall and O'Connor 1991).

Recent work by Ityokumbul (1992) suggests that the axial dispersion model is inappropriate to describe mixing in the flotation column. It is suggested that the requirement of random perturbations to describe solid mixing is not met in the collection zone. Ityokumbul (1992) develops a model based on interphase mass transfer to describe the mixing and kinetics in the collection zone.

2.1.1 THE AXIAL DISPERSION MODEL

The overall recovery of a mineral is dependent on the collection and cleaning zone recoveries,

$$R_{fc} = f(R_f, R_c) \qquad (1.14)$$

Using the axial dispersion model the collection zone recovery can be predicted as a function of the following:

$$R_c = f(k, \tau, D/uL) \qquad (1.15)$$

where k is the first order rate parameter, τ is the mean residence time (τ = L/u where L is the collection zone length and u is solid interstitial velocity) and D/uL is the vessel dispersion number (or the inverse of the Peclet number), where D is the mixing parameter viz. the vessel dispersion coefficient.

The axial dispersion model is well documented in the literature (eg. Levenspiel, 1972). An outline of the model derivation and assumptions is as follows. The change in mineral concentration in the pulp is considered to be a function of three factors:

1. Transport due to eddy dispersion.
2. Transport due to bulk or plug flow.
3. Disappearance due to particle collection.

An unsteady-state mass balance of the material is taken over an annulus of the column, of thickness Δx. The terms of the mass balance are as follows:

Entering by axial dispersion = $-(D\ A_{col}\ dC/dx)_x$
Exiting by axial dispersion = $-(D\ A_{col}\ dC/dx)_{x+\Delta x}$

Entering by bulk flow = $C(x)\ u\ A_{col}$
Exiting by bulk flow = $C(x + \Delta x)\ u\ A_{col}$

Disappearance by reaction = $(-k\ C)\ A_{col}\ \Delta x$

where C is the mineral concentration at x, x being the vertical distance from the pulp/froth interface, u the interstitial particle velocity and A_{col} the column cross sectional area. Combining the above terms, dividing by $A_{col}\ \Delta x$, and taking the limits as Δx approaches zero, yields the following differential equation:

$$D \frac{\delta^2 C}{\delta x^2} - u \frac{\delta C}{\delta x} - k\ C = 0 \qquad (1.16)$$

Danckwerts (1953) presented an analytical solution for Equation 1.16, based on the following boundary conditions:

$$C_0 = C(x) - D/u \; dC(x)/dx \text{ at } x=0$$
$$\text{and } dC/dx = 0 \text{ at } x=L$$

where L is the length of the collection zone viz. the length of the pulp zone from the pulp/froth interface to the spargers. The solution is

$$\frac{C(x)}{C_0} = \exp\left(\frac{u\,x}{2\,D}\right)\left[\frac{2\,(1+a)\exp\left(\frac{u\,a}{2\,D}(L-x)\right) - 2\,(1-a)\exp\left(\frac{u\,a}{2\,D}(x-L)\right)}{(1+a)^2\exp\left(\frac{a}{2\,N_p}\right) - (1-a)^2\exp\left(\frac{a}{2\,N_p}\right)}\right] \quad (1.17a)$$

$$a = (1 + 4\,k\,\tau\,N_p)^{1/2} \quad (1.17b)$$

$$N_p = D/uL \quad (1.17c)$$

where N_p is the vessel dispersion number. Wehner and Wilhelm (1956) showed that Equation (1.17) is valid for all entrance and exit conditions. Fractional recovery (at x=L) is given by

$$R_C = 1 - \frac{4\,a\exp(1/(2\,N_p))}{(1+a)^2\exp(a/(2\,N_p)) - (1-a)^2\exp(-a/(2\,N_p))} \quad (1.18a)$$

$$a = (1 + 4\,k\,\tau\,N_p)^{1/2} \quad (1.18b)$$

Levenspiel (1979) recommends that the axial dispersion model is likely to be an inappropriate model choice if the vessel dispersion number exceeds 1. Theoretically as the degree of mixing moves from plug flow through to a completely mixed system, with a constant mean residence time and assuming an unchanging first order rate constant, the predicted recovery will decrease.

2.1.2 THE TANKS-IN-SERIES MODEL

The tanks-in-series model is also well documented in the literature (Levenspiel, 1972). With the tanks-in-series model the collection zone recovery can be predicted as a function of

$$R_C = f(k, \tau, N) \qquad (1.19)$$

where N is the number of tanks-in-series, k is the first order rate parameter and τ is the mean residence time. In this model the actual reactor is simulated by N ideal stirred tanks-in-series. The total volume of the tanks is the same as the volume of the actual reactor. Thus for a given flow rate the total mean residence time is also the same. Equation (1.13), for which N is equal to 1, can be generalised as follows:

$$R_C = 1 - (1 + k\,(\tau/N))^{-N}. \qquad (1.20)$$

The model can be fitted to data ranging from a completely mixed system, where N = 1, to a plug flow system, where N tends to infinity. The model does not have limitations as does the axial dispersion model. The families of curves obtained from the two models for the various degrees of mixing are distinctly different (Levenspiel, 1979). However as each model approaches plug flow i.e.. when N approaches infinity and N_p approaches zero, the curves have a similar shape.

2.2 RESIDENCE TIME DISTRIBUTION STUDIES

The measurement of the residence time distribution has been described by several authors (eg. Levenspiel, 1972). The technique generally used in flotation columns is the pulse injection of a tracer at the top of the collection zone. The tracer is detected at the tailings outlet. From the RTD data the mean residence time τ and variance σ^2 can be easily determined. If the tracer in the tailings is sampled at discrete time intervals, t_i, then

$$\tau = \frac{\Sigma\, t_i\, C_i\, \Delta t_i}{\Sigma\, C_i\, \Delta t_i} \qquad (1.21)$$

and

$$\sigma^2 = \frac{\Sigma\, t_i^2\, C_i\, \Delta t_i}{\Sigma\, C_i\, \Delta t_i} - \tau^2 \qquad (1.22)$$

where C_i is the tracer exit concentration at time t_i and Δt_i is the time interval between samples. The above two parameters can be used to estimate the mixing parameters from the RTD data.

2.2.1 FITTING THE AXIAL DISPERSION MODEL TO EXPERIMENTAL DATA

The modelling of tailings residence time distribution curves of a flotation column has involved extensive use of the axial dispersion model. This model is in common use in chemical engineering and methods for its use are well documented (Levenspiel, 1972 and Wen and Fan, 1975). However the model has not been used to any great extent in minerals processing. In order to use the axial dispersion model it is necessary to solve Equation (1.16) for the set of boundary conditions which apply to the system being studied. Following this a method for determining the vessel dispersion number from the RTD data must be chosen. In the application of the model to describe mixing in a flotation column various methods and equations to determine the vessel dispersion number have been used. This section lists the various sets of boundary conditions and methods used to determine the vessel dispersion number.

Using the fact that kC = dC/dt and transferring Equation (1.16) into a dimensionless form using the following dimensionless groups,

$E = C/C_0$
$x = Z/L$
$\theta = t/\tau$

where C_0 is the initial equilibrium concentration, L is the collection zone length and τ is the mean residence time, yields the following,

$$\frac{D}{uL}\frac{\delta^2 E}{\delta Z^2} - \frac{\delta E}{\delta Z} - \frac{\delta E}{\delta Z} = 0 \qquad (1.23)$$

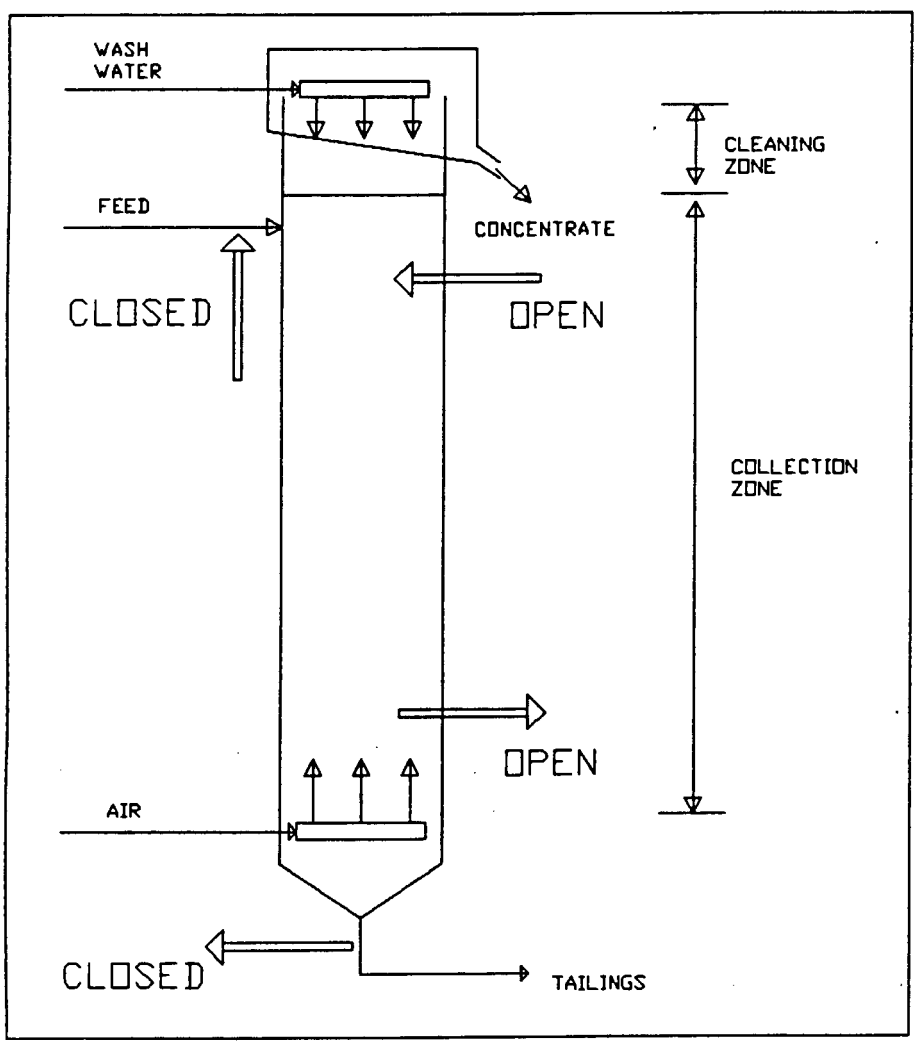

Figure 1.4: Schematic of a Flotation Column indicating Tracer injection and detection Points for different Boundary Conditions

Equation (1.23) can now be solved to yield a predicted age distribution curve. The choice of the tracer injection and detection points determines the set of boundary conditions used to solve Equation 1.23 (Levenspiel,

1979). A choice of three boundary conditions exist, viz. closed-closed, closed-open and open-open. Figure 1.4 indicates the positioning of tracer input and detection points for the different boundary conditions. In most of the tracer studies that have been performed the tracer is injected into the feed stream entering the column and detected in the tailings stream exiting the column (Laplante et al., 1988). It is assumed that tracer leaving in the froth is negligible and therefore the column is explicitly defined by closed-closed boundary conditions. There are a few studies where different injection points have been used. Rice et al. (1974) used open-open conditions and Goodall and O'Connor (1991) used closed-open conditions.

2.2.1.1 Open-Open Boundary Conditions

The open-open solution of Equation (1.23) can be determined analytically and yields the following equation (Levenspiel and Smith, 1957):

$$E(\theta) = [1/(4\pi N_d\theta)]^{1/2} \exp[-(1-\theta)^2/(4\theta N_d)] \qquad (1.24)$$

where $E(\theta)$ is the dimensionless response ($E(\theta) = \tau E(t)$, t is time and τ is mean residence time), and θ is dimensionless time ($\theta = t/\tau$). Previous workers have used the following equation for the open-open conditions (Rice et al. (1974), Xu and Finch (1991a and b), Alford et al. (1991), Kho and Sohn (1989)):

$$E(\theta) = [1/(4\pi N_d\theta^3)]^{1/2} \exp[-(1-\theta)^2/(4\theta N_d)] \qquad (1.25)$$

This solution is incorrect in the θ^3 term. Equations (1.24) and (1.25) yield quite different solutions as can be seen in Figure 1.5. The experimental result in Figure 1.6 is the tailings response curve of a liquid tracer injected into the feed stream of a 0.9m diameter column and detected in the tailings pipe (Yianatos and Bergh, 1990). It is not possible to get any reasonable fit of the experimental result using Equation (1.24). However the erroneous Equation (1.25) suggests that the open-open analytical solution may be appropriate.

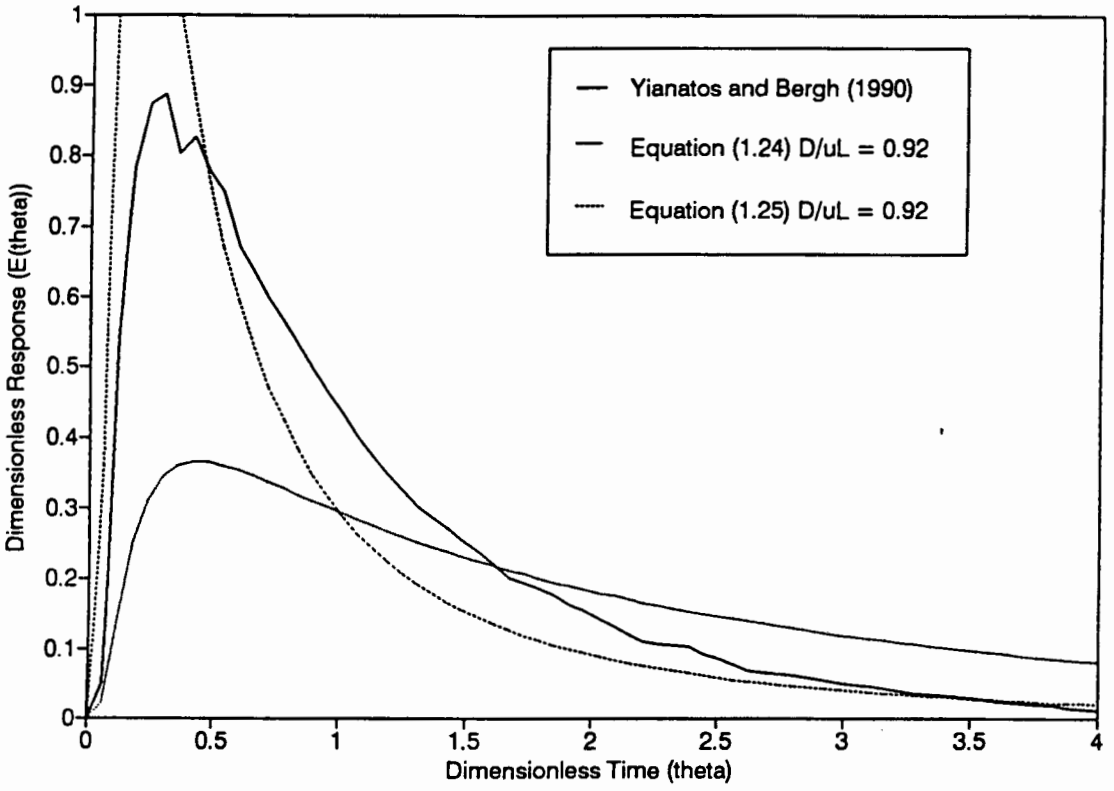

Figure 1.5: Tailings Response Curve of a 0.9m Diameter Flotation Column and Model Response Curves using Equations (1.24) and (1.25)

For testwork where the open-open boundary conditions apply, viz. the tracer is injected and detected as illustrated in Figure 1.4, N_d can be determined by two methods. Equation (1.24) can be fitted to experimental data using a direct search (least squares) method to determine N_d (Xu and Finch, 1991a). An estimate of the vessel dispersion number can also be determined by equating model and experimental variances. This is known as moments matching and the following equation is used for the open-open conditions (Levenspiel, 1979)

$$\frac{\sigma^2}{\tau^2} = 2\frac{D}{uL} + 8\left(\frac{D}{uL}\right)^2 \qquad (1.26)$$

where σ^2 and τ are determined from Equations (1.21) and (1.22) respectively.

2.2.1.2 Closed-Closed Boundary Conditions

For closed-closed boundary conditions Equation (1.23) does not yield an analytical solution. A numerical solution is required to obtain the dimensionless response curves. There are two reported methods for determining the response curves. Xu et al. (1991) describe a finite difference method and Wen and Fan (1975) an inversion Laplace transform method. In order to determine N_d a direct search method is used in conjunction with the numerical solution. N_d can also be determined using moments matching (Xu and Finch, 1991a and Levenspiel, 1979). The equation for the closed-closed conditions is

$$\frac{\sigma^2}{\tau^2} = 2\frac{D}{uL} - 2\left(\frac{D}{uL}\right)^2\left(1 - \exp\left(-\frac{uL}{D}\right)\right). \qquad (1.27)$$

2.2.1.3 Closed-Open Boundary Conditions

The closed-open solution of Equation (1.23) also requires a numerical solution. Only one study was found in the literature using these conditions (Goodall and O'Connor, 1991) and moments matching was used to determine N_d. The equation for the open-closed conditions is

$$\frac{\sigma^2}{\tau^2} = 2\frac{D}{uL} + 3\left(\frac{D}{uL}\right)^2. \qquad (1.28)$$

The numerical solution can also be determined using the same methods as in the closed-closed case (Wen and Fan, 1975).

2.2.2 FITTING THE TANKS-IN-SERIES MODEL TO EXPERIMENTAL DATA

The tanks-in-series model is simpler to use than the axial dispersion model, but is only suitable for tracer studies where closed-closed boundary conditions have been used. The reason for this relates to the basis of the model viz. a series of completely mixed tanks with closed

inputs and outputs. The model is easier to apply since the age distribution curve is described analytically whereas the axial dispersion model and closed-closed boundary conditions require a numerical solution. In this case the residence time distribution curve is given by:

$$E(\theta) = \frac{N\,(N\,\theta)^{N-1}}{(N-1)!}\,e^{-N\theta} \qquad (1.29)$$

where E is the exit age distribution function, N is the number of tanks-in-series and θ the dimensionless time. Although this model only allows for integer values of N, Buffham and Gibilaro (1968) have generalised it so that N can assume real values as well

$$E(\theta) = \frac{N\,(N\,\theta)^{N-1}}{\Gamma(N)}\,e^{-N\theta} \qquad (1.30)$$

where $\Gamma(N)$ is the gamma function of N. A value of N can be determined by fitting Equation (1.30) to the experimental RTD curve using a direct search method (least squares).

The experimental variance and mean residence time are found to be related to N in the following way

$$\frac{\sigma^2}{\tau^2} = \frac{1}{N}. \qquad (1.31)$$

The value of N can therefore be estimated from the above equation. For mixing conditions close to plug flow the tanks-in-series and dispersion models can be interrelated by equating Equations (1.31) and (1.27) (Levenspiel, 1962).

2.3 REVIEW OF RESIDENCE TIME DISTRIBUTION STUDIES

Modelling of the RTD in the collection zone in column flotation is largely based on the models and correlations used for the more extensively studied bubble columns. This review will detail previous two phase RTD studies in bubble columns, then three phase studies in bubble columns and finally RTD studies in flotation columns.

2.3.1 TWO PHASE RTD STUDIES IN BUBBLE COLUMNS

A large portion of previous bubble column work has involved two phase systems. Plug flow models with axial dispersion are used to model flow in bubble columns. The columns are either operated in cocurrent or countercurrent mode and the models used for both modes are similar. The spargers used generate bubbles > 1cm in diameter and both liquid and gas superficial velocities are generally higher than those used in column flotation.

Laplante et al. (1988) have divided work on bubble columns into three regimes of the superficial gas velocity, j_g. These are: (i) j_g < 0.5cm/s; (ii) 0.5 < j_g < 3cm/s (Column flotation conditions); and (iii) j_g > 3cm/s.

Ulbrecht and Baykara (1981) have reported on work performed at j_g values below 0.5cm/s, where the bubbles rise in a centrally located plume, in which the dispersion coefficient was proportional to the liquid rise velocity in the central plume. Reith et al. (1968) determined dispersion coefficients in columns from 5 to 29cm in diameter, at superficial gas velocities, j_g, between 10 and 45cm/s. In this range of j_g slugging was observed. They found that the liquid dispersion coefficient, D_l, was directly proportional both to column diameter and j_g. Ohki and Inoue (1970) confirmed that D_l was directly proportional to j_g, in columns from 4 to 16cm in diameter, and at superficial gas velocities between 5 and 25cm/s.

In the j_g range used in column flotation neither slugging nor a centrally located plume of rising bubbles is observed. The bubble wakes interact and the liquid phase is uniformly turbulent.

For the range $0.5 < j_g < 7$cm/s correlations for the dispersion coefficient in the bubble column have been developed. Using dimensional analysis Baird and Rice (1975) showed that in the case of eddy diffusivity

$$D_l = K\, l^{1.33}\, P_m^{0.33} \qquad (1.32)$$

where K is a dimensionless constant, l a primary length parameter and P_m the specific energy dissipation rate. The primary length parameter is the column diameter d_c (m) and the energy dissipation rate is primarily related to j_g (cm/s). By analysing numerous previous studies, Baird and Rice showed that for unbaffled columns

$$D_l = 0.035\, d_c^{1.33}\, j_g^{0.33}. \qquad (1.33)$$

Equation (1.32) is a generally accepted correlation used for determining the dispersion coefficient, D_l (m^2/s), in bubble columns. Other correlations have also been proposed (Joshi and Sharma (1979), Joshi (1980)) and these are in good agreement with Equation (1.33).

2.3.2 THREE PHASE RTD STUDIES IN BUBBLE COLUMNS

Work has been performed on three phase bubble column systems by a number of investigators (Imafuka et al. (1968), Cova (1966) and Suganuma and Yamanishi (1966)). In order to predict the concentration distribution of suspended solid particles in liquid within the bubble column, Cova (1966) assumed that the dispersion coefficient of solid particles was the same as that of liquid, which was obtained in the column without solid particles, at the same superficial gas velocity. He also assumed that the settling velocity of solid particles was equal to the terminal velocity of a single particle in a stagnant liquid. However, he did not give sufficient experimental data to confirm these assumptions. Suganuma and Yamanishi (1966) presented an empirical correlation to predict the concentration distribution of solid particles in the bubble column with continuous circulating flow of liquid but they did not separately determine the dispersion coefficient and the settling velocity of solid particles from their experimental results. Therefore, the application of their correlation is limited. Imafuku et al. (1968) performed work on 5, 10,

20cm diameter continuous cocurrent pachuca tanks. The experiments were performed at high superficial liquid velocities and high superficial gas velocities (2-10cm/s) in order to ensure the solids did not settle in the tank. The bubbles generated were > 1 cm and the solid particle size range used was 60-180μm. For the above set of conditions they showed that it was valid to apply the dispersion model to the continuous phase by confirming that the radial concentration distribution of solid particles was uniform. They also showed that the values of the solids dispersion coefficient, D_p, coincide well with the dispersion coefficient of liquid in the bubble column without suspended solid particles, D_l, at the same superficial gas rate.

2.3.3 RTD STUDIES IN FLOTATION COLUMNS

Rice et al. (1974) performed one of the first comprehensive studies of the collection zone using both solid and liquid tracers. Their study was performed on a laboratory column (0.076m diameter and 4.6m height) using low air rates (<1.5cm/s) and solids concentrations (2-3%). They found the solids and liquid dispersion coefficients to be similar, although the dispersion coefficients measured indicate virtual plug flow. A later study by Dobby and Finch (1985) was performed on 0.46m and 0.91m diameter columns each 13 m high. The operating conditions were typical of those used in column flotation although the feed only contained about 3% solids. The liquid and solids flow was monitored in the columns using fluorescein and non-floatable manganese dioxide tracers respectively. Both these tracers were problematic in their application, the flourescein was adsorbed on the particles in the system and the feed material contained a small amount of MnO_2. A liquid tracer and four solid tracers of different particle sizes viz. +38-53, +53-75, +75-106 and +106-150μm were used. The dispersion coefficient was found to be equivalent for all these tracers. It was assumed that the collection zone could be modelled according to previous bubble column work, viz. the continuous phase could be modelled using the axial dispersion model and that the solids dispersion coefficient, D_p, is equivalent to the liquid dispersion coefficient, D_l. Their investigation confirmed the first assumption for the liquid phase in both columns and for the solid phase in the 0.46 m column. The second assumption was confirmed by comparing the results obtained from both the

solid and liquid tracer in the 0.46m column at the same operating conditions. From their work and by referring to previous bubble column studies Dobby and Finch suggested the following correlation for the solids dispersion coefficient, D_p:

$$D_p = D_l = 0.063\ d_c. \qquad (1.34)$$

This correlation applies for flotation columns with d_c>0.2m and operating at gas velocities between 1 and 3cm/s. In a later paper Dobby and Finch (1986a) expanded the above correlation, again using bubble column theory, to apply to columns of any diameter. They proposed that

$$D_p = D_l = 0.063\ d_c\ (j_g/1.6)^{0.3}. \qquad (1.35)$$

Subsequent to their work RTD studies published have made similar assumptions and consequently liquid tracers have been used to model the collection zone. Laplante et al. (1988) developed the following empirical relationship for the dispersion coefficient in a flotation column:

$$D_p = D_l = 0{,}124\ d_c^{1.31}\ j_g^{0.33}\ e^{(-0.025\ S)} \qquad (1.36)$$

where S is the feed percent solids. This correlation is based on the RTD results obtained using a liquid tracer by a number of investigators (Yianatos et al. (1987), Espinosa-Gomez (1987) and Dobby and Finch (1985)). Recently Xu and Finch (1991b) have recommended the use of the relationship proposed by Luttrell et al. (1990),

$$D_l/u_i L = 1.85\ [(d_c/L)(j_g/j_l)]^{0.63} \qquad (1.37)$$

where j_l is superficial liquid downward velocity. Work published by Mavros et al. (1989) presented two phase liquid tracer studies performed on a laboratory flotation column system. They used a tanks-in-series model to describe the liquid phase mixing and found that increased gas flowrates enhanced mixing and increased liquid flowrates caused the behaviour of the column to approach plug flow.

Recent work by Yianatos and Bergh (1990) indicates that there is a difference between the mixing of liquid and of solids of different

particle sizes. The mean residence time and variance of solids decreased with increasing particle size and were always less than those of the liquid.

2.4 ASPECTS OF COLLECTION ZONE MIXING ADDRESSED IN THE PRESENT STUDY

Residence time distribution experiments were performed in the present study to address a number of issues related to the description of solids and liquid mixing in the collection zone. This section discusses the particular aspects of the modelling of the collection zone mixing characteristics which are investigated in the present study.

The approach to modelling collection zone mixing was developed from the more extensively studied bubble column. The operating conditions utilised in bubble columns cover a much wider range than those used in column flotation and the axial dispersion model is generally used to predict mixing in these columns. Previous flotation column investigators selected a specific range of conditions from which to obtain correlations to predict mixing in flotation columns. Table 1.2 compares this range of conditions with those used in column flotation.

Parameter	Flotation Column	Bubble Column
Superficial Gas Rate	0.5-3cm/s	0.5-7cm/s
Superficial Tailings Rate	0.5-2cm/s	1-7cm/s
Superficial Wash Water Rate	0.3-0.8cm/s	-
Superficial Bias Rate	0.1-0.3cm/s	-
Froth Depth	0.5-1.5m	-
Average Bubble Size	0.8-2.0mm	>10mm
Height/Diameter Ratio	>10/1	>10/1
Number of Phases	3	2 or 3
Mode of Operation	countercurrent	cocurrent

Table 1.2: Comparison of Bubble Column and Flotation Column Operating Conditions

Although the operating conditions used are similar, there are important differences between the two systems. Bubble columns are usually operated in cocurrent mode with high liquid/pulp velocities, which lead to less dynamic interaction between the dispersed and continuous phase when solids are present in the system. This is especially the case for three phase work in bubble columns where high liquid and gas velocities are used in order to keep the solids suspended (Imafuku et al., 1968). In industrial scale bubble columns the bubble size is >1cm and in laboratory scale bubble columns (d<20cm) the bubble size is <1cm. In general the ratio of column diameter to bubble diameter in bubble columns is <50. In flotation columns the ratio of column diameter to bubble size varies, the ratio being about 100 for laboratory columns and for industrial columns the ratio exceeds 500. It is possible that a decrease in bubble size will increase mixing. However this has not been previously investigated and the present study addresses this issue.

It is clear from the above discussion that industrial bubble columns are operated at conditions which lead to lower degrees of mixing than equivalent sized flotation columns viz. large bubbles and high liquid velocities. For industrial flotation columns where the degree of mixing is large it is possible that the dispersion model is an inappropriate model choice. In this study the tanks-in-series and axial dispersion models are fitted to the RTD data in order to evaluate the appropriateness of each model for a range of column diameters.

Rice et al. (1974) and Dobby and Finch (1985) found the solid and liquid dispersion coefficients to be equivalent for the operating parameters used in each study. The work of Yianatos and Bergh (1990) and Goodall and O'Connor (1989) indicate that this may not be the case for all column operating conditions. The solid and liquid dispersion coefficients may only be equivalent when the pulp passing through a column is relatively unmixed. In the present study RTD testwork is performed using both solid and liquid tracers in order to compare the solid and liquid dispersion coefficients at typical operating conditions for a range of column diameters. Furthermore an investigation is carried out to ascertain whether tracer particle size affects the resultant solid dispersion coefficient.

Tracers used to investigate solids mixing in the collection zone are normally hydrophilic i.e. tailings material (Dobby and Finch, 1985 and Yianatos and Bergh, 1990). However in the study performed by Goodall and O'Connor (1991) feed material which contains both hydrophobic and hydrophilic material was used as a tracer. It is possible that the use of feed material as a tracer will confound the tailings age distribution. RTD studies are performed in this study to compare the tailings age distribution curves obtained using feed and tailings material for a range of column diameters.

Finally a number of investigators have performed RTD studies of the collection zone of the flotation column and various approaches and correlations have been used to estimate the vessel dispersion number (Dobby and Finch (1986), Kho and Sohn (1989) and Xu and Finch (1991a and b)). As pointed out in Chapter 1 Sec. 2.2 incorrect correlations as well as inappropriate boundary conditions have been used to determine D/uL. The present study investigates the appropriateness and accuracy of the different methods which can be used.

3. MODELLING OF THE KINETICS OF THE COLLECTION ZONE

This section begins by reviewing methods which can be used to determine the overall and collection zone rate constants in a column flotation cell. Following this a particle collection model developed by Finch and Dobby (1990) to predict the collection zone rate constant is presented and the effect of flotation variables on particle collection is reviewed. Finally the particular aspects of the modelling of collection zone kinetics which are addressed in the present study are discussed.

3.1 REVIEW OF METHODS TO DETERMINE EXPERIMENTALLY THE COLLECTION ZONE RATE CONSTANT

The process of flotation in a flotation column can be divided into two sections viz. recovery from the collection zone, R_C, and recovery from the

cleaning zone, R_f (related to the drop back from the froth). A recycle process exists between the collection and cleaning zone whereby hydrophobic material enters the froth, drops back into the pulp and is then subject to recollection. Overall recovery can be predicted using the following relationship (Finch and Dobby, 1990)

$$R_{fc} = \frac{R_c R_f}{R_c R_f + 1 - R_c} \qquad (1.38)$$

Measurement of froth drop back, R_f, has proved to be difficult. Laboratory techniques used have been back calculation of R_f from measurements of recovery with and without froth (Shaning, 1985); solving for the R_f which satisfies measured recovery from cocurrent and countercurrent operation (Contini et al., 1988) and isolating the cleaning zone from the collection zone (Falutsu and Dobby, 1989). A tentative value for drop back in laboratory columns is about 50% (Finch and Dobby, 1990). A practical model of the behaviour of the froth zone has yet to be developed.

To simplify the process of modelling, the column is often considered to be a single stage (del Villar et al. (1988) and Alford (1990)). In this approach an overall rate constant k_{fc} is used, and the cleaning zone is not treated as a separate stage, although cleaning zone effects are recognized in terms of impact on k_{fc}. While this approach has been reported to be satisfactory for modelling large scale columns (Alford, 1990), it can be very misleading in scale-up as drop back increases substantially with increasing column diameter.

The work in this thesis focussed specifically on the effects of the physical and operating parameters on the collection zone rate constant. Previous methods to determine the collection zone rate constant, k_c are reviewed in detail. Three different approaches have been reported whereby k_c can be separately determined.

Contini et al. (1988) developed a method to determine k_c using a cocurrent/countercurrent column. The column used to determine k_c was of a specific design with an expansion zone below the interface in order that the column could be operated in both counter- and cocurrent modes. The

testwork entailed operating the column in the two different modes. By making the assumption that the collection zone rate constants for the co- and countercurrent modes were equivalent the recovery equations for the two modes could be solved to yield a collection zone rate constant. This assumption may not be valid.

Dobby and Finch (1986a) describe a method in which the cleaning zone was eliminated. This was achieved by operating the column with a shallow froth, but with a very high bias (>0.4 cm/s) and low gas flow rate to eliminate entrainment and feed short circuiting. In order to obtain incremental recovery values from which the rate constant could be determined the feed ore was passed through the column with a short residence time (1min). The tailings were decanted to remove the added wash water and passed through the column again. This process was repeated several times. The column was therefore measuring a batch-type rate constant and the column was not running at steady state.

Recently Mular and Musara (1991) presented a method to determine the rate parameter using a batch column. Tailings material was continuously recycled as feed resulting in closed system. The procedure to determine the rate constant was similar to methods used to determine rate constants in a conventional batch cell. Incremental concentrate samples were taken over a period of time. In this study the k_{fc} was determined. However if the froth zone was eliminated a similar study could yield k_c. The batch column is an improvement of the method laid out by Dobby and Finch (1986a) although there are problems related to the method. The wash water addition rate has to be kept at the same rate as the water exiting in the concentrate. The collection process occurs while the column is not running at steady state and a batch-type rate constant is being measured which may not be equivalent to the continuous rate constant.

3.2 A MODEL TO PREDICT THE COLLECTION ZONE RATE CONSTANT

The development of the particle collection model which follows is based on the model developed by Finch and Dobby (1990). The rate parameter is dependent on both a number of the operating variables as well as the

mineral hydrophobicity. The general form of the rate parameter used in this model was proposed by Jameson et al. (1977).

In the collection zone of the flotation column gas bubbles rise through the column of pulp containing hydrophobic particles at a concentration c_p (number of particles per unit volume). The collection efficiency E_K, is defined as the fraction of particles swept out by a bubble that collide with, attach to and remain attached to the bubble. To derive the relationship, consider a cubic volume of pulp with a side dimension L, the following expression describes particle collection:

rate of particle removal = rate of particle removal per bubble x number of bubbles

At a gas velocity j_g and a velocity of the bubbles relative to the slurry of U_{sg} this expression is equivalent to:

$$L^3 \frac{dc_p}{dt} = \left(-\frac{\pi}{4} d_b^2 U_{sg} c_p E_K\right) \times \left(\frac{j_g L^2}{\pi/6\, d_b^3} \frac{L}{U_{sg}}\right) \qquad (1.39)$$

Cancelling of terms yields:

$$\frac{1}{c_p} \frac{dc_p}{dt} = \frac{1.5\, j_g E_K}{d_b} \qquad (1.40)$$

Provided that E_K is independent of c_p this is equivalent to the expression for the first order process where the first order rate constant k is given by:

$$k = \frac{1.5\, j_g E_K}{d_b} \qquad (1.41)$$

The collection efficiency can be expressed as a function of three components as follows

$$E_K = E_C\, E_A\, E_D \qquad (1.42)$$

where E_C is the collision efficiency, E_A is the attachment efficiency, and E_D is the fraction of particles that remain attached throughout the flotation process. Collision efficiency E_C is the fraction of all particles swept out by the projected area of the bubble that collide with the bubble. Two types interaction occur between the particle and bubble upon collision:

1. The particle collides with the bubble and the bubble surface is strongly deformed. The particle rebounds unless attachment takes place during the first collision.

2. The particle slides along the bubble surface with a weak deformation of the bubble surface, which is not detectable experimentally.

Particle trajectory simulations by Dobby (1984) show that particle bounce is insignificant for particles less than 100μm in diameter. Schulze (1989) found for a 200μm particle that the sliding model seemed more reasonable. Which of the two interactions predominates in flotation depends on many factors and has not been investigated in detail. However in this thesis where fine and intermediate particle sizes (<180μm) were used and due to nature of the column operation high relative velocities of the particles are not expected the sliding process would seem more likely. The analysis which follows only accounts for the sliding process.

Unless attachment occurs the sliding particle maintains bubble contact until the fluid streamlines carry it radially away from the bubble surface. Attachment efficiency E_A is the fraction of all colliding particles that undergo successful attachment during the time of contact. For the work performed in this thesis it will be assumed that E_D equals one, that is, that no detachment of particles occurred. It has generally been considered in conventional flotation that an important cause of poor coarse particle flotation is particle-bubble disruption by turbulence. Estimates of critical particle size have been developed (Jowett, 1980 and Woodburn et al., 1971). Values of the critical particle size, below which detachment should be minimal, are generally about 100μm. In the quiescent

flow of a flotation column where there is no mechanical agitation it is likely that the critical particle size is substantially higher.

Development of the correlations to predict the collision and attachment efficiencies initially employs a single particle, single bubble system and this is later expanded to the real system of bubble swarms. Particle sizes dealt with in this work are less than 180μm and the correlations developed only account for fine and intermediate sized particles. It is assumed that particles below 180μm are still within the limits of the model.

3.2.1 PARTICLE-BUBBLE COLLISION

Particle-bubble collision has been studied extensively by several investigators eg. Reay and Ratcliff (1975), Anfruns and Kitchener (1977), Weber (1981), Weber and Paddock (1983) and Schulze (1989). The general method of analysis used by the above authors is based on the equation of motion of a spherical particle relative to a spherical bubble ($d_b >> d_p$) rising in an infinite pool of liquid. Hydrodynamic drag will tend to sweep the particle around the bubble, following the fluid streamlines. Particle inertia and gravity act in a combined manner to move the particle out of the fluid streamline and toward the top surface of the bubble.

Figure 1.6 illustrates the approach of the particle toward the bubble. The equations of motion in the x and y direction are

$$Sk = \frac{dv_x^*}{dt^*} u_x^* - v_x^* \qquad (1.43a)$$

$$Sk = \frac{dv_y^*}{dt^*} (u_p^* + u_y^*) - v_y^* \qquad (1.43b)$$

where the term on the left hand side is the inertial term. $v_{x,y}^*$ and $u_{x,y}^*$ are dimensionless particle and liquid velocities respectively, t^* is dimensionless time and u_p^* is the dimensionless particle terminal velocity. All the velocities are made dimensionless by dividing by the

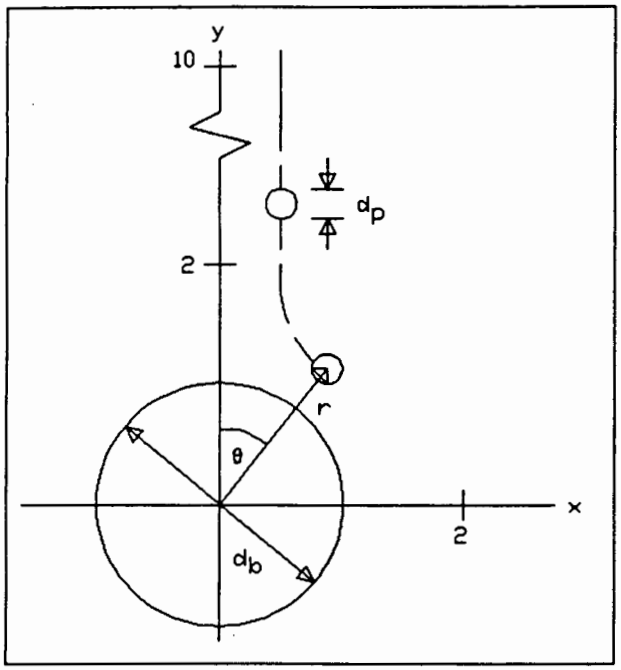

Figure 1.6: Illustration of a Particle approaching a Bubble

bubble rise velocity U_b. t^* is made dimensionless by multiplying by (u_b/d_b). Sk is the Stokes number, given by

$$Sk = -\frac{1}{9}\left(\frac{\rho_p}{\rho_l}\right)\left(\frac{d_p}{d_b}\right)^2 Re_b \qquad (1.44a)$$

where

$$Re_b = \frac{d_b\, U_b\, \rho_{sl}}{\mu_{sl}} \qquad (1.44b)$$

and U_b is the terminal rise velocity of a single bubble calculated using an adaptation by Yianatos et al. (1988b) of the multi-species settling equation of Masliyah (1979),

$$U_b = \frac{g\, d_b^2\, (\rho_{sl} - \rho_b)}{18\, \mu_{sl}\, (1 + 0.15\, Re_b^{0.687})} \qquad (1.45)$$

Equations (1.44b) and (1.45) are solved iteratively to determine both U_b and Re_b. The particle terminal velocity is calculated using Stokes' equation

$$u_p = g\, (\rho_p - \rho_l)\, d_b^2 \,/\, (18\mu_l) \qquad (1.46)$$

The collision efficiency is determined by first developing correlations for fine particles where Sk is less than 0.1 and can be assumed to be zero. The analysis is then extended to intermediate size particles.

3.2.1.1 Collision Efficiency for Fine Particles

The collision model of Weber and Paddock (1983) is the most comprehensive model to date. In their model the overall collision efficiency is the sum of gravitational and interceptional collision:

$$E_C = E_{Cg} + E_{Ci} \qquad (1.47)$$

E_{Ci} is given by (Weber and Paddock, 1983)

$$E_{Ci} = \frac{1.5}{1 + u_p} \left(\frac{d_p}{d_b}\right)^2 \left[1 + \frac{(3/16)Re_b}{1 + 0.249\, Re_b^{0.56}}\right] \qquad (1.48)$$

for $0<Re_b\leq 300$. E_{Cg} is given by, (Reay and Ratcliff, 1973)

$$E_{Cg} = \frac{u_p^*}{1 + u_p^*} \left(1 + \frac{d_p}{d_b}\right)^2 \sin^2\theta_c \qquad (1.49)$$

where θ_c is the angle, measured from the stagnation point of the bubble, where the fluid streamlines come closest to the bubble. For $20<Re_b<400$ the following correlation for θ_c applies:

$$\theta_C = 78.1 - 7.37 \ln Re_b \quad (1.50)$$

3.2.1.2 Collision Efficiency for Intermediate Particles

Collision efficiencies for Sk > 0.1 have to be calculated by determining particle trajectories using a numerical solution to the equation of motion (Equation 1.43) and finding the grazing trajectory by trial and error.

Collision efficiency for Sk > 0.1 is estimated from experimental data by the following equation (Finch and Dobby, 1990):

$$E_C = E_{Co} (1.63 Re_b^{0.06} Sk^{0.54} u_p^{*-0.16}) \quad (1.51)$$

where E_{Co} is E_C obtained from Equation (1.47) for conditions when Sk=0.

3.2.2 PARTICLE-BUBBLE ATTACHMENT

Each mineral that collides with a bubble stays in contact with the bubble surface for a time referred to as the sliding time t_s. During the period of contact the bubble film thins. If the sliding time is sufficiently long, the film will thin to point where rupture will occur (spontaneously) to form a stable three phase aggregate. The total time required for this process is known as the induction time t_i. In simple terms, if the induction time t_i is less than or equal to the sliding time t_s, then particle attachment will proceed.

3.2.2.1 Particle Sliding Time

To calculate t_s the analysis applies the fluid mechanical arguments already detailed in the collision model. No attempt is made to include surface forces as they are not readily quantified. The calculation of t_s involves determining the distribution on the bubble surface of particle collision angles, the angle at which fluid streamlines start to carry the

particle radially away from the bubble, i.e. the maximum angle of contact θ_c, and the particle sliding velocity.

The distribution of contact angles is quantified by n_θ the fraction of all colliding particles that collide between the front stagnation point and some angle θ. This is calculated using the trajectory model; a good approximation is

$$n_\theta = \frac{\sin^2\theta}{\sin^2\theta_c} \qquad (1.52)$$

where θ_c is given by Equation (1.50).

The maximum angle of contact θ_m is calculated by determining the angle at which the radial component of the particle settling velocity (directed toward the bubble surface) is equal to the radial component of the liquid velocity (directed away from the bubble surface). At $\theta > \theta_m$ the particle no longer contacts the bubble, unless attachment has already occurred. A correlation between θ_m, ρ_p and θ_c is, (Finch and Dobby, 1990)

$$\theta_m = 9 + 8.1\ \rho_p + \theta_c(0.9 - 0.09\ \rho_p) \qquad (1.53)$$

Particle sliding velocity v_θ over the bubble surface is the sum of the tangential component of the particle settling velocity, $u_p\sin\theta$, and the local tangential velocity. Assumptions of Stokes flow and potential flow to determine the local tangential velocity have been found to be invalid. The flow regime has, however, been modelled using two linear functions (Dobby and Finch, 1987). The model makes use of the parameter surface vorticity ξ_s which is the liquid tangential velocity gradient at the surface of the sphere. The following relationship holds for $0° < \theta \leq 90°$:

$$\xi_s = a + b\theta + c\theta^2 + d\theta^3. \qquad (1.54)$$

The coefficients a, b, c and d are a function of Re_b and Appendix 4 details the equations used to determine these coefficients.

For $d_p/d_b < 0.03$ particle tangential velocity v_θ,

$$v_\theta = 0.7\ \xi_s\ u_b\ (d_p/d_b) + u_p \sin\theta \qquad (1.55)$$

For $d_p/d_b > 0.03$ the particle velocity is calculated by dividing the particle into two zones, the lower part that sees a velocity gradient and the upper part that sees a constant velocity. Then v_θ is given by

$$v_\theta = 0.7\ \xi_s\ u_b \left[\frac{(d_p - 0.03d_b)}{d_p}\ 0.06 + \left(\frac{0.03d_p}{d_p}\right)\ 0.03\right] + u_p \sin\theta \qquad (1.56)$$

An average value of the particle sliding velocity $v_{\theta m}$ is determined using average values of ξ_s and $\sin\theta$. The particle sliding time t_s can now be calculated

$$t_s = ((\theta_m - \theta)/360)\pi(d_p + d_b)/v_{\theta m} \qquad (1.57)$$

where θ is in degrees.

3.2.2.2 Induction Time

A particle attaches to a bubble when the sliding time t_s equals or exceeds the induction time t_i. Prediction of the induction time has been investigated by a number of authors and a few correlations have been developed to predict the parameter. It is a difficult parameter to measure and prediction involves a number of assumptions. For sliding collisions, Schulze (1989) recommends Taylor's expression for film thinning. In this relationship the film thinning process is approximated by a sphere approaching a plane surface. If the only forces acting are gravity and the hydrodynamic drag force, induction time is given by:

$$t_i = \frac{6\mu_l \ln((d_p/2)/h_{crit})}{((2/3\ d_p(\rho_p - \rho_g)g + (36\mu_l U_b/d_b))\cos\theta} \qquad (1.58)$$

where θ_{crit} is the critical thickness of film rupture. h_{crit} is related to particle hydrophobicity. This parameter is practically impossible to determine, however reasonable values of h_{crit} are between 20 and 50nm (Alford, 1991).

Studies have been performed whereby the induction time was estimated from batch laboratory flotation tests (Jowett (1980), Shaning (1985) and Crawford and Ralston (1988)). Jowett (1980) investigated the effect of particle size on the induction time in the flotation of various ores. For a pyrite system it was found that induction time decreased from about 11 to 9msec with increasing particle size from 2 to 50μm. With increasing particle size above 50μm the induction time began to increase. In the study performed by Shaning (1985) the induction time decreased with increasing particle size for d_p<50μm. Crawford and Ralston (1988) found that for the quartz particles floated the induction time decreased with increasing particle size up to 46μm and then from the next size (99μm) onwards increased.

3.2.2.3 Attachment Efficiency

If θ' is the angle θ in Equation (1.57) when $t_s = t_i$ then after rearrangement this gives

$$\theta' = \theta_m - (360\ v_{hm}\ t_i)/(\pi(d_b+d_p)). \qquad (1.59)$$

Attachment efficiency is therefore given by

$$E_A = \frac{\sin^2 \theta'}{\sin^2 \theta_c} \qquad (1.60)$$

The collection efficiency can now be determined using Equations (1.60), (1.51) and (1.42) and the collection zone rate constant can be calculated using Equation (1.41).

3.3 THE EFFECT OF FLOTATION VARIABLES ON PARTICLE COLLECTION IN THE COLLECTION ZONE

Chapter 1 Sec. 1.1.2 discussed the effect of the various parameters on maintaining the desired bubbly flow regime. This section deals with the effect of the various parameters on the rate of particle collection.

3.3.1 PARTICLE SIZE

The influence of particle size on the rate of recovery of minerals from flotation pulps has been investigated in numerous studies (eg. Trahar and Warren (1976), Crawford and Ralston (1988) and Finch and Dobby (1990)). Particle size is recognised as being a very important variable, and major problems in flotation can be the relatively poor response of coarse and very fine particles. An optimum flotation rate usually applies to a range of particle sizes in a system. Above and below this range the flotation rate decreases forming an inverted U shaped curve. For pyrite the optimum particle size range for recovery has been reported to be between 50 and 150μm by Imaizumi and Inoue (1965). The relatively slow flotation rate of very fine particles is generally attributed to the reduced opportunity for particle-bubble collisions arising from hydrodynamic and inertial factors. The poor recovery of coarse particles has been explained by bubble-particle detachment (Woodburn et al., 1971) or by an increase in the induction time for large particle diameters (Jowett, 1980). Finch and Dobby (1990) using the model detailed above show that for a constant induction time that as d_p increases E_C increases but E_A decreases. The effect of d_p on E_A as well as E_C therefore results in an optimum particle size for recovery.

3.3.2 PARTICLE HYDROPHOBICITY

Particle hydrophobicity is related to the induction time of the particle. Finch and Dobby (1990) plot curves of the effect of particle size on collection rate using constant induction times and the model detailed above. As discussed in Chapter 1 Sec. 3.2.2.2 constant t_i with changing particle size has been shown not to be the case in a number of studies.

Hydrophobicity is likely to vary with particle size. Hydrophobicity is also inherently related to the type of ore being floated, the surface conditions of the ore (eg. oxidised) and the collector type and amount added to the system.

3.3.3 SUPERFICIAL GAS RATE

Equation (1.41) gives the relationship between the collection zone rate constant and the gas rate. The equation indicates that the rate constant is directly proportional to the gas rate. The gas rate does not affect the result of the model predicting the collection efficiency. Dobby and Finch (1986b) suggest that there is an optimum gas rate for particle collection. This proposal is based on the fact that as the gas rate increased the bubble size increased according to the following equation

$$d_b = C\ j_g^{0.25} \qquad (1.61)$$

where C is a constant. This correlation was developed from bubble sizing tests using a cloth sparger by Laplante et al. (1983). The collection zone rate constant is inversely proportional to bubble size. Consequently bubble size increases result in a reduction in the rate constant. The collection efficiency decreases with increasing bubble size further reducing the rate constant. Finch and Dobby (1990) propose that the opposing effects of bubble size and gas rate serve to produce an optimum gas rate for particle collection.

In a study performed by Mular and Musara (1991) the rate constant was found to increase sharply with increasing gas flow rate up to about 2.5cm/s. Above 2.5cm/s the rate constant increased at a lower rate. The levelling off of the rate constant above 2.5cm/s was attributed to the production of larger bubbles at high gas rates. The study was performed on a batch flotation column and coal was floated.

3.3.4 BUBBLE SIZE

Equation (1.41) shows that decreases in the bubble size result in an increase in the collection zone rate constant since the rate constant is inversely proportional to the bubble size. Decreasing the bubble size also results in an increase in both the collision and attachment efficiencies. Experimental evidence of increasing collision efficiency with decreasing d_b has been provided by Anfruns and Kitchener (1977). The increase in the attachment efficiency is because the fractional decrease in particle sliding velocity on a smaller bubble (bubble velocity decreases with decreasing d_b) exceeds the fractional decrease in sliding distance. In a study by Ahmed and Jameson (1985) the rate constant was found to increase up to one hundred fold when the bubble size was reduced from 0.655mm to 0.075mm.

3.4 ASPECTS OF THE KINETICS OF THE COLLECTION ZONE ADDRESSED IN THE PRESENT STUDY

A number of methods have been developed to determine the collection zone rate constant (Dobby and Finch (1986a), Contini et al. (1988) and Mular and Musara (1991)). However in each of the methods the collection zone of the flotation column did not operate at typical conditions. Either the column configuration was modified, the tailings material was recycled or the column was not operated at steady state. In this study a method is developed to determine the collection zone rate constant at typical column operating conditions and while the column is operating at steady state.

Using the method to determine the collection zone rate constant developed above and by injecting labelled hydrophobic material into a flotation column an evaluation of the effect of the various physical parameters on the collection zone rate constant(s) is obtained. The results of this testwork are used to evaluate the combination of first order kinetics and models describing the degree of mixing in the collection zone to predict recoveries.

The particle collection model developed by Finch and Dobby (1990) and detailed in Chapter 1 Sec. 3.2 represents a comprehensive fundamental

description of flotation kinetics. However limited experimental testwork is reported in which the model is evaluated a range of operating parameters. The results of the kinetics testwork performed in this study are also used to determine the applicability of this model for a range of typical column operating conditions.

4. FLOTATION COLUMN SCALE-UP

This section presents a brief outline of a typical scale-up procedure using the axial dispersion model to describe mixing and a single first order rate constant to describe the flotation kinetics (Finch and Dobby, 1990). The procedure illustrates how models describing the mixing characteristics and kinetics of the collection zone are incorporated into scale-up. Table 1.3 lists the parameters which are required to perform the scale-up calculation. The parameters which can be determined from pilot plant testwork are numbered with an asterisk (*). Pilot plant testwork is essential to determine not only the optimum operating conditions for the feed material to be treated but also the following information; an estimate of the collection zone rate constant and an evaluation of the froth carrying capacity. These parameters are estimated using methods detailed earlier.

Feed Conditions		Operating Conditions	
Solids Density	ρ_p	Bias Rate (*)	j_b
Feed % Solids	S	Gas Holdup (*)	ϵ_g
Volumetric		Gas Rate (*)	j_g
Feed Rate	Q_F	Carrying Capacity (*)	C_a
Collection Zone		Froth Zone Recovery	R_f
Rate Constants (*)			
Mineral 1 - valuable	k_{c1}		
Mineral 2 - gangue	k_{c2}		
Mean Particle Size	d_p		
Column Configuration		**Target Performance**	
Column Diameter	d_c	Recovery of Mineral 1	R_{fc1}
Cross Sectional Area	A_c	Grade of Mineral 1	G_{fc1}
Number of Columns	X		
Collection Zone Length	L		

Table 1.3: Data required for Flotation Column Scale-up

The mineral content of the feed material is also required to calculate the grade of Mineral 1 in the concentrate. For Minerals 1 and 2 the following procedure is carried out to determine the recovery of each mineral to the concentrate:

Overall Recovery, R_{fc}:

$$R_{fc} = \frac{R_c R_f}{R_c R_f + 1 - R_c} \qquad (1.38)$$

Froth Zone Recovery, R_f:

Froth zone recovery is estimated from previous column testwork. However there is limited experimental data for the value of R_f in industrial columns. R_f has been measured to be about 50% for laboratory columns and is expected to be less than 50% in industrial columns (Finch and Dobby, 1990).

Collection Zone Recovery, R_c:

$$R_c = 1 - \frac{4\ a\ \exp(1/(2\ N_p))}{(1+a)^2\ \exp(a/(2\ N_p)) - (1-a)^2\ \exp(-a/(2\ N_p))} \qquad (1.18a)$$

where

$$a = (1 + 4\ k_c\ \tau_p\ N_p)^{1/2} \qquad (1.18b)$$

$$N_p = D_p/u_p L \qquad (1.17c)$$

Collection Zone Rate Constant, k_c:

The collection zone rate constant is usually determined from pilot plant work. It can also be estimated from the following equation:

$$k = \frac{1.5\ j_g\ E_K}{d_b} \qquad (1.41)$$

and the particle collection model detailed earlier. Equation (1.41) also provides information as to how the rate constant will change if the industrial column is operated at different conditions to those used in the pilot column testwork (eg. bubble size and gas rate).

Particle Mean Residence Time, τ_p:

$$\tau_p = \tau_l \frac{u_l}{u_l + U_{sp}} \qquad (1.62)$$

where u_l is the interstitial liquid velocity, τ_l is the liquid mean residence time and U_{sp} is particle slip velocity. u_l and τ_l are determined from the following equations

$$u_l = j_{sl}/(1-\epsilon_g) \qquad (1.63)$$

$$\tau_l = L(1-\epsilon_g)/j_{sl} \qquad (1.64)$$

where j_{sl} is the superficial slurry velocity and is determined from

$$j_{sl} = Q_F/XA_c + j_b \qquad (1.65)$$

U_{sp} can be obtained from the general equation proposed by Masliyah (1979):

$$U_{sp} = \frac{g\, d_p^2\, (\rho_p-\rho_{sl})\, (1-\epsilon_g)^{2.7}}{18\, \mu_{sl}\, (1+0.15\, Re_p^{0.687})} \qquad (1.66a)$$

where

$$Re_p = \frac{d_p\, U_{sp}\, \rho_l\, (1-\epsilon_g)}{\mu_{sl}} \qquad (1.66b)$$

Vessel Dispersion Number, N_p

$$N_p = D_p/u_pL \qquad (1.17c)$$

where D_p is the particle dispersion coefficient and can be determined from one of the empirical correlations listed in Chapter 1 Section 2.3.3 viz. Equations (1.34), (1.35) or (1.36), u_p is the particle interstitial velocity ($u_p = u_l + U_{sp}$) and L is the collection zone length. Equation (1.37) can also be used to obtain an estimate of N_p.

The scale-up process involves varying the factor XA_c by altering either X or d_c and the scale-up procedure is repeated until the required recovery of Mineral 1 is obtained at typical values of j_{sl} viz. 0.5 - 2 cm/s. A mass balance as well as the overall recoveries of Minerals 1 and 2 will yield the grade of Mineral 1 in the concentrate.

The recovery and grade results are then used to calculate the concentrate solids rate per unit cross sectional area (M_c) for the designed column. This value is compared to the maximum carrying capacity of the froth calculated either from the pilot column testwork or the correlations listed in Chapter 1 Sec. 1.2.3. If M_c is greater than the maximum carrying

capacity of the froth this generally indicates that the column design will be dictated by the froth zone. The focus of the work performed in this thesis is the design of columns which operate below the maximum carrying capacity i.e. the volume of the collection zone combined with the cleaning action of the froth determines the recoveries and grades obtained. For this reason the design of columns which are limited by the froth zone carrying capacity is not dealt with in detail.

4. RESEARCH OBJECTIVES

The objectives of this research programme are:

1. To evaluate and improve existing models used to describe the degree of mixing in the collection zone of flotation columns.

2. To evaluate and improve existing models used to describe the flotation kinetics for the recovery of sulphide minerals from the collection zone of a flotation column.

3. To use the above results to evaluate and improve flotation column scale-up procedures.

CHAPTER 2

EXPERIMENTAL DETAILS

1. STUDY OF MIXING CHARACTERISTICS OF THE COLLECTION ZONE

The study of the mixing characteristics of the collection zone consisted of three sets of residence time distribution studies. The preliminary RTD study entailed the injection of salt labelled liquid tracers into a laboratory column. The following two RTD studies involved the use of radioactively labelled solid and liquid tracers and were performed on a pilot and an industrial column.

1.1 PRELIMINARY RESIDENCE TIME DISTRIBUTION STUDY

This testwork began by setting up a laboratory flotation column and establishing standard ore, reagent additions and operating conditions to be used in the preliminary RTD study as well as in later testwork. Following this bubble size measurements were performed to calibrate the filter cloth sparger in the laboratory column for bubble size at different gas rates and frother concentrations. The bubble size measurements were performed using a bubble size measuring device developed at the University of Cape Town. Finally the preliminary RTD study was performed using liquid tracers and was intended to link up with testwork using solid tracers performed by Goodall and O'Connor (1991) on similar equipment. Furthermore the RTD study also investigated the effect of feed percent solids, gas flow rate and frother concentration using two types of spargers on the liquid tracer tailings RTD. The RTD study was performed using sodium chloride as a tracer and conductivity meters to monitor tracer flow.

1.1.1 EQUIPMENT

The equipment used in the preliminary RTD study was a laboratory flotation column and ancillary equipment, a gas holdup measuring system, a bubble size measuring device and a residence time distribution detection system.

1.1.1.1 Laboratory Column Rig

The laboratory flotation column had been successfully used in previous projects at the University of Cape Town (Goodall and O'Connor (1991) and Schommarz (1991)). The column was constructed of flanged 600mm lengths (sections) of clear perspex pipe with an internal diameter of 54mm. By removing or inserting sections, the length of the column could be varied as desired. Certain sections of the column were manufactured with threaded ports for the feed pipe attachment, sparger insertion and tailings removal. For the testwork performed in the preliminary study the total column height was set at 2.35m, the collection zone height was 1.550m and the cleaning zone height was 0.65m.

Figure 2.1 is a schematic diagram of the column. As illustrated, the top section of the column consisted of a froth overflow weir and a concentric launder with a base angled at 18° to the horizontal to facilitate froth flow. The top section of the column was covered by a clear perspex lid. The lid had a diameter slightly larger than the froth launder and a center hole which allowed for the insertion of a wash water distributor into the froth zone. The launder lid was also fitted with a concentric rinse sprinkler. This was fixed in such a way as to irrigate the froth only in the launder (and not in the froth zone of the column) in order to promote froth breakage and concentrate removal. A second concentrate launder was placed just below the outlet of the first launder. Sample bottles were placed in this launder to collect concentrate samples. When samples were not being taken concentrate flowed through a pipe attachment at the base of the launder and a length of hosing to a settling tank.

The wash water distributor was constructed from 7mm o.d. copper tubing, consisting of a 300mm vertical length and 4 sprinkler arms attached to the base, projecting radially from the center pipe and in the form of a cross.

Each arm was 22mm in length and had five equidistant 1mm holes (on the bottom) for water distribution. The penetration depth of the sprinkler arms into the froth bed was set by simply moving the vertical pipe up or down in the center hole of the column lid. The wash water distributor was set at a depth of 1cm below the weir for column runs. For testwork performed in the preliminary study the feed pipe insertion port was placed 70cm from the top of the column, the sparger port approximately 15cm from the bottom of the column and the tailings removal hose was fitted to the base of the column.

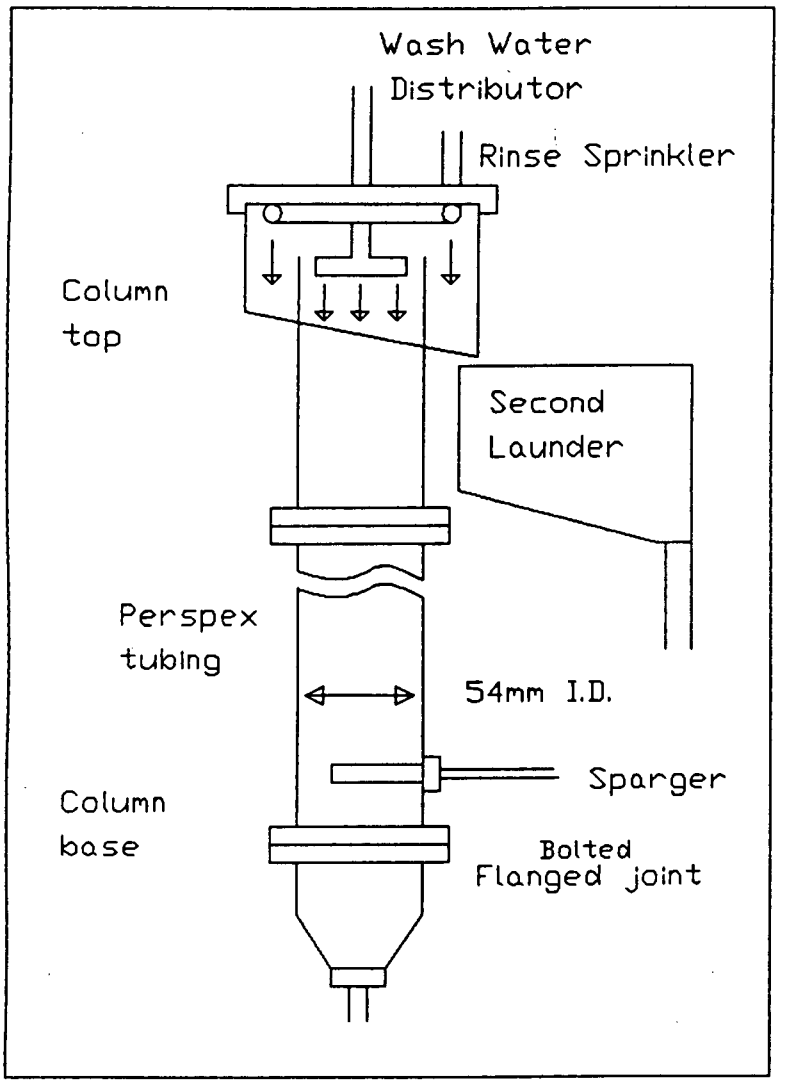

Figure 2.1: Schematic of the Laboratory Flotation Column

Gas Holdup Measurement

Pulp phase fractional holdups were determined experimentally by static head measurements. Mercury manometers were connected to ports on the laboratory column 103cm apart. The upper port was about 10cm below the pulp/froth interface.

Air Spargers

Two types of spargers were used in the preliminary study: a filter cloth sparger and an external sparger based on the United States Bureau of Mines design (USBM). These are illustrated in Figure 2.2.

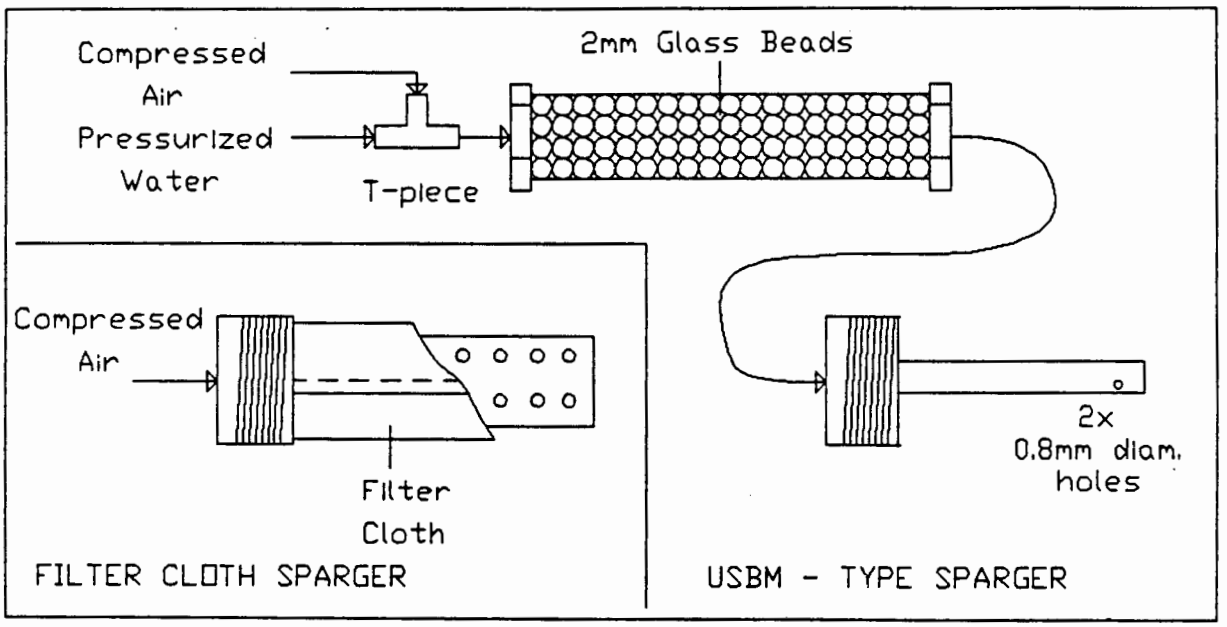

Figure 2.2: Air Spargers used in the Laboratory Column testwork

The filter cloth sparger consisted of a short length of 15mm i.d. PVC pipe with a number of 4mm holes drilled into it. Filter cloth was wrapped around the pipe and both sewn and glued into place. A large filter cloth surface area was used to keep the pressure drop low across the sparger and to prevent the mean bubble size from increasing excessively with increasing gas flow rate. The base of the sparger had a 20mm o.d. threaded section which allowed it to be screwed into the column port just above the base of the column.

The USBM sparger consisted of a T-piece joint in which air and water supplies were joined at right angles to each other. From the T-piece the mixture flowed into a cylinder, 25mm i.d. and 150mm long, packed with 2mm glass beads to improve mixing. A short section of 6mm i.d. hosing fed the water/air mixture into the column. This hosing was sealed off at the end inside the column and two 0.8mm nozzle openings were made on the underside of the pipe so that the water/air stream was directed downwards as it entered the column.

Air to the system was supplied at about 650kPa. The process air entered a regulator where pressure was maintained at about 450kPa, it then passed through a rotameter equipped with a needle valve and following this a second needle valve. The air was then fed by a length of hosing to the sparger system. Pressure in the rotameter was maintained at 400kPa using the second needle valve and flow rate was varied using the needle valve attached to the rotameter. The rotameter was calibrated at 400kPa for gas flow rates at atmospheric pressure using a soap film meter and a stop watch.

Ancillary Equipment

Figure 2.3 is a diagram of the entire rig showing the equipment layout. The solids and water were mixed in a 350l holdup tank. The solids were suspended with a marine type propellor driven by a 1.5hp three phase motor. The base of the tank was fitted with a valve and a feed hose. A narrow hosing (5mm i.d.) was used to pump pulp throughout the system to eliminate solids settling. The pulp was fed to a conditioning tank by a Watson Marlow 503S peristaltic pump. This had a maximum flow rate of 2l/min, using 6mm i.d. neoprene tubing. Reagent was mixed with the pulp through a T-piece as it entered the conditioning tank. The reagents, frother and collector, were pumped using reagent dosage peristaltic pumps with flowrates between 10 and 40ml/min. The conditioning tank was a 35l modified Denver laboratory batch flotation cell. The slurry was fed in at the top of the tank and the conditioned pulp was pumped from the tank through a hose fitting at the tank base. The pulp was pumped to the feed port using a Watson Marlow 503S pump. The tailings were pumped to a sampling tank where samples were taken by a Masterflex peristaltic pump,

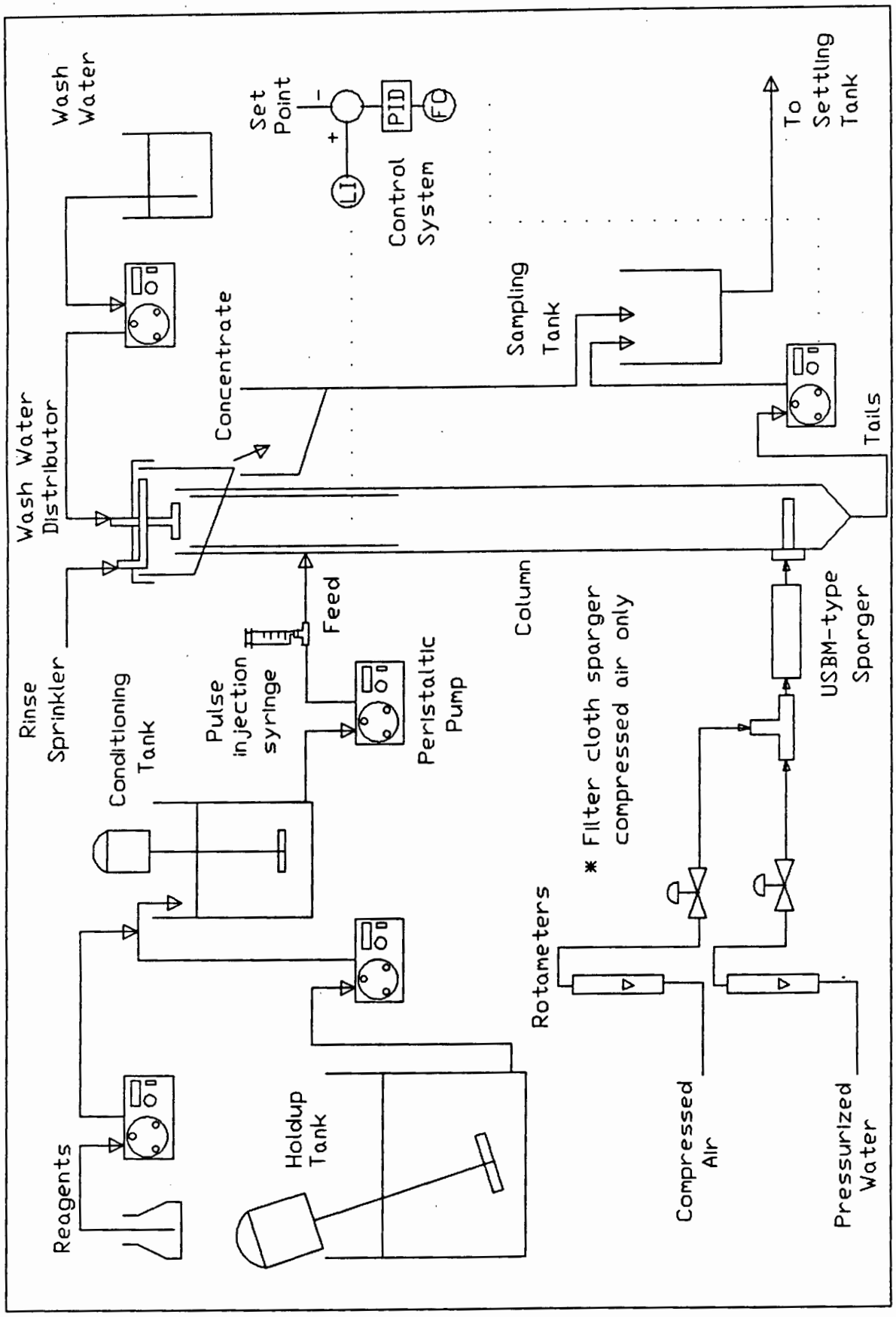

Figure 2.3: Layout of the Laboratory Column Rig

with a maximum flowrate of 13l/min. Unsampled tailings flowed from the sampling tank to a settling tank. Surge chambers were included in the feed and tailings lines to eliminate pulsing due to the peristaltic action.

Pulp level in the column was controlled using a PID controller and a detection system constructed in this study. The design of the level control system was based on a similar system developed by Ormrod (1984). The system relies on the differences in the conductivity of the froth and the pulp. Two 4ohm nichrome wires 700mm long were positioned on the inside of the column from 50mm below the froth lip and downward, thus spanning the limits of the interface. A current was passed through one of the wires and the parallel wire was a common electrode. The two wires were connected by the pulp and froth conductivity and the pulp conductivity was substantially larger than froth conductivity. Consequently the potential measured by the electrode increased linearly as the pulp-froth interface rose. The conductivity was related to interface level and the tailings pump flow rate was controlled to maintain a constant level. The controller could easily be switched to manual control and this was done when tracer was injected into the column as the tracer altered the conductivity of the pulp.

Water was supplied to the wash water distributor using a Watson Marlow 503S pump. Wash water was pumped from a 20l bucket. Water supplied to the rinse sprinkler was tap water fed through a 14S rotameter(metric). The water supply for the USBM-type sparger was obtained from a 200l polyethylene tank containing a mixture of water and frother. A centrifugal pressure water pump (maximum pressure 500kPa) was used to deliver water to the sparger through a 14S rotameter. A water pressure regulator was placed upstream of the rotameter which enabled the water supply pressure to be set at the sparger operating pressure.

1.1.1.2 Bubble Size Measuring Device

A schematic of the bubble size apparatus is provided in Figure 2.4. The device had been successfully used on the same flotation column cell by O'Connor et al. (1990). The equipment may divided into three categories; that used to collect bubbles, the electronics which detect and record the

passage of the bubbles, and the software used to read the recorded data and perform the bubble size calculations. The bubble capture equipment consisted of a glass capillary tube, a gas burette, a vacuum pump, a mercury manometer and a glass water reservoir. The electronics system comprised two photo-transistors vertically mounted a distance of 5mm apart and encased in a brass housing, an amplifier system, and a Motorola 6809 processor. The computer software was written in Borland's Turbo Pascal v4 and was run from a PC. A detailed description of the hardware components and specifics of the detection principle involved have been reported by Randall et al. (1989).

1.1.1.3 Residence Time Distribution Study Equipment

The RTD study was performed using sodium chloride to monitor liquid flow through the column. Figure 2.5 illustrates the positioning of the tracer detection meters.

A 20ml plastic syringe was attached to a T-piece 150mm before the feed port. The tracer was detected continuously by two conductivity probes at the froth lip and at the tails outlet respectively. The conductivity probe at the tailings outlet consisted of a probe mounted in a 5mm i.d. pipe. The detector was attached to the tailings outlet pipe 50mm below the tailings port and was placed vertically to ensure that bubbles did not collect in pipe. The output from the detector was fed via a meter to a flat bed recorder. The conductivity probe in the froth consisted of two nichrome wires placed 5mm apart. The output from this probe was fed directly to the flat bed recorder.

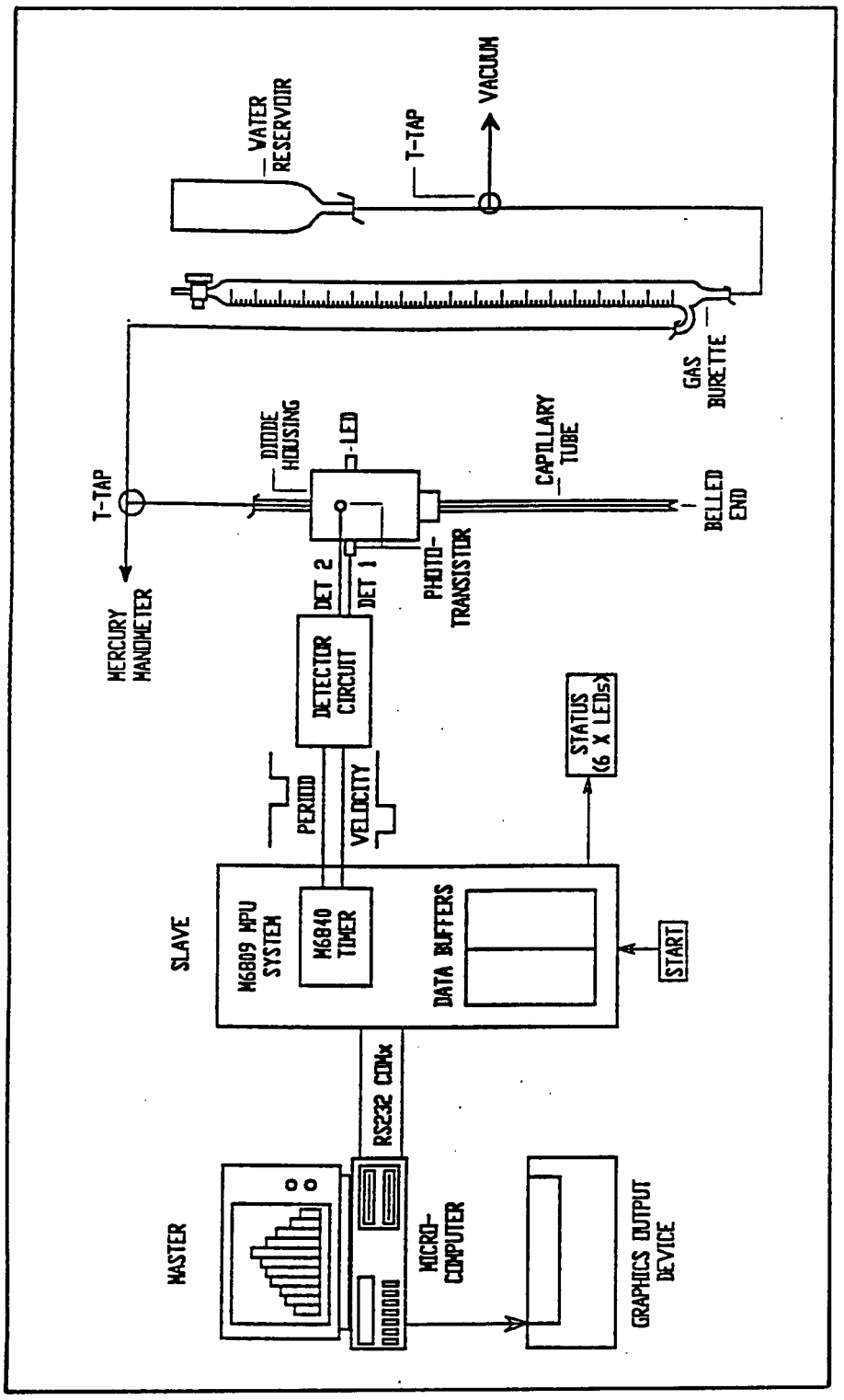

Figure 2.4: Schematic of the Bubble Size Measuring Apparatus

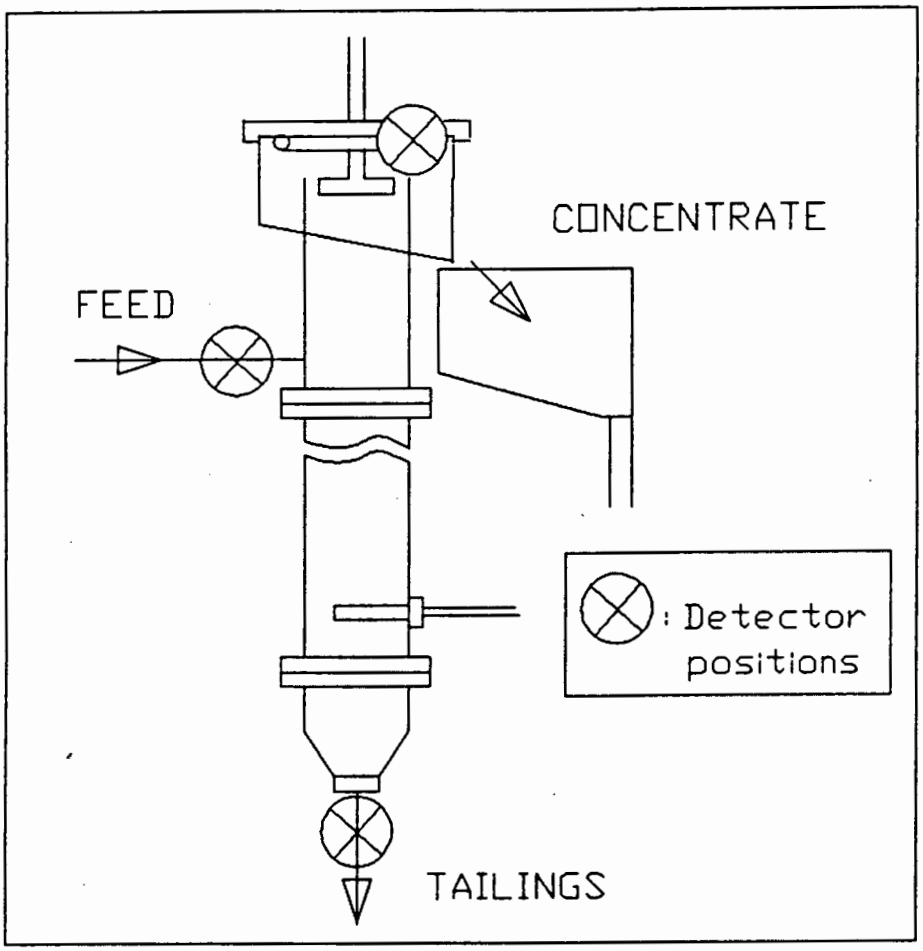

Figure 2.5: Diagram of Laboratory Flotation Column illustrating positioning of Tracer Detector Meters

1.1.2 SELECTION OF THE ORE AND THE REAGENT SUITE

The ore used in the preliminary RTD study had been used in other projects (O'Connor and Mills (1990), Goodall and O'Connor (1989) and Schommarz (1991)). The ore was both well characterised and reagent requirements had been established. The ore was a sample obtained from the St. Helena slimes dam in the Orange Free State, South Africa. Pyrite, pyrophyllite and quartz were the major constituents of the ore and it contained on average about 2 % sulphur and 10g/ton gold. The ore sample was stored under water in airtight 200l polypropylene drums to prevent excessive oxidation. This ore sample will be referred to as the standard ore throughout the thesis.

The particle size and sulphur distribution of the ore is shown in Table 2.1.

Size Fraction	Percent	% Sulphur
-38μm	51.1	3.12
+38-53μm	9.4	2.12
+53-75μm	15.7	1.20
+75-106μm	19.6	0.17
+106μm	4.2	0.19
TOTAL	100.0	2.02

Table 2.1: Particle Size and Sulphur Distribution of the Standard Ore

Work by Schommarz (1991) using the same equipment, ore and typical operating conditions found that collector dosages of between 60 and 80 g/ton sodium mercaptobenzothiozole (SMBT) and total frother dosages of about 80 g/ton DOW 200 yielded sulphur recoveries in excess of 75% and sulphur grades of about 32%. Operating conditions used in this study were over the same range and similar reagent dosages were used. Throughout the preliminary RTD study the frother and collector used were DOW200 and SMBT respectively.

1.1.3 EXPERIMENTAL METHODS

1.1.3.1 Laboratory Column Operation and Sampling

An ore/water mixture to give a required feed percent solids was made up in the holdup tank (200-300l). The tank was run for at least 30min before commencement of a set of experiments to ensure complete solids suspension. Before starting up the column it was filled up to the feed port with water at the same frother concentration as the slurry to be added in the experiment. The air was turned on and set to the desired flow rate. The intermediate feed pump was then turned on and set at the same flow rate as

the feed to the column. The collector and frother dosage pumps were also turned on at the desired reagent dosage rates. The conditioning tank was filled to a level which allowed for a 20min conditioning time when the column was running at steady state. During this time a feed sample was taken. The feed and wash water pumps were then started. The tailings flow rate was controlled manually from the control box until a froth built up and began to pour over the froth lip. The controller was then switched over to PID control.

The column was operated for at least 20min (or about 5 mean residence times) to ensure that steady state was reached. After this time the following experimental readings were taken;

1. Concentrate was sampled for 5min.
2. Tailings sampled for 30sec.
3. Gas holdup measurements were taken.
4. Bubble size measurements were taken.
5. Salt tracer was injected into the feed stream.

Feed, concentrate and tailings samples were taken in duplicate and analysed for sulphur content, mass flow rate and pulp density. The samples were analysed for total sulphur using a LECO SC32 machine with an infrared detector. From this data the sulphur recovery was determined. Reconstituted feed and actual feed assays were compared to check the accuracy of the mass balances. At the end of a run, the column was shut down by turning off the feed pump and setting the tails pump to full speed to drain the column. Any ore adhering to the column walls was flushed out by setting a very high wash water rate.

1.1.3.2 Bubble Size Measurements

The central axis of the capillary tube was positioned 10mm from radial centre of the column cell. Two capillary sizes were used: for bubbles less than 1mm a 0.5mm i.d. capillary tube was used and for bubbles larger than 1mm a 1mm i.d. tube was used. The bell-shaped end of the capillary tubes, designed to prevent bubble breakage as bubbles were drawn into the capillary, was positioned at a distance 150mm below the interface.

A vacuum of between 40-50cmHg was used to draw air bubbles into the capillary tube. Air bubbles travelled up the capillary tube, past the pair of photo-transistors, through an open T-Tap and into the (inverted) gas burette. In three phase experiments a capture flask placed between the T-tap and the burette collected the solids. At the commencement of a bubble size run the burette was filled with water to zero the calibration mark. A water line between the burette and vacuum supply prevented air bubbles from being drawn past the burette. When the bubble capture system was under vacuum, water was gravity fed to this line via a reservoir positioned 1m above the bottom of the burette.

Once a sufficient number of bubbles were collected (see below) the T-tap above the capillary tube was closed and the vacuum supply shut off. The water reservoir was detached from its mounting and moved down until the water levels in the burette and reservoir were the same. The distance (air volume) of the water level in the burette below the zero mark was recorded.

The passage of bubbles through the capillary was detected by the pair of photo-transistors. The basis for bubble detection was the difference in refractive index between air and water/slurry. As the front of an air bubble reached the lower pair of photo-transistors an "on" condition was activated and this was repeated when the bubble reached the upper transistors. "Off" conditions were restored when the rear end of the bubble passed each transistor pair. The output voltages were amplified and converted to a square wave form. Thus two timed signals were produced for each bubble, from which velocity and length pulses could be generated. These signals, together with the real time of the event, were stored in a memory "buffer". The data capture system had 56K of RAM memory which allowed up to 7000 bubbles to be processed in a single sizing run. Bubbles could be detected at a rate of up to 50 bubbles per second, a speed which far exceeds the average of about 20 bubbles measured per second during the testwork.

At the end of the measurement cycle the data was transferred to a micro-computer. Software programmes processed the data and calculated bubble volumes from the velocity and length (period) readings. The thickness of the water films (enveloping the bubbles) formed on the capillary wall was

dependent on the applied vacuum. Consequently these constituted an unknown variable; however, the applied vacuum remained essentially constant for the duration of a bubble detection run. Consequently the bubble volumes determined could be normalised with respect to the total gas volume collected and the bubble size distribution corrected for water content.

Theoretically the period and velocity groups measured during a run should have been the same byte size (if the bubbles were travelling at a constant velocity up the capillary tube); however, when the volume occupied by a bubble was less than the volume between the detectors, period and velocity pulse readings became asynchrous and fewer readings were generated. Discrepancies of 10% or less between the number of velocity and period readings are considered acceptable. Nonetheless small bubbles were better detected using smaller diameter capillaries. Table 2.2 and Figure 2.6 illustrate a typical set of results obtained from the instrument.

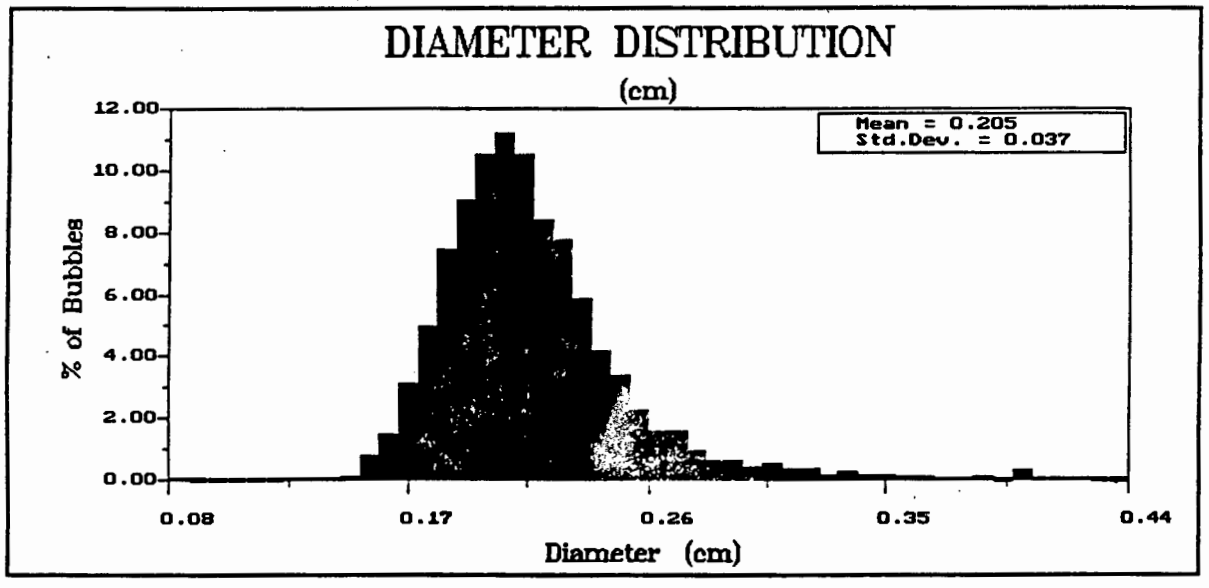

Figure 2.6: Bar Graph illustrating Bubble Size Distribution

SUMMARY OF FILE

Mean bubble volume	0.0050	(ml)
Standard deviation (volume)	0.0035	(ml)
Mean bubble diameter	0.2051	(cm)
Standard deviation (diameter)	0.0367	(cm)
Number of velocity readings	3200	
Number of period readings	3202	
% Discrepancy in readings	0.06	
Average Water Pulse Length	60.9613	
Average Air Pulse Length	6.3719	

Table 2.2: Results Obtained From the Bubble Size Measurement System

1.1.3.3 Residence Time Distribution Study Measurements

The liquid tracer was prepared by dissolving sodium chloride pellets in water. A concentrated solution of 3.4M was required to produce a good response range. 20ml of the tracer was sucked into the plastic syringe which was then placed onto the T-piece ready for injection into the column. The tracer was pulsed into the column by rapidly pushing in the plunger of the syringe and then withdrawing it slightly to ensure that the input pulse did not have a tail. The tailings flow rate was operated manually during tracer experiments as the tracer adversely effected the control system. The flat bed recorder was zeroed before each experiment and the time of tracer input was marked on the recorder. The RTD data obtained from the flat bed recorder was a continuous curve and from this discrete values were read off at 5sec intervals.

Initially tests were performed with the tailings conductivity probe placed immediately after the syringe T-piece and before the feed port. This was done to determine the shape of the input pulse. Following this the probe was placed on the tailings outlet. Both two phase and three phase tests were performed. In each case the method was similar, although in the two phase tests the conductivity probe at the froth lip was not used as the froth did not overflow.

1.1.4 TESTWORK PERFORMED

1.1.4.1 Standard Operating Conditions

Based on previous studies (Goodall, 1989 and Schommarz, 1991) a standard set of operating conditions and reagent dosage rates were chosen. Tests were performed to ensure that similar recoveries and grades as in previous studies were obtained. Table 2.3 lists the standard conditions for this study and will also be referred to as the standard conditions throughout the thesis. In all the tests performed in the preliminary RTD study the feed rate, wash water rate and collector dosage in the three phase tests were kept constant. The frother dosage is quoted in ppm to link up with the two phase tests. 25ppm is a dosage of about 50g/ton at the standard conditions.

Feed Conditions			**Reagent Addition**	
Feed Rate		Solids Density	Collector	Frother
(ml/min)	(cm/s)	(%(m/m))	(g/ton)	(ppm)
1000	0.73	15	50	25
Wash Water Rate			**Gas Rate**	
(ml/min)	(cm/s)		(l/min)	(cm/s)
340	0.25		2.32	1.69

Table 2.3: Standard Operating Conditions

1.1.4.2 Bubble Size Measurements

A series of bubble size measurements were performed to establish a bubble size versus frother concentration curve for two gas flow rates viz. 1.69cm/s and 2.11cm/s using the filter cloth sparger. The tests were performed on a two phase system. Added to the above tests bubble size measurements were also taken for each set of operating conditions used in the preliminary RTD study.

1.1.4.3 Tracer Experiments

Initial tests in the salt tracer study involved determining that the tracer input was a well shaped dirac function, ascertaining whether the salt tracer adversely affected the flotation process and finally reproducibility tests were performed at the standard conditions. The next set of experiments (see Table 2.4) involved tracer inputs for a range of column operating conditions and the two types of air spargers, in both the two phase mode and three phase mode.

Run Number	Feed % Solids	Gas Rate (cm/s)	Frother Conc. (ppm)	Sparger Type
A.1	15	1.69	25	FC
A.2	15	1.69	25	FC
A.3	15	1.69	25	FC
A.4	0	1.69	25	FC
A.5	5	1.69	25	FC
A.6	10	1.69	25	FC
A.3	15	1.69	25	FC
A.7	20	1.69	25	FC
A.8	0	0.00	25	FC
A.4	0	1.69	25	FC
A.9	0	2.11	25	FC
A.10	0	2.74	25	FC
A.11	0	1.69	0	FC
A.12	0	1.69	2	FC
A.13	0	1.69	15	FC
A.14	0	1.69	100	FC
A.15	0	1.69	2	US
A.16	0	1.69	5	US
A.17	0	1.69	10	US

FC = Filter Cloth Sparger
US = USBM-type Sparger

Table 2.4: Operating Conditions for Preliminary RTD Study Tests

1.2 RESIDENCE TIME DISTRIBUTION STUDIES PERFORMED USING RADIOACTIVELY LABELLED TRACERS

The residence time distribution studies performed in this section were performed in two phases. The first study was done on the University of Cape Town (UCT) portable pilot column rig at the Atomic Energy Corporation (AEC) in Pelindaba, Pretoria and the second on an industrial scale rougher column located on the President Steyn pyrite flotation plant in the Orange Free State. A variety of isotopically labelled tracers were used to trace liquid and hydrophobic and hydrophilic solids in both studies. The testwork followed on from the preliminary RTD study and focussed specifically on the difference between the tailings RTD of solid and liquid tracers.

1.2.1 EQUIPMENT

The equipment used in the testwork using radioactively labelled tracers comprised of the UCT pilot column cell and ancillary equipment, the President Steyn rougher column with an added pulse injection mechanism and the geiger counters, lead shields and data logging system belonging to the Atomic Energy Corporation.

1.2.1.1 Pilot Column Cell

The pilot column had been successfully used in a previous project (Schommarz (1991)). The column design and dimensions were similar to the laboratory column (see figure 2.7). The pilot column was made up of 58mm i.d. PVC sections which were joined together using screw flange fittings and only the feed and froth overflow sections were transparent. The base of the column differed from the laboratory column in that the tailings port was on the side of the column with an internal angled plate to facilitate flow to the port. This was done to enable the column to stand on its flat base. The launder, wash water distributor and rinse sprinkler setup was identical to the laboratory column. A filter cloth sparger of the same design as used in the preliminary work was used in this study.

The feed port was located 50cm from the froth lip, froth depth was 42cm, collection zone length was 190cm and the total column length was 245cm.

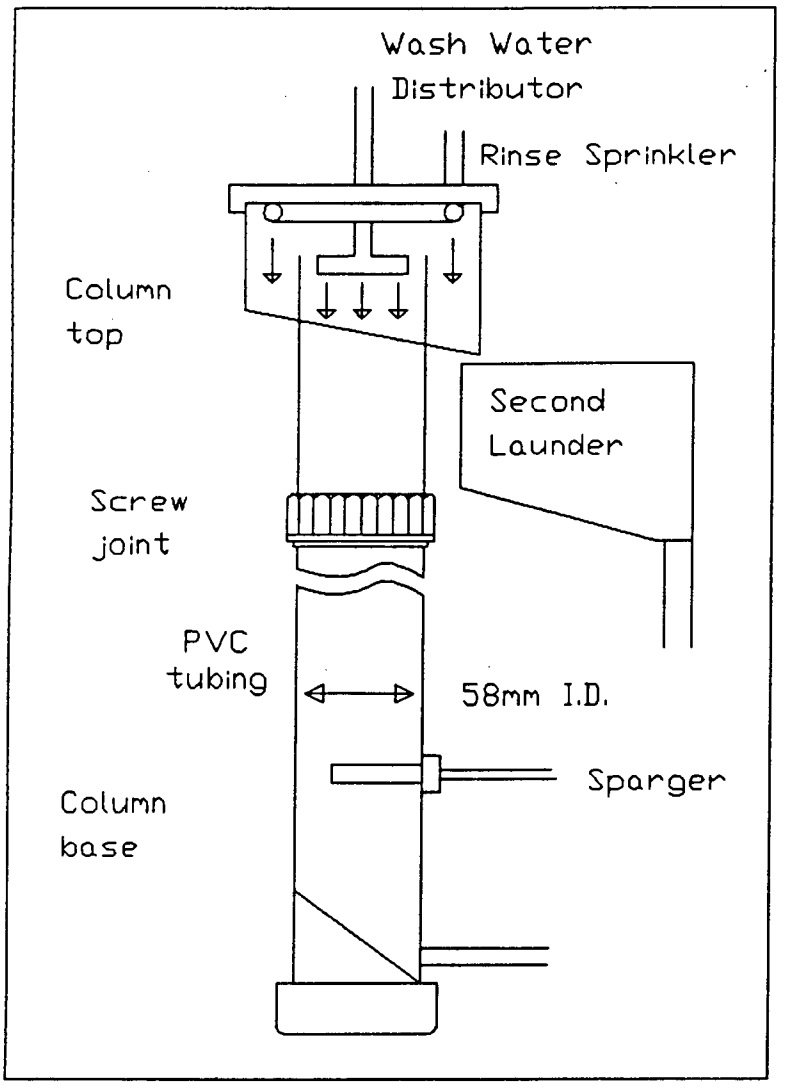

Figure 2.7: Schematic of Pilot Column

The ancillary equipment of the pilot column rig is shown in Figure 2.8, a schematic of the entire rig. The air supply system, controller, pumps and conditioning tank were all the similar to the equipment used in the laboratory column rig. A holdup tank was not used due to transportation limitations and ore was both dispersed and conditioned in the conditioning tank.

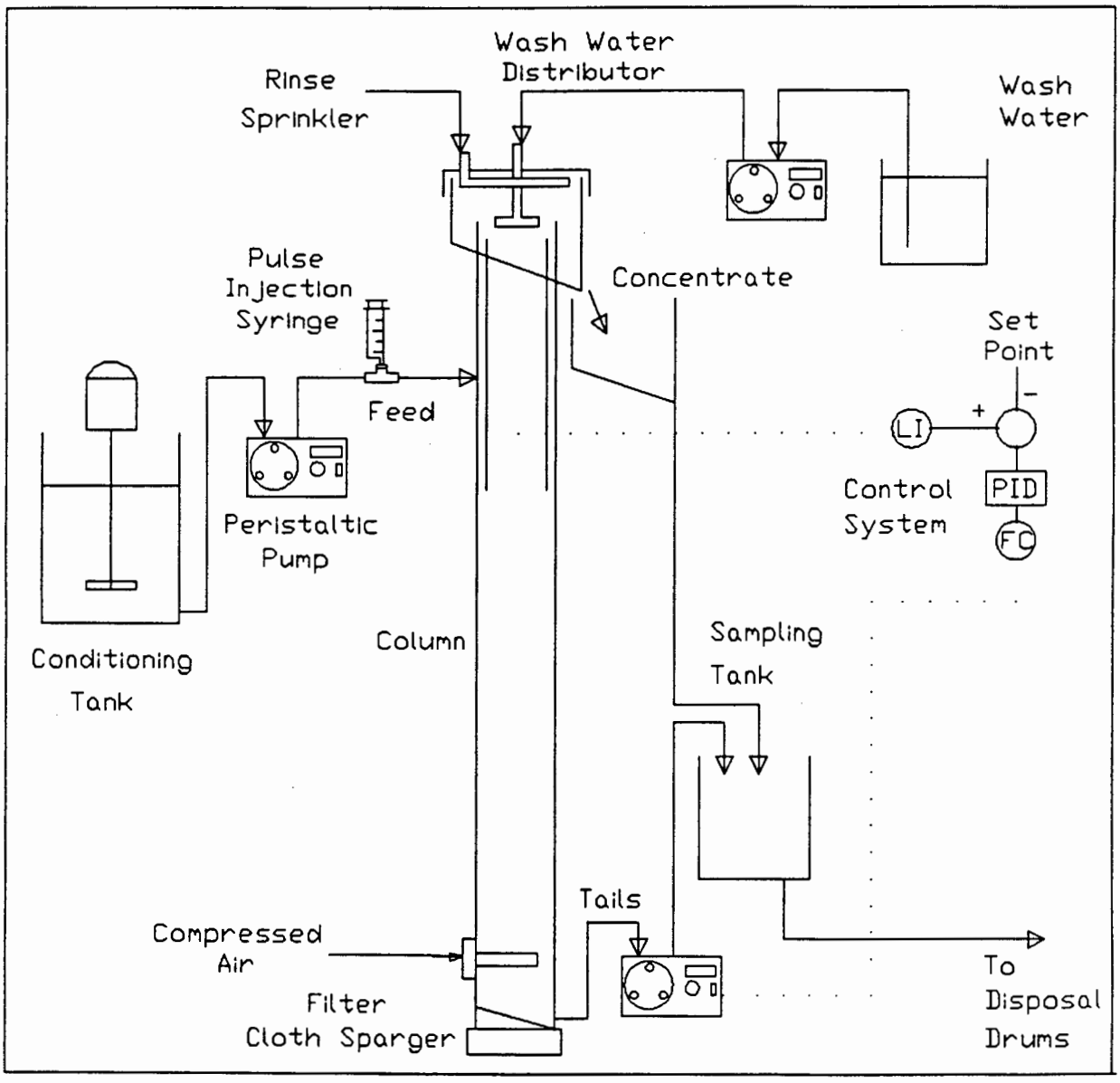

Figure 2.8: Schematic of Pilot Column Rig

1.2.1.2 President Steyn Rougher Column

The column design was similar to that of other industrial scale columns. Figure 2.9 shows the basic layout of the 1.2m i.d. column. The slurry feed was located 1.2m from the top of the column. The column operated with a froth depth of 70-75cm, a collection zone length of about 10.9m and total column length (cone tip to froth lip) of 11.9m. The concentric launder was positioned at about 30° to the horizontal to facilitate froth flow. The wash water distributor was a set of four concentric rings, with evenly

spaced 3mm holes, attached to a cross of copper tubing. The distributor was positioned 10cm below the froth lip. Figure 2.10 illustrates the froth lip and concentrate launder. The piping leading to the wash distributor in the froth is also shown.

Figure 2.10: President Steyn Column Concentrate Launder

The column was located at the head of one of the flotation plant's three rougher banks. Feed to the column was gravity fed and the flowrate was adjusted manually by means of a Saunders valve. A densitometer and

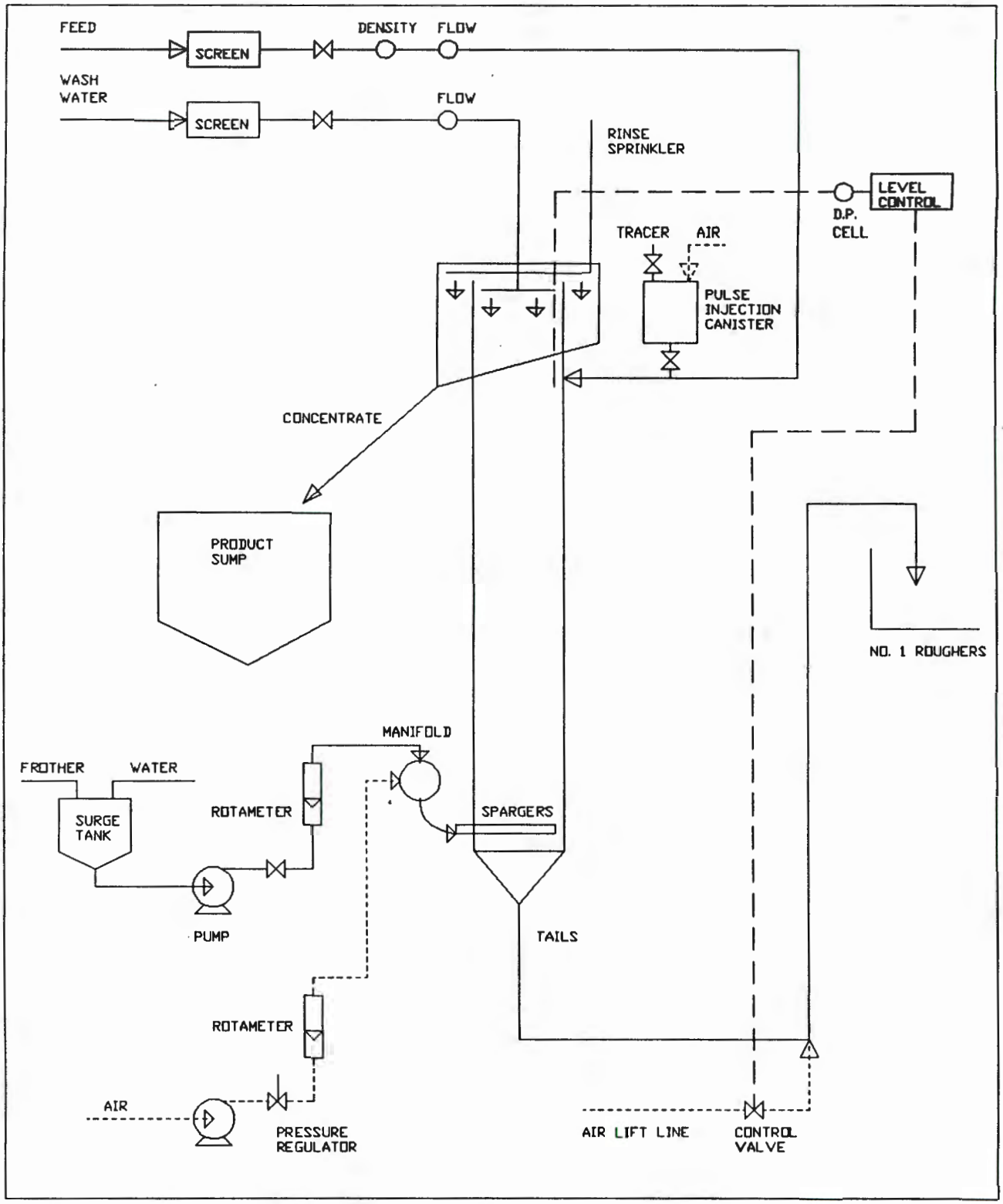

Figure 2.9: Layout of the President Steyn Rougher Column

flowmeter were attached to the feed line and values from these meters were continuously recorded. The wash water flow rate was adjusted and measured using a valve and flowmeter. A frother dosage pump delivered accurate frother dosages to the wash water. Level control was achieved using a bubble tube connected to a differential pressure cell. The cell controlled an automatic valve which varied the air flow into the airlift responsible for removing the tailings from the column. The product from the column overflowed into a weir and then flowed directly to the product sump. The column tailings were airlifted to the rougher bank and received the same treatment as the rest of the plant feed.

Air Spargers

A Cominco external air sparging system was used to aerate the column. The sparger system consisted of five thick walled stainless steel tubes with air injection holes wear-protected by tungsten carbide inserts. Air and water were premixed in a manifold at a pressure of about 450kPa. This mixture flowed through flexible hoses into the sparger tubes and was injected into the column at supersonic velocities. A sudden decrease in velocity as the mixture enters the column causes shocks that create small bubbles. The nozzles on the spargers faced downward. Figure 2.11 illustrates the sparger manifold and inlet tubes inserted into the column.

Air to the spargers was supplied by an instrument air compressor which was capable of delivering a pressure of 700kPa. The water pump delivered water to the manifold at a steady pressure of up to 470kPa. A pressure regulator on the air line was used to control the air flow to the spargers and water flow was controlled by a valve. Rotameters measured air and water rates to the spargers.

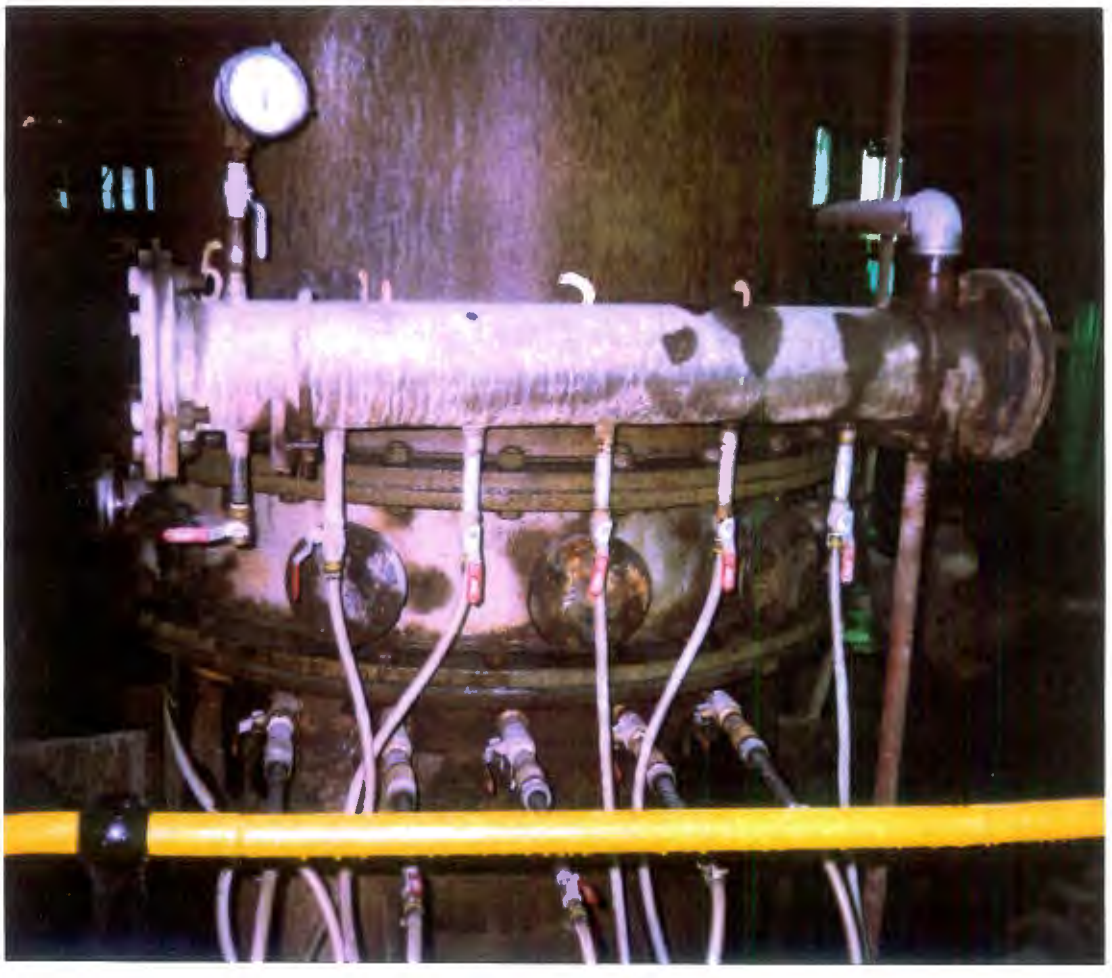

Figure 2.11: Cominco Sparger Manifold and Inlet Tubes on the President Steyn Column

Modifications to the Industrial Column for the RTD Study

For the RTD study two modifications were made to the column. Firstly a concentric rinse sprinkler was placed in concentrate launder to ensure that material recovered exited directly to the concentrate pipe. Secondly a 30l pressure cylinder was used to inject tracer into the column and this was attached to the column feed pipe about 1m before the feed port. Figure 2.12 is a photograph of the pulse injection cylinder, which had 5cm ball valves on either side and a fitting for a compressed air line and a pressure gauge on the top. The cylinder was built to withstand pressures of up to 700kPa.

Figure 2.12: Pulse Injection Cylinder attached to the Feed Pipe

1.2.1.3 Residence Time Distribution Measuring Equipment

The equipment supplied by the Atomic Energy Corporation was set up and operated by AEC personnel. Handling of the tracers was also strictly performed only by AEC personnel. Safety levels were continuously monitored to ensure that radioactive exposure was not excessive. The detection system consisted of 5 activity level detectors which were all connected to a central unit. Readings were fed from the central unit to a linked computer. A computer package written in TurboPascal set time increments between each reading and gave a continuous read out of the tracer response for each detector. After each run the data was stored on floppy disk for

later analysis. For the pilot column work the tests were performed in a laboratory and the data logging equipment was located next to the rig. In the industrial column the equipment was located in a caravan outside the flotation plant.

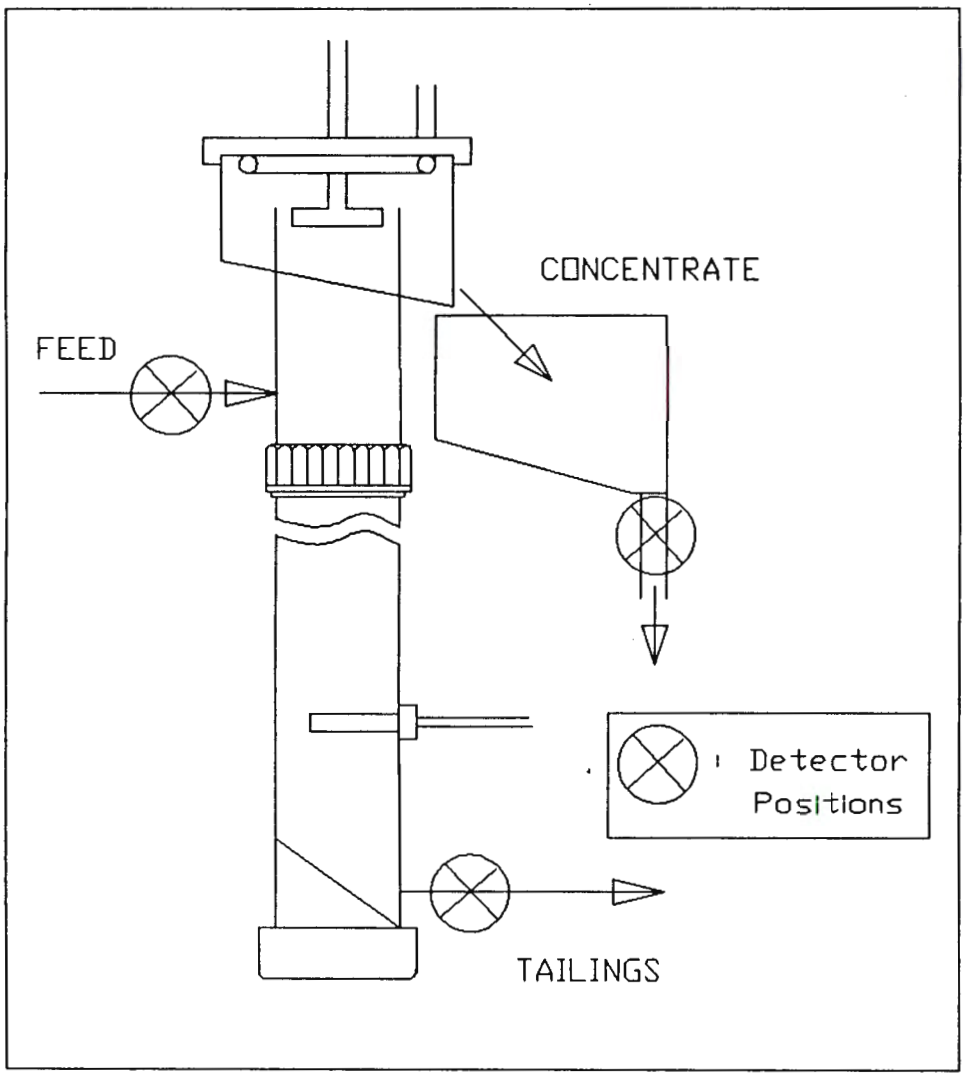

Figure 2.13: Activity Detector positioning on the Pilot Column Rig

Figures 2.13 and 2.14 illustrate the positioning of the detectors used in each of the studies. Figure 2.15 illustrates the detector positioned at the concentrate outlet of the pilot column. An essential part of the testwork was to ensure that each detector only detected activity from the required section of the column. This was done by strategically positioning lead shields around each detector. Due to the scale of the equipment this was made more difficult in the pilot column tests. A structure was built

around the column to hold up the 40mm wide lead shields which covered each of the detectors as well as the tracer injection point.

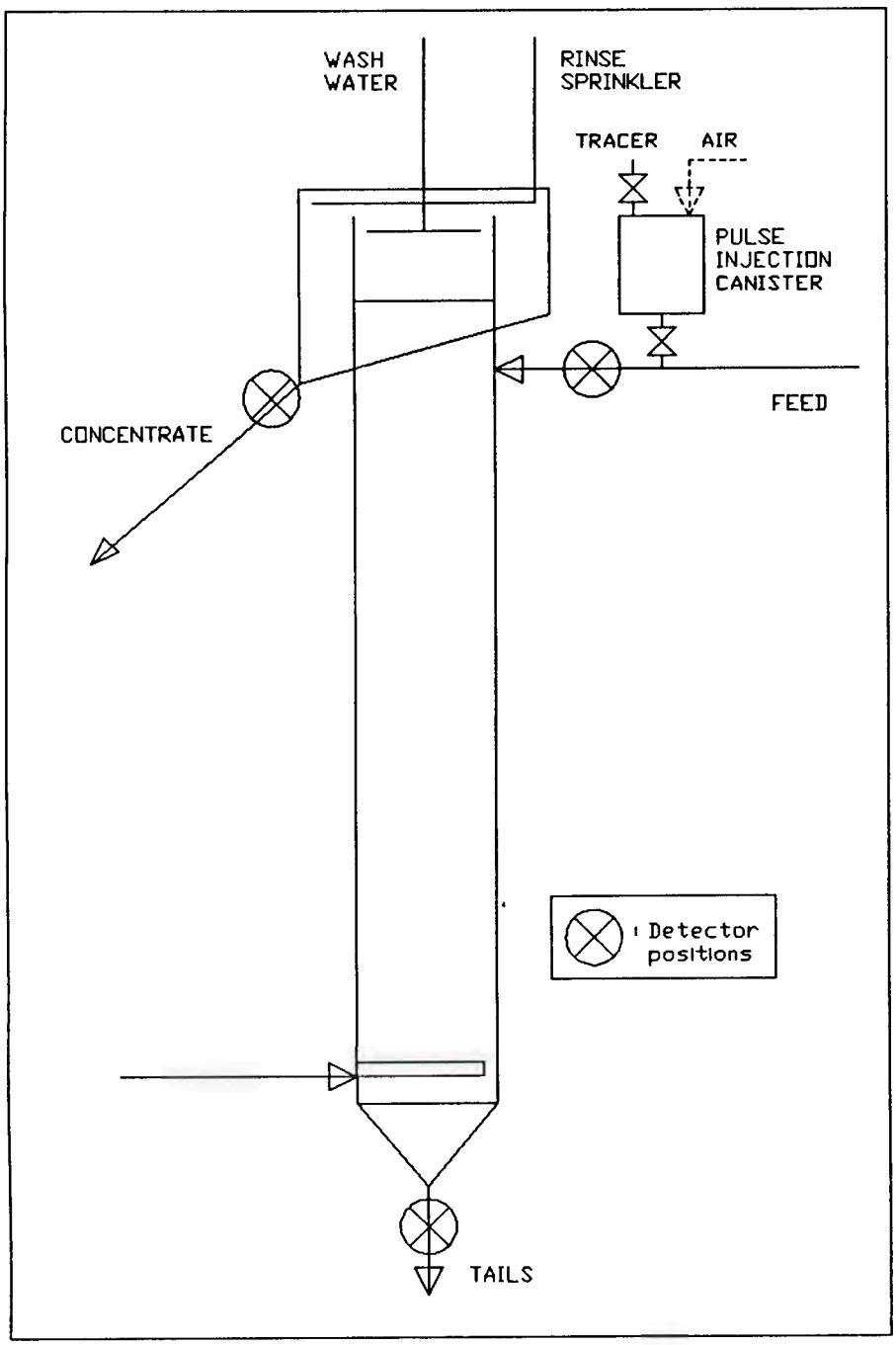

Figure 2.14: Activity Detector positioning on the Industrial Column

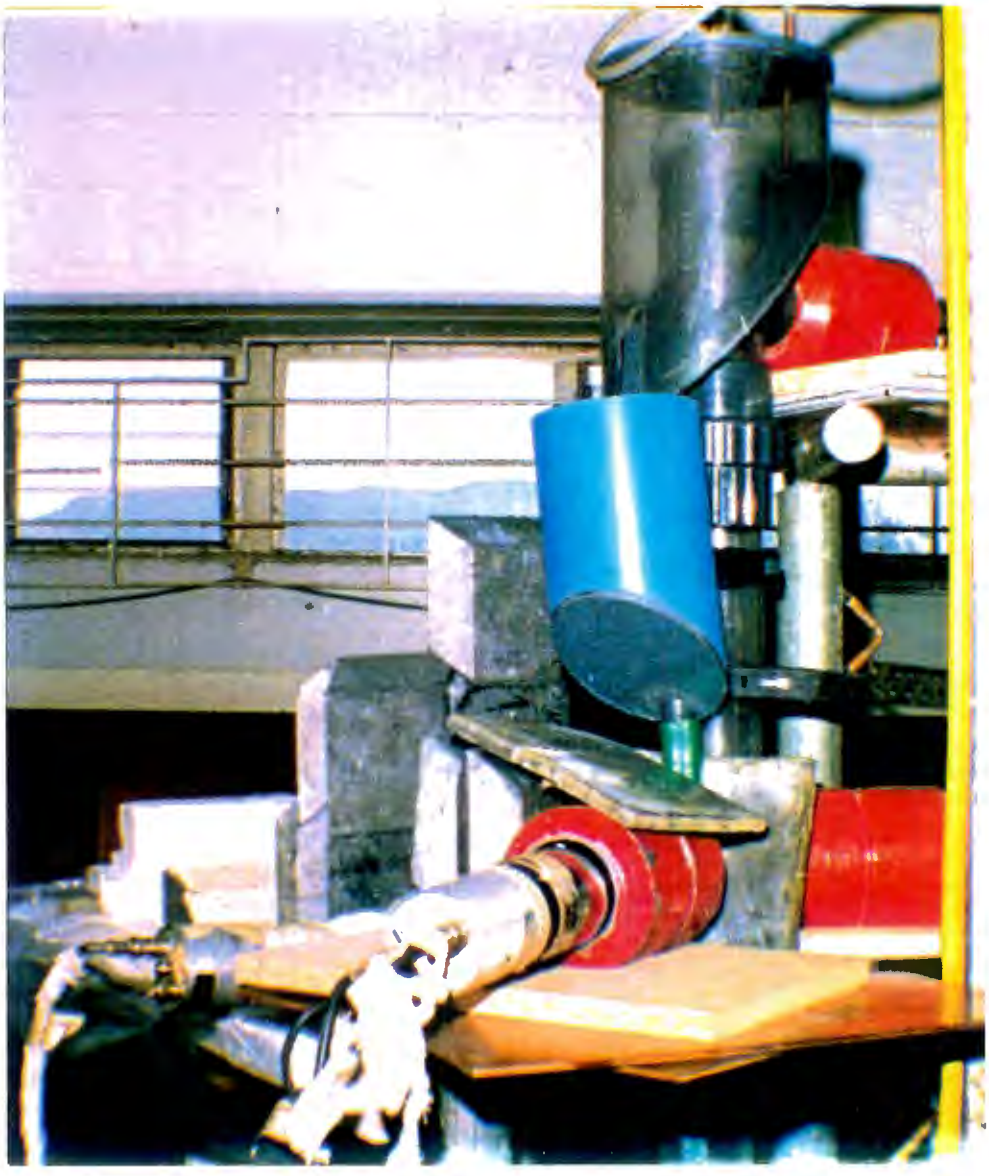

Figure 2.15: Detector positioning at the Concentrate Outlet of the Pilot Column

1.2.2 ORES, REAGENT SUITES AND OPERATING CONDITIONS

The RTD study performed on the pilot column involved the use of the same ore and reagents and similar reagent dosages as in the preliminary RTD study. The operating conditions used throughout the testwork were the standard operating conditions except that the gas flow rate was set at 2.24cm/s. The industrial column was used as a rougher in a flotation circuit which also processed an untreated ore from a tailings dam. The ore

contained on average about 1.3% sulphur and 0.6g/ton gold. Table 2.5 illustrates the particle size and sulphur distribution of the ore. The column operation involved the use of the same reagents as in the preliminary study viz. SMBT and DOW200. The column was operating at about 60% sulphur recovery and 30% gold recovery. The operating conditions of the column during the testwork are listed in Table 2.6.

Size Fraction	Percent	% Sulphur
-38μm	48.9	2.03
+38-53μm	15.7	1.21
+53-75μm	18.2	0.72
+75-106μm	9.5	0.13
+106μm	7.7	0.07
TOTAL	100.0	1.33

Table 2.5: Particle Size and Sulphur Distribution of Ore Treated in the President Steyn Rougher Column

Operating Parameter	Value
Feed Rate	1.18cm/s
Tailings Rate	1.30cm/s
Wash Water Rate	0.17cm/s
Gas Flow Rate	2.20cm/s
Pulp Density	35.1%
Bubble Size	1.5-2.0mm

Table 2.6: Operating Conditions of the President Steyn Rougher Column

1.2.3 TRACER SELECTION

Following the preliminary RTD study where sodium chloride was used to trace the liquid appropriate tracers were selected to trace both the

liquid and solids. RTD studies of flotation columns have involved the use of both solid and liquid tracers to investigate solid and liquid mixing. A range of different types of tracers and detection techniques have been used in various studies.

Lithium chloride, potassium chloride, sodium chloride, flourescein and radioactively labelled water solutions have been used to trace the liquid mixing. The use of flourescein was found to be problematic as it adsorbs onto the mineral (20%) and is light sensitive (Dobby and Finch, 1985). Yianatos et al. (1987) and Espinosa-Gomez et al. (1989) detail work using a lithium chloride tracer and atomic absorption analysis. All the above work was performed on industrial scale columns. Tracer injection time was significant (15-60sec) and it was necessary to take off-line measurements from tailings samples. Testwork performed by Mavros et al. (1989) details work using potassium chloride as tracer and an on-line conductivity meter. This provided continuous measurement of the tracer distribution and tracer injection time (<1sec) was insignificant. The work was performed on a laboratory scale column. Yianatos and Bergh (1990) detail the use of a radioactively labelled water solution (potassium bromide solution (Br^{82})) as tracer on an industrial column. Both on-line and off-line measurements were performed. Tracer injection time was insignificant due to the small amount of tracer required. A radioactively labelled water solution provides the most accurate result for both laboratory and industrial scale columns. The liquid tracer injected into the pilot and industrial columns in the present study was an isotopically labelled ammonium bromide (Br^{82}) solution. In the pilot column 5ml of liquid was used and in the industrial column 5l were injected.

Solid tracer selection is more complex since ideally a tracer is required which behaves identically to the particles in the column. Dobby and Finch (1985) performed solid tracer studies using a hydrophilic manganese dioxide tracer in a molybdenite system. Tracer concentrations were analysed off-line using atomic absorption of manganese. The reason for the selection of manganese dioxide was the small background of Mn in the tailings (10%) and it had similar density and floatability characteristics as the gangue material. Vasquez et al. (1988) and Goodall and O'Connor (1991) performed tests on laboratory columns using radioactively labelled solid tracers. However the former used non-floatable (tailings) material

as tracer and the latter used material (feed) containing both non-floatable and floatable material. Yianatos and Bergh (1990) performed a study on an industrial scale column using isotopically labelled tailings material. The tracer activity was detected from the Na^{24} isotope in preliminary on-line tests and from the Sc^{46} isotope when the samples were measured off-line. The most accurate results were obtained using radioactively labelled material which was identical to the particles in the pulp phase. Tracer input time was also negligible as only a small amount of tracer was required.

The solid tracers injected into the pilot and industrial column in the present study were isotopically labelled and Table 2.7 lists the isotopic composition and mass of different tracers used. Two types of solid tracer were used; a feed tracer which was identical to the feed material being fed to each column and a gangue tracer which was prepared by removing the floatable material from feed samples by flotation for an extended period of time. In each study the tracers were obtained from feed material for the specific column operation. The samples were prepared by being placed next to a high energy radioactive source for a length of time. This time span was longer for the industrial column tracers as the tests were only performed three days after the tracers were removed from the source and the activity of the tracers dropped rapidly due to their short half lives. For this reason scandium, iron, cobalt were also activated in the industrial column tracers, whereas for the tracers used in the pilot column sodium, which has a very short half-life, was a major source of activity.

	Percent in Ore Tracer Samples ($x10^4$)			
	Pilot Column		**Industrial Column**	
	Gangue	Feed	Gangue	Feed
Sc^{46}	-	-	7.8	4.0
Fe^{59}	-	-	-	34.8
Co^{60}	-	-	-	11.7
As^{76}	-	-	86.3	86.3
La^{140}	-	-	27.2	27.2
Au^{198}	0.3	7.5	-	0.5
Na^{24}	33.5	68.0	-	-
MASS	7g	7g	200g	200g

Table 2.7: Isotopic Composition and Mass of tracers injected into the Pilot and Industrial Columns

1.2.4 EXPERIMENTAL METHODS

1.2.4.1 Pilot Column Operation and Sampling

The ore to be used in this testwork was weighed and packed wet in plastic bags. As there was no holdup tank for each run a bag of ore was mixed with water in the conditioning tank, reagents required for the run were added to the tank and conditioned for 10min. Following this the run was begun and the same operating procedure was used as in the preliminary RTD study. Concentrate and tailings were sampled to ensure that similar recovery and grade results as in the preliminary RTD study were being obtained.

1.2.4.2 RTD Measurements On The Pilot Column

The tracer injection method used in the pilot column was the same as the method used in the preliminary RTD study. Figure 2.16 illustrates the tracer injection syringe positioned on the feed line to the pilot column. Preparation of the tracers differed for the gangue and feed tracers. The feed tracer was mixed with water in the syringe to make up a 50% solids

slurry. To this mixture collector at the same dosage as in the feed was added. The syringe was then shaken for about 5min to condition the ore. The gangue tracer was mixed with water in the syringe to make up a 50% solids mixture. Following the tracer preparation the syringe was shaken vigorously, attached to the T-piece on the feed line and injected. Data capture began and was continued until all the detector levels returned to base levels. All the detectors took readings at 1sec intervals, except the detector monitoring the pulse input which took readings at 0.2sec intervals. After each run the column was flushed thoroughly to ensure that all tracer material that may have attached to the column walls was washed out.

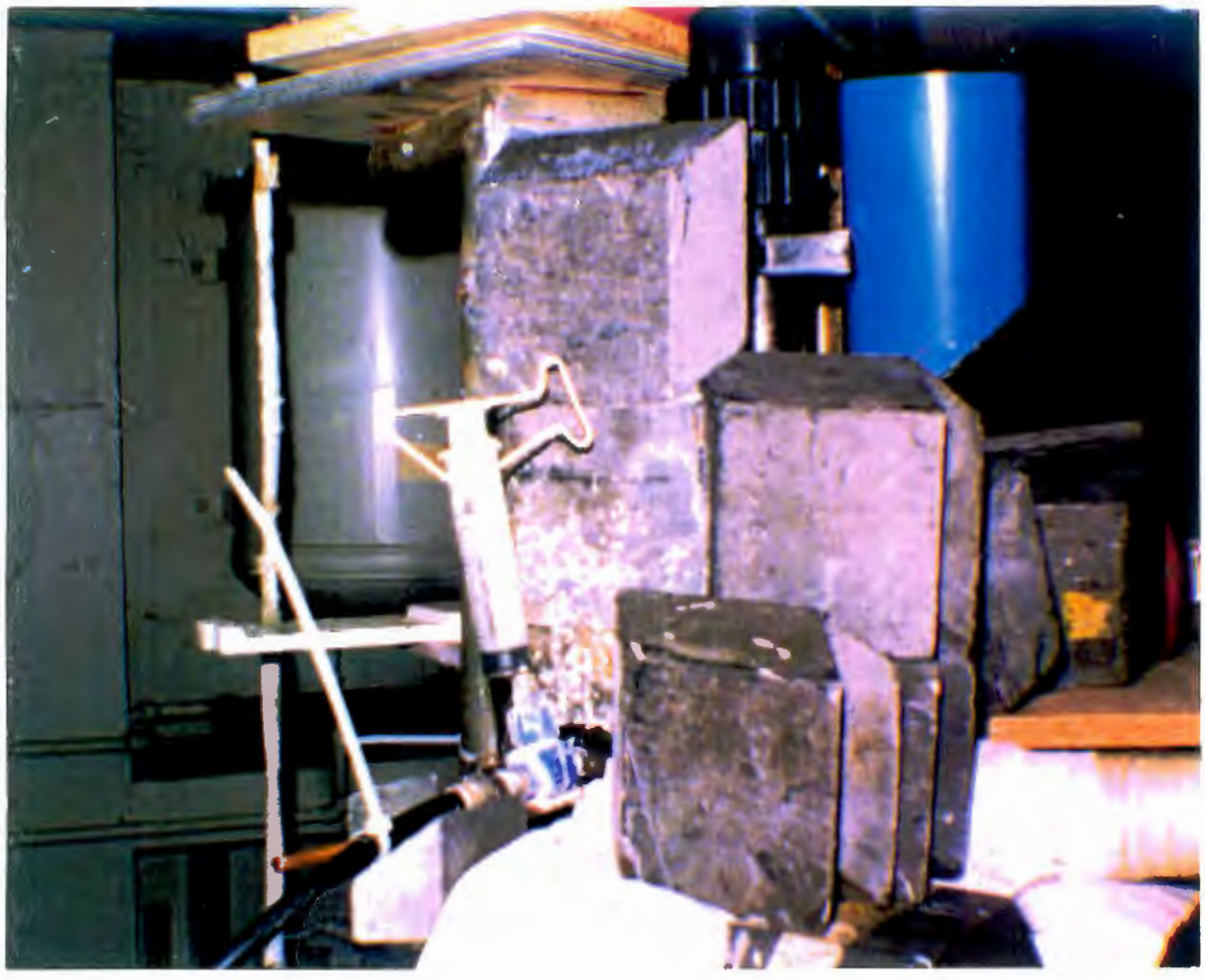

Figure 2.16: Tracer Injection Syringe on the Feed Line of the Pilot Column

1.2.4.3 RTD Measurements On The Industrial Column

Tracer preparation of the feed and gangue tracers was similar to the method used in the pilot column work. The tracer mixtures were prepared in beakers. The lower ball valve of the injection canister was shut and the upper ball valve opened and a funnel inserted. For the solid tracers the mixture was poured into the canister. Above this about 10l of water was added to ensure that the tracer was washed into the column. For the liquid tracer the sample was about 5l of solution. Once the tracer was in the canister the top ball valve was shut, the compressed air hose was attached and the canister was pressurised to about 300kPa. Recording of activity was begun and after exactly 3min the lower ball valve was opened, the tracer entered the column and the valve was again shut. It was possible to ascertain when all the tracer entered the column by monitoring the pressure gauge on the canister. Tracer injection time was about 2 to 3sec.

1.2.5 TESTWORK PERFORMED

1.2.5.1 Pilot Column RTD Study

The tests listed in Table 2.8 were performed on the pilot column cell.

Run Number	Tracer Sample
B.1	Liquid
B.2	Feed Material
B.3	Gangue Material
B.4	-38μm Gangue
B.5	+38-75μm Gangue
B.6	+75-106μm Gangue
B.7	+106-150μm Gangue

Table 2.8: RTD Testwork performed on the Pilot Column Rig

1.2.5.2 Industrial Column RTD Study

Two Reproducibility tests were performed using the gangue tracer. The tests performed are listed in Table 2.9.

Run Number	Tracer Sample
C.1	Gangue Material
C.2	Gangue Material
C.3	Liquid
C.4	Feed Material
C.2	Gangue Material
C.5	-38μm Gangue
C.6	+38-75μm Gangue
C.7	+75-106μm Gangue
C.8	+106-150μm Gangue

Table 2.9: RTD Testwork performed on the Industrial Column

1.3 RESIDENCE TIME DISTRIBUTION DATA ANALYSIS

Added to the RTD results obtained from the salt tracer and radioactive tracer testwork, the RTD data obtained by Yianatos and Bergh (1990) was also analysed. This study was performed on a zinc cleaner column located in Disputada, Chile. The operating conditions of the column are listed in Table 2.10. A radioactively labelled liquid tracer as well as a similarly labelled tailings (gangue) sample were injected into the column. After tracer injection the tailings were sampled at discrete time intervals. The activity of these samples was measured and at a later stage the samples were classified into three size classes viz. -38μm, +38-75μm and +75-150μm The activity of each size class was measured to obtain separate age distribution curves. Further detail of the experimental method is listed in Yianatos and Bergh (1990). The data obtained from the above study served to establish whether the results obtained in the present study were dependent on either the operating conditions and/or the tracers used.

Operating Parameter	Value
Tailings Rate	0.92cm/s
Gas Flow Rate	1.80cm/s
Pulp Density	16.2%
Bubble Size	1.5-2.0mm

Table 2.10: Column Operating Conditions during the RTD study of Yianatos and Bergh (1990)

For each of the RTD studies performed concentration vs. time curves were obtained. This data consisted of concentration values recorded at equally spaced time intervals. For each set of data the following was performed on a QuattroPro spreadsheet:

1. The background conductivity or radioactivity levels were subtracted from the concentration values.

2. The values were divided by the area under the curve to obtain the exit age distribution curve or E(t) curve.

3. The mean residence time and variance were determined using equations (1.21) and (1.22) respectively.

4. Using the mean residence time the dimensionless concentration vs. time or $E(\theta)$ vs. θ curve was obtained, where $\theta=t/\tau$ and $E(\theta)=\tau E(t)$.

Following this both the tanks-in-series and the axial dispersion models were fitted to each set of data.

1.3.1 FITTING THE AXIAL DISPERSION MODEL TO THE RTD DATA

For all the RTD studies performed in this thesis tracer input and detector positions represented closed-closed boundary conditions. In the study by Yianatos and Bergh (1990) the tracer injection point was inside the column at the feed entrance. The tracer detection point represented a closed condition. Due to the position of the tracer injection point it was not

completely clear which boundary conditions applied, however the shape of the age distribution curves confirmed that closed-closed conditions were applicable. The vessel dispersion number was determined using two methods viz. the method of moments and a numerical solution of the axial dispersion model in conjunction with a least squares fit. The former method involved the use of Equation (1.27) to determine D/uL by matching experimental and model variances. The latter method involved the use of a finite difference method laid out by Xu et al. (1991) to numerically solve Equation (1.23). This method was programmed on a QuattroPro spreadsheet. Figure 2.17 illustrates the results of the program for a range of vessel dispersion numbers.

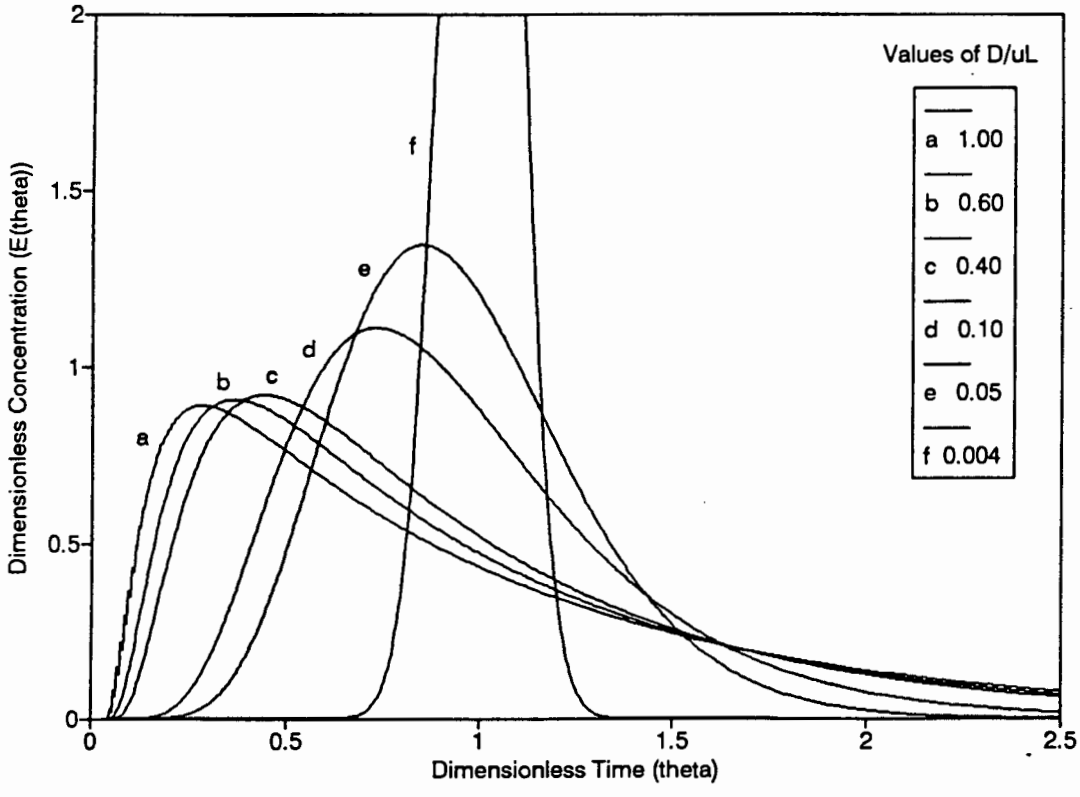

Figure 2.17: Normalised Closed-Closed Response Curves of the Dispersion Model for a Range of Vessel Dispersion Numbers

The dispersion coefficient was obtained by multiplying the experimentally determined vessel dispersion number, D/uL, by one of the following depending on whether the tracer was solid or liquid. In the case of a liquid tracer, by the interstitial liquid velocity, u_l, where $u_l=j_l/(1-\epsilon_g)$ and the collection zone length, L. In the case of a solid tracer, by the interstitial solid velocity which was determined from the relationship,

$$\frac{u_p}{u_1} = \frac{\tau_p}{\tau_1} \qquad (2.1)$$

where τ_p and τ_1 were obtained from the RTD data, and the effective collection zone length, L.

Vessel dispersion coefficients and vessel dispersion numbers were also estimated from existing prediction correlations. The method used to calculate these values was the same as that detailed in the scale-up procedure in Chapter 1 Sec. 4.

1.3.2 FITTING THE TANKS-IN-SERIES MODEL TO THE RTD DATA

The tanks-in-series model was fitted to the RTD data using Equation (1.30) and a least squares fit. Figure 2.18 illustrates the tanks-in-series response curves for a range of values of N.

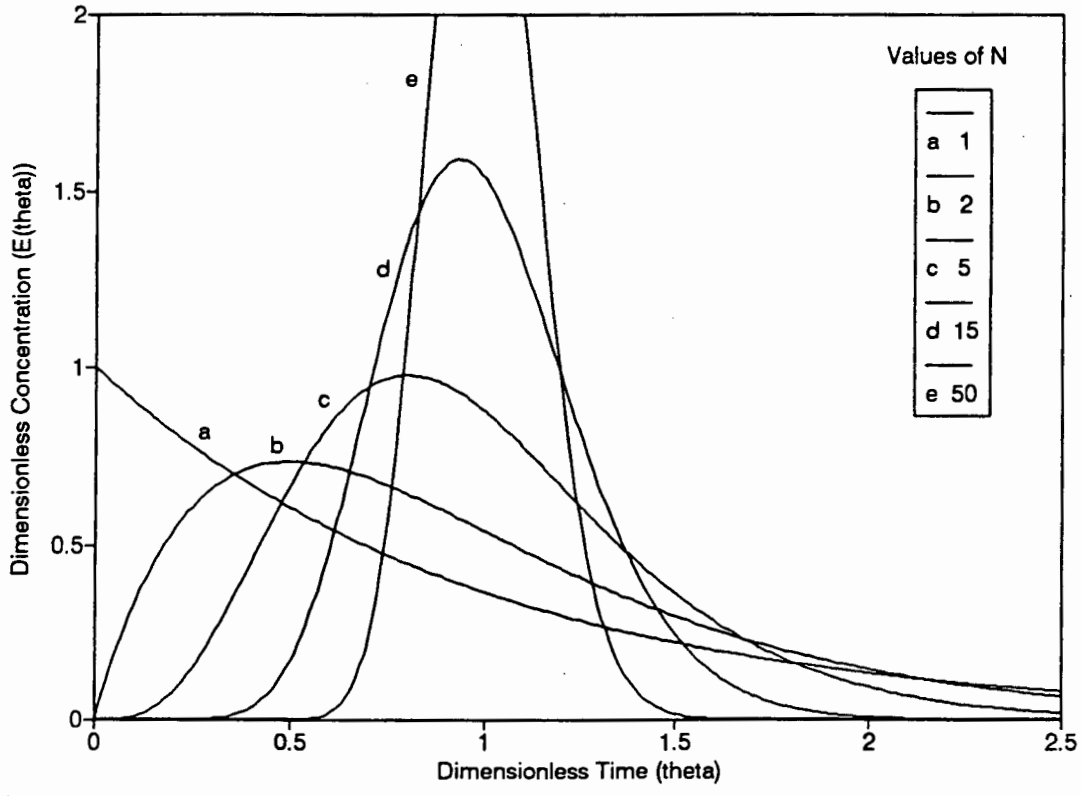

Figure 2.18: Normalised Response Curves of the Tanks-In-Series Model for a Range of Values of N

2. STUDY OF THE KINETICS OF THE COLLECTION ZONE

The study of the collection zone kinetics involved developing a method to determine the collection zone rate constant. This method was used to determine the collection zone rate constant by varying both column length and feed rate. Three sets of tests were then performed in which labelled hydrophobic tracers viz. chalcopyrite in a pyrite system and radioactively labelled pyrite were injected into the feed streams of two pilot columns and an industrial column. The results of these tests were used to evaluate the flotation kinetics of the collection zone as well as the particle collection model presented in Chapter 1 Sec. 3.2.

2.1 DEVELOPMENT OF A METHOD TO DETERMINE THE COLLECTION ZONE RATE CONSTANT

After reviewing the different methods used to determine the collection zone rate constant by a number of workers (Contini et al. (1988), Dobby and Finch (1986) and Mular and Musara (1991)) a novel method was developed to determine k_c. The goal in developing a new method was to try to fulfill the following two criteria; the method developed should determine k_c while the collection zone is operating in the countercurrent mode and at typical operating conditions and the column structure should not need to be modified.

In developing a method to determine k_c with the column operating in the countercurrent mode two criteria must be met. Firstly the cleaning zone recovery should be close to 100% i.e. $k_c \approx k_{fc}$ and secondly entrainment of gangue to the concentrate should be eliminated. In the study by Dobby and Finch (1986) the criteria were met by moving the wash water addition point downward to a point halfway between the column top and the feed entrance to eliminate drop back and by operating at a very high bias to reduce short circuiting of feed to the concentrate. The laboratory column configuration used to determine k_c in this thesis involved the following;

1. The interface was raised from about 5cm above the feed inlet to at least 50cm above the feed inlet.

2. The froth height was reduced from about 55cm to 10-15cm.

Figure 2.19 illustrates the difference between the normal column configuration and the setup used to determine k_c. Apart from the above changes the column was operated at typical operating conditions. It was not necessary to operate the column at a high bias rate as it was assumed that the zone between the feed port and the interface eliminated short circuiting of feed to the concentrate. Work by Yianatos et al. (1987) has shown that entrainment is essentially eliminated within the first 15cm of the cleaning zone. The shallow packed bubble bed served to eliminate entrainment and keep drop back and recycle of material in the froth zone at a minimum.

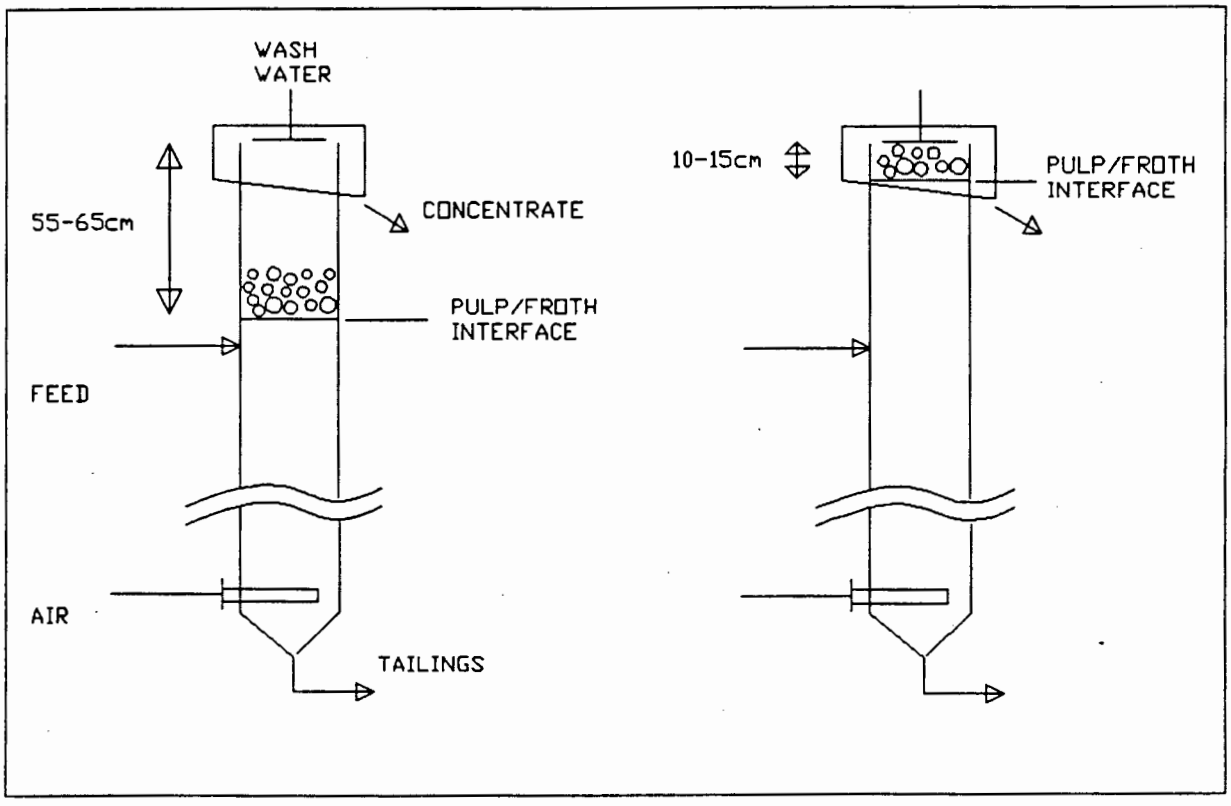

Figure 2.19: Illustration Normal Column Configuration and Column Configuration used to determine the Flotation Rate

In the testwork that follows k_c was determined using the above column operation but two different approaches. The first involved operating the column at various column lengths and feed rates in order to obtain the cumulative recovery vs. time curves. From these curves k_c could be

determined. The second method involved injecting a pulse of hydrophobic material into the feed stream of the column which was operating at steady state. The cumulative recovery vs. time curve was obtained from the tracer exiting in the concentrate.

2.2 DETERMINATION OF THE COLLECTION ZONE RATE CONSTANT BY VARYING THE COLUMN LENGTH AND FEED RATE

This section of the kinetics study was performed in order to evaluate the method developed to determine the collection rate constant. Following this the effect of gas rate on k_c was investigated using the above method.

2.2.1 EQUIPMENT

The testwork was performed on the laboratory column rig as described in Chapter 2 Sec. 1.1.1. The only difference between the two column configurations was that the collection zone length was varied by either adding or removing the 600mm long flanged sections and a specifically made 25mm long section.

2.2.2 ORE AND REAGENT SUITE

The ore and reagent suite used in this testwork was the same as the ore used in the residence time distribution studies performed on the laboratory and pilot column.

2.2.3 EXPERIMENTAL METHOD

Column operation was similar to the method used in the preliminary RTD column study. However the column was operated with the interface level positioned 10cm below the column lip. The distance between the feed port and the interface therefore increased from 5cm to 60cm. In order to obtain the collection zone recovery over a range of mean residence times the column was operated at 5 different collection zone lengths viz. 75, 100,

125, 150 and 235cm. At each collection zone length two feed rates were used viz. 1.0 l/min and 1.3 l/min.

Once column had reached steady state for the lower feed rate the following readings and samples were taken;

1. Three concentrate samples were taken over separate 5min periods.
2. Three tailings samples were taken over separate 30sec periods.
3. Gas holdup measurements were taken.

After these measurements were made the feed rate was increased to 1.3 l/min the column run for 15min in order to return it to steady state and the above samples and readings were repeated. The feed, concentrate and tailings samples were analysed in the same way as in the preliminary RTD study to obtain the sulphur grades and recoveries.

2.2.4 TESTWORK PERFORMED

Testwork performed in this section firstly involved determining the collection zone rate constant at the standard operating conditions. In doing so the method was evaluated by comparing the recoveries and grades with the results obtained for a 65cm froth in the preliminary RTD study. From this an indication of the degree of entrainment was established. Further tests were then performed to determine k_c over a range of air rates viz. 0.81, 1.69 and 2.53cm/s.

2.3 DETERMINATION OF THE COLLECTION ZONE RATE CONSTANT USING CHALCOPYRITE AND RADIOACTIVELY PYRITE TRACERS

This study involved determining the collection zone rate constant by injecting a pulse of either pure chalcopyrite or radioactively labelled pure pyrite into the feed stream of a column and monitoring the recovery of the tracer in the concentrate. Using this method an accurate measure of the flotation rate in the collection zone could be determined. Furthermore the effect of the various operating parameters on the flotation rate could be ascertained.

2.3.1 EQUIPMENT

The study using chalcopyrite as a tracer was performed on the laboratory column. The laboratory column rig was setup as in the preliminary RTD study, but with the column length increased to 3.0m. The T-piece used in the preliminary RTD study was again used to inject the chalcopyrite tracer into the column. 20ml syringes were used to inject the tracer into the column. The concentrate samples were analysed for copper using an acid digest and atomic absorption spectroscopy.

Two studies were performed using radioactively labelled pyrite tracers. The first was carried out at the Atomic Energy Corporation at the same time as the RTD study was performed on the pilot column rig. The column length was the same in the RTD study. The second study was performed on the President Steyn industrial column. The tracer injection device as used in the RTD study was used to inject the tracers into the column. The equipment used to monitor the flow of pyrite in and out of the columns was the same as described in Chapter 2 Sec. 1.2.1.3. The positioning of the detectors on the columns was the same as in the pilot and industrial column RTD studies (see Figures 2.13 and 2.14).

2.3.2 ORES AND REAGENT SUITES

In studies performed on the laboratory and pilot column the same ore and reagents and similar reagent dosages were used as in the equivalent RTD studies. An analysis of a feed sample of the standard ore indicated that there was a negligible amount of copper in the standard ore. The ore and reagent suite used in the industrial column were the same as in the RTD study performed on the column. The collector, SMBT, was used in the conditioning the tracer samples in all the studies.

2.3.3 SELECTION OF THE TRACERS

Studies using tracers to determine the collection zone rate constant had not been previously performed. The reason for using tracers was to obtain an accurate evaluation of k_c at normal operating conditions in the

collection zone. The method could then be used to determine the effects of the various flotation parameters on k_c as well as evaluate the models used to describe the particle collection process. Tracer selection in this case is dependent on two criteria; firstly the tracer should only consist of one type of material and secondly it should be possible to differentiate the material from the ore being floated in the column. If the tracer fulfills the above two criteria it is then possible to measure the kinetics of a specific material in the flotation column. A further parameter which effects the result obtained is the particle size of the tracer. The use of a tracer with a discrete particle size simplifies the modelling of the response curves (see Chapter 2 Sec. 2.4).

The chalcopyrite tracer was selected since it was possible to ascertain the amount of chalcopyrite in the concentrate by determining the copper content using atomic absorption and there was a negligible amount of copper in the feed material. The chalcopyrite used was a concentrate sample obtained from the Black Mountain Mine, South Africa. The only problem with the sample was the fact that it had already been floated and was covered with reagent. Unsized chalcopyrite samples of about 12g were injected into the column.

Pure pyrite was selected as a more preferable tracer to use on the systems being investigated as the flotation process involved the flotation of pyrite in both the pilot column and industrial column. The pyrite used was a gravity concentrated sample which was milled down to the particle size range required. The sample had therefore not been in contact with any reagent prior to the testwork. The pyrite was sized into five size fractions viz. -38μm, +38-75μm, +75-106μm, +106-150μm and +150-212μm. These samples were radioactively labelled by the Atomic Energy Corporation. The activity emanated from the iron (Fe^{59}) and gold (Au^{198}) in the samples. The discretely sized samples of about 7g and 200g were injected into the pilot and industrial columns respectively. Only the first three particle size fractions were injected into the industrial column.

2.3.4 EXPERIMENTAL METHODS

In laboratory and pilot column studies the same operating procedure was used as in the preliminary RTD study to obtain steady state conditions in the column. Unless otherwise stated the froth was maintained at 10cm. Tracer preparation involved mixing up a 50% solids solution in the syringe and to this excess reagent was added. The syringe was shaken vigorously for about 5min. Once the column had reached steady state the tracer was injected into the feed stream. In both columns concentrate passing over the froth lip was almost instantaneously washed out of the concentrate launder by the rinse sprinkler. In the industrial column study the froth depth was maintained at the minimum value viz. about 20-30cm. Concentrate was washed out of the concentrate launder by the concentric rinse sprinkler positioned in the launder.

In the chalcopyrite study concentrate samples were taken at the exit of the concentrate launder in glass flasks. Sampling time was 5sec up to 120sec after which the sampling time was increased to 30sec. The concentrate was sampled for up to 8min. The samples were filtered, weighed and analysed for copper using an acid digest and atomic absorption. From these measurements the recovery of copper over time was ascertained.

In the radioactively labelled pyrite studies tracer exiting in the concentrate was monitored by an activity detector positioned at the exit of the concentrate launder. This detector took readings over 2sec intervals in the pilot column and over 5sec intervals in the industrial column. At the same time the detectors positioned at the tailings outlet in both columns monitored the flow of tracer in the tailings pipe. Since the tracer consisted only of pure pyrite it was assumed that the activity levels were related to the mass of tracer flowing in the pipes. Activity readings were proportional to the flowrate of the pulp past the detectors. In the pilot column work the rinse sprinkler flow rate was adjusted so that the concentrate flow from the launder was about the same as the tailings flowrate. In the industrial column study the measurements were adjusted to account for the difference in flowrates. In the pilot column study the tailings and concentrate detectors were calibrated relative to each other by passing a standard slurry source past each detector while it was positioned on the column. The source flowed at the same flowrate as

was used in the tests. In the industrial column study the detectors were calibrated relative to each other using a less accurate method whereby a standard source was positioned at a fixed distance from both detectors and the reading difference was measured.

Data analysis began by subtracting the background radiation from the tailings and concentrate response curves. The areas under the incremental tracer recovered vs. time curves were then adjusted by the calibration values and for the industrial column data also by the flowrate difference. By dividing the area under the curve of tracer recovered to the concentrate vs. time by the sum of the areas under the concentrate and tailings curves a value for the overall recovery of tracer to the concentrate could be obtained. It was therefore possible to obtain a cumulative tracer recovery vs. time curve for the tracer reporting to the concentrate.

2.3.5 TESTWORK PERFORMED

The chalcopyrite testwork began with tests performed to ascertain the froth zone recovery in the laboratory column at two froth depths. Two tests were performed one with a froth depth of 60cm and one with a shallow 10cm froth. The operating conditions were the same as the standard conditions listed in Table 2.3 except that the frother concentration was 50ppm and the gas flow rate was 2.24cm/s. Two runs were performed at the 10cm froth depth to evaluate the reproducibility of the tests. Following these tests an investigation was carried out to investigate the effect of bubble size on the rate constant(s). Bubble size was varied by altering frother concentration. Tests were performed at the same operating conditions as above but at four frother concentrations viz. 4, 10, 20 and 50ppm.

The study performed on the pilot column using radioactively labelled pyrite involved an investigation into the effect of bubble size, gas flow rate and tracer particle size on the collection zone rate constant. Bubble size was again varied by altering the frother concentration. Table 2.11 gives a detailed list of the tests performed. Apart from the conditions detailed in the table the standard operating conditions as listed in Table

2.3 were used. As can be seen from the table a discrete particle size fraction viz. +38-75um was used as tracer in the tests.

Run Number	Tracer Particle Size (μm)	Gas Rate (cm/s)	Frother Conc. (ppm)
F.1	+38-75	2.00	25
F.2	+38-75	2.24	25
F.3	+38-75	2.42	25
F.4	+38-75	2.67	25
F.5	+38-75	2.86	25
F.6	+38-75	2.24	4
F.7	+38-75	2.24	7
F.8	+38-75	2.24	10
F.2	+38-75	2.24	25
F.9	+38-75	2.24	40
F.10	-38	2.24	25
F.2	+38-75	2.24	25
F.11	+75-106	2.24	25
F.12	+106-150	2.24	25
F.13	+150-212	2.24	25

Table 2.11: Kinetics Testwork performed on the Pilot Column Rig using Radioactively Labelled Pyrite Tracers

The operating conditions of the industrial column were the same as in the RTD study performed on the column. Reproducibility was determined by performing two tests using the +38-75μm size fraction. In the study three different tracer particle sizes were injected into the column viz. -38μm, +38-75μm and +75-106μm.

2.4 FITTING OF RATE CONSTANTS TO THE EXPERIMENTAL DATA

From each of the kinetic studies a set of curves showing material recovered to the concentrate vs. time were obtained. In order to obtain

values of the collection zone rate constant from a recovery vs. time curve it is necessary to select a floatability distribution to describe the flotation kinetics.

In the development of the particle collection model detailed in Chapter 1 Sec. 3.2 a single rate constant was derived. In practice each mineral is best characterised by a distribution of floatabilities. A distribution is required to account for such factors as particle size, liberation, surface roughness and surface tarnishing. Basically two types of floatability distributions are used in flotation modelling; discrete and continuous. A large variety of distributions have been examined in both batch and full scale conventional cell modelling (Dowling et al. (1985)). To date in column modelling only discrete distributions have been used. The rate constant distribution described by Kelsall (1961) is most commonly used to describe the mineral floatability (eg. Dobby and Finch (1986) and Luttrell et al. (1990)). This approach assigns the range of floatabilities of an ore into two rate constants viz. a fast and a slow floating rate constant.

Care must be exercised when choosing a floatability distribution, as the overall recovery will be dependent on the form of the distribution. Ideally the distribution should only reflect mineral properties and should not be used as a remedy for any inadequacies in the basic model structure. It is therefore better to choose a simple distribution of floatabilities to describe the system and only use more complex distributions if the modelling of the results indicate that this is necessary. With this in mind each set of recovery vs. time data was firstly modelled by assuming that the mineral floatability was described by a single rate constant. If a single rate constant did not provide an adequate fit of the flotation response then fast and slow floating rate constants were assigned to the recovered material. The following method describes how the recovery vs. time curves were modelled:

1. A model was selected to describe the hydrodynamics of the collection zone. This model could be the axial dispersion model (Equation 1.18), the tanks-in-series model (Equation 1.20), the plug flow model (Equation 1.12) or the mixed flow model (1.13).

2. Using least squares an attempt was made to fit the selected hydrodynamic model and a single rate constant to the recovery vs. time data. For each of the modelling exercises the model curve obtained was multiplied by an infinite time recovery, R_I, which was taken to be final recovery data point of the experimental curve. Furthermore in all the curve fitting procedures (Steps 2 and 3) it was necessary to insert a small lag time at the beginning of each curve to account for the time taken for the first particles to reach the concentrate lip.

3. If the above model fitting approach produced a poor fit of the data then the following equation was fitted to the experimental data using multiple linear regression

$$R_C = R_I \, [x \, R_{C(kf)} + (1-x) \, R_{C(ks)}] \qquad (2.2)$$

where R_I is the infinite time recovery determined as above, x is the fraction of fast floating material and $R_{C(kf)}$ and $R_{C(ks)}$ are the recovery predictions using the selected hydrodynamic model and the fast (k_f) and slow (k_s) floating rate constants respectively.

Generally when the material being recovered consisted of a wide range of particle sizes (eg. chalcopyrite tracer) it was necessary to use two rate constants (k_f and k_s) to describe the floatability distribution. Whereas for material recovered of a discrete size fraction (eg. pyrite tracer) a single rate constant sufficed.

2.5 FITTING THE EXPERIMENTALLY DETERMINED RATE CONSTANTS TO THE PARTICLE COLLECTION MODEL

Once the rate constants had been determined from the recovery vs. time curves the collection efficiencies (E_K) were determined for each of the rate constants using Equation (1.41) and the operating conditions used in each test. The collision efficiencies were then determined using the correlations developed in the particle collection model and following this the attachment efficiencies were determined using Equation (1.42) and the experimental collection efficiencies. An attachment efficiency that was equivalent to the experimentally determined attachment efficiency was then

calculated using the particle collection model and an iteratively fitted induction time. It was therefore possible to obtain an estimate of the induction time for the range of parameters tested using the experimental results and the assumptions and correlations of the particle collection model. Appendix 3 lists a sample calculation of the QuattroPro spreadsheet used to perform the above procedure.

CHAPTER 3

RESULTS

1. STUDY OF THE MIXING CHARACTERISTICS OF THE COLLECTION ZONE

This study consisted of three sets of residence time distribution studies and the comprehensive results of these studies are listed in Appendix 1. The data is presented as the E(t) Curves which were obtained from the raw data using the methods described in Chapter 2 Sec. 1.3.

1.1 PRELIMINARY RESIDENCE TIME DISTRIBUTION STUDY

1.1.1 STANDARD OPERATING CONDITIONS

Table 3.1 lists the results obtained for a typical test performed at the standard operating conditions. Similar grade and recovery results were obtained by Schommarz (1991) and 95% confidence levels were obtainable as in the study by Schommarz viz. 2% for sulphur recovery and 1% for sulphur grades.

Mean Residence Time (min)	Sulphur Recovery (%) 1	2	3	Average	Standard Deviation (%)	Average Concentrate Grade (%S)
2.57	72.1	73.6	73.9	73.2	1.0	34.8

Table 3.1: Metallurgical Performance at Standard Operating Conditions

1.1.2 BUBBLE SIZE MEASUREMENTS

Two sets of bubble size measurements were performed. The first involved determining the mean bubble size for different frother concentrations at two air rates, 1.69cm/s and 2.24cm/s. The second set was performed during the RTD study and will be detailed in the next section. Figure 3.1 illustrates the results for the first set of tests. It is clear that between 0 and 20ppm the bubble size decreases substantially with increasing frother concentration. From 20ppm to 50ppm the mean bubble size decreases marginally. The higher air rate yields larger bubbles for concentrations less than 20ppm, however for concentrations above 20ppm air rate does not effect the bubble size.

1.1.3 RESIDENCE TIME DISTRIBUTION MEASUREMENTS

Before commencement of the tests two analyses were performed. The first involved determining whether the tracer adversely affected column operation and in the second the pulse input shape was determined. For a run performed at standard conditions ore samples were taken before and after the salt tracer had been added to column. The results indicated no change in the sulphur grades and recoveries with presence of tracer in the column. Froth stability and colour remained unchanged upon the addition of tracer. It was therefore assumed that the tracer did not affect the flotation process.

Figure 3.2 illustrates the shape of the pulse input curve. This curve was obtained with the tailings conductivity probe positioned at the feed inlet. The variance and mean residence time for this curve were $5.3 \times 10^{-4} min^2$ and 0.02min respectively. The input time was negligible compared to the mean residence of the system of about 150sec. The shape of the input was close to delta input and it was assumed that the input for the experiments was a perfect dirac delta function.

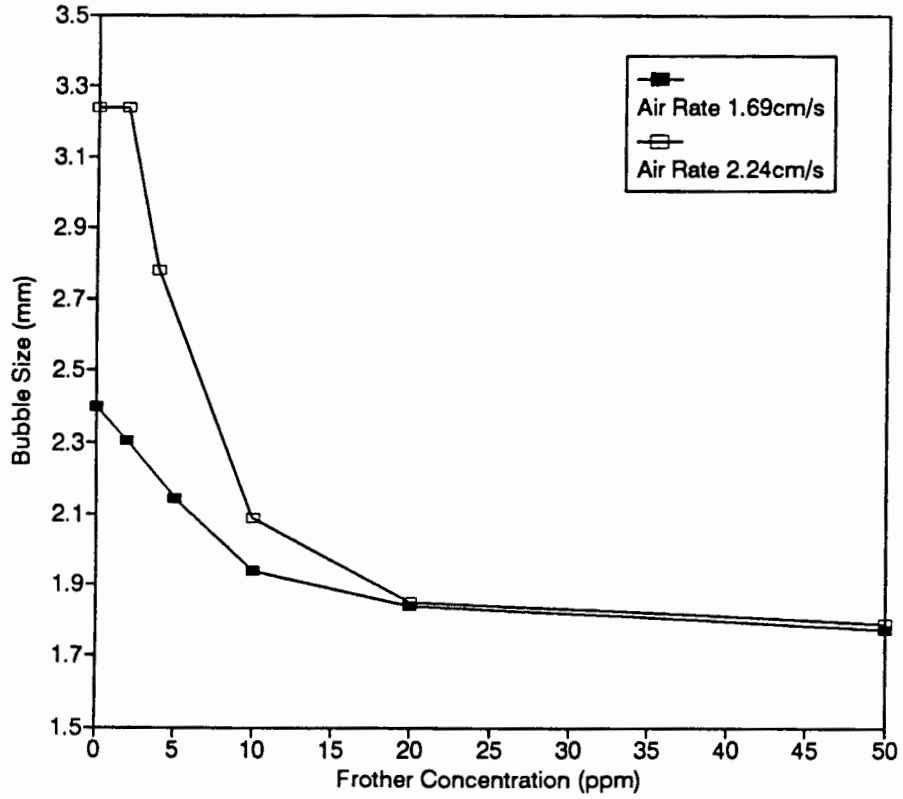

Figure 3.1: Effect of Frother Concentration on Mean Bubble Size for Two Air Rates

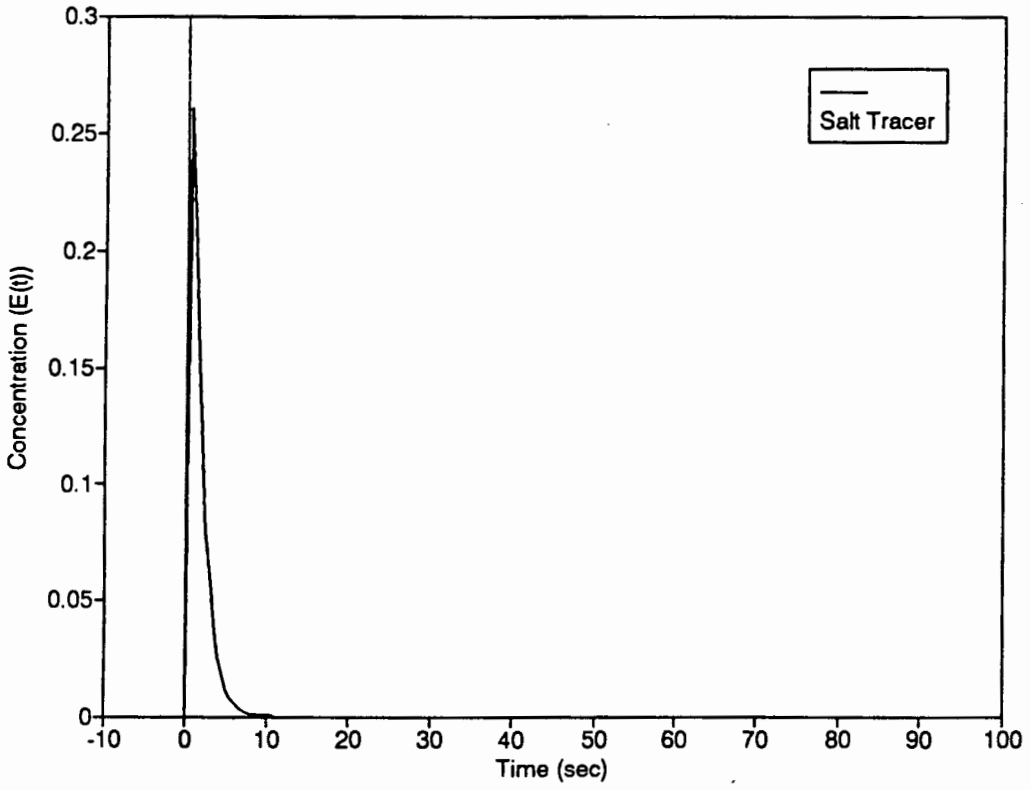

Figure 3.2: Salt Tracer Pulse Input Curve

Table 3.2 lists mean residence times, variances and model fitting results for all the tests performed in the preliminary RTD study. The tanks-in-series model was fitted to the data using least squares and the vessel dispersion number was determined using the method of moments.

Run Number	Mean Residence Time (min)	Variance (min^2)	No. of Tanks-In-Series (N)	Vessel Dispersion Number
Reproducibility				
A.1	2.53	0.423	15	0.0342
A.2	2.57	0.430	15	0.0336
A.3	2.55	0.395	16	0.0314
Feed % Solids				
A.4	2.60	0.423	15	0.0323
A.5	2.61	0.453	15	0.0343
A.6	2.62	0.421	16	0.0317
A.3	2.55	0.395	16	0.0314
A.7	2.62	0.424	16	0.0322
Gas Flow Rate				
A.8	2.59	0.311	22	0.0238
A.4	2.60	0.437	16	0.0323
A.9	2.51	0.582	11	0.0484
A.10	2.40	0.578	10	0.0530
Frother Concentration (Filter Cloth)				
A.11	2.65	0.461	15	0.0341
A.12	2.72	0.497	15	0.0349
A.13	2.60	0.579	12	0.0450
A.14	2.59	0.946	7	0.0763
Frother Concentration (USBM-type)				
A.15	2.50	0.505	12	0.0424
A.16	2.44	0.583	10	0.0516
A.17	2.42	1.029	6	0.0978

Table 3.2: Experimental Results and Model Parameters obtained in the Salt Tracer RTD Study

1.1.3.1 Reproducibility Tests

Figure 3.3 illustrates the age distribution curves of the reproducibility tests performed at the standard conditions. The mean residence times and variances for the reproducibility runs were similar to within 5 percent (Table 3.2). This was assumed to be the experimental error for this set of experiments. The conductivity probe positioned at the froth outlet did not detect tracer during any of the reproducibility tests.

Figure 3.4 illustrates a tailings age distribution curve at the standard conditions and the tanks-in-series model fit. The shape of the two curves are similar and it was assumed that the model gave a good fit of the experimental data.

1.1.3.2 The Effect of Feed Percent Solids on the Tailings Rtd

Figure 3.5 illustrates the liquid phase tailings age distribution curves for the range of feed percent solids investigated and the curve for a two phase experiment at the same conditions. It is clear from Figure 3.5 and the listed results in Table 3.2 that for the two phase system as well as for increasing percent solids the liquid phase response curves remained the same within the experimental error.

1.1.3.3 The Effect of Air Rate on the Tailings RTD

Figure 3.6 illustrates the tailings RTD curves for air rates ranging from 0 to 2.74cm/s. These tests were performed on a two phase system. From Table 3.2 it can be seen that the mean residence times decreased and the variances increased with increasing air rate. This increase in mixing with increased air rate is illustrated by the tanks-in-series model fit where N decreased from 22 to 9 over the range tested.

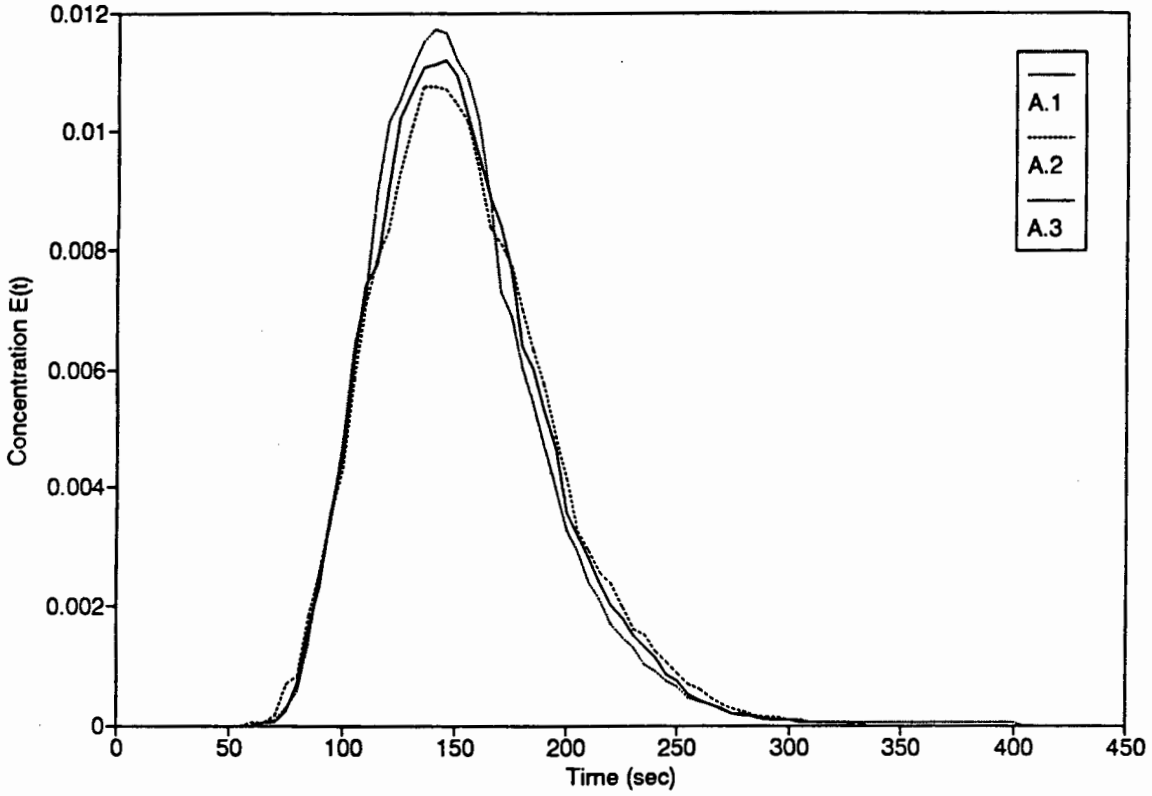

Figure 3.3: Tailings Age Distribution Curves for the Reproducibility Tests

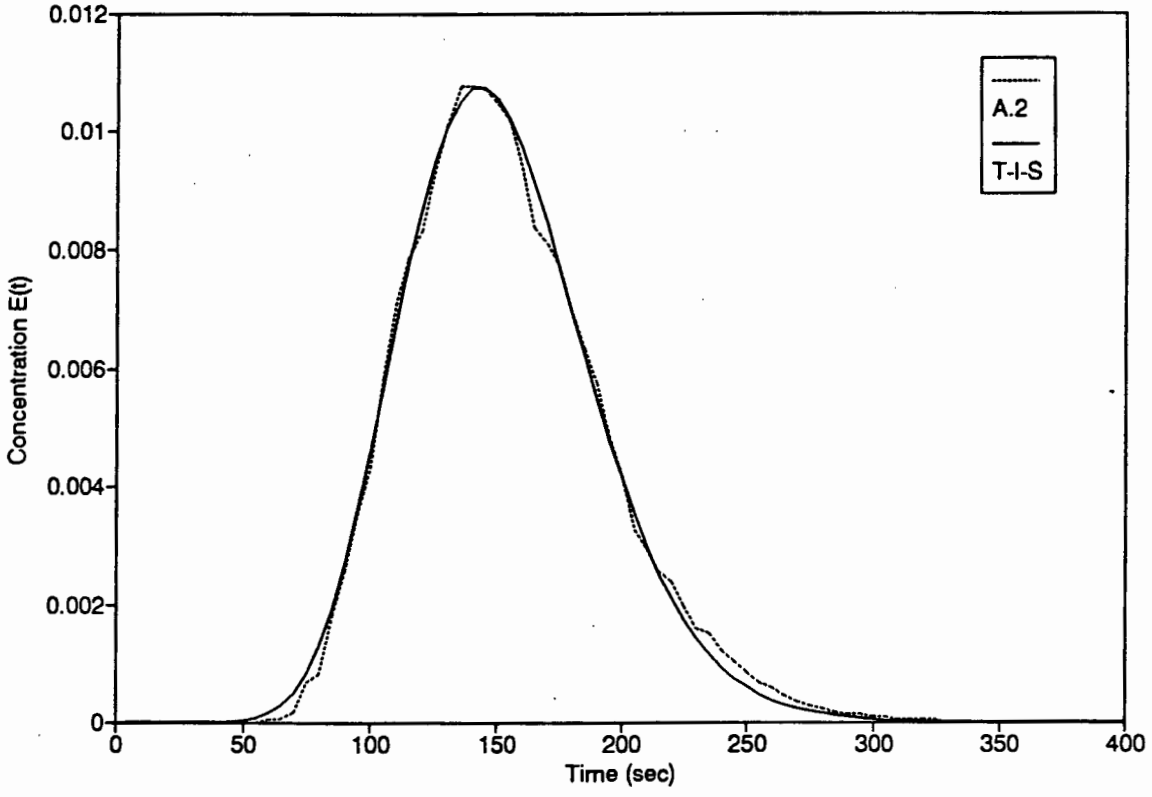

Figure 3.4: Tanks-in-Series Model Fit of Tailings Age Distribution Curve

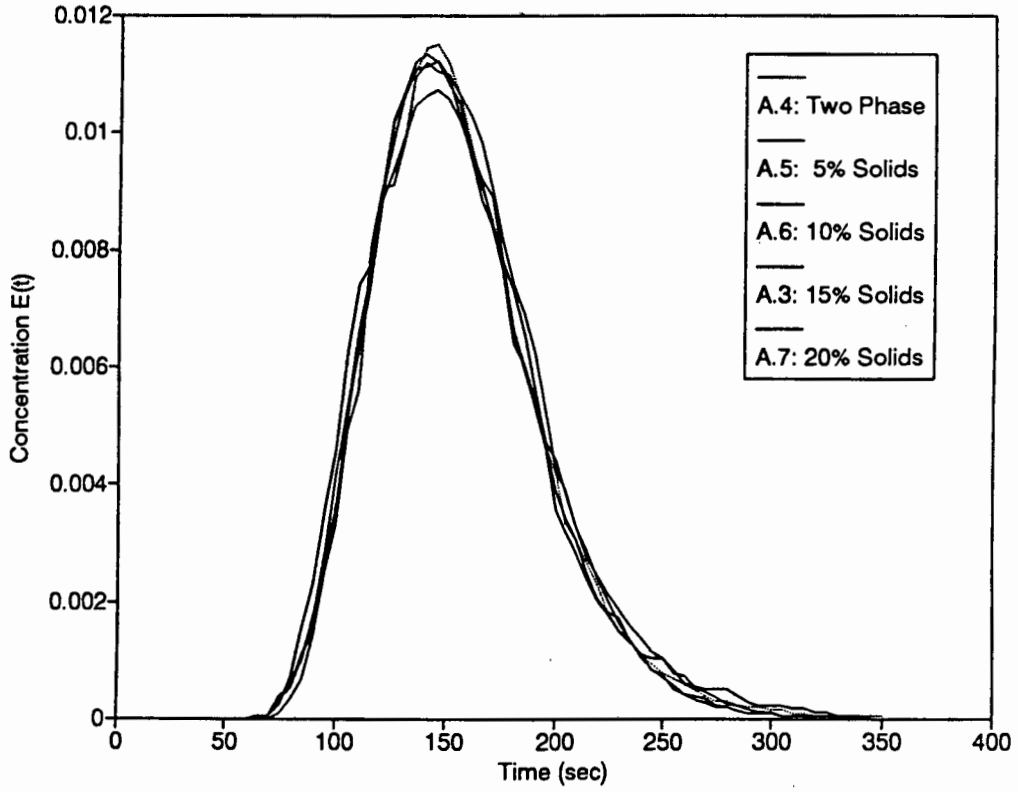

Figure 3.5: Tailings RTD Curves for a Range Feed Percent Solids

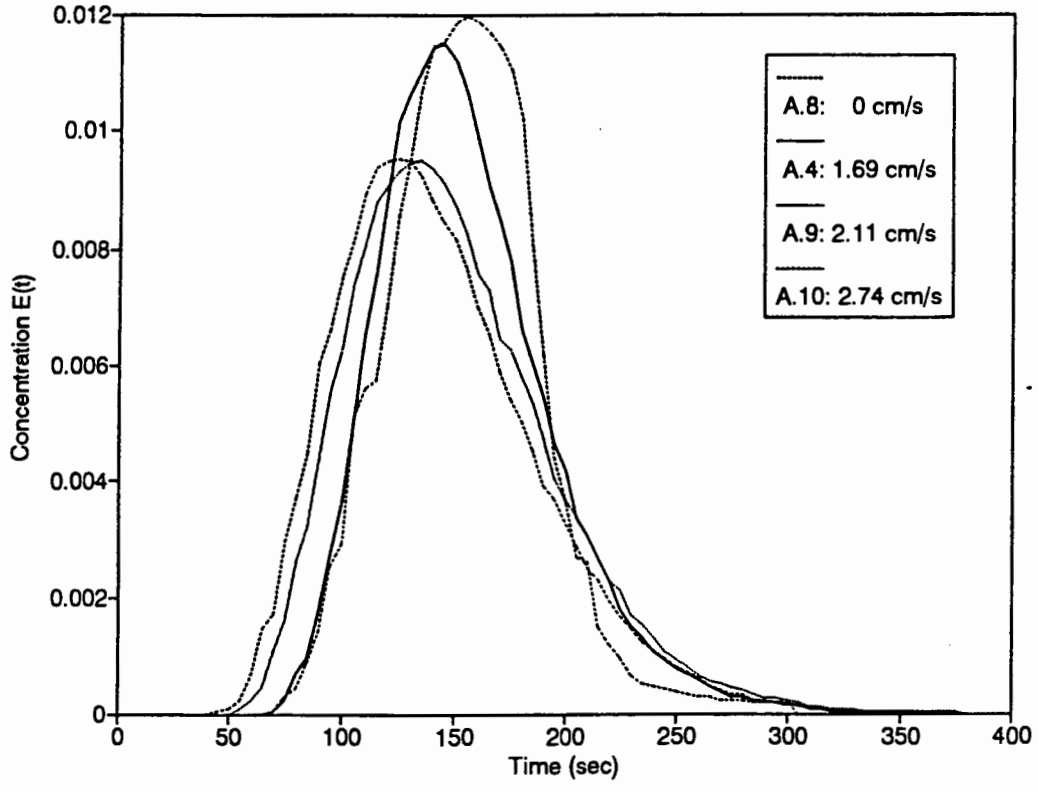

Figure 3.6: Tailings RTD Curves for a Range of Air Rates

1.1.3.4 The Effect of Frother Concentration on the Tailings RTD

Tests to determine the effects of frother concentration on mixing were performed on a two phase system using both the filter cloth and the USBM-type spargers. Figure 3.7 illustrates the tailings RTD curves for a range of frother concentrations using the filter cloth sparger and Figure 3.8 illustrates similar curves for the USBM-type sparger. From Table 3.2 it can seen that for both types of sparger the mean residence time decreased and the variance increased with increasing frother concentration. The USBM-type sparger yielded greater degrees of mixing at lower frother concentrations. The number of tanks-in-series ranged from 9 to 16 for the filter cloth sparger and 4 to 13 for the USBM-type sparger. Bubble size measurements were taken at each frother concentration (see Chapter 3 Sec. 1.1.3.5). Figure 3.9 illustrates that for both the filter cloth and USBM-type spargers the degree of mixing increased with decreasing bubble size.

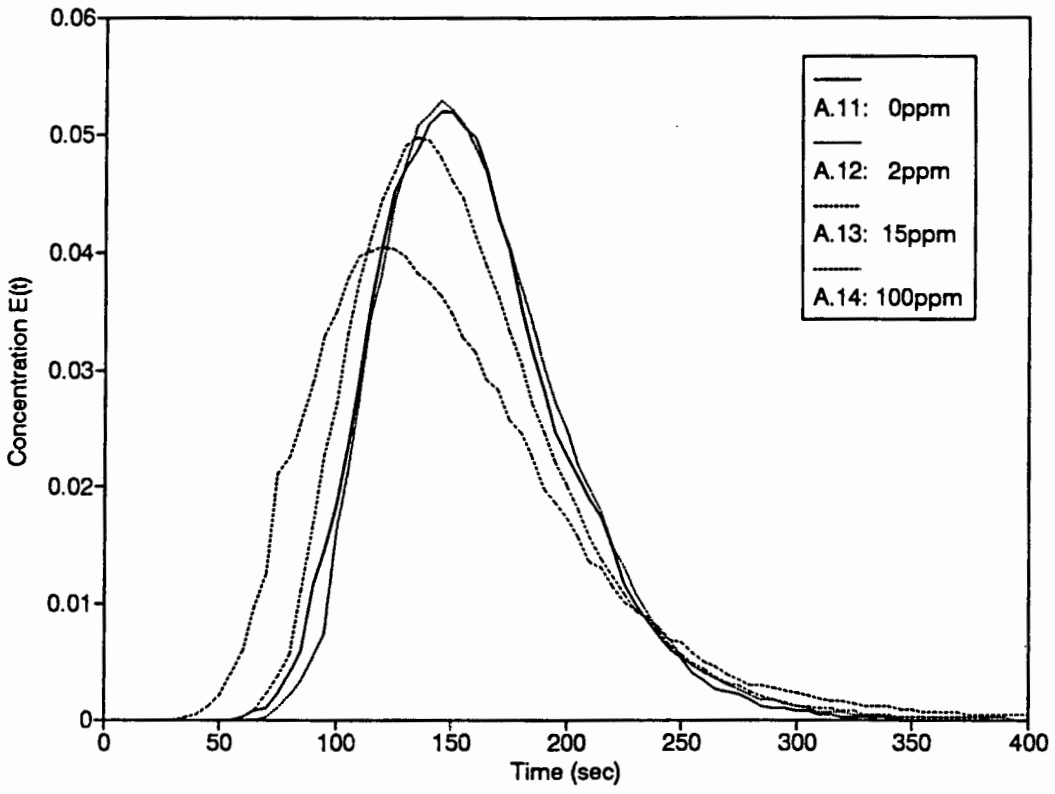

Figure 3.7: Tailings RTD Curves for a Range of Frother Concentration using the Filter Cloth Sparger

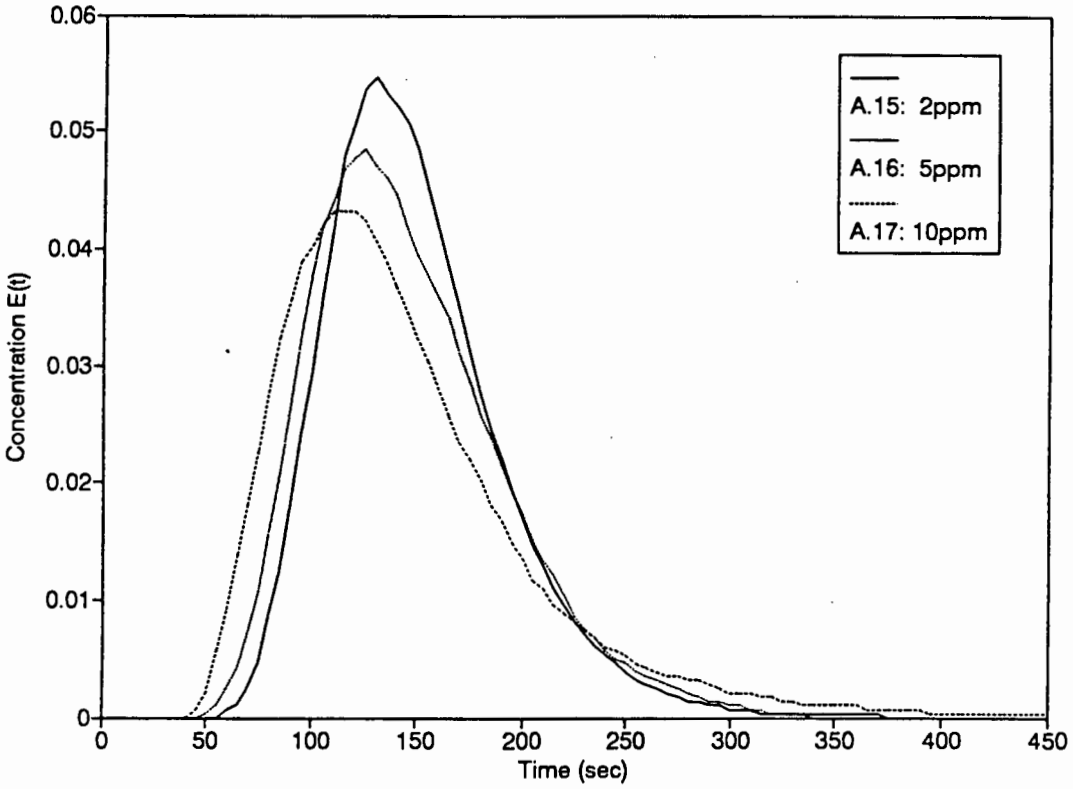

Figure 3.8: Tailings RTD Curves for a Range of Frother Concentration using the USBM-type Sparger

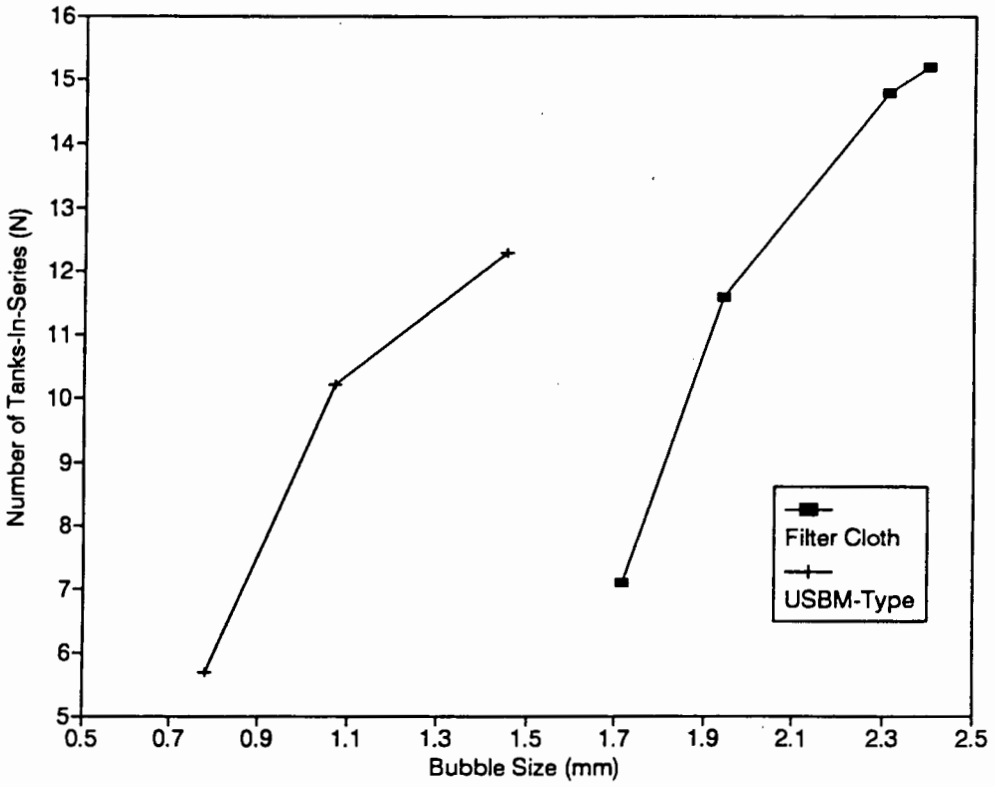

Figure 3.9: The Effect of Bubble Size on the Degree of Mixing using the Filter Cloth And USBM-Type Spargers

1.1.3.5 Gas Holdup and Bubble Size Measurements in the Preliminary RTD Study

Table 3.3 illustrates the results of the bubble size measurements for the tests performed in the RTD study. The standard deviations listed are an indication of the width of the bubble size distribution and not the error for a range of readings. It is clear that with increasing air rate at a frother concentration of 25ppm the bubble size remained relatively constant. However for the range of frother concentrations tested the bubble size decreased substantially with increasing frother concentration up to about 20ppm, this was in agreement with the initial bubble size measurements. The USBM-type sparger yielded substantially smaller bubble sizes than the filter cloth sparger.

Table 3.3 also details the gas holdup measurements. Gas holdup increased substantially with increasing air rate and only slightly with increasing feed percent solids. As frother concentration was increased for both the filter cloth and USBM-type sparger tests the gas holdup increased. The USBM-type sparger produced larger gas holdups than the filter cloth sparger.

Run Number	Gas Holdup (ϵ_g)	Mean Bubble Diam.(mm)	Standard Deviation (mm)
Reproducibility			
A.1	0.114	1.722	0.064
A.2	0.112	1.728	0.080
A.3	0.110	1.725	0.057
Feed % Solids			
A.4	0.102	1.755	0.088
A.5	0.105	1.741	0.084
A.6	0.108	1.738	0.058
A.3	0.110	1.725	0.080
A.7	0.115	1.725	0.061
Gas Flow Rate			
A.8	0.000	0.000	0.000
A.4	0.102	1.755	0.088
A.9	0.142	1.765	0.052
A.10	0.195	1.773	0.071
Frother Concentration (Filter Cloth)			
A.11	0.076	2.400	0.312
A.12	0.089	2.307	0.247
A.13	0.115	1.940	0.121
A.14	0.168	1.716	0.042
Frother Concentration (USBM-type)			
A.15	0.175	1.450	0.087
A.16	0.182	1.070	0.049
A.17	0.190	0.780	0.045

Table 3.3: Gas Holdup and Bubble Size Measurements in the RTD Study

1.2 RESIDENCE TIME DISTRIBUTION STUDIES USING RADIOACTIVELY LABELLED TRACERS

Results of the analysis of data obtained from the RTD studies performed on the UCT pilot column rig and the President Steyn industrial column are presented in this section. Data obtained from an RTD study performed on a cleaner column in Disputada, Chile by Yianatos and Bergh (1990) were analysed and these results are also presented.

1.2.1 PILOT COLUMN RTD STUDY

Figure 3.10 illustrates the pulse inputs of the liquid and gangue tracers measured by the detector positioned at the feed inlet. The input curve is similar to the salt tracer input curve which is also plotted. However both the gangue and liquid radioactive tracer pulse inputs have tails. This is due to the fact it was difficult to shield the detector positioned at the feed inlet from all radiation emanating from the tracers flowing through

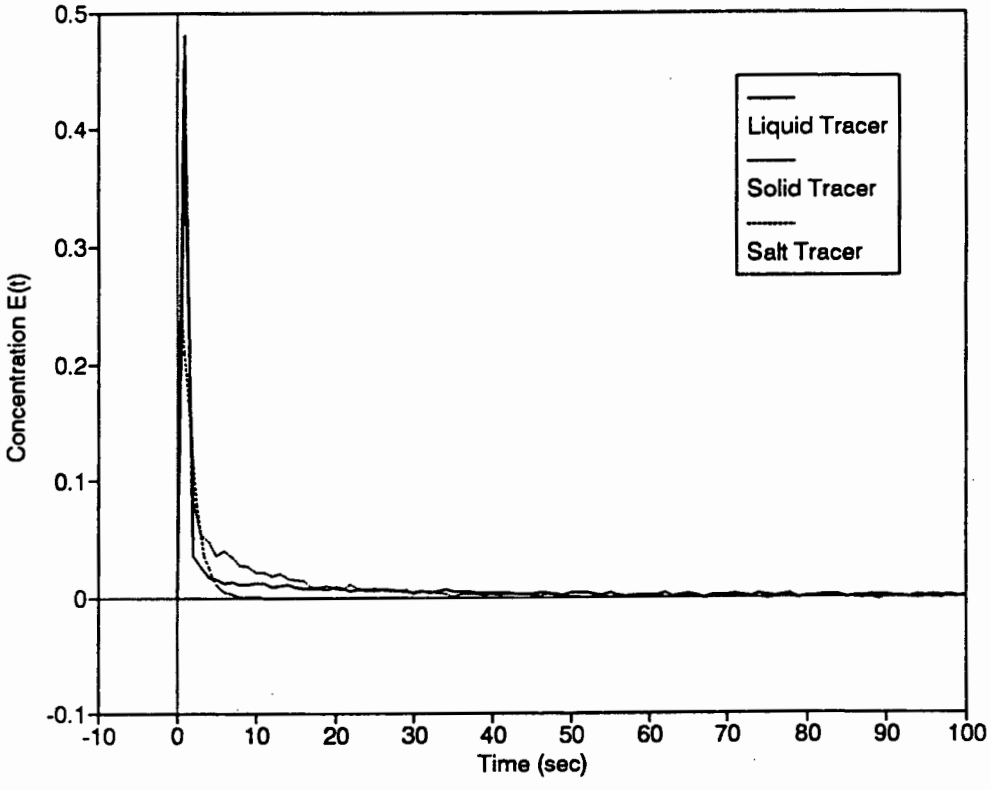

Figure 3.10: Salt Tracer and Radioactive Gangue and Liquid Tracers Pulse Inputs

the column. It was assumed for modelling purposes that the pulse input for the experiment was a perfect dirac delta function.

From the results of the preliminary RTD study as well as the results shown in Chapter 3 Sec. 1.2.2.1 and the work of Goodall and O'Connor (1989) where similar tracers and equipment were used it was assumed that the experimental error for the measured mean residence times and variances was 5 percent. Negligible activity levels were measured at the concentrate detector when the gangue and liquid tracers were injected. However for the feed tracer a significant portion of the tracer activity was detected in the concentrate overflow. Table 3.4 lists the experimental results and model parameters obtained from the application of the tanks-in-series and dispersion models. The tanks-in-series model and the numerical solution of the axial dispersion model were fitted to the data using least squares. The method of moments was also used to obtain an estimate of the vessel dispersion number. The determination of the vessel dispersion number using the method of moments and the least squares fit of the numerical solution of the dispersion model yielded similar results for all the curves, except for the larger particle sizes. The axial dispersion coefficients listed in Table 3.4 were calculated using the vessel dispersion number obtained from the least squares fit.

1.2.1.1 The Tailings RTD of the Feed, Liquid and Gangue Tracers

Figure 3.11 illustrates the tailings age distribution curves for the feed, gangue and liquid tracers. From Table 3.4 and Figure 3.11, the gangue and feed tracers had similar mean residence times and variances. The liquid tracer had a longer mean residence time and larger variance than the feed and gangue tracers.

Figure 3.12 illustrates the $E(\theta)$ vs. θ curves for the feed, liquid and gangue tracers. The curves are similar and all very close to plug flow. At this degree of mixing the tanks-in-series model and dispersion model yield similarly shaped curves. Figure 3.11 illustrates the tanks-in-series model fit of the response curves. It is clear that the model fits the data well. The tanks-in-series and dispersion model indicate an increase in mixing from liquid to solid tracer. The dispersion coefficients of the gangue and

feed tracers are significantly higher than the liquid dispersion coefficient.

UCT Pilot Column: d_c = 0.054m and L = 1.90m

Run Number	Tracer Sample	Residence Time (min)	Tracer Vel. (u) ($x10^2$m/s)	Variance (min^2)	Tanks-In-Series (N)	Disp. Number Method of Moments	Disp. Number Least Squares	Disp. Coeff. ($x10^3$) (m^2/s)
B.1	LIQUID	3.30	1.15	0.596	19	0.028	0.027	0.59
B.2	FEED	1.95	1.95	0.308	15	0.042	0.035	1.28
	GANGUE							
B.3	Combined	1.61	2.37	0.223	16	0.045	0.032	1.44
B.4	-38μm	2.98	1.28	0.547	19	0.032	0.027	0.65
B.5	+38-75μm	2.03	1.88	0.294	16	0.037	0.032	1.14
B.6	+75-106μm	1.62	2.35	0.245	15	0.049	0.035	1.53
B.7	+106-150μm	1.57	2.43	0.395	9	0.088	0.059	2.71

Table 3.4: Experimental Results and Model Parameters obtained from the Pilot Column Response Curves

1.2.1.2 The Tailings RTD of Gangue Tracers over a Range of Particle Sizes

Figure 3.13 illustrates the age distribution curves for the different tracer particle sizes. From Table 3.4 and Figure 3.13 it is clear that as particle size increases the mean residence time and the variance decrease up to the +75-106μm fraction. The variance for the +106-150μm fraction is significantly larger than that of the former size fraction. Figure 3.14 illustrates the $E(\theta)$ vs. θ curves for the range of particle sizes. Apart from the +106-150μm fraction the curves are all similar in shape and represent close to plug flow behaviour.

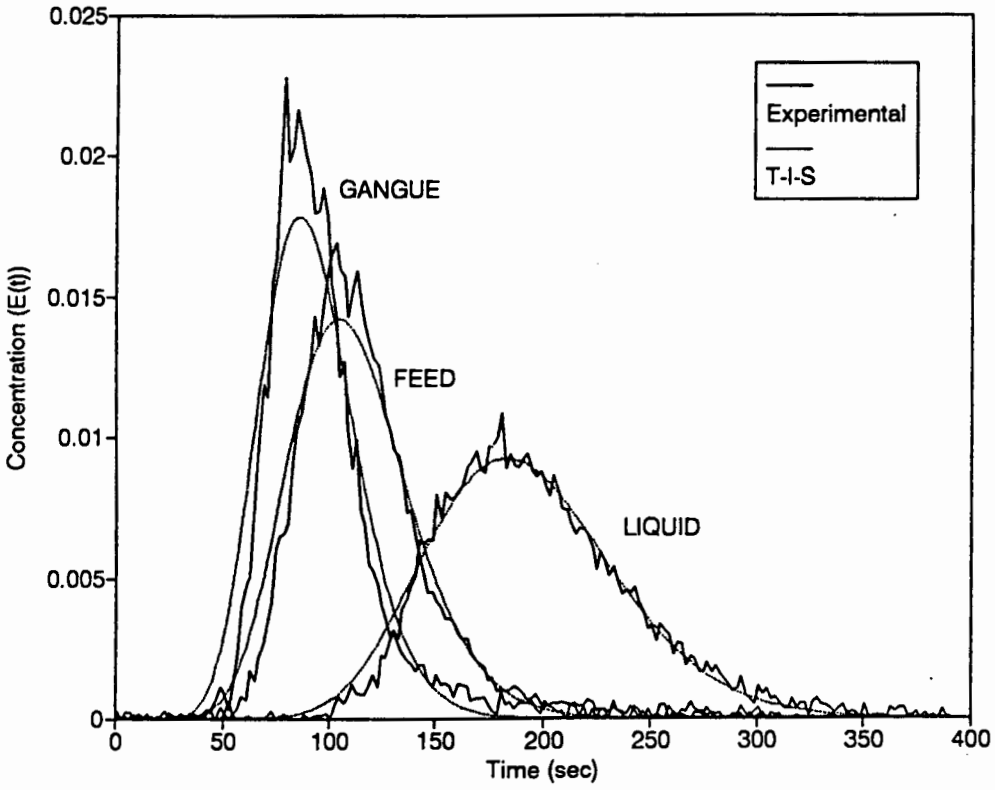

Figure 3.11: Tailings Age Distribution Curves for the Gangue, Feed and Liquid Tracers

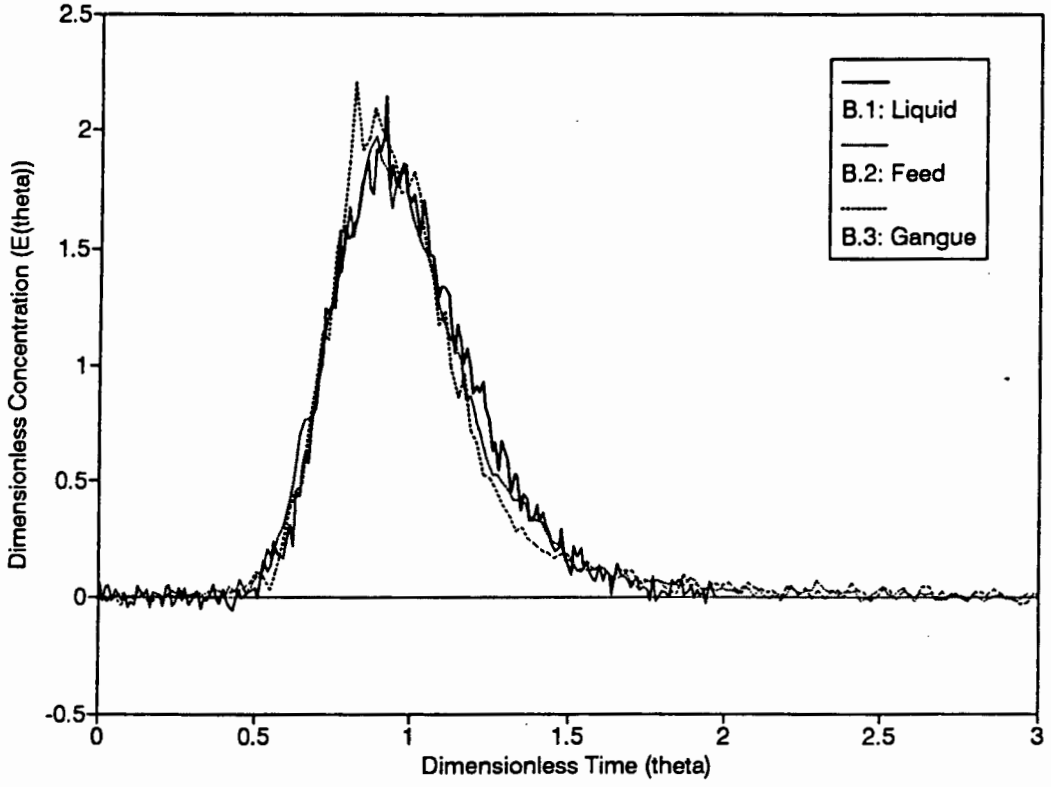

Figure 3.12: Normalised Response Curves for the Feed, Gangue and Liquid Tracers

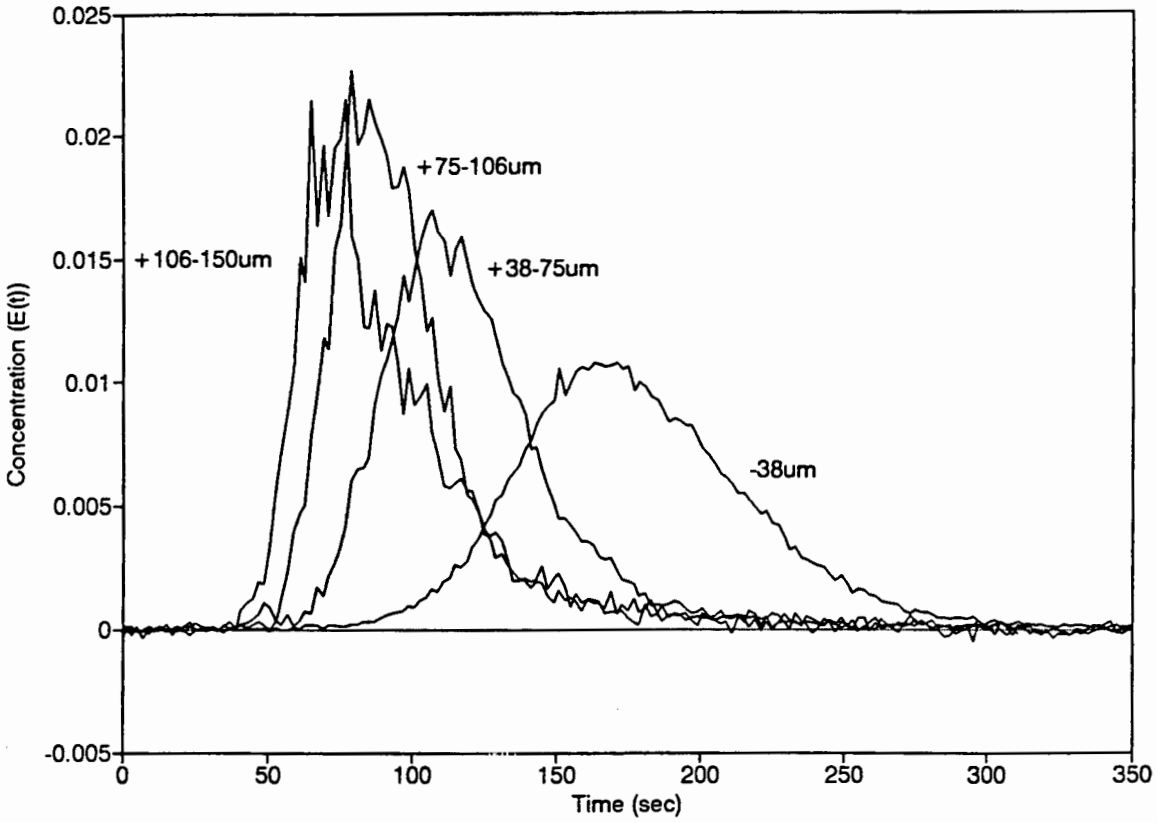

Figure 3.13: Age Distribution Curves of Gangue Tracers over a Range of Particle Sizes

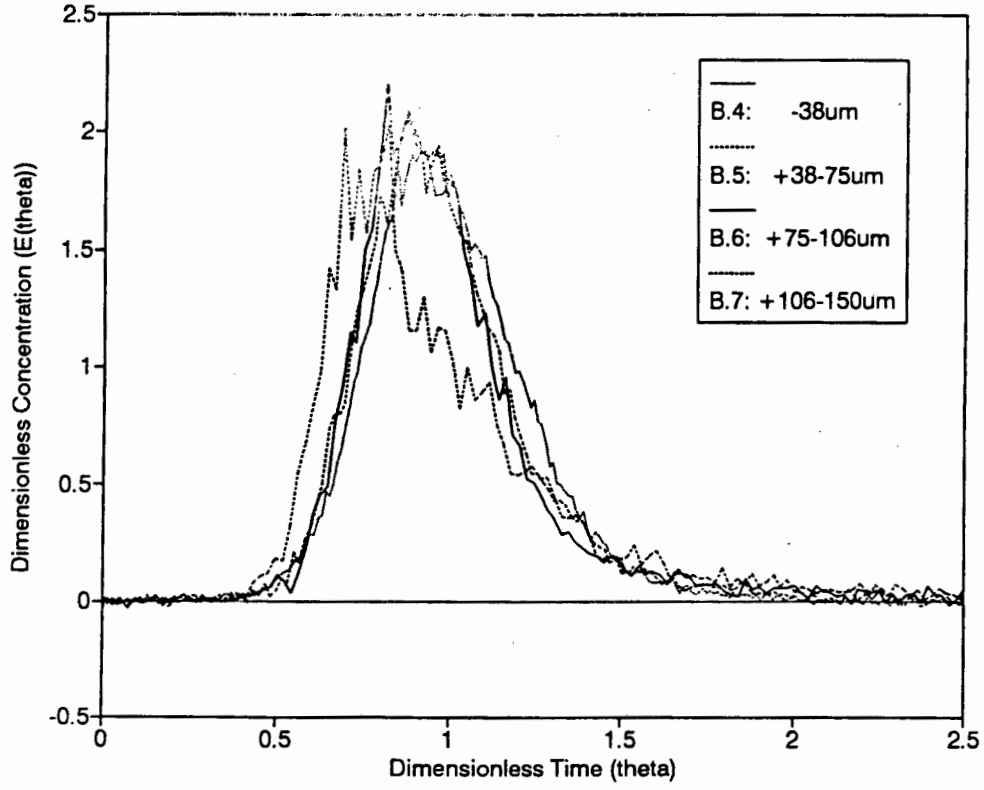

Figure 3.14: Normalised Response Curves of Gangue Tracers over a Range of Particle Sizes

Figures 3.15 and 3.16 illustrate the tanks-in-series model fit of the -38μm fraction and the +106-150μm fraction respectively. The tanks-in-series model fits the age distribution curve of the -38μm fraction well and the same applies to the +38-75μm and +75-106μm fractions. However as can be seen by Figure 3.16 the model does not provide a good fit of the +106-150μm fraction.

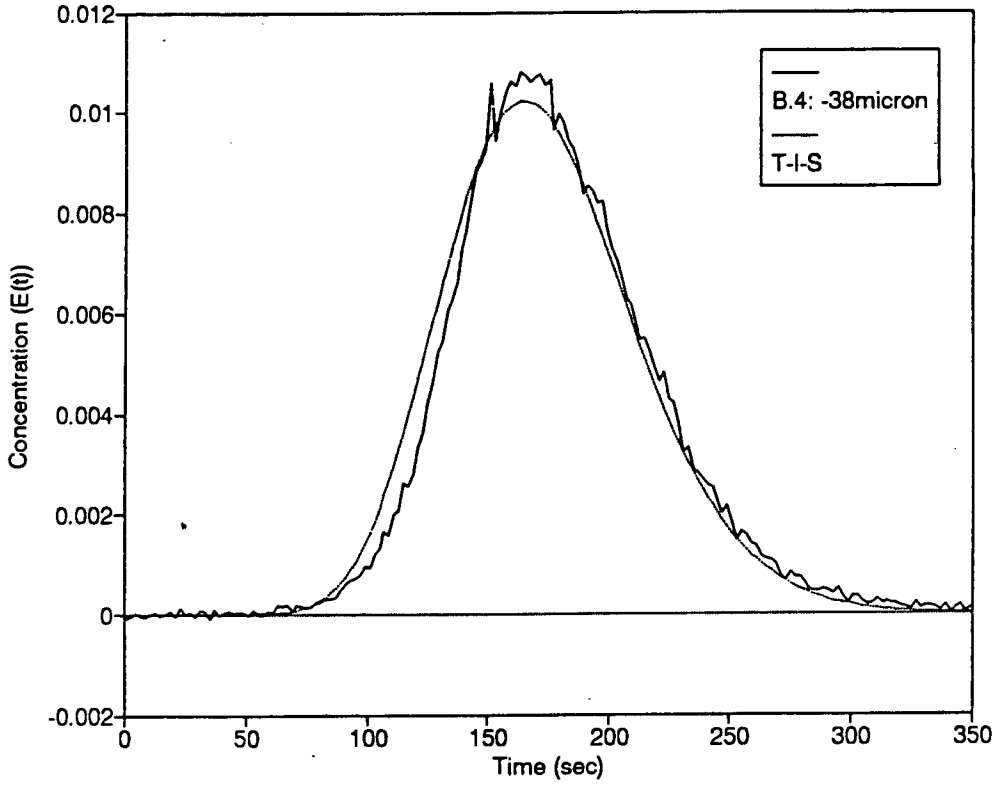

Figure 3.15: Age Distribution Curve of the -38μm Fraction and the Tanks-In-Series Model Fit

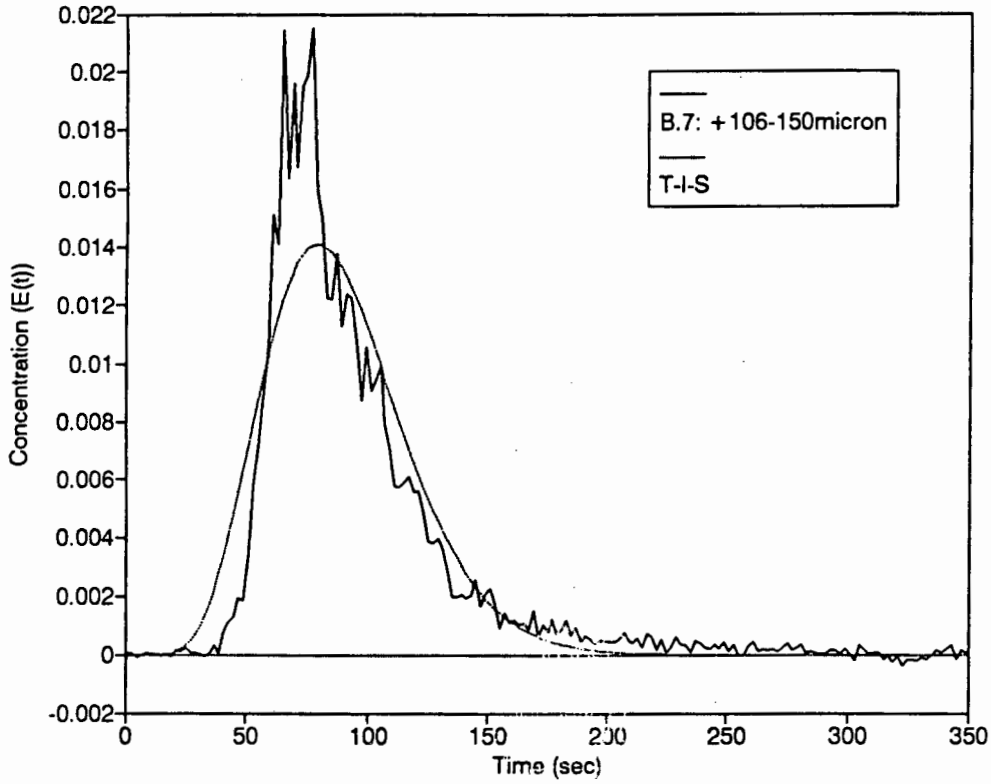

Figure 3.16: Age Distribution Curve of the +106-150µm Fraction and the Tanks-In-Series Model Fit

1.2.2 PRESIDENT STEYN ROUGHER COLUMN RTD STUDY

Figure 3.17 illustrates a typical pulse input curve produced using the pressurised tracer injection canister and measured by the detector positioned on the feed line. The tail of the pulse is due to the fact that the detector could not be completely shielded from the column. If the tail was subtracted from the pulse input curve a function close to a dirac delta function would be observed. The mean residence time of the tracer input was about 3-5 seconds. For modelling purposes it was assumed that the input time was negligible and the input pulse was a perfect dirac function.

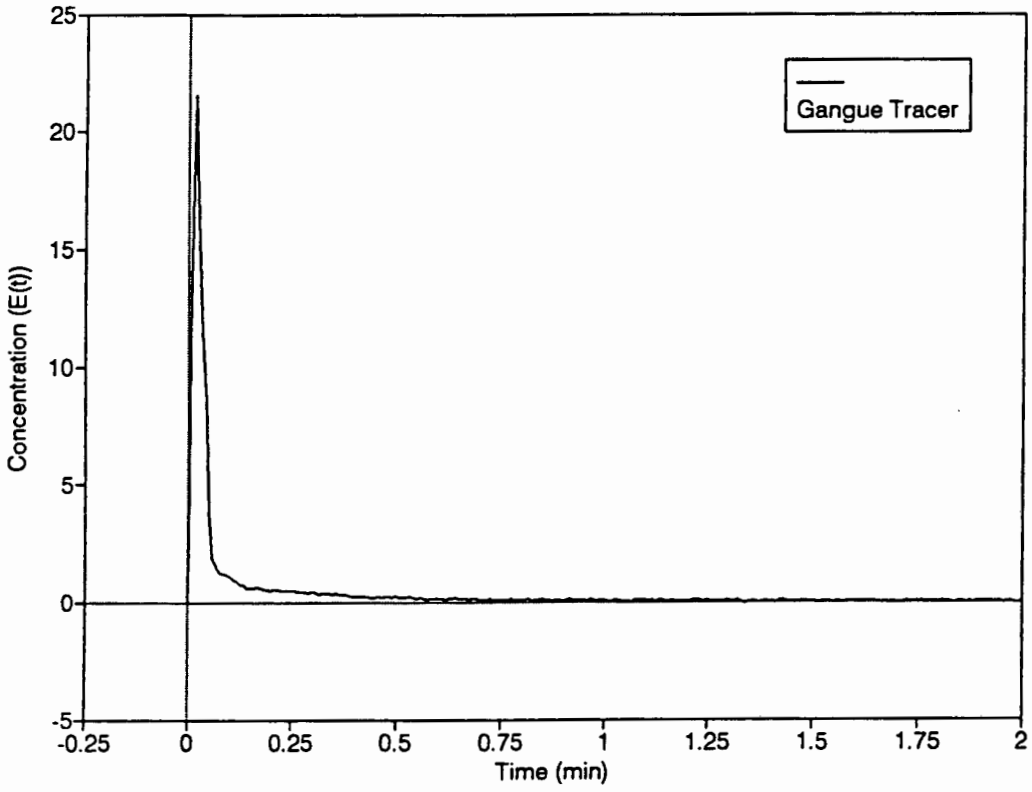

Figure 3.17: Typical Pulse Input Curve for the President Steyn Column

Table 3.5 lists the mean residence times, variances and model fitting results for all the tests performed in the industrial column RTD study. As in the study performed on the pilot column rig the tanks-in-series model and the numerical solution of the axial dispersion model were fitted to the data using least squares. The method of moments was also used to obtain an estimate of the vessel dispersion number. The vessel dispersion numbers determined using the method of moments were consistently lower than those obtained by the least squares fit. The axial dispersion coefficients listed in Table 3.5 were calculated using the vessel dispersion numbers obtained from the least squares fit. For all the tests performed, except where feed material was injected, negligible activity was detected by the detector positioned on the concentrate outlet pipe. For the feed tracer test a significant portion of the tracer activity was detected in the concentrate outlet pipe.

President Steyn Rougher Column: d_c = 1.20m and L = 10.9m

Run Number	Tracer Sample	Residence Time (min)	Tracer Vel. (u) ($x10^2$m/s)	Variance (min^2)	Tanks-In-Series (N)	Disp. Number Method of Moments	Disp. Number Least Squares	Disp. Coeff. ($x10^3$) (m^2/s)
C.1	GANGUE	9.66	1.63	56.24	1.80	0.472	0.68	0.121
C.2	GANGUE	9.42	1.67	53.20	1.80	0.469	0.70	0.122
C.3	LIQUID	11.42	1.38	70.03	1.60	0.448	0.63	0.094
C.4	FEED	9.34	1.68	48.82	1.80	0.584	0.68	0.125
	GANGUE							
C.2	Combined	9.42	1.67	53.20	1.80	0.469	0.70	0.122
C.6	-38μm	10.42	1.51	66.85	1.75	0.600	0.70	0.115
C.7	+38-75μm	8.92	1.76	44.23	1.90	0.479	0.63	0.121
C.8	+75-106μm	8.59	1.83	41.22	1.90	0.484	0.58	0.116
C.9	+106-150μm	8.11	1.94	35.56	1.90	0.454	0.56	0.118

Table 3.5: Experimental Results and Model Parameters obtained from the President Steyn Column Response Curves

1.2.2.1 Reproducibility Tests

Figure 3.18 illustrates the age distribution curves of the reproducibility tests. The two tests were performed on separate days during the study. The mean residence times and variances were similar to within 5 percent (see Table 3.5). This was assumed to be the experimental error for the study.

1.2.2.2 The Tailings RTD of the Feed, Liquid and Gangue Tracers

Figure 3.19 illustrates the tailings age distribution curves of the gangue and feed tracers. The two tracers produced virtually identical response curves and the mean residence times and variances of the curves are similar within the limits of the experimental error (see Table 3.5).

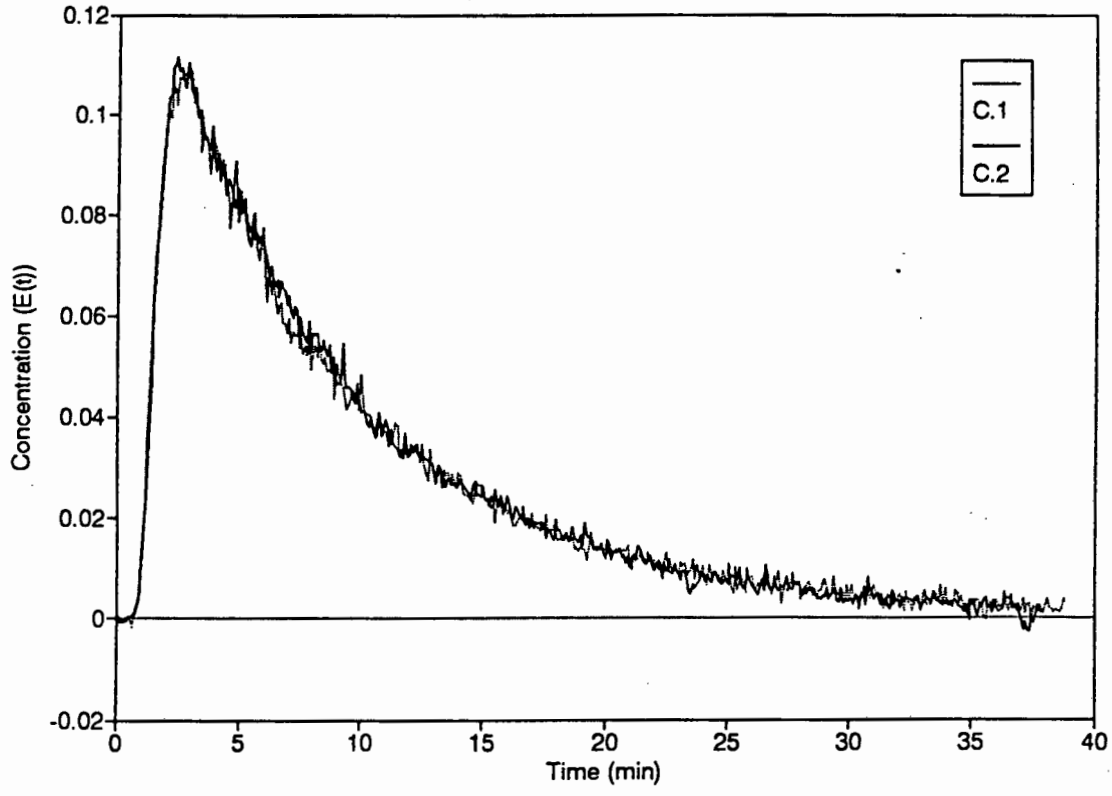

Figure 3.18: Tailings Response Curves of Reproducibility Tests performed on the President Steyn Column

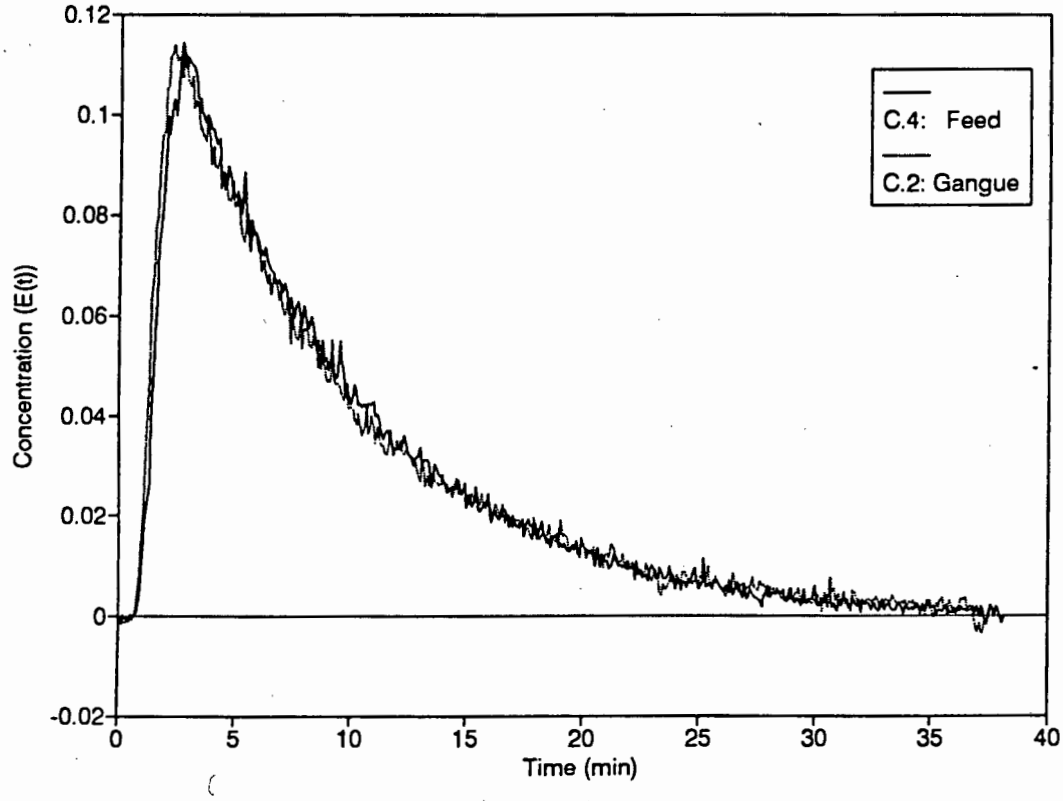

Figure 3.19: Tailings Response Curves of the Feed and Gangue Tracers

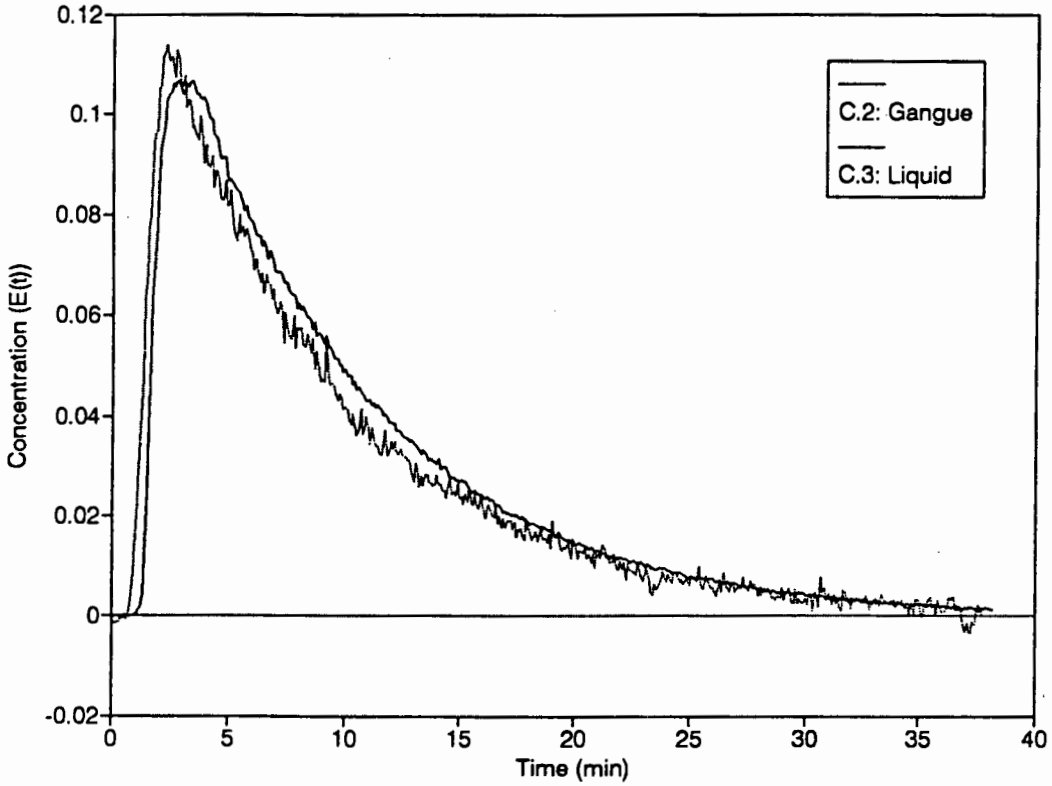

Figure 3.20: Tailings Response Curves of the Gangue and Liquid Tracers

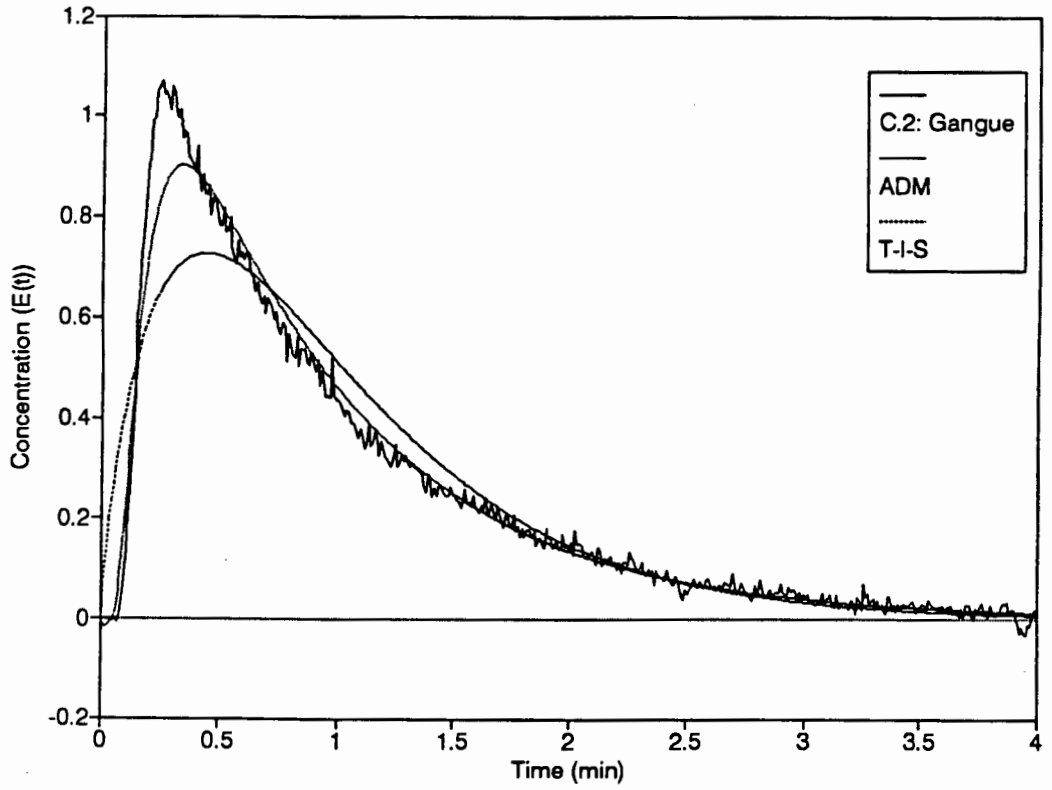

Figure 3.21: Normalised Tailings Response Curve of the Gangue Tracer and the Least Squares Fits of the Axial Dispersion and the Tanks-In-Series Models

Figure 3.20 illustrates the tailings response curves of the gangue and liquid tracers. From this figure and the results in Table 3.5 it can be seen that the mean residence time and variance decreased from liquid to solid tracer. Figure 3.21 illustrates the tanks-in-series and dispersion model least squares fits of the gangue tracer response curve. The dispersion model gives a better fit of the curve. From Table 3.5 it can be seen that the feed and gangue vessel dispersion numbers and vessel dispersion coefficients were significantly larger than the liquid values.

1.2.2.3 The Tailings RTD of the Gangue Tracers over a Range of Particle Sizes

Figure 3.22 illustrates the age distribution curves of the -38μm, the +75-106μm and the +106-150μm fractions. From Table 3.5 it can be seen that as particle size increased the mean residence time and variance decreased. Figure 3.23 and 3.24 show the least squares fit of the tanks-in-series and dispersion models to the -38μm and +106-150μm fractions respectively. As with the combined gangue tracer the tanks-in-series model did not give a good fit of the curves. However the dispersion model provides a good fit of all four particle size fractions. The vessel dispersion number decreased with increasing particle size. The vessel dispersion coefficients remained constant within the experimental error for the range of particle sizes and were similar to the combined gangue dispersion coefficient.

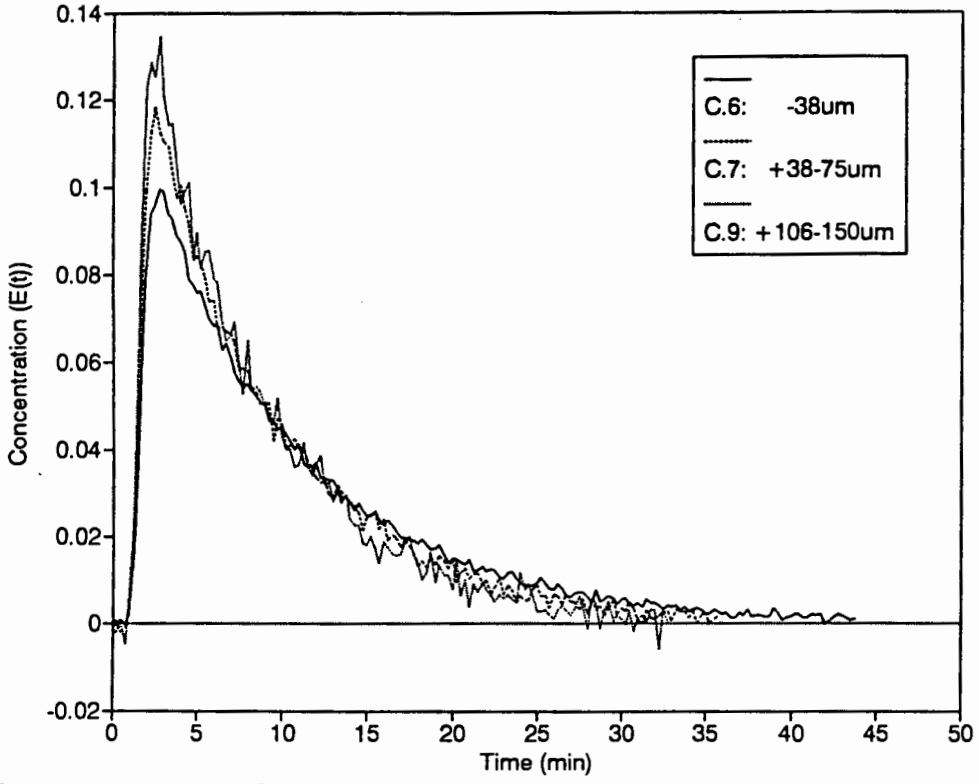

Figure 3.22: Tailings Response Curves of the -38μm, the +75-106μm and the +106-150μm Fractions

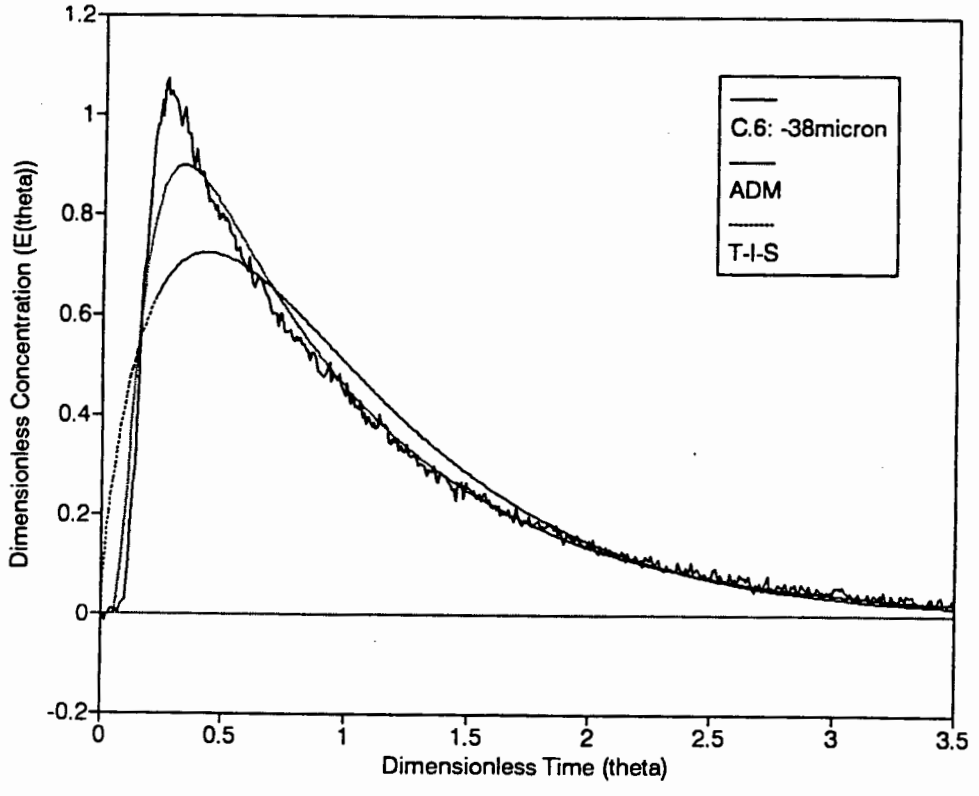

Figure 3.23: Normalised Tailings Response Curve of the -38μm Fraction and the Least Squares Fits of the Axial Dispersion and the Tanks-In-Series Models

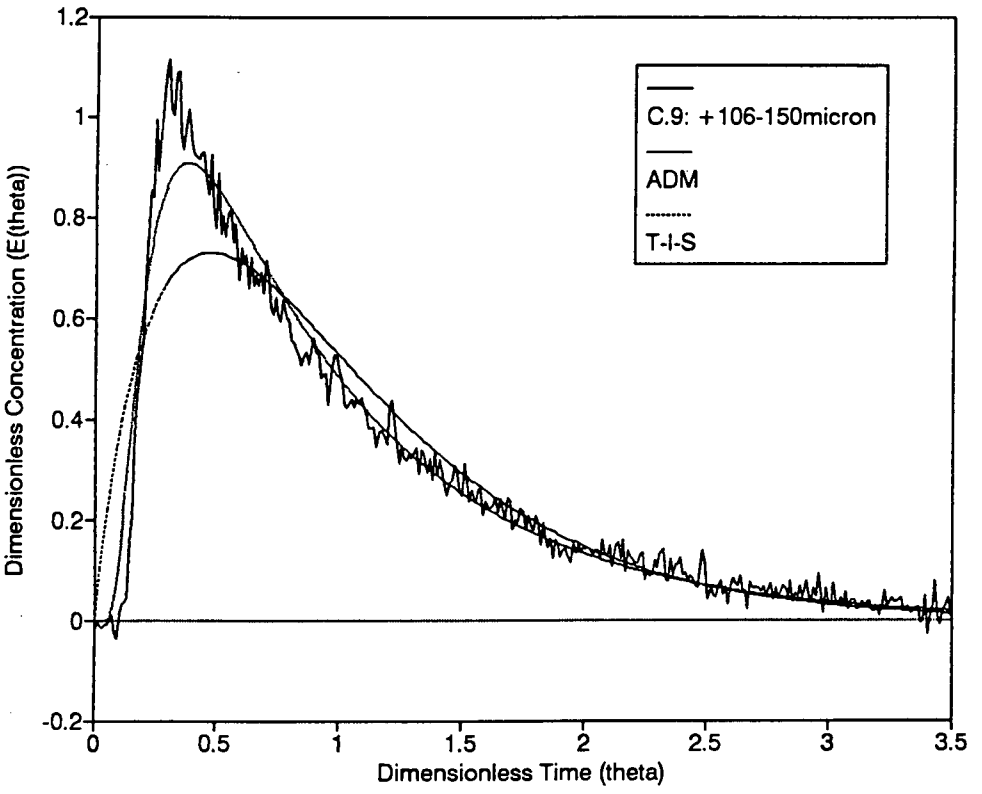

Figure 3.24: Normalised Tailings Response Curve of the +106-150μm Fraction and the Least Squares Fits of the Axial Dispersion and the Tanks-In-Series Models

1.2.3 DISPUTADA CLEANER COLUMN RTD STUDY

Detailed results of the Disputada cleaner column study are also listed in Appendix 1. Table 3.6 lists the mean residence times, variances and model fitting results for the tests performed. As in the two previous studies the tanks-in-series model and the numerical solution of the axial dispersion model were fitted to the data using least squares. The method of moments was also used to obtain an estimate of the vessel dispersion number. The vessel dispersion numbers determined using the method of moments differed significantly from those obtained using the least squares fit and did not follow the same trend. The axial dispersion coefficients listed in Table 3.6 were calculated using the vessel dispersion numbers obtained from the least squares fit.

Disputada Cleaner Column: d_c = 0.91m and L = 11.0m

Tracer Sample	Residence Time (min)	Tracer Velocity (u) ($x10^2$m/s)	Variance (min^2)	Tanks-In-Series (N)	Disp. Number Method of Moments	Disp. Number Least Squares	Disp. Coeff. ($x10^3$) (m^2/s)
LIQUID	16.75	0.92	174.28	1.25	0.613	0.92	0.093
GANGUE							
Combined	12.68	1.21	116.43	1.10	0.945	0.85	0.113
-38μm	15.29	1.01	155.60	1.15	0.730	0.95	0.105
+38-75μm	12.44	1.24	107.18	1.15	0.819	0.82	0.112
+75-150μm	8.77	1.76	48.50	1.05	0.634	0.56	0.108

Table 3.6: Experimental Results and Model Parameters obtained from the Disputada Cleaner Column Response Curves

1.2.3.1 The Tailings RTD of the Feed, Gangue and Liquid Tracers

Figure 3.25 illustrates the gangue and liquid tracer response curves. Also shown are the tanks-in-series and dispersion model least squares fits for each of the curves. The mean residence time and variance decreased from liquid to solid tracer (see Table 3.6). The tanks-in-series model does not fit the data well whereas the dispersion model gives a good fit of the data. From Table 3.6 it can be seen that the vessel dispersion coefficient of the gangue tracer was significantly larger than the liquid dispersion coefficient.

1.2.3.2 The Tailings RTD of Gangue Tracers over a Range of Particle Sizes

Figure 3.26 illustrates the tailings response curves of the -38μm, +38-75μm and +75-150μm fractions. It also shows the dispersion model curve fits for each size fraction. As can be seen in Table 3.6 with increasing particle size the mean residence time and variance decreased. The dispersion model gives a good fit of the data over the range of particle sizes. The vessel dispersion coefficients for the range of particle sizes

remained constant within the experimental error and were similar to the combined gangue dispersion coefficient.

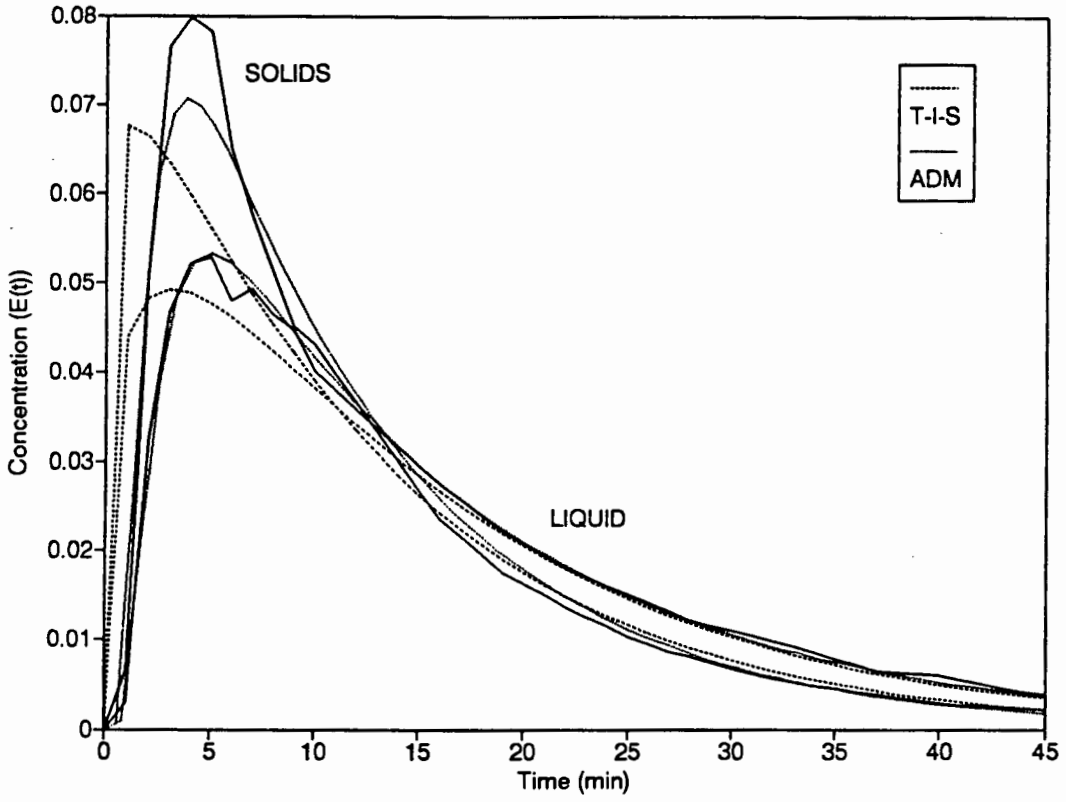

Figure 3.25: Tailings Response Curve of Gangue and Liquid Tracers and the Least Squares Fits of the Axial Dispersion and the Tanks-In-Series Models

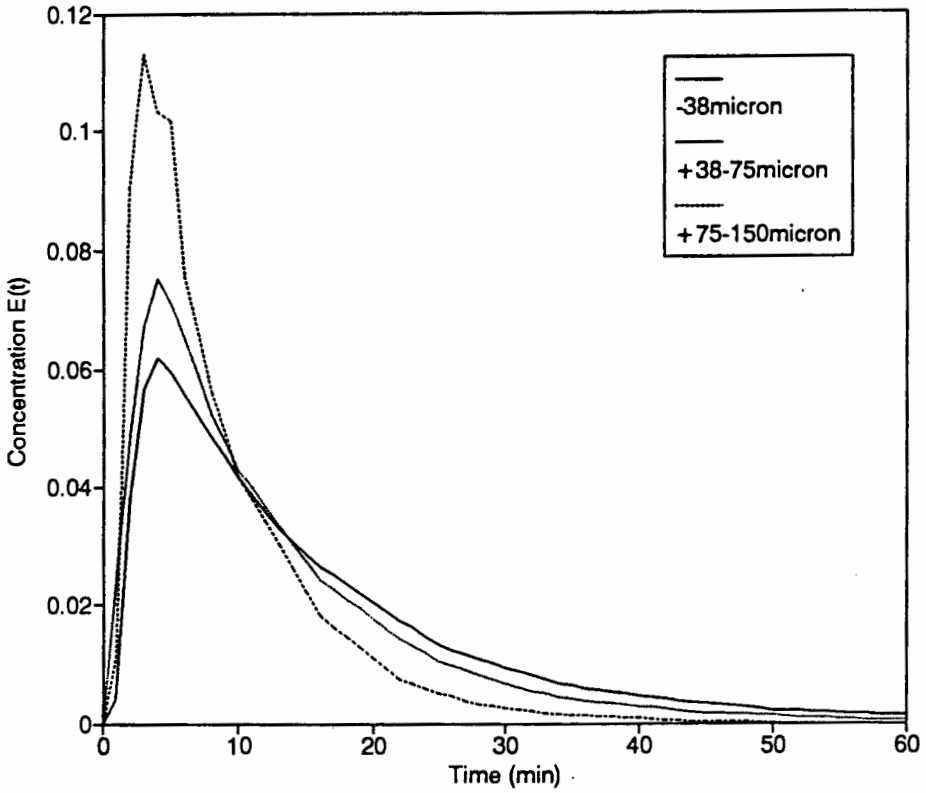

Figure 3.26: Tailings Response Curves of the -38µm, the +38-75µm and the +75-150µm Fractions and the Least Squares Fit of the Dispersion Model

2. STUDY OF THE KINETICS OF THE COLLECTION ZONE

2.1 DETERMINATION OF THE COLLECTION ZONE RATE CONSTANT BY VARYING COLUMN LENGTH AND FEED RATE

Table 3.7 lists the grade and recovery results obtained by varying the column length and feed rate at the standard operating conditions. The grade and recovery results for a 60cm froth are also listed in the table. In the evaluation of the method to determine the collection zone rate constant the recoveries and grades obtained at similar mean residence times for the 10cm and 60cm froth can be compared. The recovery for the 60cm froth is significantly lower than the recovery in the 10cm froth. The

grades obtained in the 10cm froth test are marginally lower than those obtained in the 60cm froth test.

Mean Residence Time (min)	Sulphur Recovery (%) 1	2	3	Average	Standard Deviation (%)	Average Concentrate Grade (%S)
Run Number: D.2						
10cm Froth						
0.00	0.0	0.0	0.0	0.0	0.0	0.0
0.78	62.2	52.4	60.1	58.2	5.3	38.3
1.00	64.3	68.3	63.7	65.4	2.6	36.7
1.57	77.5	79.9	79.1	78.5	1.2	35.2
2.01	78.1	80.1	79.7	79.3	1.0	34.3
2.88	80.2	79.2	78.6	79.3	1.0	32.4
3.71	75.8	80.2	79.3	78.4	2.6	31.5
60cm Froth						
2.57	72.1	73.6	73.9	73.2	1.0	34.8

Table 3.7: Sulphur Recovery and Grade Results at the Standard Operating Conditions over a Range of Mean Residence Times

From Table 3.7 it can be seen that the standard deviations of the recovery measurements were relatively high for recoveries measured at low mean residence times. Figure 3.27 illustrates the recovery vs. mean residence time curve at the standard conditions showing the standard deviation for each recovery measurement.

2.1.1 EFFECT OF GAS FLOW RATE ON SULPHUR RECOVERY

Appendix 2 lists the results for the tests performed at three air rates viz. 0.81cm/s, 1.69cm/s and 2.53cm/s. Figure 3.28 illustrates the sulphur recovery curves for the three air rates. Recovery at 0.81cm/s was substantially lower than the higher air rates. For all three rates the standard deviation for each recovery measurement was between 2 and 5% (See

Appendix 2) and the recovery vs. time curves for the two higher air rates were similar within the standard deviations of the measurements.

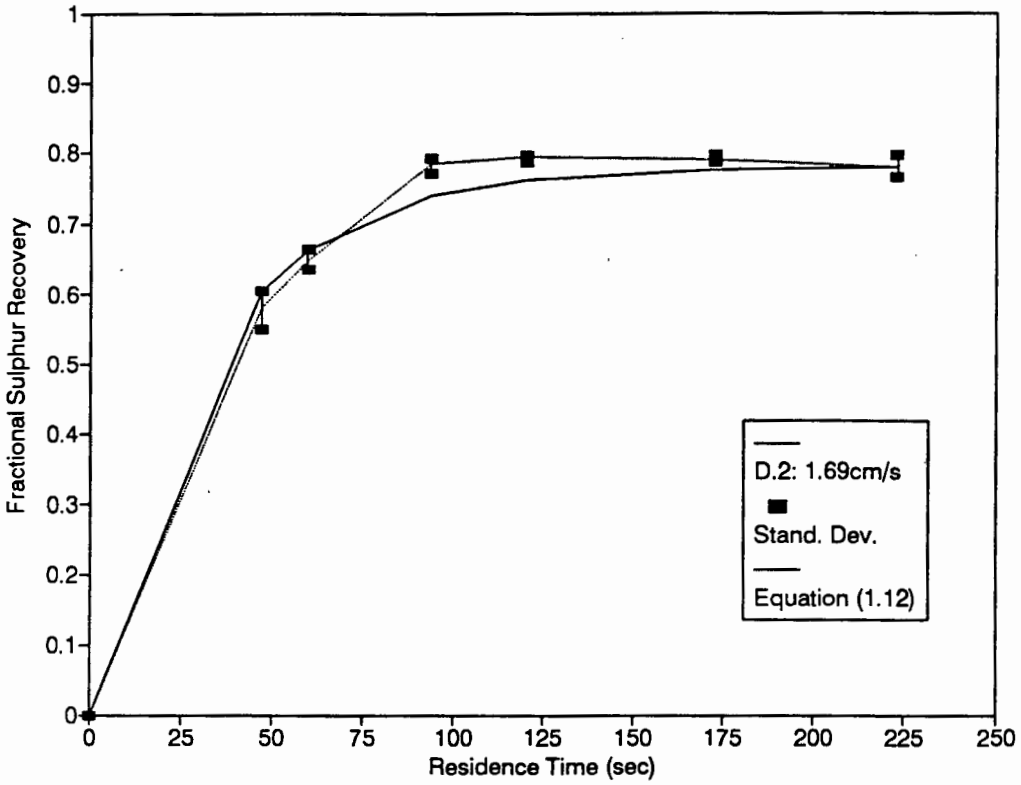

Figure 3.27: Sulphur Recovery vs. Mean Residence Time for the Standard Operating Conditions

Run Number	Gas Rate (cm/s)	Fraction of Fast Floating Material	Fast Floating Rate Constant (min^{-1})	Slow Floating Rate Constant (min^{-1})	Final Recovery R_c (%)
D.1	0.81	0.95	1.01	0.77	56.0
D.2	1.69	1.00	1.90	0.00	77.9
D.3	2.53	1.00	1.50	0.00	80.3

Table 3.8: Model Parameters obtained in the Curve Fitting of the Sulphur Recovery Curves

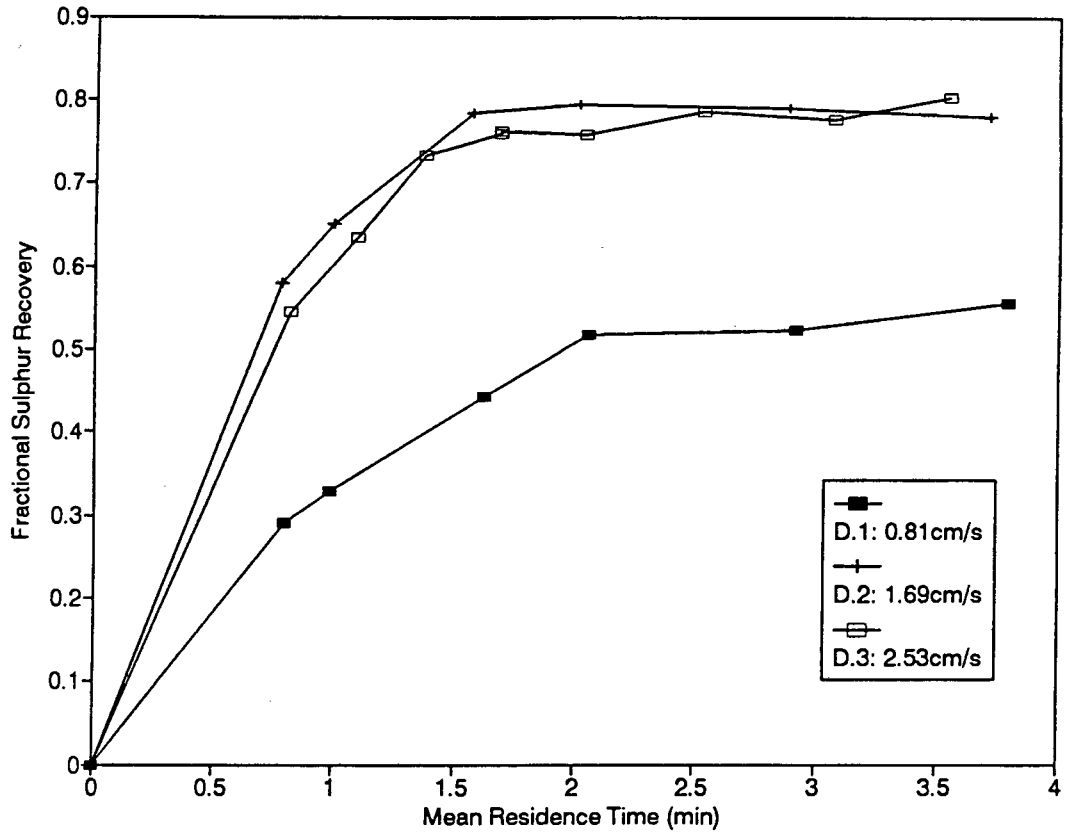

Figure 3.28: Sulphur Recovery vs. Mean Residence Time Curves for Three Gas Rates

Table 3.8 lists the modelling results of the above curves. For the lower air rate it was necessary to model the experimental curve using fast and slow floating rate constants to obtain a good fit. However the fraction of slow floating material was very small. For the two higher air rates a single rate constant provided an adequate fit of the data. In this case the plug flow model was used to determine the rate constants. From 0.81cm/s to 1.69cm/s the fast floating rate constant increased. The rate constant was lower for the air rate of 2.53cm/s than 1.69cm/s. However the standard deviations of the recovery measurements indicate that the two curves cannot be differentiated.

2.2 DETERMINATION OF THE COLLECTION ZONE RATE CONSTANT USING CHALCOPYRITE TRACERS

Appendix 2 lists the results obtained in this section. For each test the incremental mass of copper and cumulative recovery vs. time data are listed. Figure 3.29 presents curves of the cumulative copper recovered to the froth vs. time for the reproducibility tests. It is clear from this figure that the experiments were highly reproducible. The short lag time between the time of tracer injection and the appearance of tracer in the froth was also reproducible.

Figure 3.30 shows curves of the incremental mass of copper recovered to the froth vs. time obtained for the tests performed with a 10cm and 60cm froth. The curve obtained for the 60cm froth differs from that obtained with the 10cm froth in two ways. Firstly the initial peak is lower for the 60cm froth than for the 10cm froth and secondly the 10cm froth yields a smooth curve after the initial peak while the 60cm froth produces further smaller peaks after the initial peak.

Table 3.9 lists the modelling results for the tests performed using the chalcopyrite tracer. A single rate constant did not provide a good fit of the data and it was necessary to model the recovery vs. time curves using fast and slow floating rate constants. The axial dispersion model was used to determine the rate constants. Figure 3.31 illustrates the copper recovery vs. time curves for the 10cm froth and the similar test performed with a 60cm froth. Using Equation (1.38) and the collection zone recovery (R_c) vs. time curve for the 10cm froth the froth zone recovery (R_f) was determined to be 0.48 by fitting the resultant curve (R_{fc}) to the experimental data obtained for the 60cm froth. Figure 3.31 also illustrates this fit of the 60cm froth curve.

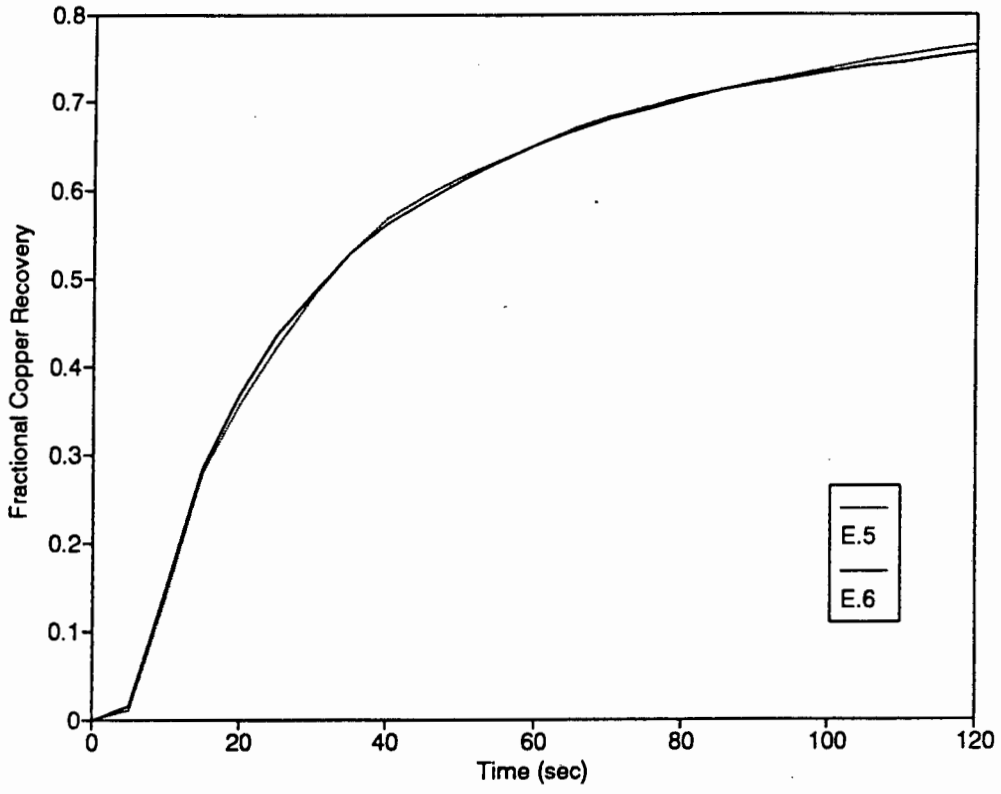

Figure 3.29: Copper Recovery vs. Time Curves for the Reproducibility Tests

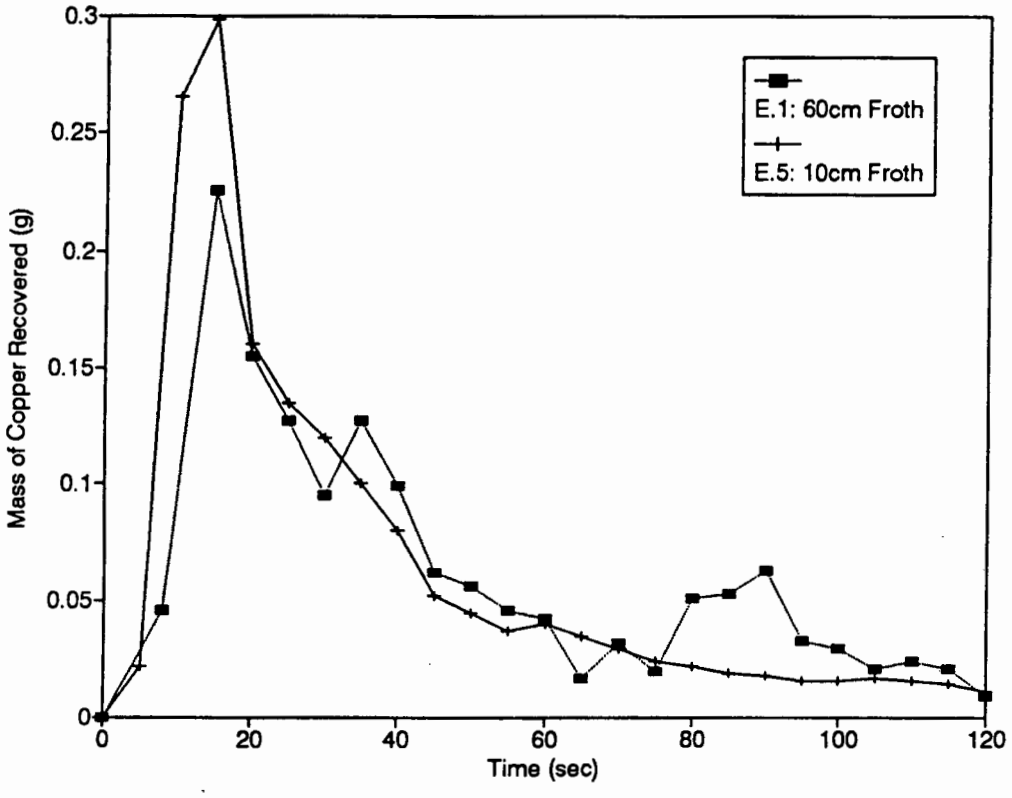

Figure 3.30: Incremental Mass of Copper Recovered to the Froth vs. Time Curves for a 10cm and 60cm froth

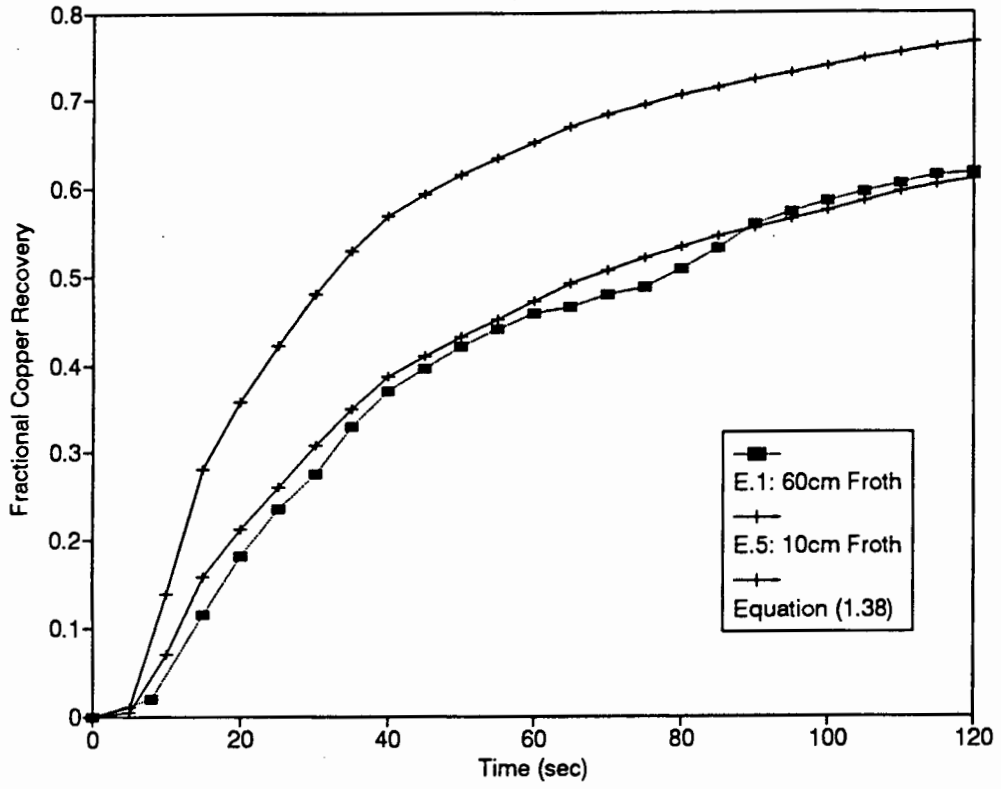

Figure 3.31: Copper Recovery vs. Time for a 10cm and 60cm Froth

Run Number	Frother Conc. (ppm)	Bubble Size (mm)	Fraction of Fast Floating Material	Fast Floating Rate Constant (min^{-1})	Slow Floating Rate Constant (min^{-1})	Final Recovery R_c (%)	Vessel Disp. Number
60cm Froth (R_f=0.48)							
E.1	50	1.73	0.69	3.6	0.53	87.81	0.07
10cm Froth (R_f=1.00)							
E.2	4	2.70	0.68	2.7	0.55	76.18	0.03
E.3	10	2.08	0.68	2.9	0.55	85.16	0.04
E.4	20	1.83	0.69	3.3	0.57	87.56	0.05
E.5	50	1.73	0.69	3.6	0.52	87.14	0.07
E.6	50	1.73	0.69	3.6	0.53	87.81	0.07

Table 3.9: Model Parameters obtained in the Curve Fitting of the Copper Recovery Curves

2.2.1 THE EFFECT OF BUBBLE SIZE ON COPPER RECOVERY

Figure 3.32 illustrates the effect of frother concentration and indirectly bubble size on the copper recovery vs. time curves. Increasing frother concentration and decreasing bubble size resulted in faster kinetics and increased final recoveries. Table 3.9 lists the modelling results for the various frother concentrations. Using the axial dispersion model and fast and slow floating rate constants an excellent fit was obtained for each of the curves. Figure 3.33 illustrates the curve fit of the model to the recovery vs. time curve obtained at the standard operating conditions (20ppm). The bubble sizes for the various frother concentrations were obtained from the curve in Figure 3.1. In Table 3.9 it can seen that with increasing bubble size the fraction of fast floating material and the slow floating rate constant remained relatively constant. Table 3.9 shows that the final recovery of copper increased with decreasing bubble size, but below a d_b of about 1.9mm the recovery levelled off. Figure 3.34 illustrates the change in the fast floating rate constant with increasing bubble size. The rate constant decreased markedly with increasing bubble size.

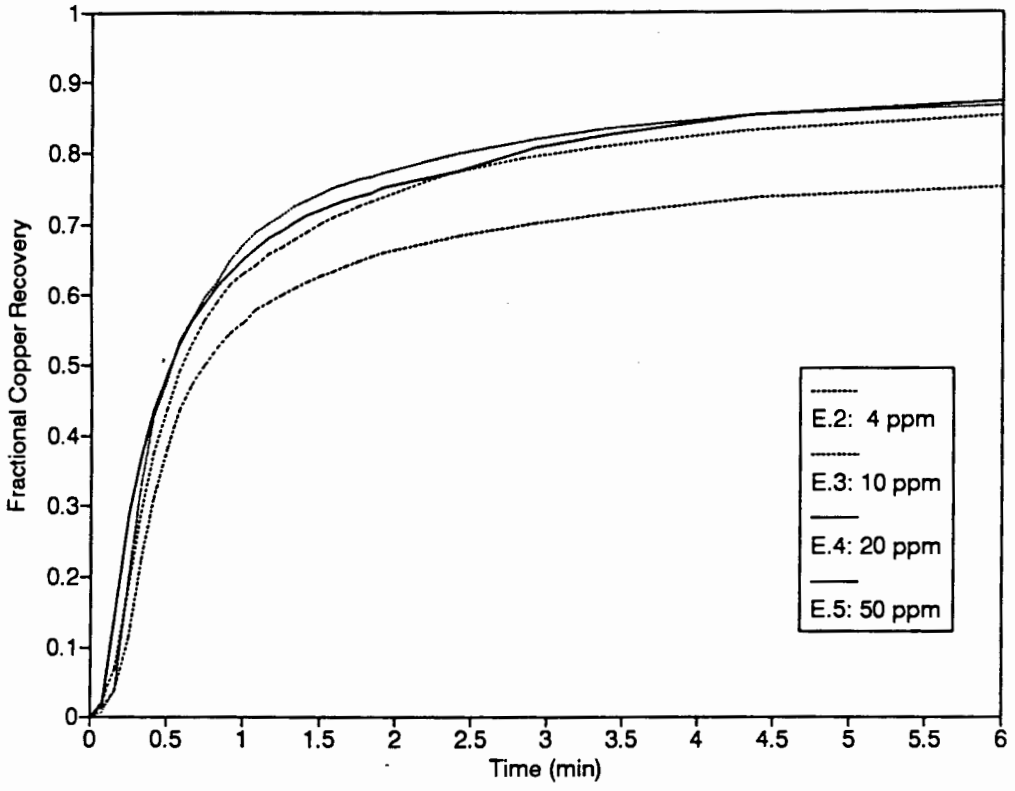

Figure 3.32: Copper Recovery vs. Time Curves for a Range of Frother Concentrations

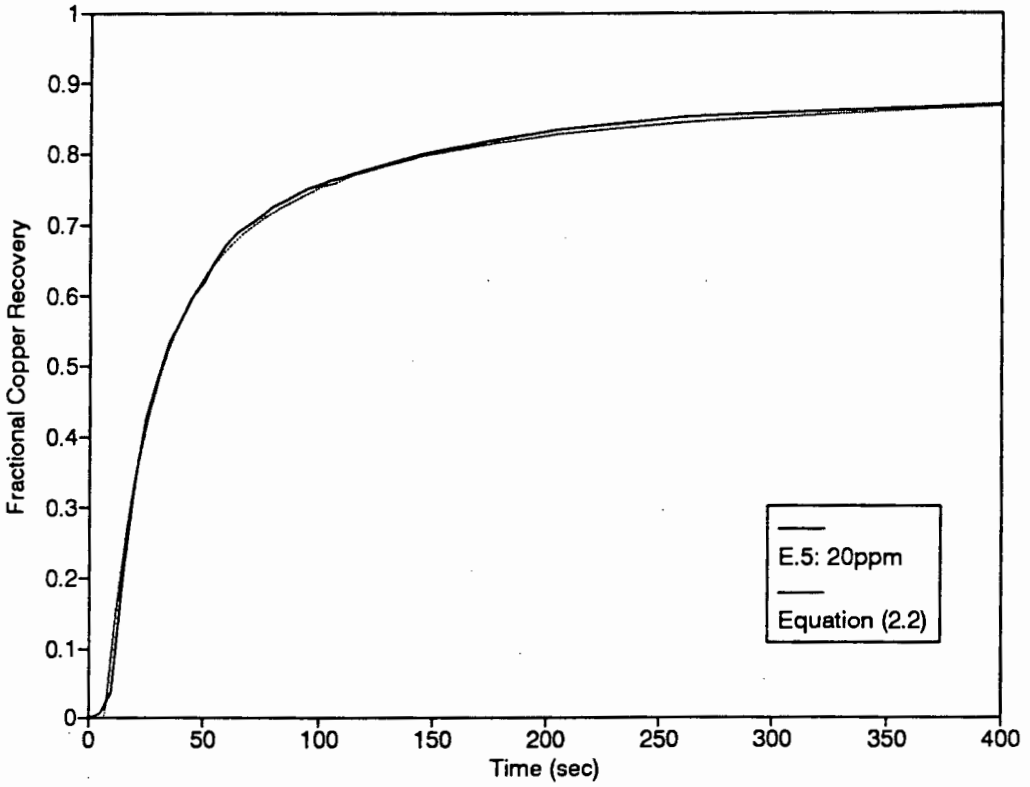

Figure 3.33: Model Fit of the Copper Recovery vs. Time Curve obtained at the Standard Operating Conditions

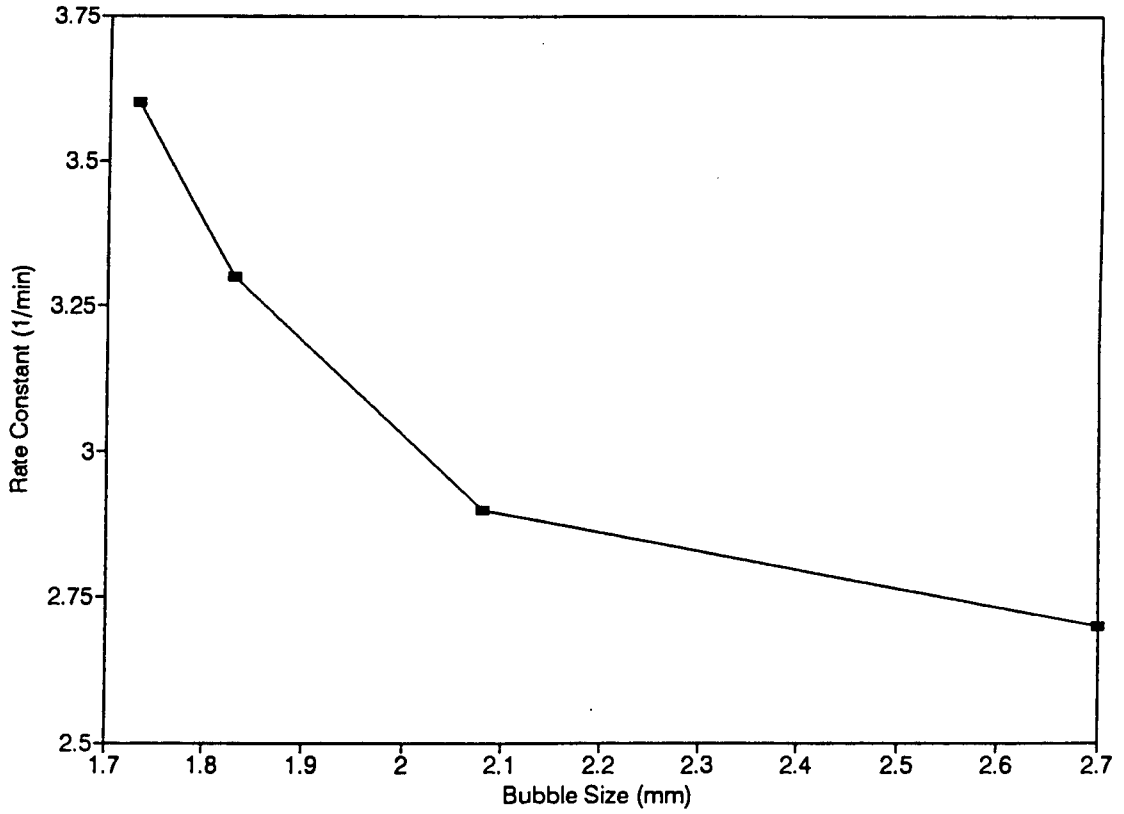

Figure 3.34: The Effect of Bubble Size on the Fast Floating Rate Constant

2.3 DETERMINATION OF THE COLLECTION ZONE RATE CONSTANT USING RADIOACTIVELY LABELLED PYRITE TRACERS

The recovery of radioactively labelled pyrite to the concentrate over time data for the tests performed in this section are listed in Appendix 2.

2.3.1 PILOT COLUMN STUDY

A similar column configuration and experimental procedure was used as in the chalcopyrite study and it was therefore assumed that the same reproducibility was obtainable. Table 3.10 lists the modelling results for the tests performed at the various operating conditions. For these tests a single rate constant and the axial dispersion model provided an excellent fit of the data. Figure 3.35 illustrates the model fit of the recovery vs. time curve obtained at the standard operating conditions. Also shown are the plug and mixed flow curves using the same rate constant. Equation (1.18) provided an excellent fit of almost all the curves obtained. Figure 3.35 also shows one of the curves for which the fit was not as good.

Run Number	Tracer Mean Particle Size (μm)	Gas Rate (cm/s)	Frother Conc. (ppm)	Bubble Size (mm)	Rate Constant (min^{-1})	Final Recovery R_c (%)	Vessel Disp. Number
F.1	56.5	2.00	25	1.83	1.26	69.87	0.032
F.2	56.5	2.24	25	1.83	1.31	73.17	0.032
F.3	56.5	2.42	25	1.83	1.47	75.02	0.032
F.4	56.5	2.67	25	1.83	1.57	77.86	0.032
F.5	56.5	2.86	25	1.83	1.65	78.94	0.032
F.6	56.5	2.24	4	2.70	0.90	62.39	0.021
F.7	56.5	2.24	7	2.25	1.00	69.02	0.024
F.8	56.5	2.24	10	2.08	1.10	73.09	0.027
F.2	56.5	2.24	25	1.83	1.31	73.17	0.032
F.9	56.5	2.24	40	1.73	1.97	72.91	0.040
F.10	19.0	2.24	25	1.83	0.86	28.79	0.027
F.2	56.5	2.24	25	1.83	1.31	73.17	0.032
F.11	90.5	2.24	25	1.83	1.87	72.98	0.035
F.12	128.0	2.24	25	1.83	1.62	50.25	0.059
F.13	181.0	2.24	25	1.83	1.28	35.55	0.070

Table 3.10: Model Parameters obtained in the Curve Fitting of the Pilot Column Pyrite Recovery Curves

2.3.1.1 The Effect of Gas Flow Rate on Pyrite Recovery

Figure 3.36 illustrates the recovery vs. time curves for the range of gas rates. Final recovery increased with increasing gas flow rate. From Table 3.10 and Figure 3.37 it can seen that the rate constant increased almost linearly with increasing gas flow rate.

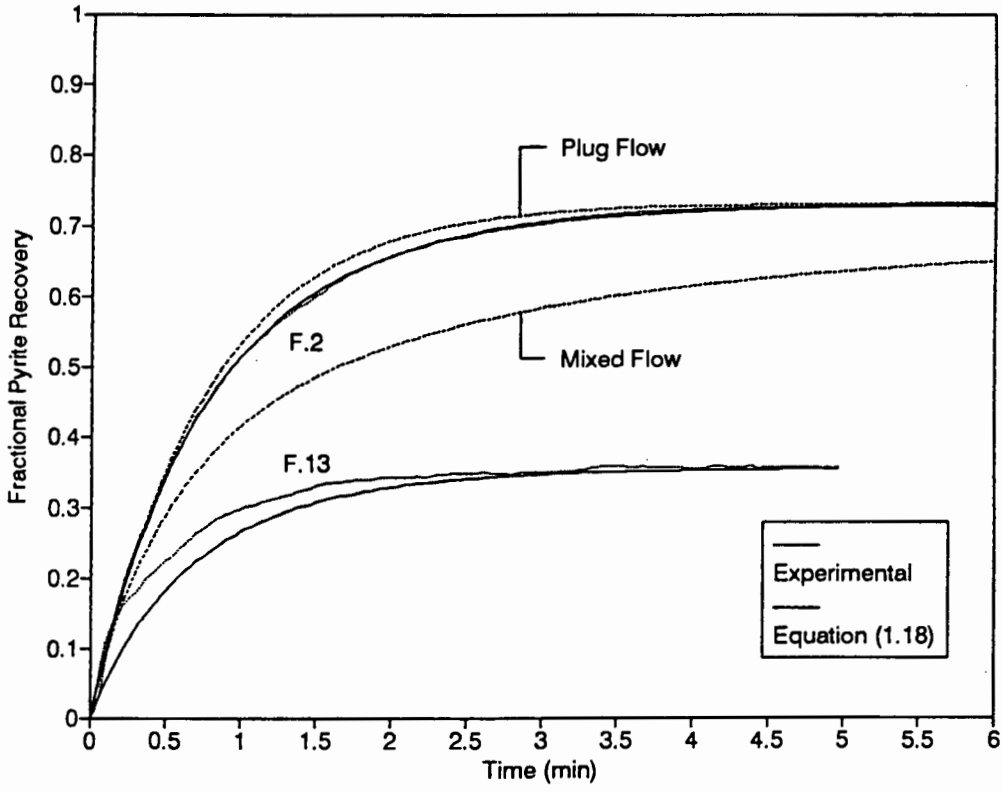

Figure 3.35: Model Fit of the Pyrite Recovery vs. Time Curves for Tests F.2 and F.13

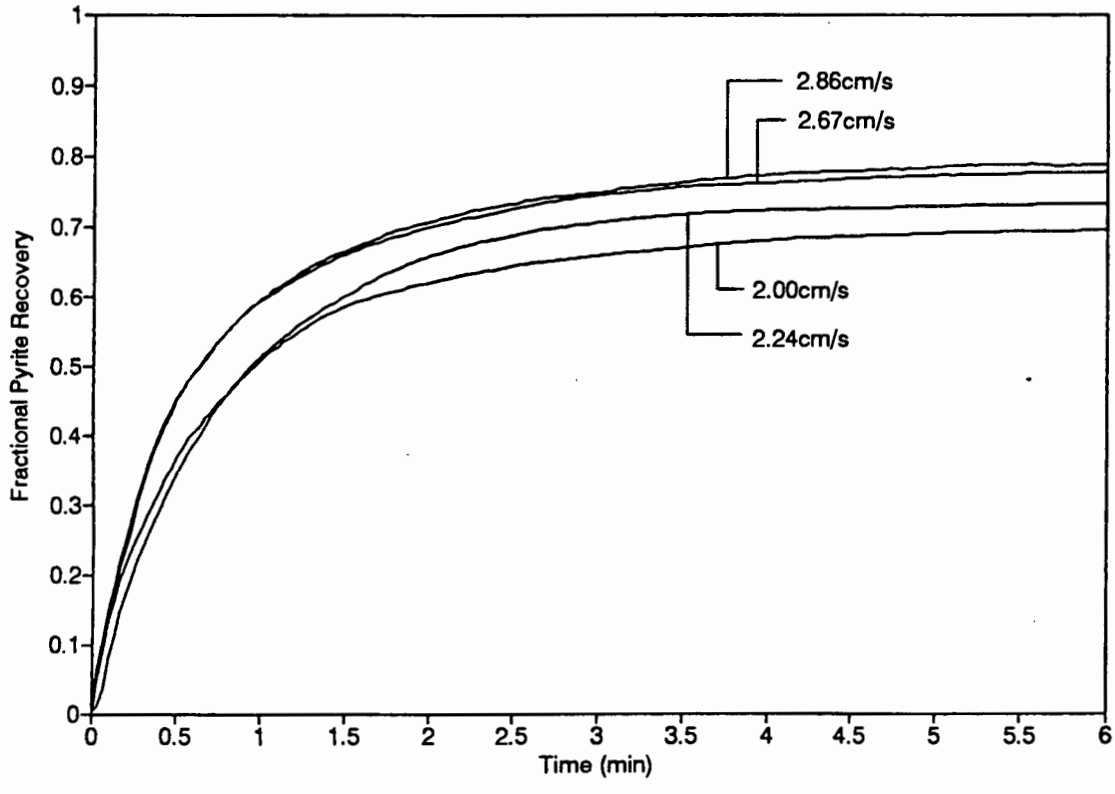

Figure 3.36: Pyrite Recovery vs. Time Curves for a Range of Gas Flow Rates

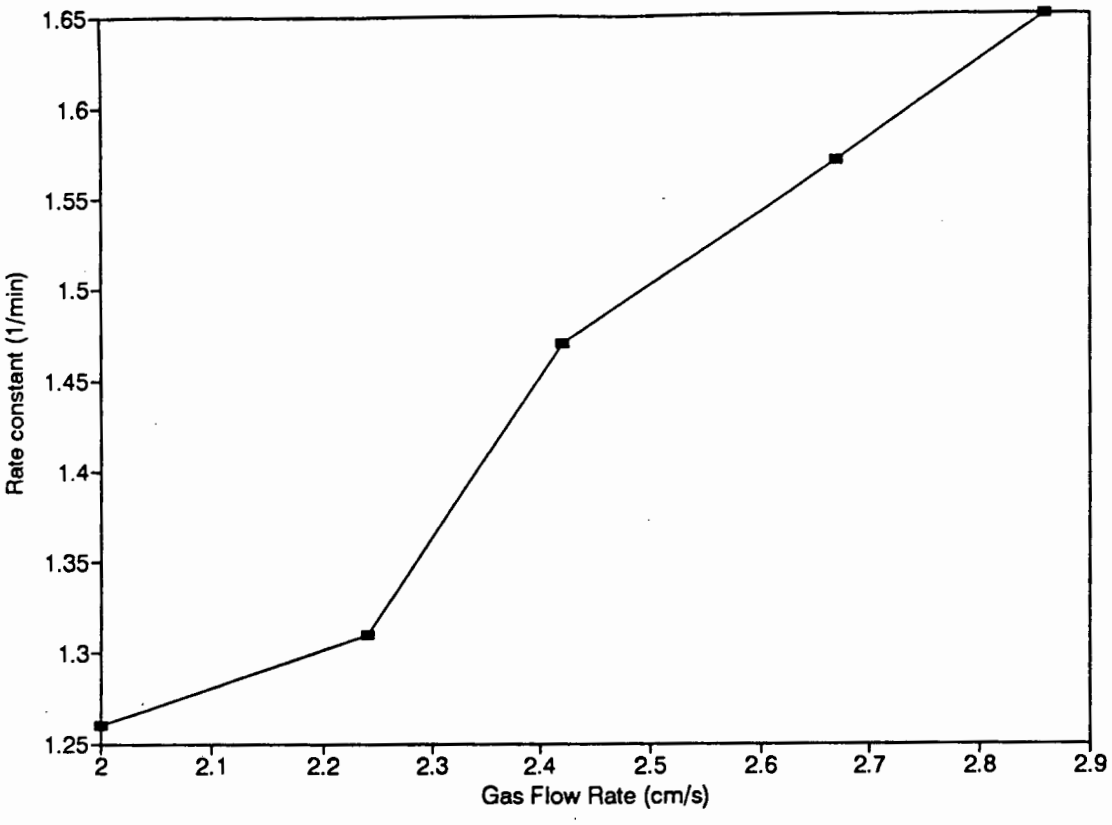

Figure 3.37: The Effect of Gas Flow Rate on the Rate Constant

2.3.1.2 The Effect of Bubble Size on Pyrite Recovery

Figure 3.38 illustrates the recovery vs. time curves for three of the frother concentrations. The curve illustrated in Figure 3.1 was again used to determined the bubble sizes at the various frother concentrations. From Table 3.10 it can be seen that with decreasing bubble size the final recovery increased down to a d_b of about 2.1mm below this bubble size the recovery levelled off. Figure 3.39 illustrates the rate constants obtained at the different bubble sizes. The rate constant decreased with increasing bubble size.

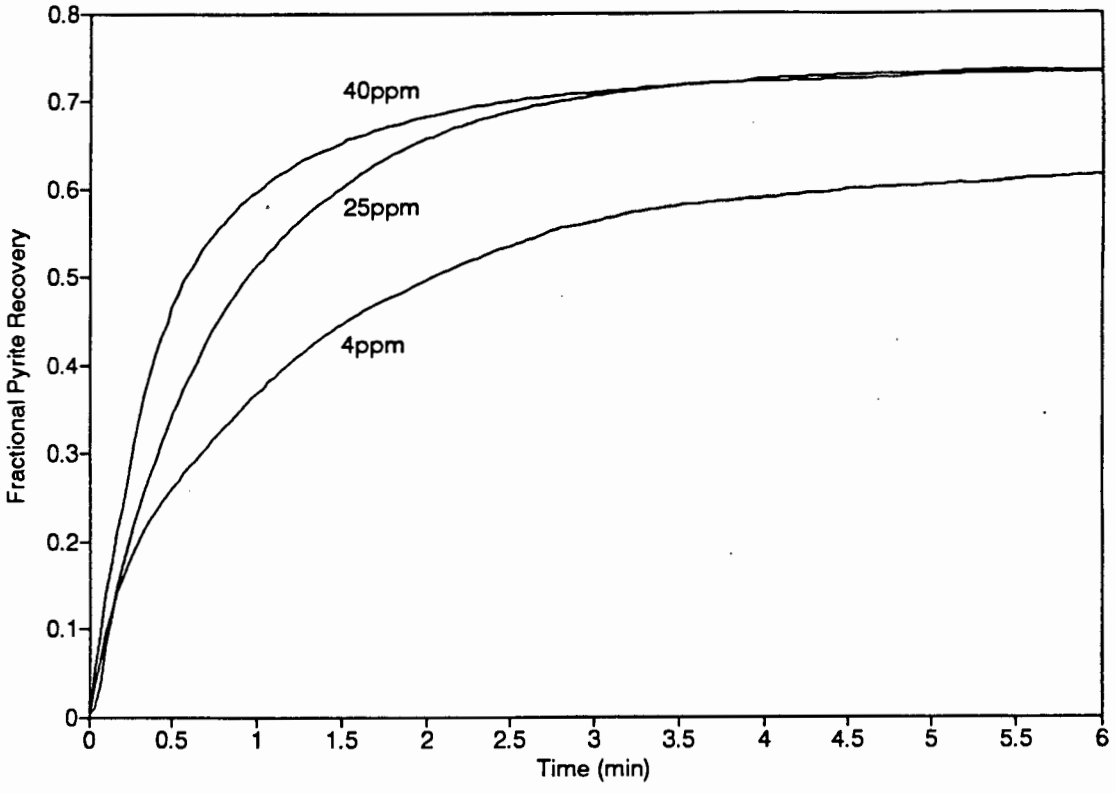

Figure 3.38: Pyrite Recovery vs. Time Curves for a Range of Frother Concentrations

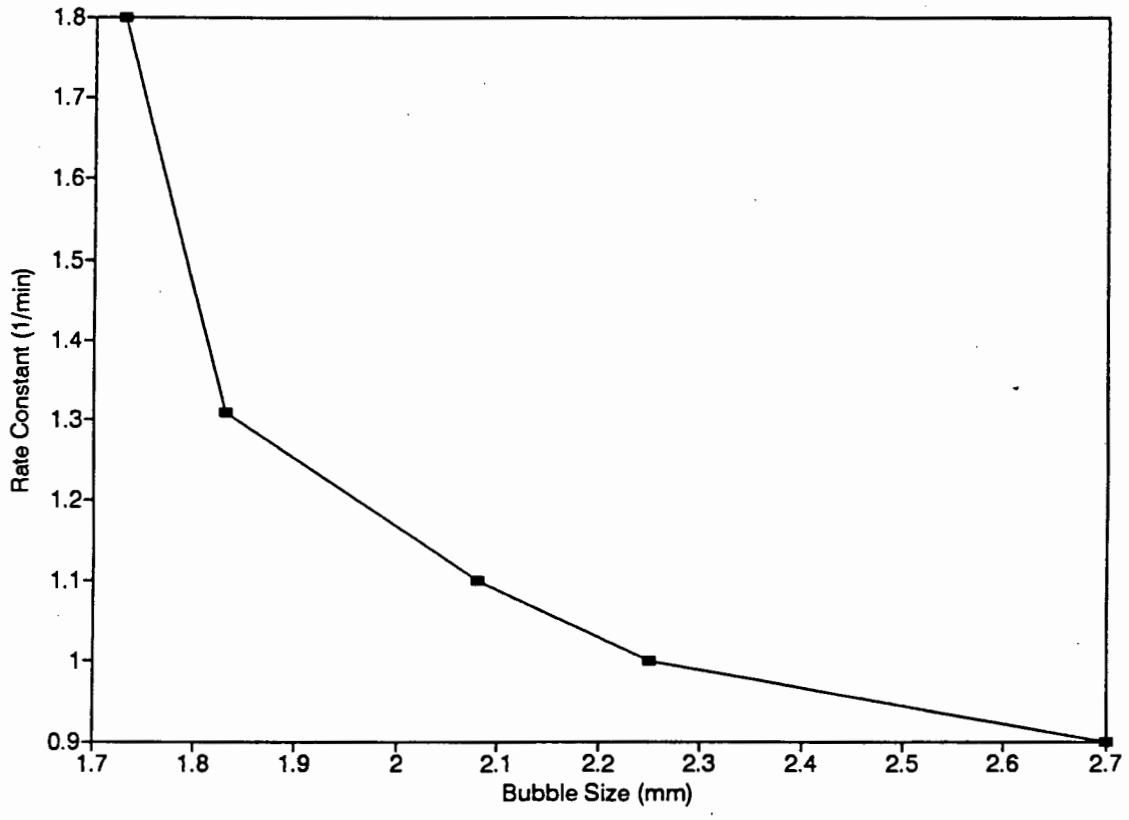

Figure 3.39: The Effect of Bubble Size on the Rate Constant

2.3.1.3 The Effect of Particle Size on Pyrite Recovery

Figure 3.40 illustrates the tracer recovered vs. time curves for the range of tracer particle sizes used. The shape of curve obtained for the largest particle size fraction (+150-212μm) did not match the other curves and the model fit of this curve was poor (see Figure 3.35). Figure 3.41 illustrates the final recovery of pyrite for the different particle sizes. The curve has an optimum over the 50μm to 90μm size range. Figure 3.42 illustrates the change in the rate constant with particle size. This curve also has an optimum value which is at about 90μm.

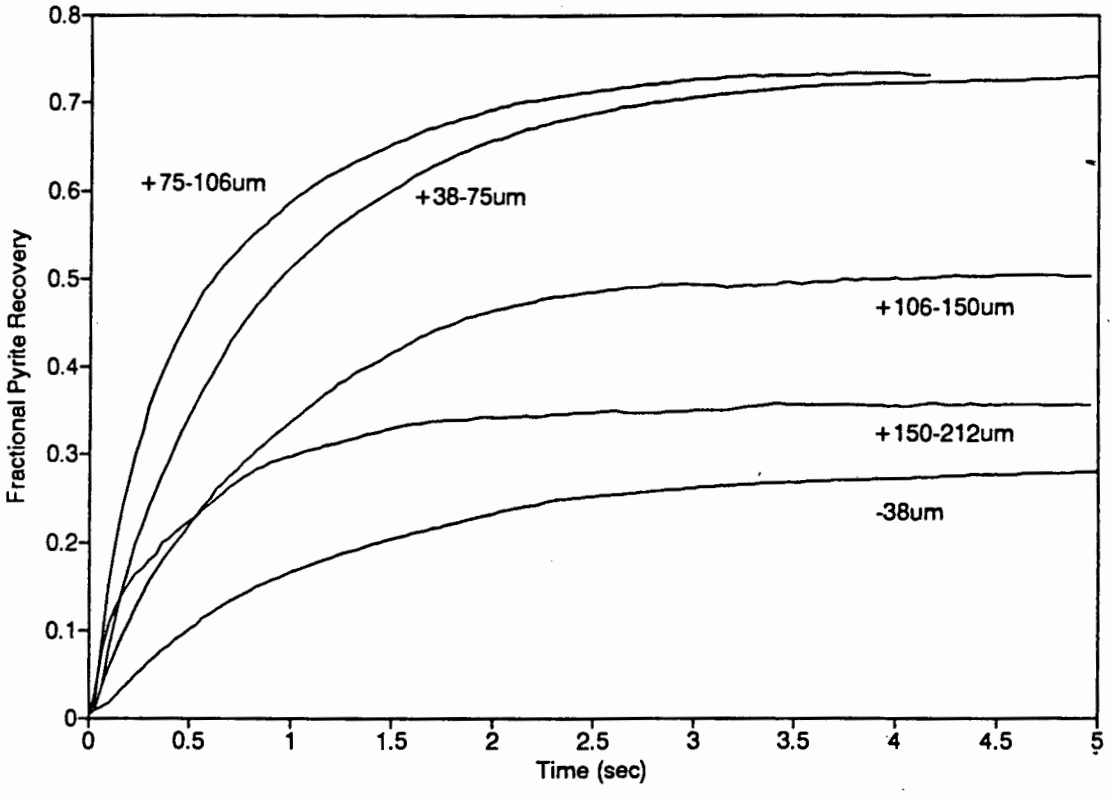

Figure 3.40: Pyrite Recovery vs. Time Curves for a Range of Particle Size Fractions

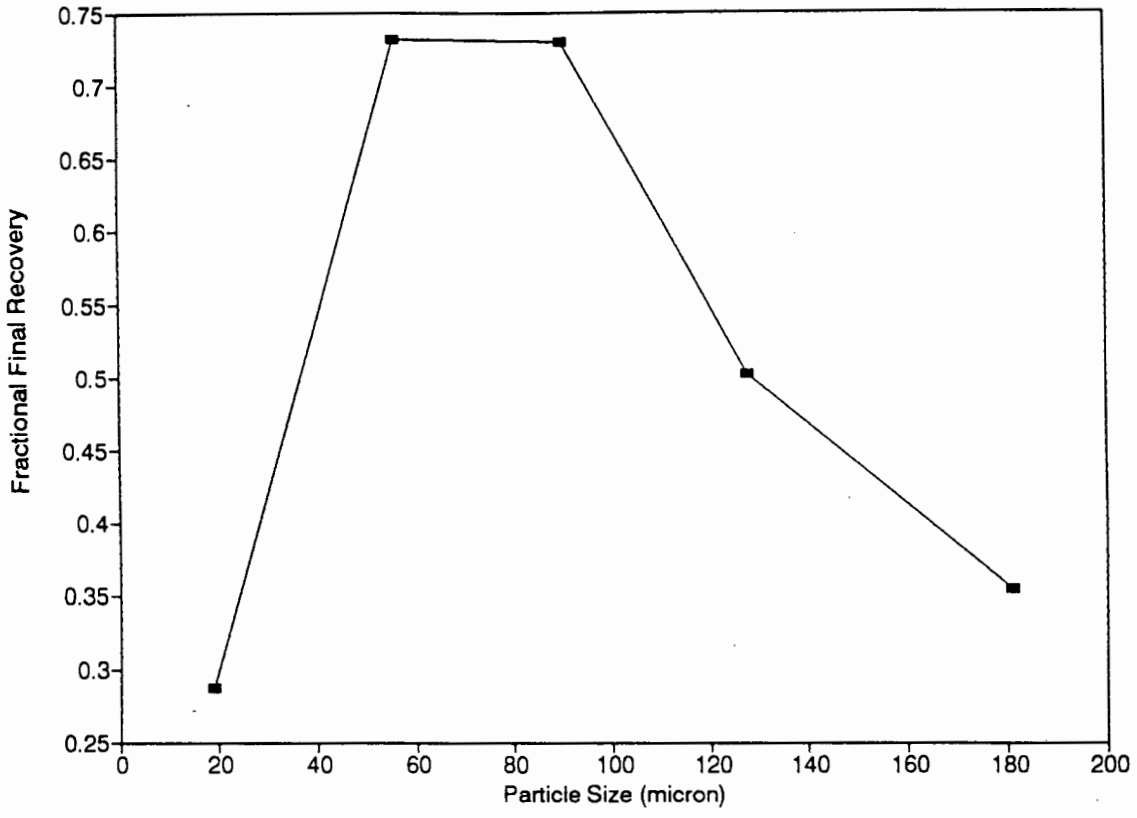

Figure 3.41: The Effect of Particle Size on the Final Recovery

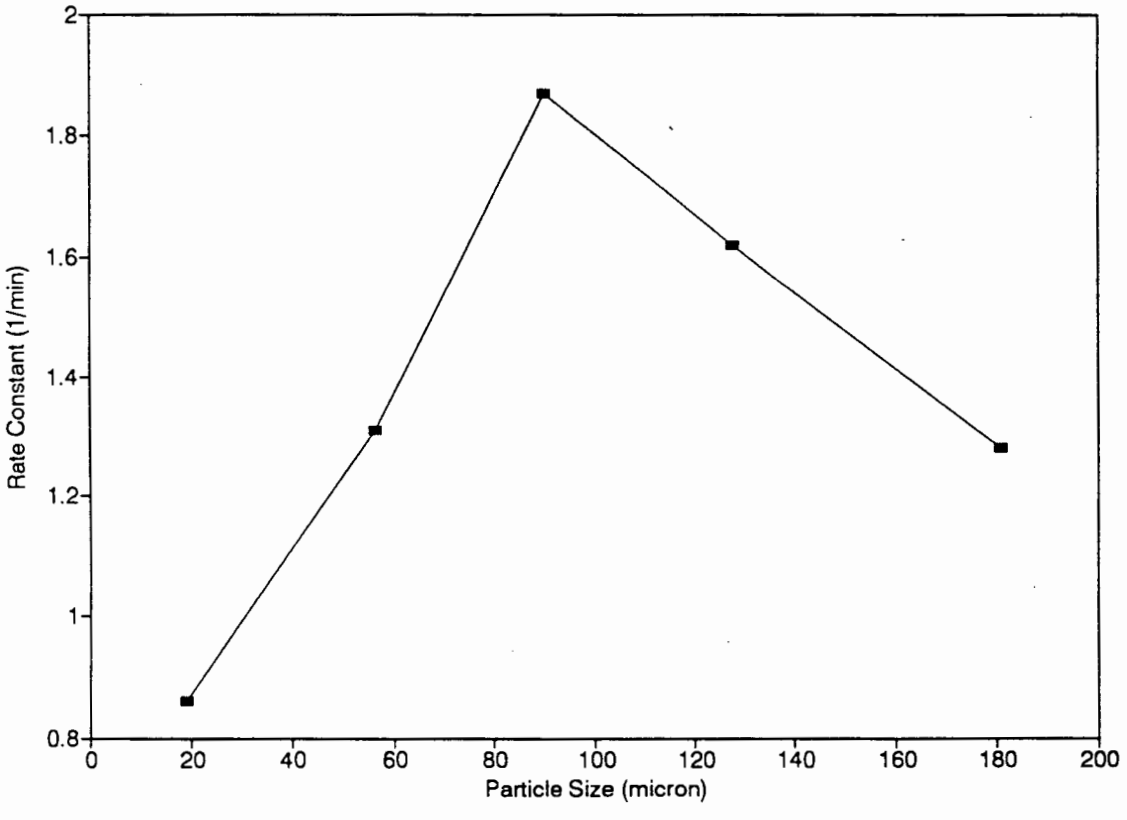

Figure 3.42: The Effect of Particle Size on the Rate Constant

2.3.2 PRESIDENT STEYN INDUSTRIAL COLUMN STUDY

Figure 3.43 illustrates the tracer recovered over time curves for all the tests performed on the industrial column. The two runs performed using the +38-75μm fraction indicate that the tests were reproducible. The tracer recoveries were significantly lower than the recoveries obtained in the pilot column. A single rate constant and the axial dispersion model produced good curve fits of the recovery vs. time curves. Figure 3.44 shows the curve fit for the +38-75μm fraction as well as the plug and mixed flow curves for the same rate constant. Table 3.11 lists the curve fitting results for the tests performed. As in the previous kinetics tests froth zone recovery was assumed to be 100%. The rate constants obtained were substantially lower than the rate constants measured for the equivalent tracers in the pilot column. An attempt was made to obtain a fit of the curves by varying the froth zone recovery and using Equation (1.38) however this proved to be unsuccessful.

Run Number	Tracer Sample	Rate Constant (min^{-1})	Final Recovery (%)	Vessel Dispersion Number
G.1	-38μm	0.22	11.01	0.750
G.2	+38-75μm	0.31	49.00	0.630
G.3	+38-75μm	0.34	48.70	0.630
G.4	+75-106μm	0.20	48.00	0.580

Table 3.11: Model Parameters obtained in the Curve Fitting of the President Steyn Column Pyrite Recovery Curves

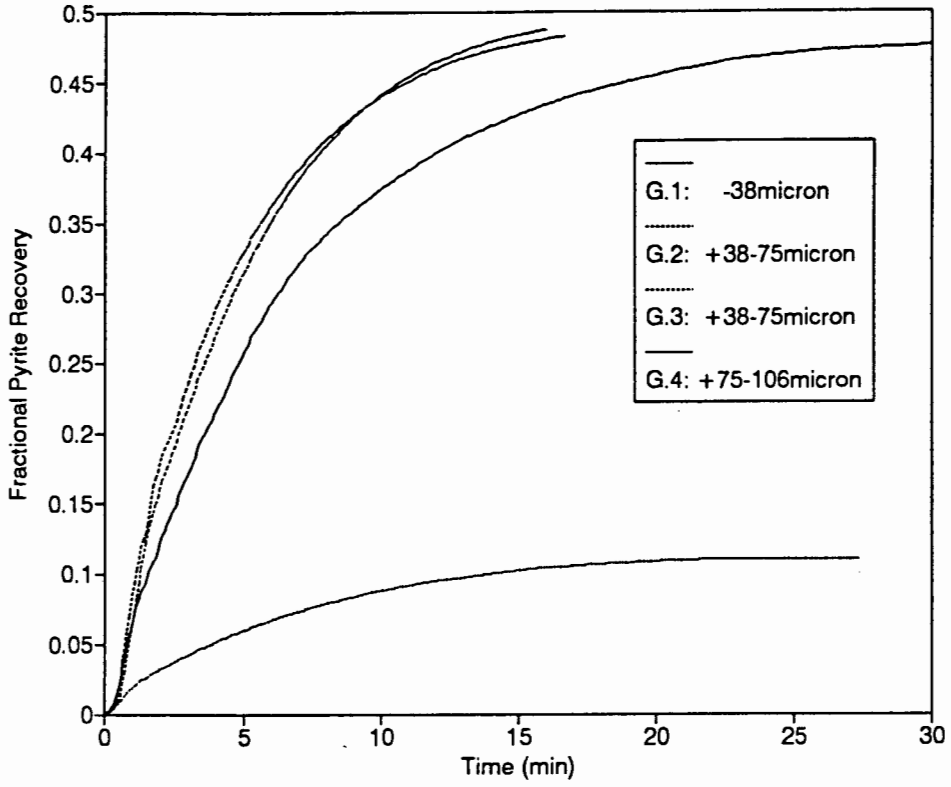

Figure 3.43: Recovery of Pyrite vs. Time Curves obtained in President Steyn Column Testwork

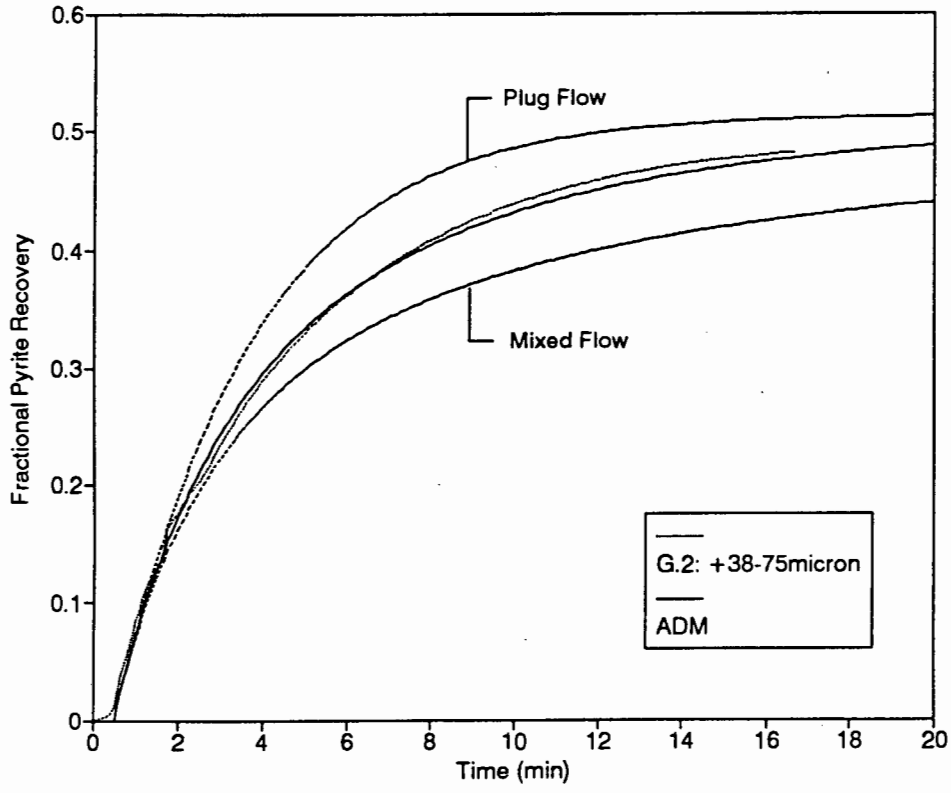

Figure 3.44: Model Fit of the Pyrite Recovered for the +38-75µm Fraction vs. Time Curve

2.3.2.1 Prediction of Industrial Column Performance using Pilot Column Results

Figure 3.45 shows the recovery vs. time curve for the +38-75μm fraction in the industrial column. Also shown is the curve fit using Equation (1.18) and a curve using Equation (1.18) and the collection zone rate constant obtained for the same tracer and similar operating conditions in the pilot column. It is clear from this figure that the assumption of equivalent collection zone rate constants in the pilot and President Steyn industrial columns did not hold.

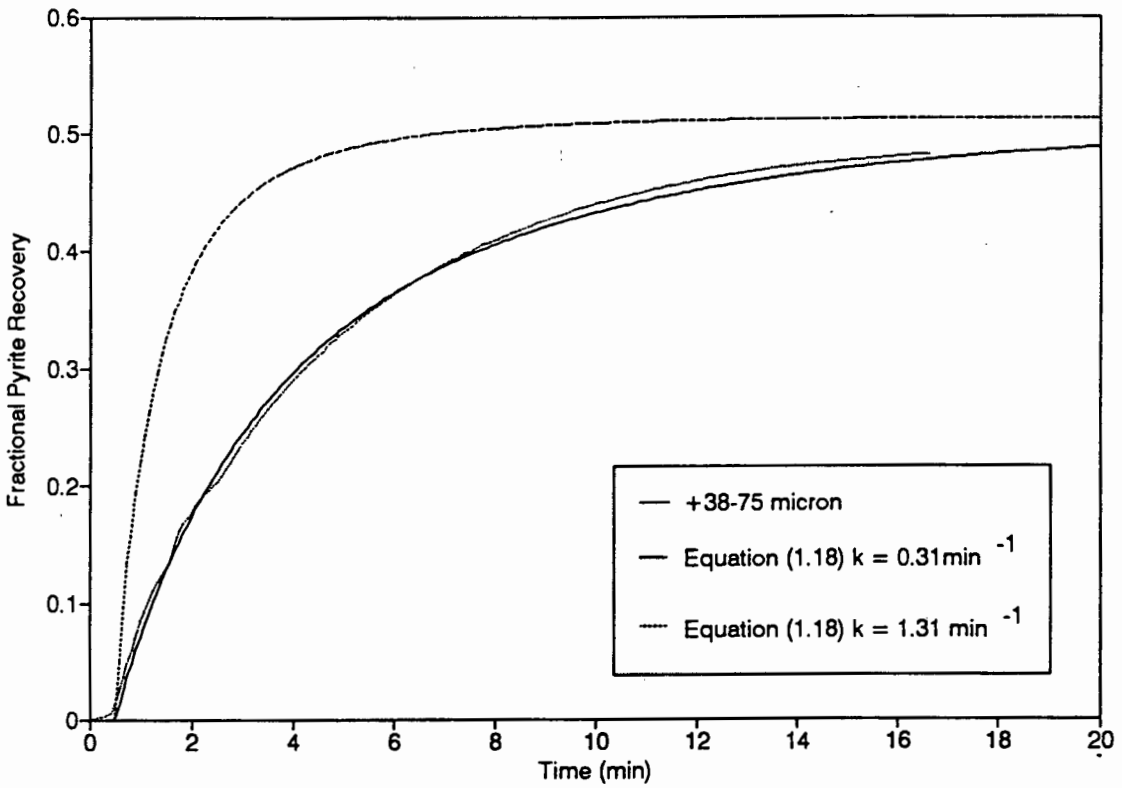

Figure 3.45: Curve of Pyrite Recovered for the +38-75μm Fraction vs. Time and Equation (1.18) using Industrial and Pilot Column Collection Zone Rate Constants

2.4 FITTING THE EXPERIMENTALLY DETERMINED RATE CONSTANTS TO THE PARTICLE COLLECTION MODEL

For the tests performed using the chalcopyrite tracers on the laboratory column and the pyrite tracers on the pilot column Equation (1.41) was used to determine the collection efficiencies. Figure 3.46 illustrates the experimental collection efficiencies for the range of operating conditions tested. The collection efficiency curve for the range of tracer particle sizes tested has an optimum at a d_p of about 90μm. For both the chalcopyrite and pyrite tracers the collection efficiency decreased with increasing bubble size, however in both cases for the largest bubble size (2.70mm) E_K increased from the lower bubble size. The collection efficiency remained virtually constant with increasing air rate.

Table 3.12 lists results obtained from the particle collection model as detailed in Chapter 1 Sec. 3.2. Figure 3.47 illustrates the effect of the different parameters on the collision efficiency as determined by the model. As discussed earlier particle size has a large effect on the collision efficiency; increasing particle size results in an increase in E_C. With increasing bubble size E_C decreased marginally while the model showed no effect of air rate on E_C.

Figure 3.48 illustrates the effect of the range of parameters on the attachment efficiencies determined using Equation (1.42) and the collision efficiencies determined above. The attachment efficiency increased with decreasing particle size. For the smallest particle size E_A increased tenfold over the larger particle sizes. The effect of bubble size on the attachment efficiency was similar for the chalcopyrite and pyrite tracers although the chalcopyrite values were significantly higher. Initially E_A decreased with increasing d_b but with larger bubble sizes it began to increase. The attachment efficiency was unaffected by the gas rate.

Figure 3.49 shows the iteratively determined induction times for range of parameters investigated. With increasing particle size the induction time decreased markedly. The chalcopyrite and pyrite tracers exhibited similar trends for the range of bubble sizes tested; t_i remained virtually constant except for the largest d_b (2.70mm) were it decreased. The chalcopyrite induction times were lower than those determined using the

pyrite tracers. The induction times did not change over the range of air rates tested. Figure 3.49 also illustrates the induction times determined using Equation (1.58). The values predicted by the equation are significantly lower than the experimental induction times.

Run Number	Collection Efficiency (%)	Collision Efficiency (%)	Attachment Efficiency (%)	Induction Time (msec)
Frother Concentration (Chalcopyrite)				
E.2	0.33	2.7	12.4	18.4
E.3	0.30	2.5	12.0	18.4
E.4	0.30	2.2	14.0	18.3
E.5	0.31	1.6	19.7	11.4
Gas Flow Rate				
F.1	0.13	2.9	4.5	21.4
F.2	0.12	2.9	4.2	21.5
F.3	0.12	2.9	4.2	21.5
F.4	0.12	2.9	4.2	21.5
F.5	0.12	2.9	4.2	21.5
Frother Concentration				
F.6	0.12	1.8	6.6	14.1
F.7	0.11	2.2	5.1	20.5
F.8	0.11	2.4	4.7	21.5
F.2	0.12	2.9	4.2	21.5
F.9	0.17	3.0	5.4	20.1
Particle Size				
F.10	0.08	0.2	46.5	47.3
F.2	0.12	2.9	4.2	21.5
F.11	0.17	8.7	1.9	15.7
F.12	0.15	19.4	0.8	13.2
F.13	0.12	42.4	0.3	10.8

Table 3.12: Model Parameters obtained from the Particle Collection Model for the Testwork Performed

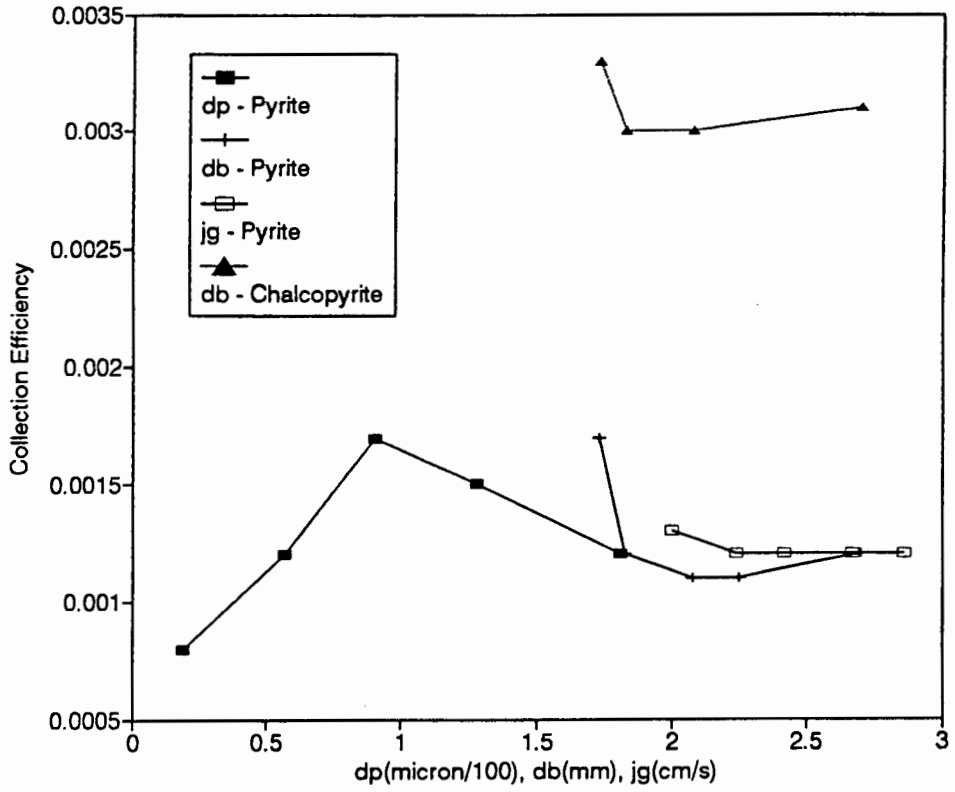

Figure 3.46: The Effect of Gas Flow Rate, Bubble Size and Particle Size on the Collection Zone Efficiency

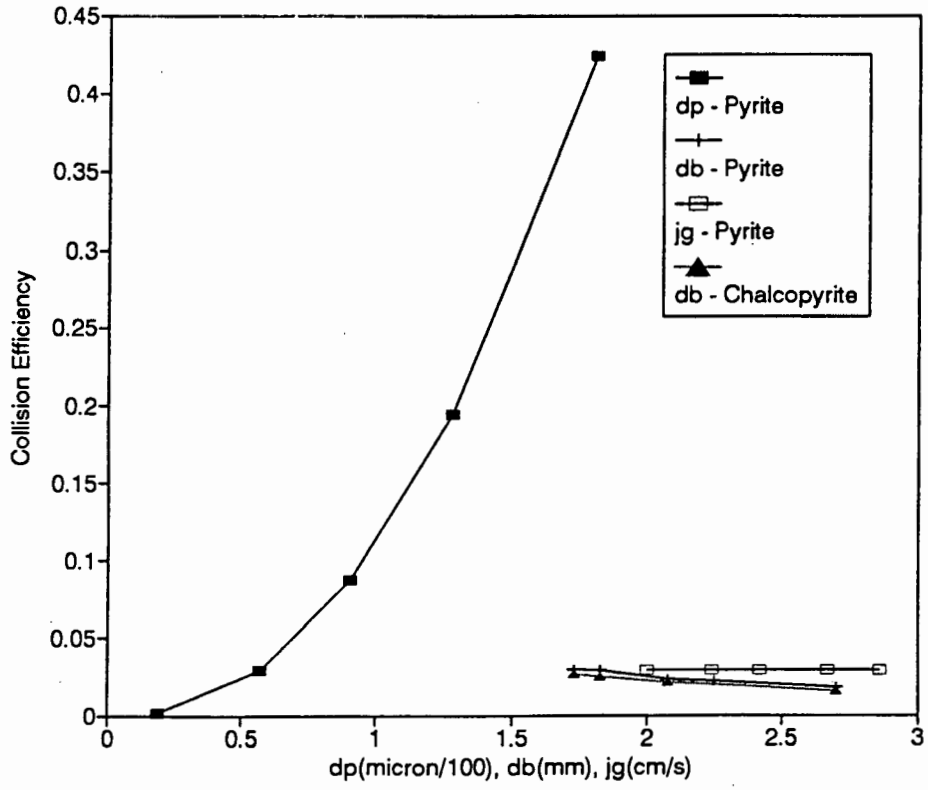

Figure 3.47: The Effect of Gas Flow Rate, Bubble Size and Particle Size on the Collision Efficiency

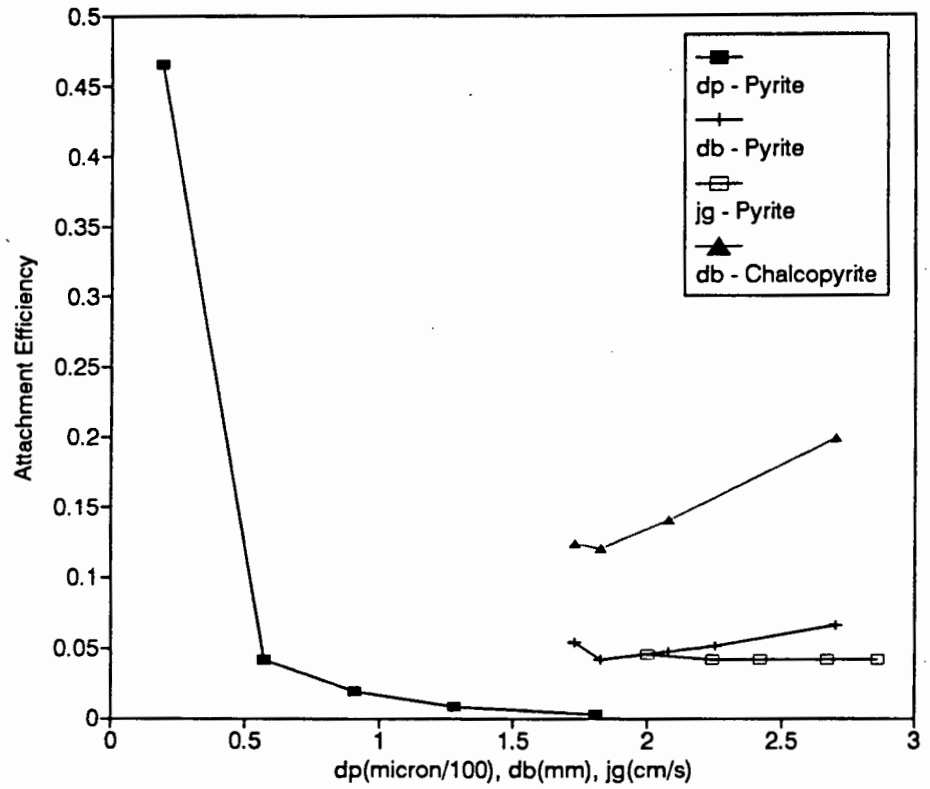

Figure 3.48: The Effect of Gas Flow Rate, Bubble Size and Particle Size on the Attachment Efficiency

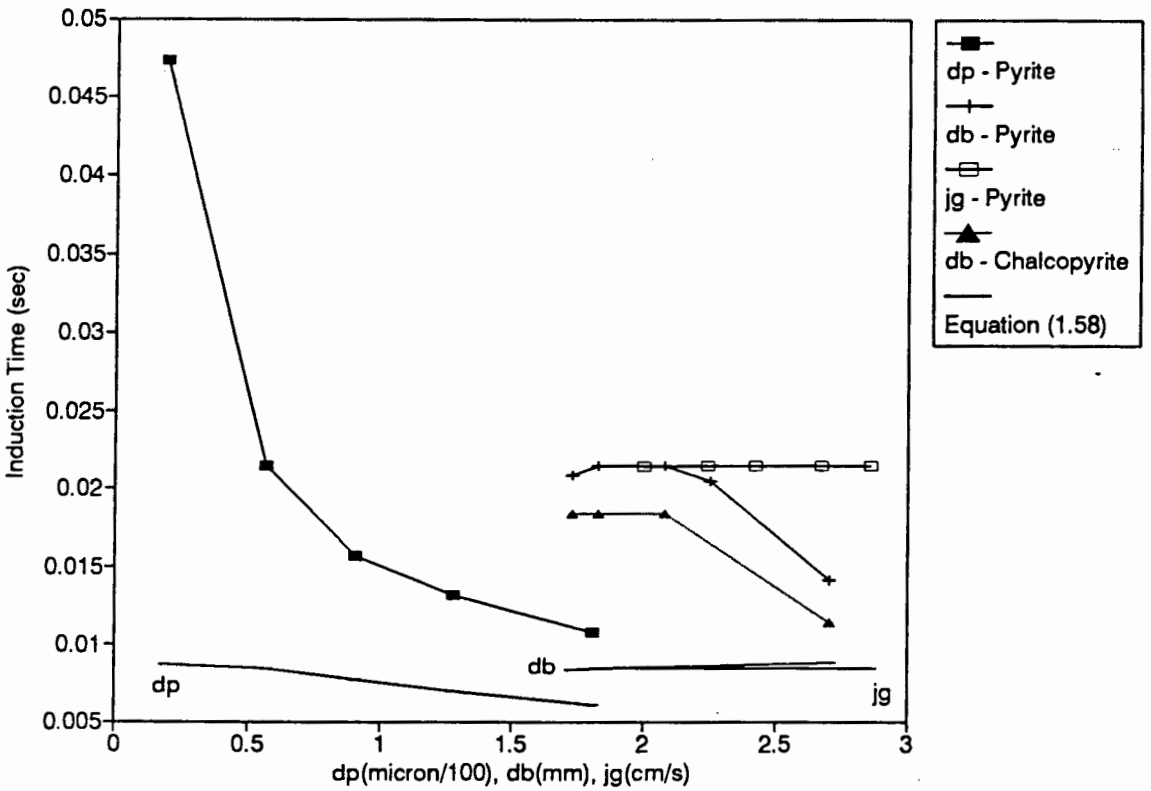

Figure 3.49: The Effect of Gas Flow Rate, Bubble Size and Particle Size on Induction Time

CHAPTER 4

DISCUSSION

1. STUDY OF THE MIXING CHARACTERISTICS OF THE COLLECTION ZONE

The study of the mixing characteristics of the collection zone began with the preliminary liquid tracer RTD study performed on a laboratory column. Two further RTD studies using radioactively labelled solid and liquid tracers were performed in order to validate results obtained in the preliminary study for a range of column diameters. The results of the preliminary study are discussed in the next section. Following this section the curve fitting of RTD data using the axial dispersion model is discussed. Finally an analysis of the data obtained from the radioactively labelled tracer RTD studies as well as similar data of Yianatos and Bergh (1990) is presented.

1.1 PRELIMINARY RTD STUDY

The preliminary RTD study was performed in order to link up with the solid tracer RTD study of Goodall and O'Connor (1991). The following sections discuss the effect of the feed percent solids and superficial gas rate on the degree of mixing of the solid and liquid tracers in the collection zone. Furthermore liquid tracer testwork performed to establish the effect of bubble size on collection zone mixing is discussed. The final section compares the vessel dispersion numbers determined using solid and liquid tracers and calculated using empirical correlations.

1.1.1 THE EFFECT OF THE FEED PERCENT SOLIDS ON THE DEGREE OF MIXING

Figure 4.1 illustrates the effect of varying the feed percent solids on the vessel dispersion number of the liquid salt tracer used in the preliminary RTD study and the radioactively labelled solid tracer used in

the study performed by Goodall and O'Connor (1991). Except for the fact that a sintered glass frit was used to aerate the column the operating conditions, column configuration, ore and reagent suite used in the study of Goodall and O'Connor (1991) were all the same as used in the preliminary RTD study. With increasing feed percent solids the liquid tracer vessel dispersion number remained constant within the experimental error, whereas the solid tracer dispersion numbers were substantially higher than the liquid tracer dispersion numbers and decreased with increasing feed percent solids. The fact that the solid dispersion numbers (D_p/u_pL) were larger than the liquid dispersion numbers (D_l/u_lL) indicates that the solid dispersion coefficients were larger than the liquid coefficients (solid interstitial velocities (u_p) are higher than the liquid velocities (u_l) due to the added contribution of terminal settling velocities to the solid interstitial velocities). Increasing the feed percent solids affected the liquid and solid dispersion number differently thus also indicating that the dispersion coefficients may not have been equivalent in the laboratory column.

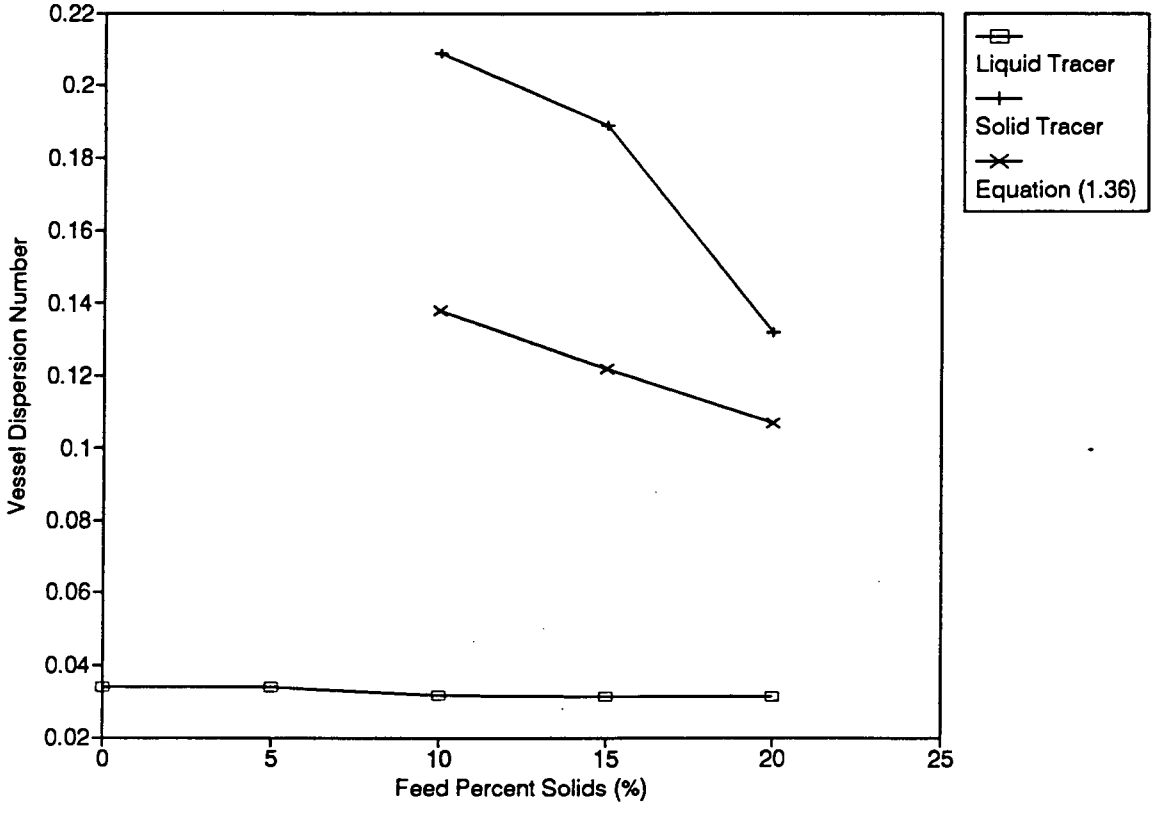

Figure 4.1: The Effect of the Percentage of Solids in the Feed on the Degree of Mixing

1.1.2 THE EFFECT OF THE SUPERFICIAL GAS RATE ON THE DEGREE OF MIXING

After ascertaining that the presence of solids did not significantly affect the liquid mixing the rest of the preliminary study RTD tests were performed without the presence of solids. Figure 4.2 illustrates the effect of the varying the superficial gas rate on the vessel dispersion number of the liquid salt tracer used in the preliminary RTD study and the radioactively labelled solid tracer used in the study performed by Goodall and O'Connor (1991). The liquid and solid vessel dispersion numbers increased with increasing gas rate. This is in agreement with dispersion coefficient prediction correlations for example Equation (1.36) where the dispersion coefficient is proportional to $j_g^{0.33}$. The bubble size was found to remain constant for the range of gas flow rates used in the preliminary RTD study (1.69 to 2.74cm/s) due to the level of frother concentration (25ppm) and the design of the sparger. It is proposed that the increase in mixing with increasing superficial gas velocity was due to the increase in the number of bubbles. A tracer test (A.8) performed in the absence of bubbles showed that the flow character was typical of plug flow. Mixing in the collection zone is due to the presence of bubbles and the interaction of both the liquid and solids with these bubbles. Therefore an increase in the number of bubbles will result in increased liquid and solid interaction with bubbles resulting in increased mixing. Bubble size measurement work performed in a recent study by Saxena et al. (1990) showed that for a range of gas flow rates in a 30.5cm diameter bubble column viz. 3.6 - 9.2cm/s the bubble size was independent of gas velocity. It is likely that the effect of gas velocity on the vessel dispersion coefficient in both Equation (1.33), which was developed for bubble columns operating at gas flow rates between 0.5 and 7cm/s and Equation (1.36) is due to increases in the number of bubbles. As in the tests where the feed percent solids was varied the solid dispersion numbers were larger than the liquid dispersion numbers.

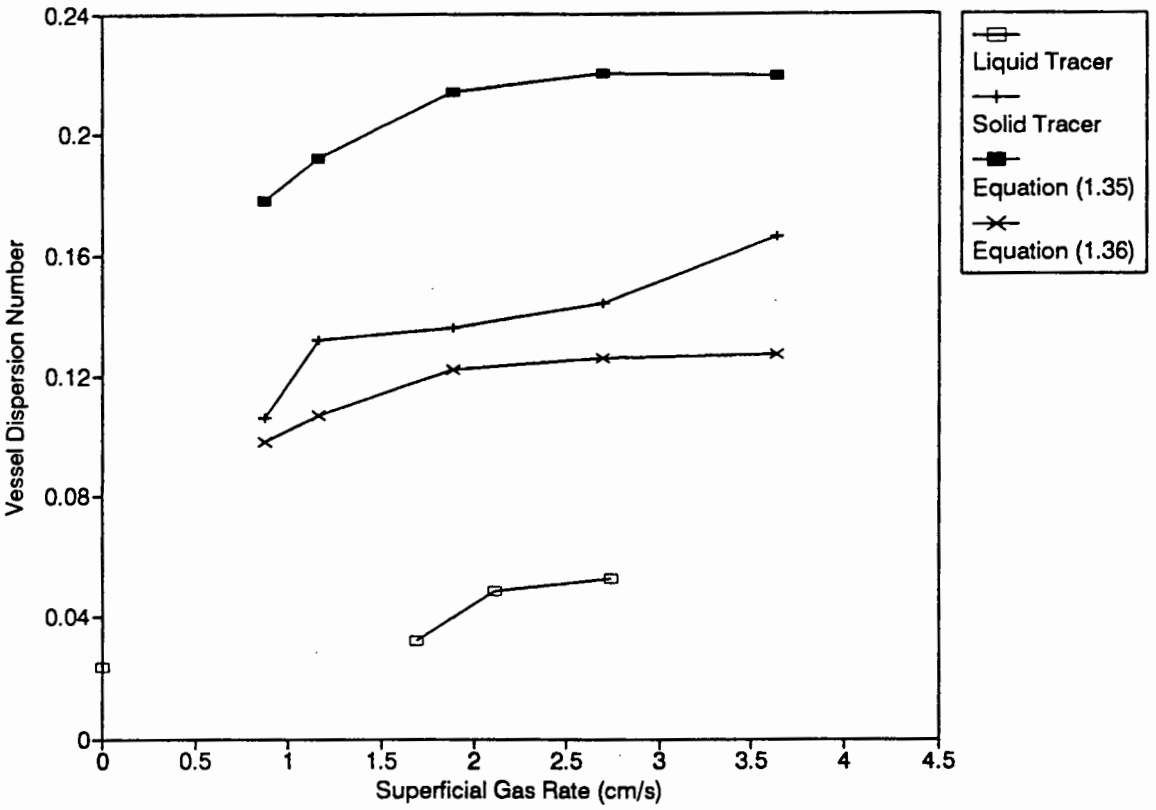

Figure 4.2: The Effect of Superficial Gas Rate on the Degree of Mixing

1.1.3 THE EFFECT OF BUBBLE SIZE ON THE DEGREE OF MIXING

Figure 3.9 shows that the degree of mixing increases substantially with decreasing bubble size for the two types of sparger used in the liquid tracer RTD testwork. It is clear from this figure that for the range of bubble sizes used in flotation columns the degree of mixing is dependent on the bubble size. The mixing conditions at the same frother concentrations also varied for the USBM-type and filter cloth spargers. This could have been due to a difference in the bubble size distributions produced and the way in which the air was induced into the column by the two types of spargers. In the present testwork the gas flowrate was kept constant, bubble size was reduced by adding more frother and this resulted in substantial increases in the number of bubbles. As discussed earlier, this resultant increase in mixing is attributed to the increase in the number of bubbles. By extrapolating this result to industrial columns it is clear that flotation columns, which have smaller and substantially more bubbles, will be more mixed than bubble columns.

1.1.4 COMPARISON OF PREDICTED AND EXPERIMENTAL VESSEL DISPERSION NUMBERS

A number of correlations are presented in the literature to predict the solids vessel dispersion coefficient in flotation columns (see Chapter 1 Sec. 2.3.3). These correlations were developed from liquid tracer RTD studies on flotation and bubble columns and predict the solid vessel dispersion number by assuming solid and liquid dispersion coefficients to be equivalent. Figures 4.1 and 4.2 illustrate the prediction of the solid vessel dispersion numbers for varying feed percent solids and superficial gas rate for two of these correlations (Equations (1.35) and (1.36)). Equation (1.36) gives an adequate prediction of the solid dispersion number for the range of operating conditions investigated in the solid tracer studies. However these correlations are based on the assumption that the liquid and solid tracer dispersion coefficients are equivalent and therefore predictions of the vessel dispersion numbers for the liquid phase would be significantly higher than for the solids (since $D/u_l L > D/u_p L$). This is not in agreement with the results obtained in the preliminary RTD study.

Although the results of the preliminary study indicate that the solid dispersion coefficients were larger than the liquid dispersion coefficients for equivalent operating conditions in the laboratory column it was not possible to conclude from this testwork that this result would apply to flotation columns in general. The solid and liquid tracer studies discussed above were performed using different spargers. Bubble sizing work on the sintered glass disc and the filter cloth spargers used in the above studies by Schommarz (1991) indicates that the sintered glass sparger produced smaller bubbles than the filter cloth sparger. This would result in an increased degree of mixing and consequently higher vessel dispersion numbers using the sintered glass disc sparger (see Chapter 4 Sec. 1.1.3). Added to this the solid tracer used by Goodall and O'Connor (1991) was feed material consisting of both hydrophobic and hydrophilic material and it was suspected that possible interaction of this tracer with the gas phase may have confounded the tailings RTD. Therefore in each of the following RTD studies liquid, feed and gangue tracers were injected using identical operating conditions and spargers in an attempt to validate and explain the above results.

1.2 RESIDENCE TIME DISTRIBUTION STUDIES PERFORMED USING RADIOACTIVELY LABELLED TRACERS

Once the preliminary RTD study had been performed further RTD studies were performed focussing specifically on the effect of different tracers viz. liquid, feed and gangue samples on the tailings response curves. This section begins by discussing the various methods used to determine the vessel dispersion number and following this the tanks-in-series and dispersion model fits are evaluated. The modelling results of the RTD studies performed on the UCT pilot column rig, the President Steyn rougher column and the Disputada cleaner column are then used to analyse the different tracer response curves obtained using radioactively labelled tracers.

1.2.1 DETERMINING THE VESSEL DISPERSION NUMBER FROM RTD DATA

As detailed in Chapter 1 Sec. 2.2.1 the solution of Equation (1.23) is dependent on the boundary conditions set out by the tracer injection and detection points. Three possible sets of boundary conditions exist; closed-open, open-open and closed-closed. The family of curves obtained using the three sets of boundary conditions are very different (Levenspiel, 1979). However for small degrees of mixing all the curves tend towards a similar solution. Therefore when RTD studies are performed on a laboratory scale column, where mixing approaches plug flow, an incorrect choice of boundary conditions used in the solution will not adversely affect the fit and the N_d obtained. In an industrial column however, where the degree of mixing is far greater, this is not the case and it is essential that the correct boundary conditions are used. The choice of tracer injection and detection points in RTD studies performed on industrial columns usually prescribe closed-closed boundary conditions. However in the case of the open-open boundary conditions Equation (1.24) should be used to determine the predicted response curve.

Of the methods used to determine the vessel dispersion number moments matching has the advantage of being a simple technique and can give a reasonable indication of the vessel dispersion number in both the laboratory and industrial scale columns. The drawback of using this

technique is that in the closed-closed case the resultant theoretical response curve for the N_d determined using the moments matching method cannot be plotted. Modelling of the tailings residence time distribution in a column has largely been used to develop correlations to predict mixing for scale-up purposes. RTD studies can also be extremely useful in understanding why an industrial column is not performing according to design specifications. Figure 4.3 illustrates the liquid tracer response curve for a baffled 1.8m diameter column (Alford, 1991). Using the method of moments N_d was calculated to be 1.85. A plot of the response curve for an N_d of 1.85 determined from the numerical solution of Equation (1.23) for closed-closed boundary conditions is also shown in Figure 4.3. It is clear that the column mixing deviates significantly from the predicted result using moments matching and that a portion of the tracer was bypassed to the tails outlet. The method of moments would not give any indication of this occurrence. For this reason the moments matching method should be used with caution since it does not yield any information as to whether the experimental response curve is similar to the model and does not indicate what sort of deviations there are from the model prediction.

The determination of N_d using a numerical solution is more detailed than using the method of moments. The inversion Laplace transform method and the finite difference method both provide equally good solutions. It has been found that a direct search method (least squares) provides a satisfactory fit of the numerical solution to experimental data (Xu and Finch (1991) and Xu et al. (1991)). As explained in Chapter 2 Sec. 1.3 the vessel dispersion numbers were therefore determined in the following RTD studies using the finite difference method and a least squares fit detailed by Xu et al. (1991). The method of moments was also used in order to compare the resultant vessel dispersion numbers with those obtained using the numerical solutio...

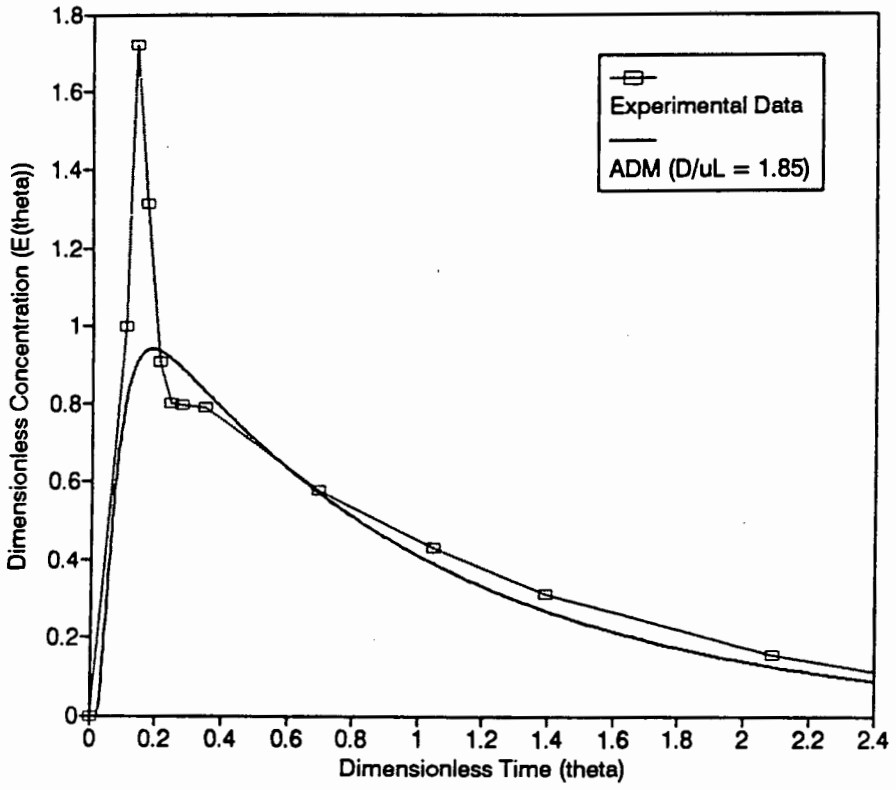

Figure 4.3: Tailings Response Curve of a 1.8m Diameter Flotation Column and Model Response Curve using Closed-Closed Boundary Conditions and the Method of Moments

1.2.2 SUMMARY OF THE MODEL FITTING OF RTD DATA OBTAINED FROM THE STUDIES USING RADIOACTIVELY TRACERS

Table 4.1 gives a summary of the modelling results obtained for the four sets of RTD data analysed. To simplify the discussion the three columns are referred to as follows

Column I: UCT pilot column rig
Column II: President Steyn rougher column
and Column III: Disputada cleaner column.

The analysis of the experimental data using the method of moments and the least squares fit of the numerical solution of Equation (1.23) are shown in Table 4.1. For the large columns the results obtained using the former method are quite different to those obtained using the least squares fit

Tracer Sample	Residence Time (min)	Variance (min^2)	Tanks-In Series (N)	Disp. Number Method of Moments	Disp. Number Least Squares	Disp. Coeff. ($x10^3$) (m^2/s)
Column I						
V/Q	3.33					
LIQUID	3.30	0.596	19	0.028	0.027	0.59
FEED	1.95	0.308	15	0.042	0.035	1.28
GANGUE						
Combined	1.61	0.223	16	0.045	0.032	1.44
-38μm	2.98	0.547	19	0.032	0.027	0.65
+38-75μm	2.03	0.294	16	0.037	0.032	1.14
+75-106μm	1.62	0.245	15	0.049	0.035	1.53
+106-150μm	1.57	0.395	9	0.088	0.059	2.71
Column II						
V/Q	11.15					
LIQUID	11.42	70.03	1.60	0.448	0.63	94
FEED	9.34	48.82	1.80	0.584	0.68	125
GANGUE						
Combined	9.42	53.20	1.80	0.469	0.70	122
-38μm	10.42	66.85	1.75	0.600	0.70	115
+38-75μm	8.92	44.23	1.90	0.479	0.63	121
+75-106μm	8.59	41.22	1.90	0.484	0.58	116
+106-150μm	8.11	35.56	1.90	0.454	0.56	118
Column III						
V/Q	16.50					
LIQUID	16.75	174.28	1.25	0.613	0.92	93
GANGUE						
Combined	12.68	116.43	1.10	0.945	0.85	113
-38μm	15.29	155.60	1.15	0.730	0.95	105
+38-75μm	12.44	107.18	1.15	0.819	0.82	112
+75-150μm	8.77	48.50	1.05	0.634	0.56	108

Table 4.1: Model Parameters obtained from the Response Curves of Columns I, II and III

of the numerical solution. However for the laboratory column the results are similar. Michell and Furzer (1972) in a study of an industrial scale packed column also found that the method of moments prediction of the dispersion number did not match the least squares fit of the experimental data. It is clear from the above results that the method of moments may not be accurate in determining the dispersion number in a large column. The following two sections discuss the modelling fitting results presented in Table 4.1.

1.2.3 COMPARISON OF THE TANKS-IN-SERIES AND DISPERSION MODEL FITS OF THE RTD DATA

The choice of a model to describe the particle hydrodynamics in the collection zone of flotation columns has been found to be dependent on the column diameter. For the laboratory column RTD studies both models fit the data equally well due to the small deviation from plug flow. As a general guideline it can be concluded that for laboratory columns (< 10cm) the tanks-in-series model and the dispersion model are both suitable.

For columns with diameters between 10cm and 180cm the dispersion model provides a better fit than the tanks-in-series model. The best fit of the tanks-in-series model and the closed-closed solution of the dispersion model for the gangue tracer in Column II and the liquid and gangue tracers in Column III are shown in Figures 3.21 and 3.25 respectively. Visual inspection of the curves shows clearly that for the two industrial columns the dispersion model fits the experimental data better than the tanks-in-series model. This is in agreement with the findings of Xu and Finch (1991). The question arises as to whether the poor fit of the tanks-in-series model would effect scale-up predictions. Table 4.2 shows the predicted overall recoveries using the axial dispersion and tanks-in-series models for the two industrial columns (II and III). The mean residences times, solid interstitial velocities and values of N and D_p were taken from the results for the combined gangue tracers. A collection zone rate constant of $1.0min^{-1}$ and a typical industrial column froth zone recovery of 40% (Finch and Dobby, 1990) were used in the calculations. The overall recovery predictions using the two models were similar for Column II but substantially different for Column III. This result indicates that

the use of the tanks-in-series model in scale-up procedures is likely to result in inaccurate overall recovery predictions.

Model Parameters	Column II	Column III
Axial Dispersion Model		
Solid Dispersion Coefficient, D_p (m^2/s)	0.125	0.113
Solid Settling Velocity, u_p (m/s)	0.0167	0.0121
Solid Mean Residence Time (min)	9.42	12.68
Final Recovery (%)	100.0	100.0
Collection Zone Length, L (m)	10.9	11.0
Collection Zone Rate Constant (min^{-1})	1.0	1.0
Froth Zone Recovery (%)	40.0	40.0
Vessel Dispersion Number, D_p/u_pL	0.6977	0.8490
Predicted Overall Recovery (Eqns. 1.18 and 1.38)		
Axial Dispersion Model (%)	93.71	95.99
Tanks-In-Series Model		
Number of Tanks-In-Series (N)	1.80	1.10
Predicted Overall Recovery (Eqns. 1.20 and 1.38)		
Tanks-in-Series Model (%)	91.21	85.82
Mixed Flow Model (Eqns. 1.13 and 1.38)		
Required Solid Mean Residence Time to obtain Overall Recoveries Equivalent to the Axial Dispersion Model (min)	37.5	59.5

Table 4.2: Prediction of the Overall Recoveries of Columns II and III using the Axial Dispersion, Mixed Flow and Tanks-In-Series Models

Figure 4.4 illustrates the liquid tracer tailings distribution for an unbaffled 2.5m diameter and 13m high column (Espinosa-Gomez et al., 1989). It is clear that a single stirred tank reactor describes the curves better than the upper limit of the vessel dispersion number viz. D/uL = 1. For columns greater than 180cm in diameter it is likely that the dispersion number exceeds 1 and the degree of mixing approaches that of a single stirred tank. It is proposed that these columns are best modelled as single stirred tank vessels.

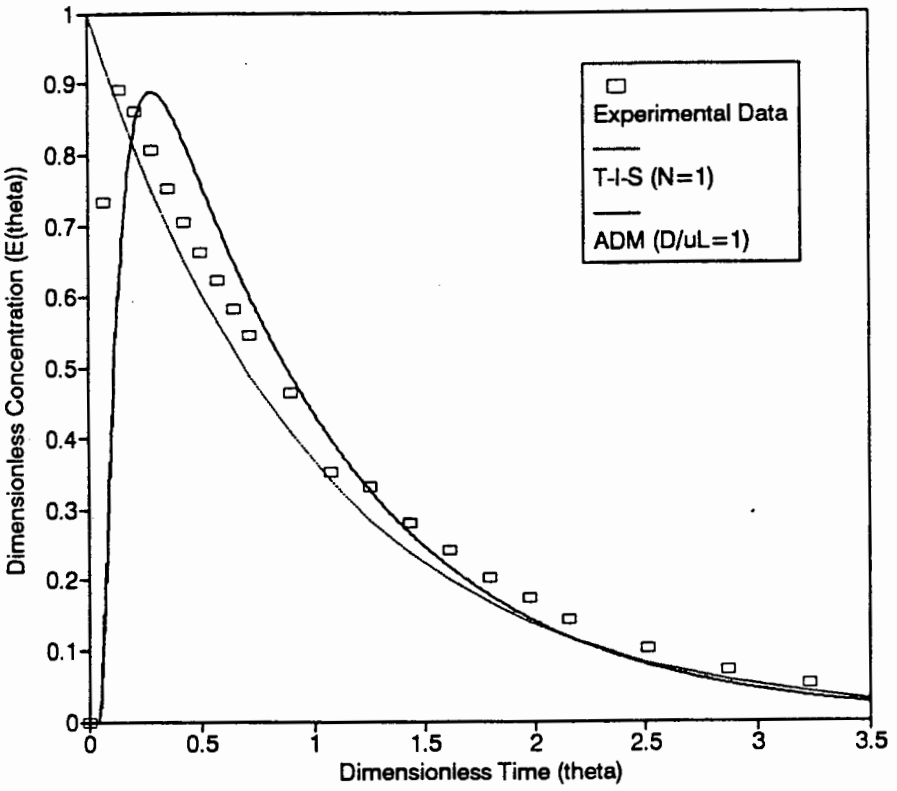

Figure 4.4: Tailings Response Curve for an Unbaffled 2.5m Diameter Column (after Espinosa-Gomez et al., 1989)

In the scale-up procedure an overprediction of the degree of mixing leads to the preferable result of a conservative estimate of recovery in scale-up. Consequently some investigators (Amelunxen, 1990) use a single stirred tank to describe the degree of mixing in industrial columns. Table 4.2 shows that the required mean residence times using the mixed flow model are more than four times the mean residence times used in the dispersion model to obtain the same overall recoveries. From this result it is clear that using the mixed flow model would result in unnecessary overdesign of industrial flotation columns with effective diameters less than 180cm.

1.2.4 THE RTD OF VARIOUS TRACERS IN THE THREE COLUMNS

The validity of tracer studies requires firstly that a tracer should perform in exactly the same way as the bulk material being measured, i.e. if only the flow regime in a reactor is to be determined, then the tracer

should not interact with any other phases in the system. Secondly the mass of tracer entering and leaving the system should be equal (Levenspiel, 1972).

It is possible that if feed material, which contains both hydrophobic and hydrophilic particles, is used as a tracer it will produce a substantially different tailings age distribution than would be obtained when tailings (hydrophilic) material is used. When gangue material is used as a tracer the response measured at the tails outlet will be representative of the overall flow regime of the hydrophilic particles since only a minimal amount of this tracer will report to the froth outlet. When a feed tracer, containing both hydrophobic and hydrophilic particles, is injected it is proposed that essentially two types of tracer are being injected in one input pulse. The hydrophilic portion of the tracer should behave in a similar manner as the gangue tracer referred to above. The hydrophobic portion of the tracer will be recovered in the froth phase and the concentrate detector will measure the age distribution curve of this material. Thus when using a gangue or feed tracer the distribution curves obtained from the tailings detector should have a similar shape and yield similar degrees of mixing. The results of injected gangue and feed tracers into Columns I and II are illustrated in Figures 3.11 and 3.19 respectively. It can be seen that the tailings response curves of the feed and gangue are similar in both columns. Table 4.1 shows that the dispersion coefficients of the feed and gangue material in both Column I and Column II are equivalent within the limits of experimental error. These results confirm the above proposal.

Table 4.1 indicates that in both the laboratory and the industrial columns the vessel dispersion coefficients of the solids were always greater than that of the liquid. Clearly these results show that it is not generally correct to assume that the solid and liquid dispersion coefficients are the same. The table also shows that the degree of mixing in the large columns was substantially greater than in the laboratory column. This is in agreement with dispersion coefficient prediction correlations for example Equation (1.36) which indicates that the dispersion coefficient is proportional to $d_c^{1.31}$.

Table 4.1 lists the experimental results and the model parameters for the three columns using various tracer particle sizes. Figure 4.5 shows the relationship between particle size and the dispersion coefficient in Column I. As particle size increased the dispersion coefficient increased. The zero particle size point represents the value for the liquid tracer. It is difficult to make any strong conclusions from these results for two reasons. Firstly the axial dispersion model provided a poor fit of the +106-150μm size fraction response curve and the model result is thus not a good indication of the hydrodynamics. It is possible that for this particle size in the laboratory column a small degree of settling at the base of the column affected the response curve. The large particles could have settled momentarily at the base of the column before finally being washed out resulting in an erratic response curve. Secondly it should be noted that the mixing in Column I was very close to plug flow and the increase in the dispersion coefficients over the range of particles sizes did not substantially change the response curves for the -38μm, +38-75μm and +75-106μm size fractions.

Figure 4.6 shows the relationship between particle size and the dispersion coefficient for Columns II and III. The zero particle size point again represents the value for the liquid tracer. The liquid dispersion coefficient in both columns was significantly smaller than the solid dispersion coefficients. For these columns the solid dispersion coefficients were constant within the experimental error as particle size increased. For Columns II and III the average dispersion coefficients for the various particle sizes were respectively 29% and 21% larger than the corresponding liquid dispersion coefficients (Mills et al., 1992). In a subsequent study by Xu and Finch (1992) the solid dispersion coefficient was found to be about 21% larger than the liquid dispersion coefficient, thus confirming the results obtained in this study. In the design of an industrial scale column using the axial dispersion model and a single first order rate constant this difference does not however produce a substantial difference in the overall recovery prediction. Table 4.3 lists the results obtained using both the liquid and solid dispersion coefficients to predict overall recoveries in the two industrial columns (II and III). The model parameters were taken from the combined gangue and liquid tracer results in Table 4.1. The predicted overall recoveries using the liquid dispersion coefficients are 1 to 2% higher than the recoveries

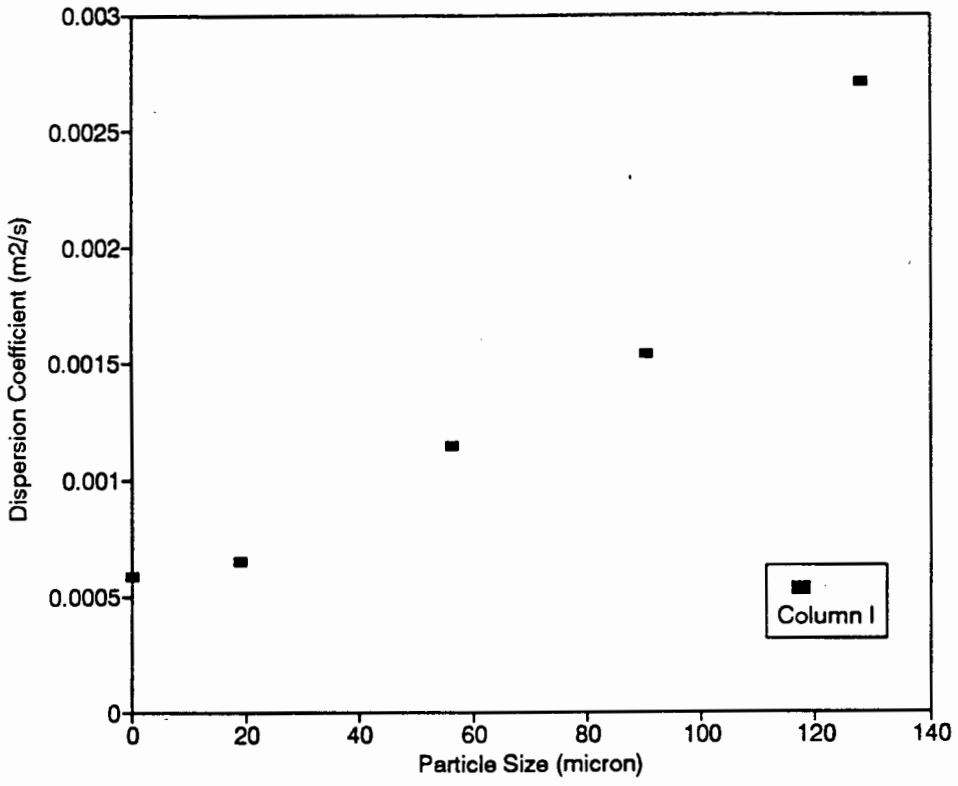

Figure 4.5: The Effect of Particle Size on the Dispersion Coefficient in Column I (Zero Particle Size indicates Liquid Tracer Result)

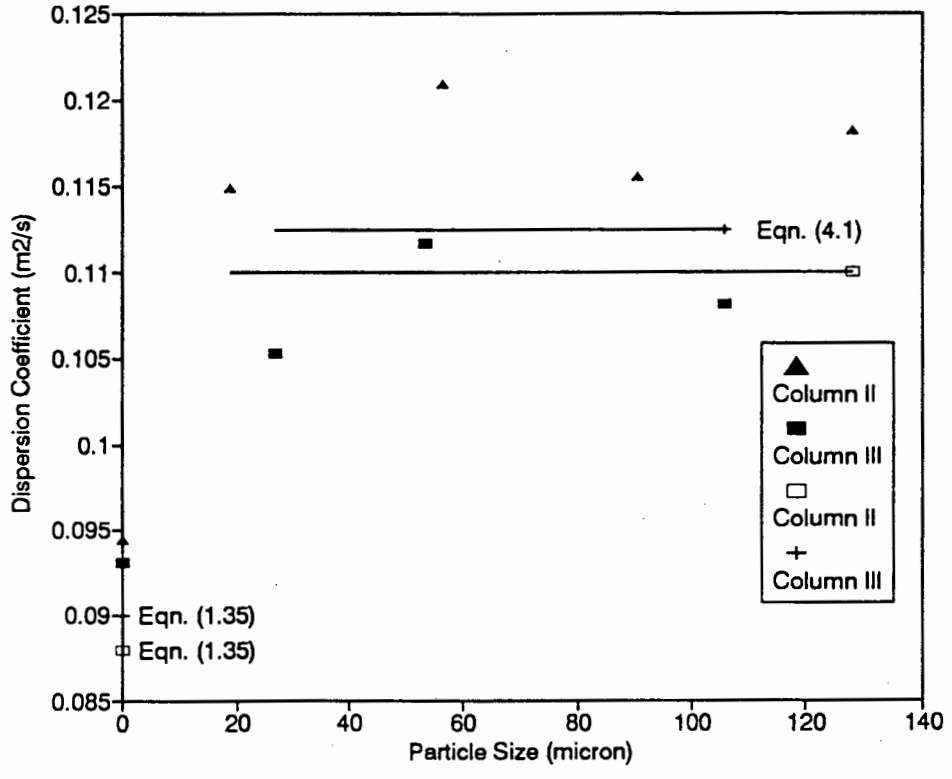

Figure 4.6: The Effect of Particle Size on the Dispersion Coefficient in Columns II and III (Zero Particle Size indicates Liquid Tracer Result)

calculated using the solid dispersion coefficients. It is unlikely that this difference would affect the scale-up operation.

Model Parameters	Column II	Column III
Liquid Dispersion Coefficient, D_l (m^2/s)	0.094	0.093
Solid Dispersion Coefficient, D_p (m^2/s)	0.127	0.113
Solid Settling Velocity, u_p (m/s)	0.0167	0.0121
Solid Mean Residence Time (min)	9.42	12.68
Final Recovery (%)	100.0	100.0
Collection Zone Length, L (m)	10.9	11.0
Collection Zone Rate Constant (min^{-1})	1.0	1.0
Froth Zone Recovery (%)	40.0	40.0
Vessel Dispersion Numbers		
1. D_l/u_pL	0.5164	0.6987
2. D_p/u_pL	0.6977	0.8490
Predicted Overall Recovery (Eqns. 1.18 and 1.38)		
1. using D_l/u_pL	95.25	96.76
2. using D_p/u_pL	93.71	95.99

Table 4.4: Prediction of Overall Mineral Recovery in Columns II and III using the Liquid and Solid Dispersion Coefficients

Column	Dispersion Coefficient ($x10^3$ m^2/s)			
	Liquid Tracer	Equation (1.35)	Equation (1.36)	Equation (1.37)
Column I	0.59	3.8	2.4	6.1
Column II	940.0	830.0	890.0	910.0
Column III	930.0	590.0	900.0	590.0

Table 4.5: Predicted and Fitted Liquid Dispersion Coefficients for Columns I, II and III

Table 4.5 shows the liquid dispersion coefficients predicted using Equations (1.35), (1.36) and (1.37) and the fitted liquid dispersion coefficients for Columns I, II and III. Equation (1.36) provides the best

fit to the experimental data. Columns II and III were operated at substantially different feed percent solids and Equation (1.35) is the only correlation which accounts for this parameter. Although the preliminary RTD study in this thesis has shown that the feed percent solids is not a significant parameter in laboratory columns, this may not be the case in industrial columns. From the results obtained in this testwork it suggested that, when estimating the solids dispersion coefficient for a flotation column, Equation (1.36) be modified as follows:

$$D_p = 1.25\ (0.124\ d_c^{1.31}\ j_g^{0.33}\ e^{-0.025S}). \qquad (4.1)$$

Although the solid dispersion coefficients were found to be constant within the experimental error for the range of particle sizes tested in Columns II and III the lowest solid dispersion coefficient in each column was that of the -38μm tracer. Flint and Howarth (1971) using a hydrodynamic analysis predicted that ultra-fine particles follow the liquid streamlines around a bubble rather than intercepting the bubble itself. From this it is proposed that ultra-fine particles interact with bubbles to the same degree as the liquid. This in turn results in similar degrees of mixing of the ultra-fines and the liquid. However as particles increase in size they are intercepted by bubbles rising through the pulp. This increased interaction of the larger particles with the bubbles results in an increase in the degree of mixing of these particles. This proposal is confirmed by the results obtained in the pilot column as well as the two industrial columns.

2. STUDY OF THE KINETICS OF THE COLLECTION ZONE

This section begins with an evaluation of the method developed to determine the collection zone rate constant. Following this the results obtained either by varying the column length and feed rate or by injecting labelled hydrophobic material into the feed in order to determine the collection zone rate constant are discussed. The experimental results are used to evaluate models used to describe the kinetics and hydrodynamics of

the collection zone of flotation columns as well as the particle collection model presented in Chapter 1 Sec. 3.2.

2.1 EVALUATION OF THE METHOD DEVELOPED TO DETERMINE THE COLLECTION ZONE KINETICS

A comparison the sulphur recoveries and grades obtained for the 10cm and 60cm froth in the laboratory column illustrate the differences in the two operating conditions (Table 3.7). Firstly the small drop in concentrate grade from the 60cm to the 10cm froth indicates that entrainment in the froth was minimal. Secondly the higher recoveries measured for the 10cm froth indicates that drop back of floatable material occurred in the deeper froth. The tests performed using 10cm and 60cm froths and the chalcopyrite tracer further illustrate the difference in the results obtained at the two froth depths. Figure 3.30 shows a succession of peaks in the recovery of copper vs. time curve for the 60cm froth indicating recycling of chalcopyrite in the froth phase before it was finally recovered. However the recovery vs. time curve for the 10cm froth was smooth following the initial peak indicating that material entered the froth and then was recovered to the concentrate. Furthermore the curve fit of the recovery vs. time curves in Figure 3.31 with R_f set at 1 in the 10cm froth test produced a value of 0.48 for R_f in the 60cm froth test. This value is in agreement with values quoted by Finch and Dobby (1990) who suggest that froth drop back in laboratory columns is about 50% i.e. $R_f = 0.50$.

The above discussion illustrates that the method developed fulfills the criteria for determining the collection zone kinetics. Firstly entrainment and bypassing of the feed to the concentrate does not occur to a significant extent and secondly the froth zone recovery was close to 100%. The method was therefore assumed to give a good approximation of particle recovery in the collection zone at typical column operating conditions.

2.2 ANALYSIS OF DATA OBTAINED IN THE KINETICS STUDIES

2.2.1 DATA OBTAINED ON THE LABORATORY COLUMN BY VARYING COLUMN LENGTH AND FEED RATE

An initial study was carried out to determine the effect of gas rate on the flotation kinetics. The collection zone rate constant was determined by varying the collection zone length and feed rate. This method is similar to typical methods used to determine the flotation kinetics in a pilot column (Finch and Dobby, 1990). Relatively large standard deviations, eg. 5%, were observed at the low mean residence times and recoveries. It is likely that this was due to changes in the characteristics of the feed to the column over the different sampling times. The plug flow model and first order rate constants provided a reasonable fit of the data. However due to the above mentioned standard deviations in the measurements it was not possible to accurately determine the effect of gas rate on the flotation rate.

2.2.2 DATA OBTAINED USING CHALCOPYRITE AND RADIOACTIVELY LABELLED PYRITE TRACERS

As can seen from Figure 3.29 this approach yielded highly reproducible recovery vs. time curves of the tracer exiting in the concentrate of the laboratory column. The chalcopyrite tracer sample injected into the laboratory column consisted of particles less than 150μm. Due to this large size range and presumably a distribution of rate constants with size the curves were modelled using fast and slow floating rate constants. Equation (2.2) and the axial dispersion model produced an excellent fit of the (recovery of copper) vs. time curves. In the tests performed on the pilot column using radioactively labelled pyrite tracers, the samples consisted of discrete particle size ranges and therefore a single first order rate constant and the axial dispersion model provided an excellent fit of the recovery vs. time data. The above results illustrate that the axial dispersion model and first order kinetics are an appropriate choice to describe mixing and kinetics in a pilot column. Figure 3.35 shows the pyrite recovery curve for the +38-75μm fraction as well as the axial dispersion model fit at standard conditions in the pilot

column. It also shows the two extremes of plug and mixed flow using the same rate constant. It is clear from this figure that the axial dispersion model provides the best fit of the data.

The question arises as to whether the good fit obtained of the recovery vs. time curves above is merely due to a surplus of parameters in the models used. This could be argued to be the case in the chalcopyrite testwork where there were three fitted variables viz. k_f, k_s and x, the fraction of fast floating material. However in the pyrite testwork the only unknown was the collection zone rate constant and an excellent fit was still obtained, thus indicating the appropriateness of the axial dispersion model in predicting the recovery vs. time data.

Figure 3.44 illustrates the two extremes of plug and mixed flow as well as the experimental data and the axial dispersion model fit of the pyrite recovery using the +38-75μm pyrite fraction in the industrial column. From this figure it is clear firstly that the experimental data could be adequately modelled using the axial dispersion model and first order kinetics and secondly that the experimental recovery vs. time curve is in between the plug and mixed flow curves and the plug and mixed flow models would not provide good fits of the experimental data.

The operating conditions of the President Steyn industrial column during the pyrite tracer testwork were similar to the standard operating conditions in the similar pilot column testwork. The gas flow rates in both columns were about 2.2cm/s and the industrial column used Cominco spargers which produced bubble sizes similar to those in the pilot column (Tucker et al., 1992). A comparison of tests where identical tracers were used, viz. the +38-75μm fraction, indicates that the collection zone rate constant decreased by a factor of about 4 from the pilot to the industrial scale column (see Tables 3.10 and 3.11). This decrease cannot be attributed to poor modelling of the hydrodynamics in the columns since the RTD testwork comprehensively characterised the mixing characteristics of the solids in both columns. There are two possible explanations for this observed decrease in flotation rate from the pilot to the industrial column. Firstly, it was thought that the column was operating at or more likely above the carrying capacity limit of the froth. The feed rate to the column was high (1.22cm/s) and the feed percent solids was 35%. In

determining the flotation rate of the collection zone it is essential that the column is operating below carrying capacity or else the froth becomes the limiting factor in particle recovery. Even though the froth was made shallower for the kinetics experiments it was not possible to make it less than about 30cm and it is possible that the froth affected recovery of material. From this result it could be concluded that the pilot column rate constant viz. $1.31min^{-1}$ is the optimum achievable flotation rate in the industrial column.

The second possible explanation is that the increase in aspect ratio resulted in a decrease in the flotation rate constant. Amelunxen (1990) discusses conventional cell design in which the pilot rate constant is divided by 2.5 in the scale-up procedure and mentions that this factor could be higher in flotation column scale-up. Equation (1.41) is an equation generally used to predict the collection zone rate constant in flotation columns. Gas flow rate and bubble size were kept constant in the pilot and industrial columns and the only other variable in Equation (1.41) is collection efficiency and it is unlikely that this variable is affected by the aspect ratio. It is therefore not clear why the collection zone rate constant could be affected by the aspect ratio. It is suggested that the decrease in the rate constant from the pilot to the industrial column is a result of a combination of the two possible explanations. The rate constant in the industrial column was low due to the poor operation of the column outlined above. However it is unlikely that a rate constant of $1.31min^{-1}$ could be achieved in the industrial column if it was operating below carrying capacity. It is suggested that the approach of Amelunxen (1990) whereby a scale-up factor is used to reduce the predicted rate constant in the industrial column would apply to most flotation column scale-up procedures. This factor is probably between 2.5 and 4.

The tests performed by injecting the pyrite and chalcopyrite tracers into the different columns produced both reproducible and accurate recovery vs. time curves. This approach was used to gain insight into the effect of various operating parameters as well as the effect of the hydrophobic particle characteristics on the flotation rate.

2.2.3 THE EFFECT OF VARIABLES ON THE FLOTATION KINETICS

2.2.3.1 The Effect of the Superficial Gas velocity on the Flotation Rate

Figure 3.37 shows the effect of gas flow rate on the collection zone rate constant. The increase in the rate constant with increasing gas rate is an expected result and has been obtained by other investigators (Mular and Musara (1991) and Finch and Dobby (1990)). However Finch and Dobby (1990) discuss a possible optimum rate constant due to the increase in bubble size with increasing gas rate. For the operating conditions used in their work and using the particle collection model the calculated optimum was found to be at an air rate of about 0.7cm/s. In the present study an analysis of the bubble size with increasing air rate indicated that the bubble size remained virtually constant for the range of gas flow rates tested (2.00 to 2.86cm/s). Consequently it was unlikely that an optimum gas flow rate would be measured. However it is likely that an optimum flotation rate constant would exist at higher gas flow rates (>3cm/s) where slugging begins to occur. The rate constant vs. gas rate curve for a complete range of gas rates in pilot column would probably emulate the curve obtained by Mular and Musara (1991) where the rate constant began to level off at air rates above 3.5cm/s. It is proposed that this curve shape will be emulated by most flotation processes in a pilot column. The linear increase in pyrite recovery with increasing gas rate is an expected result for a column not operating at carrying capacity.

For the range of gas flow rates used in typical column operation viz. 1.5 to 3.0cm/s the rate constant has been shown to increase linearly with increasing gas flow rate in the present study (Figure 3.37). This is in agreement with Equation (1.41) where j_g is proportional to the rate constant. The collection efficiencies predicted using the experimental rate constants and Equation (1.41) remained constant with increasing gas rate. The collision efficiency also remained unchanged with increasing gas rate and consequently the attachment efficiency and induction time remained constant. The values obtained for the collection efficiencies and induction times viz. about 0.0012 and 0.0215sec respectively were in the same range as previously reported values (Dobby and Finch (1990) and Schulze (1989). Since the bubble size did not change with gas rate it is

likely that the induction time would remain constant as gas rate has not been found to effect induction time (Schulze, 1989). From the above discussion it can be concluded that Equation (1.41) provides an adequate prediction of the rate constant over the range of air rates investigated.

2.2.3.2 The Effect of Bubble Size on the Flotation Rate

The effect of bubble size on the flotation rate constant was investigated using both the chalcopyrite and pyrite tracers. The rate constants decreased markedly with increasing bubble size for both tracers although the rate constants obtained using the chalcopyrite tracer were significantly higher. It has been reported that chalcopyrite floats at a faster rate than pyrite (King, 1982) and furthermore the chalcopyrite sample used was already coated with reagent while it is likely that the pyrite sample became oxidised to some extent during the radioactive labelling period resulting in a lower rate of recovery. The decrease in flotation rate with particle size is an expected result and has been shown to be the case in conventional batch cell tests (Ahmed and Jameson, 1977). Experimental studies examining the effect of bubble size on the flotation rate at typical column operating conditions had not been done previously studied. However Equation (1.41) which is commonly used to predict the rate constant in column flotation indicates that the collection zone rate constant is inversely proportional to bubble size at a constant gas flow rate. The results obtained in this study indicate the large effect bubble size has on the collection zone rate constant over the range of d_b investigated. This reaffirms the fact that bubble size control is essential in column flotation.

The bubble size was found in the RTD studies to affect the degree of mixing significantly. Decreasing bubble size resulted in an increase in the degree of mixing. A column which approaches plug flow will yield the highest recovery. However the conditions for a small degree of mixing are large bubble sizes which are not conducive to particle collection. Increasing the bubble diameter in the kinetics study resulted in a sharp decrease the rate constant and optimum recovery occurred between bubble diameters of 1 and 2mm. Therefore the reduced mixing due to larger bubble sizes did not serve to improve recoveries. Flotation columns are usually

operated at bubble sizes between 1 and 2mm and the present work shows that this is the range for optimum final recovery (see Tables 3.9 and 3.10). Further reductions in bubble size served only to improve the rate of recovery.

The collection efficiencies predicted using Equation (1.41) and the experimental rate constants followed the same trend as set out in the literature (Finch and Dobby, 1990) viz. as bubble size increased collection efficiency decreased. However for the largest bubble size (2.70mm) E_K increased slightly from the lower bubble size for both tracer curves. The collision efficiencies calculated indicated a small decrease in E_C with increasing bubble size. However the attachment efficiencies calculated from Equation (1.42) only decreased with increasing bubble size initially but then increased linearly with increasing bubble size for both tracers. The fitted induction times remained constant with increasing bubble size but decreased for the largest bubble size (2.70mm). The above result conflicts with the expected result of decreasing collection and attachment efficiency with increasing bubble size. From Table 3.3 it can be seen that the standard deviation of the bubble size distribution increased with bubble size. The bubble size measurements refer to average bubble size of the bubble swarm, however for the larger bubble sizes there were naturally smaller bubbles being produced at the same time. For these bubble sizes this may have lead to a higher rate constant than would actually occur for a swarm of bubbles all with a d_b of 2.70mm. Lower rates at the larger bubble sizes would have led to a steeper curve and therefore decreasing collection and attachment efficiencies with increasing bubble size. The results obtained using Equation (1.41) again indicate that this equation provides an adequate prediction of the collection zone rate constant over the bubble sizes tested.

2.2.3.3 The Effect of Particle Size on the Flotation Rate

In the study performed on the pilot column the curve obtained for the effect of particle size on the rate constant had an optimum at 90μm. Finch and Dobby (1990) obtained a similarly shaped rate constant vs. particle size curve in the flotation of galena but with the optimum at about 30μm. The final recovery of tracer vs. time curve obtained had an optimum over

the 50μm to 90μm size range. This result is in agreement with the work of Imaizumi and Inoue (1965) who report the optimum to be between 50 and 150μm in conventional flotation.

The collection efficiencies determined using the experimental rate constants and Equation (1.41) have an optimum at about 90μm. This is expected since particle size is not a separate parameter in Equation (1.41) and therefore the change in rate with particle size is reflected in E_K. The calculated collision efficiencies increased dramatically with increasing particle size while the attachment efficiencies determined from Equation (1.42) decreased with increasing particle size. This in agreement with the proposal of Finch and Dobby (1990) that the opposing changes in E_A and E_C result in an optimum particle size for collection. The resultant iteratively determined induction times decreased with increasing particle size. This trend is similar to both previous experimental work in conventional flotation (Jowett, 1980) and the prediction of t_i using Equation (1.58). The increase in t_i with decreasing d_p is more marked in the column cell than in the conventional work. Furthermore Jowett (1980) showed that t_i decreased with increasing d_p up to 50μm but above this particle size began to increase. This increase was not detected in the present study and it is likely that it would occur but at a larger d_p as the flotation column is known to collect larger particle sizes more effectively. Finally the induction times determined from the particle collection model compare well with previously determined values and trends (Schulze, 1990 and Jowett, 1980) thus indicating the model provides an adequate description of flotation kinetics in the collection zone of a pilot column.

CHAPTER 5

CONCLUSIONS AND RECOMMENDATIONS

In the study of the mixing characteristics of the collection zone three independent residence time distribution studies were performed and analysed. Furthermore the RTD data of Yianatos and Bergh (1990) were also analysed. From these studies it was possible to ascertain the appropriateness of the tanks-in-series and axial dispersion models to describe mixing. The choice of model to describe the degree of mixing in the collection zone is dependent on the column diameter. For laboratory columns (d_c < 10cm) both the axial dispersion model and the tanks-in-series model fit RTD data equally well due to the small deviation from plug flow. For column diameters between 10cm and 180cm the dispersion model provides a better fit than the tanks-in-series model and it is recommended that the dispersion model be used for columns in this diameter range. For column diameters greater than 180cm the column is best modelled as a single stirred tank. However use of the mixed flow model to design columns less than 180cm can lead to unnecessary overdesign.

It is proposed that increases in mixing with increasing gas rate are due, among other possible factors, to increases in the number of bubbles. The increase in mixing with decreasing bubble size measured in the preliminary RTD study was attributed to the increase in the number of bubbles. By extrapolating this result to industrial columns it is clear that flotation columns, which have smaller and substantially more bubbles, will be more mixed than bubble columns.

The analysis of the RTD data showed the importance of choosing the correct boundary conditions when ascertaining the vessel dispersion number. The following points should also be considered when using the axial dispersion model. Firstly for open-open boundary conditions the theoretical response curves should be calculated using Equation (1.24). Secondly moments matching should be used with caution as this method does not give any indication of the deviation of the theoretical response curve from the

experimental result. Finally for closed-closed boundary conditions the numerical solution and curve fit using finite difference and a least squares technique detailed by Xu and Finch (1991) should be used to determine the theoretical response curves.

The injection of feed, liquid and gangue tracers into the different columns yielded the following results. The feed and gangue tracers produce similar tailings age distribution curves for a range of column diameters and therefore either material can be used to evaluate collection zone mixing. For all the columns investigated the liquid dispersion coefficients were significantly smaller than the solid dispersion coefficients. Furthermore for a range of tracer particle sizes injected into both industrial columns the solid dispersion coefficients were similar and a factor of about 1.25 larger than the respective liquid dispersion coefficients. It is proposed that ultra-fine particles have a similar degree of mixing as the liquid due to the fact that they follow the liquid streamlines around a bubble rather than intercepting the bubble itself. However as particles get larger they begin to intercept with the bubbles thus leading to a greater dispersion as observed in the present study. The correlation of Laplante et al. (1988) to predict the solid dispersion coefficient was modified to account for the difference between solid and liquid dispersion coefficients. However it was shown that this difference does not substantially affect overall recovery predictions in the industrial columns.

A method to determine the collection zone rate constant(s) at typical column operating conditions and while the column was operating at steady state was developed. An evaluation of this method indicated that it fulfilled the requirements for determining the collection zone rate constant viz. minimal entrainment of gangue and minimal recycling of hydrophobic material in the froth zone. The method provided an adequate prediction of the collection zone rate constant(s) for scale-up. However using this method and by injecting hydrophobic tracers into the feed stream of a column an accurate evaluation of the collection zone rate constant could be ascertained for a range of operating parameters.

The results of the residence time distribution studies were used in the evaluation of collection zone kinetics. First order kinetics and the axial

dispersion model provided an excellent prediction of the recovery of hydrophobic material in the concentrate for a range of operating parameters in the laboratory columns. The dispersion model combined with first order kinetics also provided a good fit of similar data obtained from the industrial column. The collection zone rate constants determined in the industrial column kinetic study were found to be a factor of about 4 less than the rate constants determined using an identical tracer at the same operating conditions in the pilot column study. This difference is partly attributed to the fact that the industrial column could have been operating above the carrying capacity limits of the froth. However it is also suggested that industrial column rate constants are a factor of between 2.5 and 4 smaller than pilot column rate constants. It is possible that the industrial column rate constant is a more complex parameter than the pilot rate constant, however it not clear why there is a difference between the two values.

The effect of gas flow rate, bubble size and particle size on the collection zone rate constant in the laboratory columns was evaluated. Model parameters of the particle collection model were also calculated for each of the operating conditions. The effect of each of the operating parameters investigated on the flotation rate and the particle collection model parameters is presented below.

The final recovery and rate constant increased with increasing gas flow rate for the range investigated. It is proposed that a maximum rate constant and final recovery will usually occur at a gas rate of about 3.0cm/s. Above this value the gas flow will begin to approach slugging and the recovery and rate will level off. The collection efficiency as well as the induction times remained constant with the change in gas rate. Increasing the bubble diameter in the kinetics study resulted in a sharp decrease in the rate constant and optimum recovery occurred between bubble diameters of 1 and 2mm. Flotation columns are usually operated at bubble sizes between 1 and 2mm and the present work shows that this is the range for optimum final recovery. Further reductions in bubble size serve only to improve the rate of recovery.

The effect of particle size on the final recovery and rate constants followed the same trend as in previous studies. The optimum particle size

range for the final recovery of pyrite was found to be between 50 and 90μm. The rate constants as well as the collection efficiencies had an optimum at about 90μm. The induction time was found to decrease with increasing particle size. It is expected that for particle sizes larger than the maximum size used in the testwork the induction time would begin to increase.

For each of the operating conditions investigated Equation (1.41) and the particle collection model of Finch and Dobby (1990) were found to fit the experimentally determined rate constants well. The model can therefore be used with confidence in the prediction of collection zone kinetics in laboratory flotation columns. The injection of hydrophobic tracers into a flotation column has been found to provide an accurate estimate of collection zone kinetics in pilot and industrial columns. This method could used in future testwork to evaluate in more detail collection zone kinetics in industrial columns, to determine the kinetics of other flotation systems and to investigate froth zone behaviour.

REFERENCES

Ahmed, N. and Jameson, G.J. "The effect of bubble size on the rate of flotation of fine particles", *Int. J. Min. Proc.*, 14 (1985) 195-215.

Alford R.A. "An improved method for the design of industrial column flotation circuits in sulphide applications" in *Sulphide Deposits - Their Origin and Processing* (P. Gray, ed.), I.M.M. (1990).

Alford R.A. "Modelling and design of flotation column circuits", *Ph.D Thesis*, Univ. of Queensland (1991).

Alford R.A., Baguley P.J., Artone E. and Bijok A. "Column flotation circuit design at Peak Gold" in Proceedings of *Column '91*, International Conference on Column Flotation, Sudbury, Canada (1991) 123-135.

Amelunxen R.L. "Column Flotation: New carrying capacity considerations for scale-up", Presented at *Expomineria '90*, Santiago, Chile (1990).

Anfruns J.F. and Kitchener J.A. "Rate of capture of small particles in flotation", *Trans. I.M.M.*, 86 (1977) C9-15.

Baird M.H.I and Rice R.G. "Axial dispersion in large unbaffled columns", *Chem. Eng. J.*, 9 (1975) 171-174.

Boutin P. and Wheeler D.A. "Column Flotation", *Mining World*, 20(3) (1962) 47-50.

Buffham B.A. and Gibilaro L.G. "A generalization of the tanks-in-series model", *A.I.Che. J.*, 14(5) (1968) 805-806.

Clingan B.V. and Macgregor D.R. "Column flotation experiences at Magma Copper Co.", *Min. and Met. Proc.*, 3(3) (1987) 121-125.

Coffin V.L. and Misczak J."Column flotation at Mines Gaspe" in Proceedings of *14th International Mineral Processing Congress*, Toronto, Canada (1982).

Contini N.J., Wilson S.W. and Dobby G.S. "Measurement of rate data in flotation columns" in Proceedings of *Column Flotation '88* (K.V.S. Sastry, ed.), S.M.E. Annual Meeting, Phoenix, Arizona (1988) 81-89.

Cova D.R., I. and E.C. "Catalyst Suspension in gas agitated tubular reactors", *I. and E.C. Proc. Des. and Dev.*, 5(20) (1966) 20

Crawford R. and Ralston J. "The influence of particle size and contact angle in mineral flotation", *Int. J. Min. Proc.*, 23 (1988) 1-29.

Danckwerts P.V. "Continuous flow systems - distribution of residence times", *Chem. Eng. Sci.*, 2 (1953) 1-13.

del Villar R., Finch J.A., Yianatos J and Laplante A.R. "Column flotation simulation" in *Computer Applications in the Mineral Industry*, First Canadian Conference (K. Fytas, J.L. Collins and R.K. Singhal eds.) A.A. Balkema, Rotterdam (1988).

Dobby G.S. "A fundamental flotation model and flotation column scale-up", *Ph.D Thesis*, McGill University, Montreal, Canada (1984).

Dobby G.S. and Finch J.A. "Mixing characteristics of industrial flotation columns", *Chem. Eng. Sci.*, 40(7) (1985) 1061-1068.

Dobby G.S. and Finch J.A. "Flotation column scale-up and modelling", *C.I.M. Bulletin*, 79(889) (1986a) 259-264.

Dobby G.S. and Finch J.A. "Particle collection in columns - gas rate and bubble size effects", *Can. Met. Q.*, 25(1) (1986b) 9-13.

Dobby G.S. and Finch J.A. "Particle size dependence in flotation derived fron a fundamental model of the capture process", *Int. J. Min. Proc.*, 21 (1987) 241-260.

Dowling E.C., Klimpel R.R. and Aplan F.F. "Model discrimination in the flotation of a porphyry ore", *Min. and Met. Proc.*, May (1985) 87-101.

Espinosa-Gomez R. "Recovery of Pyrochlore from slimes discarded at Niobec by column flotation", *Ph.D. Thesis*, McGill Univ., Montreal Canada (1987).

Espinosa-Gomez R., Finch J.A., Yianatos J.B. and Dobby G.S. "Column carrying capacity: particle size and density effects", *Min. Eng.*, 1(1) (1988) 77-79.

Espinosa-Gomez R., Johnson N.W., Pease J.D. and Munro P.D. "The commissioning of the first flotation columns at Mount Isa Limited", *Processing of Complex Ores* (G.S. Dobby and S.R. Rao ed.), Pergamon Press, New York (1989) 293-302.

Falutsu M. and Dobby G.S. "Direct measurement of collection zone recovery and froth drop back in a laboratory flotation column", *Min. Eng.*, 2(3) (1989) 377-386.

Finch J.A. and Dobby G.S. "Column Flotation", Pergamon Press (1990).

Flint L.R. and Howarth W.J. "The collision efficiency of small particles with spherical air bubbles", *Chem. Eng Sci.*, 26 (1975) 1155-1168.

Goodall C.M. and O'Connor C.T. "Residence time distribution studies of the solid and liquid phases in a laboratory column flotation cell" in Proceedings of S.A.I.M.M. Int. Colloquium: *Developments in Froth Flotation*, Gordons Bay, South Africa Vol. 2 (1989).

Goodall C.M. and O'Connor C.T. "Residence time distribution studies in a flotation column. Part 1: the modelling of residence time distributions in a laboratory column cell", *Int. J. Min. Proc.*, 31 (1991) 97-113.

Imafuka K., Wang T., Koide K. and Kubota H. "Behaviour of suspended solid particles in the bubble column", *J. Chem. Eng. Japan*, 1(2) (1968) 153-158.

Imaizumi T. and Inoue T. "Kinetic consideration of froth flotation" in Proceedings of *6th Int. Min. Proc. Congr.* (A. Roberts ed.), Cannes (1965) 581-589.

Ityokumbul M.T. "A new modelling approach to flotation column design", *Min. Eng.*, 5(6) (1992) 685-693.

Jameson G.J., Nam S. and Moo-Young M. "Physical factors affecting recovery rates in flotation", *Min. Sci. Eng.*, 9(3) (1977) 103-118.

Joshi J.B. "Axial mixing in multiphase contactors - a unified correlation", *Trans. I. Chem. Eng.*, 58 (1980) 155-165.

Joshi J.B. and Sharma M.M. "A circulation model for bubble columns", *Trans. I. Chem. Eng.*, 57 (1979) 244-251.

Jowett A. "Gangue mineral contamination of froth", *Brit. Chem. Eng.*, 2(5) (1966) 330-333.

Jowett A. "Formation and distribution of particle-bubble aggregates in flotation", *Fine Particles Processing*, International Symposium, Chapter 37 (1980).

Kelsall D.F. "Application of probability assessment of flotation systems", *Trans. Inst. Min. and Met.*, 70(4) (1961) 161-220.

Kho C.J. and Sohn H.J. "Column flotation of talc", *Int. J. Min. Proc.*, 27 (1989) 157-167.

King R.P. "Principals of flotation", *S. Afr. Inst. Min. Met. Monogr. Ser.*, 3 (1982) 159-182.

Laplante A.R., Toguri J.M. and Smith H.W. "The effect of air flow rate on the kinetics of flotation, part 1: the transfer of material from the slurry to the froth", *Int. J. Min. Proc.*, 11 (1983) 203-219.

Laplante A.R., Yianatos J.B. and Finch J.A. "On the mixing characteristics of the collection zone in flotation columns" in Proceedings of *Column Flotation '88* (K.V.S Sastry ed.), S.M.E. Annual Meeting Phoenix, Arizona (1988) 69-80.

Levenspiel O. and Smith W.K. "Notes on the diffusion-type model for the longitudinal mixing of fluids in flow", *Chem. Eng. Sci.*, 6 (1957) 227-233.

Levenspiel O. "Comparison of the tanks-in-series and the dispersion models for non ideal flow of fluid", *Chem. Eng. Sci.*, 17 (1962) 576

Levenspiel O. "Chemical Reaction Engineering", Second ed., *Wiley*, N.Y. (1972) Chapter 9.

Levenspiel O. "The Chemical Reactor Omnibook", *OSU Book Stores*, Corvallis, Oregon (1979) Chapters 61-64.

Luttrell G.H., Yan S., Adel G.T. and Yoon R.H., "A computer-aided package for column flotation", *SME Meeting*, Salt Lake City (1990) Preprint no. 90-173.

Masliyah J.H. "Hindered settling in a multi-species system" *Chem. Eng. Sci.*, 34 (1979) 1166-1168.

Mavros P., Lazaridis N.K. and Matis K.A. "A study and modelling of liquid-phase mixing in flotation column", *Int. J. Min. Proc.*, 26 (1989) 1-16.

Michell R.W. and Furzer I.A. "Mixing in trickle flow through packed beds", *Chem. Eng. J.*, 4 (1972) 53-63.

Mills P.J.T., Yianatos J.B. and O'Connor C.T. "The mixing characteristics of solid and liquid phases in a flotation column", Minerals Engineering '92, Vancouver, Canada, 14-16 April, (1992), (*Minerals Engineering*, in press).

Mular A.L. and Musara W.T. "A batch flotation column for rate data measurement" in Proceedings of *Column '91*, International Conference on Column Flotation, Sudbury, Canada (1991) 63-74.

O'Connor C.T. and Mills P.J.T. "The effect of temperature on the pulp and froth phases in the flotation of pyrite", *Min. Eng.*, 3(6) (1990) 615-624.

O'Connor C.T., Randall E.W. and Goodall C.M. "Measurement of the effects of physical and chemical variables on bubble size", *Int. J. Min. Proc.*, 28 (1990) 139-149.

Ohki Y. and Inoue H. "Longitudinal mixing of the liquid phase in bubble columns", *Chem. Eng. Sci.*, 25 (1970) 1-16.

Ormrod G.T.W. "Development of a system for the measurement of the pulp-froth level in flotation", *Mintek Report No. M147*, Mintek, South Africa, (1984).

Randall E.W., Goodall C.M., Fairlamb P.M., Dold P.L. and O'connor C.T. "A method for measuring the sizes of bubbles in two- and three-phase systems", *J. Phys. E. Sci. Instrum.*, 22 (1989) 827-833.

Reay D. and Ratcliff G.A. "Removal of fine particles from water by dispersed air flotation: effects of bubble size and particle size on collection efficiency", *Can. J. Chem. Eng.*, 51(4) (1973) 178-185.

Reay D. and Ratcliff G.A. "Experimental testing of the hydrodynamic collision model of fine particle flotation", *Can. J. Chem. Eng.*, 53(10) (1975) 481-486.

Reith T., Renken S. and Israel B.A., "Gas hold-up and axial mixing in the fluid phase of bubble columns", *Chem. Eng. Sci.*, 23 (1968) 619-629.

Rice R.G., Oliver A.D., Newman J.P. and Wiles R.J. "Reduced dispersion using baffles in column flotation", *Powder. Tech.*, 10 (1974) 201-210.

Saxena A.C., Rao N.S. and Saxena S.C. "Bubble size distributions in bubble columns", *Can. J. Chem. Eng.*, 68 (1990) 159-161.

Schommarz K.H. "The determination of the effects of the physical and chemical parameters on the column flotation cell performance in the flotation of pyrite", *M.Sc. Thesis*, Univ. of Cape Town (1991).

Schulze H.J. "Hydrodynamics of bubble-mineral particle collisions", *Min. Proc. and Extract. Met. Review*, 5 (1989) 43-76.

Shaning Y. "Particle collection in a flotation column", *M.Sc. Thesis*, McGill Univ., Montreal, Canada (1985).

Suganuma T. and Yamanishi T. "Behaviour of solid particles in bubble columns", *Chem. Eng. Japan*, 30 (1966) 1136.

Trahar W.J. and Warren L.J. "The flotability of very fine particles - a review", *Int. J. Min. Proc.*, 3 (1976) 103-131.

Tucker J.P., Francidis J.-P. and O'Connor C.T. "The effect of physical and chemical parameters on bubble size distributions in a COMINCO air sparging test rig", in Proceedings of *Column '91*, International Conference on Column Flotation, Sudbury, Canada (1991) 289-302.

Ulbrecht J.J. and Baykara Z.S. "Significance of the central plume velocity for the correlation of liquid phase mixing in bubble columns", *Chem. Eng. Comm.*, 10 (1981) 165-185.

Vasquez J., Yianatos J.B. and Nunez P.M. "Analysis of mineral recovery in flotation columns", *VII J. Trans. Mat. J.*, Univ. of Chile, Santiago, Chile (1988) 42-43.

Warren L.J. "Determination of the contributions of true flotation and entrainment in batch flotation tests", *Int. J. Min. Proc.*, 14 (1985) 33-44.

Wehner J.F. and Wilhelm R.H. "Boundary Conditions of flow reactors", *Chem. Eng. Sci.*, 6 (1956) 89-93.

Weber M.E. "Collision efficiencies for small particles with a spherical collector at intermediate Reynolds numbers" *J. Separ. Proc. Tech.*, 2(1) (1981) 29-33.

Weber M.E. and Paddock D. "Interceptional and gravitational collision efficiencies for single collectors at intermediate Reynolds numbers", *J. Coll. Int. Sci.*, 94(2) (1983) 328-335.

Wen C.Y. and Fan L.T. "Models for flow systems and chemical reactors", Chem. Proc. Eng. Vol. 3 (L.F. Albright, R.N. Maddox andJ.J. McKetta ed.), *Marcel Dekker Inc.*, New York (1975) 114-151.

Woodburn E.T., King R.P. and Colborn R.P. "The effect of particle size distribution and the performance of a phosphate flotation process", *Met. Trans.*, 2 (1971) 3163-3174.

Xu M. and Finch J.A. "The axial dispersion model in flotation column studies", *Min. Eng.*, 4 (1991a) 553-562.

Xu M. and Finch J.A. "Estimating vessel dispersion numbers in flotation columns" in Proceedings of *Column '91*, International Conference on Column Flotation, Sudbury, Canada (1991b) 437-466.

Xu M., Finch J.A. and Laplante A.R. "Numerical solution of the axial dispersion model in flotation column studies", *Can. Met. Q.*, 30(2) (1991) 71-77.

Xu M. and Finch J.A. "Solids mixing in the collection zone of flotation columns", 5(9) (1992) 1029-1039.

Yianatos J.B., Finch J.A. and Laplante A.R. "The cleaning action in column in column flotation froths", Trans. Inst. Min. Met., 96 (1987) 1061-1068.

Yianatos J.B., Finch J.A. and Laplante A.R. "Selectivity in column flotation froths", *Int. J. Min. Proc.*, 15 (1988a) 11-14.

Yianatos J.B., Finch J.A., Dobby G.S. and Xu M. "Bubble size estimation in a bubble swarm", *J. Coll. Inter. Sci.*, 126(1) (1988b) 37-44.

Yianatos J.B. "Column flotation, Modelling and technology" in Proceedings of S.A.I.M.M. Int. Colloquium: *Developments in Froth Flotation*, Gordons Bay, South Africa Vol. 2 (1989).

Yianatos J.B. and Bergh L.G. "Radiactive tracer technique applied to industrial flotation columns" in Proceedings of *3rd Int. Min. Proc. Symp.* (G. Onal ed.), Istanbul, Turkey (1990) 537-544.

Ynchausti R.A., McKay J.D. and Foot D.G. Jr. "Column flotation parameters-their effects" in Proceedings of *Column Flotation '88* (K.V.S. Sastry ed.), SME Annual Meeting, Phoenix, Arizona (1988) 157-172.

APPENDIX 1

RESIDENCE TIME DISTRIBUTION TESTWORK DATA

A. Preliminary RTD Study

B. Pilot Column RTD Study

C. President Steyn Industrial Column Study

RTD data of Yianatos and Bergh (1990)

A. PRELIMINARY RTD STUDY (Laboratory Column)

	REPRODUCIBILITY						
Time	A.1 Run 1	A.2 Run 2	A.3 Run 3		A.1 Run 1	A.2 Run 2	A.3 Run 3
(sec)	E(t)	E(t)	E(t)	(sec)	E(t)	E(t)	E(t)
0	0.0000	0.0000	0.0000	215	0.0021	0.0026	0.0024
5	0.0000	0.0000	0.0000	220	0.0017	0.0024	0.0020
10	0.0000	0.0000	0.0000	225	0.0015	0.0020	0.0018
15	0.0000	0.0000	0.0000	230	0.0013	0.0016	0.0015
20	0.0000	0.0000	0.0000	235	0.0010	0.0015	0.0013
25	0.0000	0.0000	0.0000	240	0.0009	0.0012	0.0011
30	0.0000	0.0000	0.0000	245	0.0008	0.0011	0.0008
35	0.0000	0.0000	0.0000	250	0.0007	0.0009	0.0008
40	0.0000	0.0000	0.0000	255	0.0005	0.0007	0.0005
45	0.0000	0.0000	0.0000	260	0.0004	0.0006	0.0004
50	0.0000	0.0000	0.0000	265	0.0004	0.0005	0.0003
55	0.0000	0.0000	0.0000	270	0.0003	0.0004	0.0003
60	0.0000	0.0000	0.0000	275	0.0002	0.0003	0.0002
65	0.0001	0.0000	0.0000	280	0.0002	0.0002	0.0002
70	0.0001	0.0002	0.0000	285	0.0002	0.0002	0.0001
75	0.0003	0.0007	0.0002	290	0.0001	0.0001	0.0001
80	0.0006	0.0008	0.0007	295	0.0001	0.0001	0.0001
85	0.0014	0.0018	0.0016	300	0.0001	0.0001	0.0001
90	0.0026	0.0026	0.0023	305	0.0001	0.0001	0.0000
95	0.0034	0.0035	0.0036	310	0.0001	0.0000	0.0000
100	0.0048	0.0043	0.0046	315	0.0001	0.0000	0.0000
105	0.0064	0.0058	0.0062	320	0.0001	0.0000	0.0000
110	0.0072	0.0071	0.0074	325	0.0001	0.0000	0.0000
115	0.0090	0.0079	0.0077	330	0.0001	0.0000	0.0000
120	0.0102	0.0083	0.0090	335	0.0001	0.0000	0.0000
125	0.0106	0.0093	0.0102	340	0.0001	0.0000	0.0000
130	0.0111	0.0101	0.0107	345	0.0001	0.0000	0.0000
135	0.0115	0.0108	0.0111	350	0.0001	0.0000	0.0000
140	0.0117	0.0108	0.0111	355	0.0001	0.0000	0.0000
145	0.0117	0.0107	0.0112	360	0.0001	0.0000	0.0000
150	0.0112	0.0105	0.0109	365	0.0001	0.0000	0.0000
155	0.0109	0.0102	0.0103	370	0.0001	0.0000	0.0000
160	0.0102	0.0094	0.0096	375	0.0001	0.0000	0.0000
165	0.0089	0.0084	0.0089	380	0.0001	0.0000	0.0000
170	0.0073	0.0081	0.0084	385	0.0001	0.0000	0.0000
175	0.0069	0.0077	0.0077	390	0.0001	0.0000	0.0000
180	0.0060	0.0070	0.0064	395	0.0001	0.0000	0.0000
185	0.0054	0.0063	0.0060	400	0.0001	0.0000	0.0000
190	0.0047	0.0057	0.0053	405	0.0000	0.0000	0.0000
195	0.0040	0.0049	0.0046	410	0.0000	0.0000	0.0000
200	0.0033	0.0041	0.0036	415	0.0000	0.0000	0.0000
205	0.0029	0.0033	0.0032	420	0.0000	0.0000	0.0000
210	0.0024	0.0029	0.0028	425	0.0000	0.0000	0.0000

A. PRELIMINARY RTD STUDY (Laboratory Column)

	FEED % SOLIDS								
	A.4	A.5	A.6	A.7	Time	A.4	A.5	A.6	A.7
Time	0	5	10	20		0	5	10	20
(sec)	E(t)	E(t)	E(t)	E(t)	(sec)	E(t)	E(t)	E(t)	E(t)
0	0.0000	0.0000	0.0000	0.0000	180	0.0066	0.0066	0.0073	0.0074
5	0.0000	0.0000	0.0000	0.0000	185	0.0060	0.0059	0.0066	0.0069
10	0.0000	0.0000	0.0000	0.0000	190	0.0054	0.0053	0.0056	0.0062
15	0.0000	0.0000	0.0000	0.0000	195	0.0047	0.0047	0.0047	0.0053
20	0.0000	0.0000	0.0000	0.0000	200	0.0042	0.0039	0.0044	0.0042
25	0.0000	0.0000	0.0000	0.0000	205	0.0033	0.0034	0.0039	0.0039
30	0.0000	0.0000	0.0000	0.0000	210	0.0030	0.0031	0.0033	0.0033
35	0.0000	0.0000	0.0000	0.0000	215	0.0027	0.0025	0.0028	0.0029
40	0.0000	0.0000	0.0000	0.0000	220	0.0023	0.0021	0.0024	0.0024
45	0.0000	0.0000	0.0000	0.0000	225	0.0018	0.0018	0.0021	0.0020
50	0.0000	0.0000	0.0000	0.0000	230	0.0015	0.0017	0.0019	0.0016
55	0.0000	0.0000	0.0000	0.0000	235	0.0013	0.0013	0.0016	0.0013
60	0.0000	0.0000	0.0000	0.0000	240	0.0011	0.0011	0.0014	0.0011
65	0.0000	0.0000	0.0000	0.0000	245	0.0009	0.0011	0.0011	0.0009
70	0.0000	0.0001	0.0001	0.0000	250	0.0008	0.0011	0.0010	0.0007
75	0.0002	0.0004	0.0003	0.0001	255	0.0007	0.0008	0.0008	0.0006
80	0.0007	0.0006	0.0005	0.0003	260	0.0006	0.0006	0.0007	0.0004
85	0.0010	0.0011	0.0010	0.0007	265	0.0005	0.0006	0.0005	0.0004
90	0.0018	0.0015	0.0017	0.0014	270	0.0004	0.0005	0.0005	0.0003
95	0.0027	0.0028	0.0028	0.0025	275	0.0003	0.0005	0.0004	0.0002
100	0.0037	0.0034	0.0042	0.0033	280	0.0003	0.0005	0.0003	0.0002
105	0.0050	0.0053	0.0053	0.0049	285	0.0002	0.0004	0.0002	0.0001
110	0.0065	0.0066	0.0063	0.0056	290	0.0002	0.0003	0.0002	0.0001
115	0.0076	0.0076	0.0074	0.0080	295	0.0002	0.0002	0.0001	0.0001
120	0.0089	0.0090	0.0088	0.0091	300	0.0001	0.0002	0.0001	0.0001
125	0.0102	0.0099	0.0094	0.0091	305	0.0001	0.0002	0.0001	0.0000
130	0.0107	0.0107	0.0099	0.0099	310	0.0001	0.0002	0.0001	0.0000
135	0.0110	0.0112	0.0105	0.0109	315	0.0001	0.0002	0.0001	0.0000
140	0.0114	0.0113	0.0106	0.0112	320	0.0000	0.0001	0.0000	0.0000
145	0.0115	0.0112	0.0107	0.0110	325	0.0000	0.0001	0.0000	0.0000
150	0.0112	0.0108	0.0106	0.0110	330	0.0000	0.0001	0.0000	0.0000
155	0.0107	0.0105	0.0102	0.0106	335	0.0000	0.0001	0.0000	0.0000
160	0.0099	0.0097	0.0097	0.0103	340	0.0000	0.0001	0.0000	0.0000
165	0.0091	0.0092	0.0092	0.0098	345	0.0000	0.0000	0.0000	0.0000
170	0.0085	0.0084	0.0089	0.0091	350	0.0000	0.0000	0.0000	0.0000
175	0.0078	0.0077	0.0078	0.0081	355	0.0000	0.0000	0.0000	0.0000

A. PRELIMINARY RTD STUDY (Laboratory Column)

	GAS RATE (cm/s)						
	A.8	A.9	A.10		A.8	A.9	A.10
Time	0.00	2.11	2.74		0.00	2.11	2.74
(sec)	E(t)	E(t)	E(t)	(sec)	E(t)	E(t)	E(t)
0	0.0000	0.0000	0.0000	215	0.0015	0.0027	0.0023
5	0.0000	0.0000	0.0000	220	0.0012	0.0023	0.0020
10	0.0000	0.0000	0.0000	225	0.0010	0.0021	0.0017
15	0.0000	0.0000	0.0000	230	0.0007	0.0017	0.0015
20	0.0000	0.0000	0.0000	235	0.0005	0.0016	0.0012
25	0.0000	0.0000	0.0000	240	0.0005	0.0013	0.0011
30	0.0000	0.0000	0.0000	245	0.0004	0.0011	0.0010
35	0.0000	0.0000	0.0000	250	0.0004	0.0010	0.0008
40	0.0000	0.0000	0.0000	255	0.0003	0.0008	0.0007
45	0.0000	0.0000	0.0000	260	0.0003	0.0007	0.0006
50	0.0000	0.0000	0.0001	265	0.0003	0.0006	0.0005
55	0.0000	0.0001	0.0002	270	0.0002	0.0005	0.0004
60	0.0000	0.0002	0.0007	275	0.0002	0.0005	0.0003
65	0.0000	0.0005	0.0015	280	0.0002	0.0004	0.0003
70	0.0000	0.0011	0.0017	285	0.0002	0.0003	0.0002
75	0.0003	0.0016	0.0030	290	0.0002	0.0003	0.0002
80	0.0004	0.0026	0.0037	295	0.0002	0.0003	0.0002
85	0.0009	0.0032	0.0045	300	0.0002	0.0002	0.0002
90	0.0014	0.0044	0.0060	305	0.0000	0.0002	0.0001
95	0.0025	0.0055	0.0066	310	0.0000	0.0001	0.0001
100	0.0029	0.0063	0.0076	315	0.0000	0.0001	0.0001
105	0.0051	0.0074	0.0082	320	0.0000	0.0001	0.0001
110	0.0056	0.0081	0.0090	325	0.0000	0.0001	0.0000
115	0.0057	0.0088	0.0094	330	0.0000	0.0001	0.0000
120	0.0071	0.0091	0.0095	335	0.0000	0.0000	0.0000
125	0.0086	0.0093	0.0095	340	0.0000	0.0000	0.0000
130	0.0095	0.0095	0.0095	345	0.0000	0.0000	0.0000
135	0.0107	0.0095	0.0092	350	0.0000	0.0000	0.0000
140	0.0114	0.0094	0.0088	355	0.0000	0.0000	0.0000
145	0.0115	0.0091	0.0085	360	0.0000	0.0000	0.0000
150	0.0119	0.0087	0.0082	365	0.0000	0.0000	0.0000
155	0.0120	0.0083	0.0077	370	0.0000	0.0000	0.0000
160	0.0119	0.0076	0.0070	375	0.0000	0.0000	0.0000
165	0.0117	0.0073	0.0066	380	0.0000	0.0000	0.0000
170	0.0114	0.0065	0.0059	385	0.0000	0.0000	0.0000
175	0.0110	0.0063	0.0054	390	0.0000	0.0000	0.0000
180	0.0102	0.0058	0.0050	395	0.0000	0.0000	0.0000
185	0.0080	0.0054	0.0046	400	0.0000	0.0000	0.0000
190	0.0062	0.0048	0.0039	405	0.0000	0.0000	0.0000
195	0.0044	0.0040	0.0037	410	0.0000	0.0000	0.0000
200	0.0036	0.0037	0.0033	415	0.0000	0.0000	0.0000
205	0.0027	0.0034	0.0029	420	0.0000	0.0000	0.0000
210	0.0026	0.0030	0.0025	425	0.0000	0.0000	0.0000

A. PRELIMINARY RTD STUDY (Laboratory Column)

	FROTHER CONCENTRATION (ppm) - FILTER CLOTH SPARGER								
	A.11	A.12	A.13	A.14	Time	A.11	A.12	A.13	A.14
Time	0	2	15	100		0	2	15	100
(sec)	E(t)	E(t)	E(t)	E(t)	(sec)	E(t)	E(t)	E(t)	E(t)
0	0.0000	0.0000	0.0000	0.0000	215	0.0035	0.0036	0.0028	0.0026
5	0.0000	0.0000	0.0000	0.0000	220	0.0030	0.0030	0.0025	0.0023
10	0.0000	0.0000	0.0000	0.0000	225	0.0023	0.0026	0.0022	0.0020
15	0.0000	0.0000	0.0000	0.0000	230	0.0020	0.0022	0.0019	0.0019
20	0.0000	0.0000	0.0000	0.0000	235	0.0017	0.0019	0.0018	0.0018
25	0.0000	0.0000	0.0000	0.0000	240	0.0015	0.0016	0.0015	0.0016
30	0.0000	0.0000	0.0000	0.0000	245	0.0012	0.0014	0.0013	0.0014
35	0.0000	0.0000	0.0000	0.0000	250	0.0011	0.0011	0.0011	0.0013
40	0.0000	0.0000	0.0000	0.0001	255	0.0008	0.0009	0.0010	0.0012
45	0.0000	0.0000	0.0000	0.0002	260	0.0007	0.0008	0.0009	0.0010
50	0.0000	0.0000	0.0000	0.0004	265	0.0005	0.0007	0.0007	0.0009
55	0.0000	0.0000	0.0000	0.0008	270	0.0005	0.0006	0.0006	0.0008
60	0.0000	0.0000	0.0000	0.0012	275	0.0004	0.0005	0.0006	0.0007
65	0.0001	0.0000	0.0001	0.0019	280	0.0003	0.0004	0.0005	0.0006
70	0.0002	0.0000	0.0004	0.0025	285	0.0002	0.0003	0.0004	0.0006
75	0.0004	0.0002	0.0007	0.0042	290	0.0002	0.0003	0.0003	0.0006
80	0.0008	0.0004	0.0011	0.0045	295	0.0002	0.0003	0.0003	0.0005
85	0.0012	0.0007	0.0022	0.0051	300	0.0001	0.0002	0.0002	0.0005
90	0.0023	0.0011	0.0034	0.0058	305	0.0001	0.0002	0.0002	0.0004
95	0.0029	0.0015	0.0045	0.0066	310	0.0001	0.0001	0.0002	0.0004
100	0.0037	0.0032	0.0054	0.0070	315	0.0001	0.0001	0.0002	0.0003
105	0.0047	0.0042	0.0066	0.0076	320	0.0000	0.0001	0.0001	0.0003
110	0.0058	0.0055	0.0075	0.0079	325	0.0000	0.0001	0.0001	0.0003
115	0.0071	0.0069	0.0082	0.0080	330	0.0000	0.0001	0.0001	0.0002
120	0.0081	0.0076	0.0089	0.0081	335	0.0000	0.0001	0.0001	0.0002
125	0.0090	0.0088	0.0094	0.0081	340	0.0000	0.0000	0.0001	0.0002
130	0.0094	0.0095	0.0098	0.0079	345	0.0000	0.0000	0.0000	0.0002
135	0.0098	0.0102	0.0100	0.0076	350	0.0000	0.0000	0.0000	0.0002
140	0.0102	0.0103	0.0099	0.0075	355	0.0000	0.0000	0.0000	0.0001
145	0.0104	0.0106	0.0096	0.0073	360	0.0000	0.0000	0.0000	0.0001
150	0.0104	0.0104	0.0092	0.0070	365	0.0000	0.0000	0.0000	0.0001
155	0.0101	0.0102	0.0089	0.0065	370	0.0000	0.0000	0.0000	0.0001
160	0.0100	0.0098	0.0083	0.0063	375	0.0000	0.0000	0.0000	0.0001
165	0.0094	0.0094	0.0078	0.0059	380	0.0000	0.0000	0.0000	0.0001
170	0.0086	0.0085	0.0073	0.0057	385	0.0000	0.0000	0.0000	0.0001
175	0.0081	0.0081	0.0067	0.0052	390	0.0000	0.0000	0.0000	0.0001
180	0.0070	0.0074	0.0061	0.0049	395	0.0000	0.0000	0.0000	0.0001
185	0.0063	0.0068	0.0054	0.0045	400	0.0000	0.0000	0.0000	0.0001
190	0.0056	0.0060	0.0049	0.0040	405	0.0000	0.0000	0.0000	0.0001
195	0.0050	0.0055	0.0044	0.0037	410	0.0000	0.0000	0.0000	0.0000
200	0.0045	0.0050	0.0040	0.0035	415	0.0000	0.0000	0.0000	0.0000
205	0.0042	0.0044	0.0036	0.0031	420	0.0000	0.0000	0.0000	0.0000
210	0.0038	0.0040	0.0032	0.0027	425	0.0000	0.0000	0.0000	0.0000

A. PRELIMINARY RTD STUDY (Laboratory Column)

	FROTHER CONCENTRATION (ppm) - USBM-TYPE SPARGER						
	A.15	A.16	A.17		A.15	A.16	A.17
Time	2	5	10		2	5	10
(sec)	E(t)	E(t)	E(t)	(sec)	E(t)	E(t)	E(t)
0	0.0000	0.0000	0.0000	235	0.0012	0.0014	0.0014
5	0.0000	0.0000	0.0000	240	0.0011	0.0012	0.0012
10	0.0000	0.0000	0.0000	245	0.0009	0.0010	0.0011
15	0.0000	0.0000	0.0000	250	0.0008	0.0009	0.0011
20	0.0000	0.0000	0.0000	255	0.0006	0.0008	0.0009
25	0.0000	0.0000	0.0000	260	0.0006	0.0007	0.0009
30	0.0000	0.0000	0.0000	265	0.0005	0.0007	0.0008
35	0.0000	0.0000	0.0000	270	0.0004	0.0006	0.0007
40	0.0000	0.0000	0.0000	275	0.0004	0.0005	0.0007
45	0.0000	0.0000	0.0001	280	0.0003	0.0004	0.0006
50	0.0000	0.0001	0.0004	285	0.0003	0.0004	0.0006
55	0.0000	0.0002	0.0011	290	0.0002	0.0003	0.0006
60	0.0001	0.0005	0.0019	295	0.0002	0.0003	0.0005
65	0.0002	0.0009	0.0028	300	0.0001	0.0002	0.0004
70	0.0005	0.0015	0.0036	305	0.0001	0.0002	0.0004
75	0.0009	0.0022	0.0046	310	0.0001	0.0001	0.0004
80	0.0017	0.0031	0.0056	315	0.0001	0.0001	0.0004
85	0.0025	0.0041	0.0065	320	0.0001	0.0001	0.0004
90	0.0037	0.0054	0.0071	325	0.0001	0.0001	0.0003
95	0.0048	0.0065	0.0078	330	0.0001	0.0001	0.0003
100	0.0059	0.0076	0.0081	335	0.0001	0.0001	0.0002
105	0.0071	0.0084	0.0084	340	0.0001	0.0000	0.0002
110	0.0083	0.0089	0.0086	345	0.0001	0.0000	0.0002
115	0.0096	0.0094	0.0086	350	0.0001	0.0000	0.0002
120	0.0101	0.0096	0.0086	355	0.0001	0.0000	0.0002
125	0.0107	0.0097	0.0085	360	0.0001	0.0000	0.0002
130	0.0109	0.0094	0.0081	365	0.0001	0.0000	0.0001
135	0.0106	0.0092	0.0078	370	0.0001	0.0000	0.0001
140	0.0104	0.0089	0.0073	375	0.0000	0.0000	0.0001
145	0.0101	0.0083	0.0069	380	0.0000	0.0000	0.0001
150	0.0097	0.0079	0.0065	385	0.0000	0.0000	0.0001
155	0.0090	0.0075	0.0061	390	0.0000	0.0000	0.0001
160	0.0083	0.0072	0.0056	395	0.0000	0.0000	0.0001
165	0.0076	0.0068	0.0051	400	0.0000	0.0000	0.0001
170	0.0070	0.0062	0.0047	405	0.0000	0.0000	0.0001
175	0.0062	0.0057	0.0044	410	0.0000	0.0000	0.0001
180	0.0055	0.0052	0.0041	415	0.0000	0.0000	0.0001
185	0.0049	0.0048	0.0036	420	0.0000	0.0000	0.0001
190	0.0044	0.0043	0.0034	425	0.0000	0.0000	0.0001
195	0.0039	0.0038	0.0030	430	0.0000	0.0000	0.0001
200	0.0034	0.0035	0.0027	435	0.0000	0.0000	0.0001
205	0.0029	0.0030	0.0024	440	0.0000	0.0000	0.0001
210	0.0026	0.0027	0.0022	445	0.0000	0.0000	0.0001
215	0.0022	0.0019	0.0019	450	0.0000	0.0000	0.0001
220	0.0019	0.0021	0.0018	455	0.0000	0.0000	0.0001
225	0.0017	0.0017	0.0016	460	0.0000	0.0000	0.0001
230	0.0014	0.0015	0.0015	465	0.0000	0.0000	0.0000

B. PILOT COLUMN RTD STUDY

B.1	TRACER: Liquid								
Time (sec)	E(t)	Time (sec)	E(t)	Time (sec)	E(t)	Time (sec)	E(t)	Time (sec)	E(t)
0	0.0003	91	0.0001	183	0.0094	275	0.0020	367	0.0004
1	-0.0001	93	0.0001	185	0.0090	277	0.0016	369	0.0001
3	0.0002	95	0.0001	187	0.0089	279	0.0019	371	0.0001
5	0.0003	97	0.0002	189	0.0092	281	0.0016	373	0.0003
7	-0.0000	99	-0.0000	191	0.0094	283	0.0014	375	-0.0000
9	0.0002	101	0.0005	193	0.0087	285	0.0012	377	0.0002
11	0.0001	103	0.0008	195	0.0086	287	0.0010	379	0.0000
13	-0.0001	105	0.0006	197	0.0088	289	0.0011	381	0.0001
15	0.0001	107	0.0007	199	0.0083	291	0.0015	383	-0.0001
17	-0.0003	109	0.0012	201	0.0079	293	0.0008	385	0.0003
19	-0.0001	111	0.0009	203	0.0086	295	0.0007	387	0.0001
21	-0.0002	113	0.0009	205	0.0080	297	0.0005	389	0.0000
23	0.0003	115	0.0008	207	0.0074	299	0.0011		
25	0.0001	117	0.0012	209	0.0074	301	0.0009		
27	0.0001	119	0.0016	211	0.0070	303	0.0011		
29	0.0002	121	0.0011	213	0.0065	305	0.0007		
31	-0.0003	123	0.0023	215	0.0067	307	0.0008		
33	0.0001	125	0.0022	217	0.0067	309	0.0005		
35	0.0001	127	0.0028	219	0.0065	311	0.0004		
37	0.0001	129	0.0032	221	0.0060	313	0.0003		
39	-0.0002	131	0.0029	223	0.0053	315	0.0007		
41	0.0002	133	0.0039	225	0.0059	317	0.0003		
43	0.0003	135	0.0042	227	0.0055	319	0.0006		
45	-0.0002	137	0.0047	229	0.0051	321	0.0005		
47	-0.0001	139	0.0051	231	0.0054	323	0.0001		
49	0.0002	141	0.0063	233	0.0049	325	0.0006		
51	-0.0001	143	0.0062	235	0.0044	327	0.0007		
53	0.0002	145	0.0063	237	0.0046	329	0.0005		
55	-0.0002	147	0.0063	239	0.0044	331	0.0005		
57	-0.0001	149	0.0080	241	0.0047	333	0.0004		
59	0.0001	151	0.0071	243	0.0041	335	0.0002		
61	0.0001	153	0.0081	245	0.0039	337	0.0003		
63	-0.0003	155	0.0078	247	0.0032	339	0.0005		
65	0.0000	157	0.0078	249	0.0034	341	0.0002		
67	-0.0001	159	0.0081	251	0.0027	343	0.0002		
69	0.0001	161	0.0083	253	0.0034	345	0.0002		
71	0.0003	163	0.0090	255	0.0031	347	-0.0001		
73	-0.0000	165	0.0091	257	0.0030	349	0.0005		
75	-0.0001	167	0.0095	259	0.0023	351	-0.0001		
77	0.0002	169	0.0089	261	0.0027	353	0.0001		
79	-0.0001	171	0.0087	263	0.0026	355	0.0001		
81	-0.0002	173	0.0097	265	0.0019	357	0.0001		
83	-0.0003	175	0.0096	267	0.0022	359	0.0000		
85	-0.0000	177	0.0100	269	0.0021	361	0.0004		
87	0.0002	179	0.0108	271	0.0017	363	0.0003		
89	-0.0000	181	0.0089	273	0.0017	365	0.0004		

B. PILOT COLUMN RTD STUDY

B.2	TRACER: Feed Material						
Time (sec)	E(t)	Time (sec)	E(t)	Time (sec)	E(t)	Time (sec)	E(t)
0	0.0000	91	0.0126	183	0.0010	275	0.0002
1	-0.0001	93	0.0143	185	0.0010	277	0.0001
3	-0.0000	95	0.0133	187	0.0011	279	0.0002
5	-0.0001	97	0.0145	189	0.0011	281	0.0002
7	0.0000	99	0.0157	191	0.0009	283	0.0002
9	0.0001	101	0.0165	193	0.0007	285	-0.0001
11	0.0000	103	0.0169	195	0.0007	287	-0.0001
13	0.0000	105	0.0160	197	0.0009	289	0.0001
15	0.0002	107	0.0157	199	0.0006	291	0.0002
17	0.0000	109	0.0143	201	0.0004	293	0.0004
19	-0.0002	111	0.0154	203	0.0005	295	0.0001
21	0.0000	113	0.0159	205	0.0006	297	0.0000
23	-0.0000	115	0.0147	207	0.0006	299	0.0002
25	0.0000	117	0.0139	209	0.0006	301	0.0004
27	0.0001	119	0.0133	211	0.0005	303	0.0001
29	-0.0001	121	0.0128	213	0.0005	305	-0.0002
31	0.0002	123	0.0126	215	0.0005	307	0.0002
33	0.0001	125	0.0118	217	0.0004	309	0.0001
35	0.0001	127	0.0107	219	0.0004	311	0.0001
37	0.0002	129	0.0101	221	0.0007	313	-0.0001
39	0.0001	131	0.0095	223	0.0006	315	-0.0001
41	0.0002	133	0.0093	225	0.0003	317	-0.0001
43	0.0003	135	0.0087	227	0.0003	319	0.0001
45	0.0002	137	0.0073	229	0.0003	321	0.0000
47	-0.0000	139	0.0074	231	0.0003	323	-0.0001
49	0.0004	141	0.0064	233	0.0004	325	-0.0002
51	0.0002	143	0.0058	235	0.0003	327	0.0001
53	0.0006	145	0.0051	237	0.0003	329	-0.0000
55	0.0002	147	0.0045	239	0.0001	331	-0.0002
57	0.0004	149	0.0045	241	0.0004	333	-0.0000
59	0.0008	151	0.0042	243	0.0003	335	0.0000
61	0.0007	153	0.0039	245	0.0000	337	0.0001
63	0.0018	155	0.0036	247	0.0002	339	-0.0001
65	0.0014	157	0.0036	249	0.0000	341	-0.0000
67	0.0022	159	0.0034	251	-0.0000	343	-0.0001
69	0.0027	161	0.0030	253	0.0002	345	-0.0000
71	0.0034	163	0.0028	255	0.0001	347	0.0001
73	0.0042	165	0.0029	257	-0.0000		
75	0.0060	167	0.0024	259	0.0004		
77	0.0065	169	0.0021	261	0.0002		
79	0.0066	171	0.0020	263	0.0001		
81	0.0069	173	0.0018	265	0.0003		
83	0.0090	175	0.0013	267	0.0003		
85	0.0103	177	0.0015	269	0.0006		
87	0.0109	179	0.0010	271	0.0003		
89	0.0117	181	0.0010	273	0.0002		

B. PILOT COLUMN RTD STUDY

B.3	TRACER: Gangue Material						
Time (sec)	E(t)	Time (sec)	E(t)	Time (sec)	E(t)	Time (sec)	E(t)
0	0.0000	91	0.0193	183	0.0005	275	0.0001
1	0.0001	93	0.0179	185	0.0006	277	0.0004
3	-0.0002	95	0.0180	187	0.0003	279	0.0002
5	0.0001	97	0.0189	189	0.0006	281	-0.0000
7	-0.0004	99	0.0179	191	0.0006	283	-0.0001
9	-0.0000	101	0.0155	193	0.0005	285	-0.0004
11	-0.0001	103	0.0143	195	0.0006	287	-0.0003
13	-0.0000	105	0.0121	197	0.0003	289	0.0001
15	0.0002	107	0.0127	199	0.0001	291	0.0001
17	-0.0002	109	0.0103	201	0.0006	293	0.0002
19	0.0001	111	0.0089	203	0.0004	295	-0.0005
21	0.0000	113	0.0099	205	0.0004	297	0.0002
23	0.0003	115	0.0074	207	0.0002	299	-0.0000
25	-0.0000	117	0.0069	209	0.0003	301	0.0001
27	-0.0000	119	0.0054	211	-0.0002	303	0.0002
29	0.0001	121	0.0053	213	0.0005	305	-0.0000
31	0.0000	123	0.0048	215	0.0004	307	-0.0002
33	-0.0000	125	0.0041	217	0.0001	309	-0.0000
35	-0.0000	127	0.0036	219	0.0004	311	-0.0002
37	-0.0000	129	0.0029	221	-0.0001		
39	0.0001	131	0.0031	223	0.0003		
41	0.0002	133	0.0026	225	-0.0001		
43	0.0002	135	0.0024	227	0.0003		
45	0.0004	137	0.0021	229	0.0003		
47	0.0006	139	0.0020	231	-0.0000		
49	0.0011	141	0.0017	233	0.0006		
51	0.0009	143	0.0019	235	0.0003		
53	0.0003	145	0.0019	237	0.0002		
55	0.0012	147	0.0014	239	-0.0002		
57	0.0024	149	0.0011	241	0.0000		
59	0.0040	151	0.0016	243	0.0004		
61	0.0048	153	0.0012	245	0.0003		
63	0.0051	155	0.0013	247	-0.0001		
65	0.0079	157	0.0011	249	0.0003		
67	0.0096	159	0.0007	251	0.0001		
69	0.0119	161	0.0012	253	-0.0000		
71	0.0114	163	0.0012	255	0.0005		
73	0.0155	165	0.0011	257	0.0005		
75	0.0164	167	0.0006	259	-0.0001		
77	0.0192	169	0.0007	261	0.0002		
79	0.0228	171	0.0007	263	-0.0000		
81	0.0198	173	0.0007	265	0.0001		
83	0.0203	175	0.0005	267	0.0000		
85	0.0216	177	0.0003	269	-0.0001		
87	0.0207	179	0.0002	271	0.0002		
89	0.0200	181	0.0010	273	0.0002		

B. PILOT COLUMN RTD STUDY

B.4	TRACER: -38 micron Gangue Material								
Time (sec)	E(t)	Time (sec)	E(t)	Time (sec)	E(t)	Time (sec)	E(t)	Time (sec)	E(t)
0	-0.0000	91	0.0006	183	0.0094	275	0.0008	367	-0.0000
1	-0.0001	93	0.0007	185	0.0093	277	0.0007	369	-0.0001
3	-0.0001	95	0.0007	187	0.0089	279	0.0007	371	0.0000
5	0.0000	97	0.0008	189	0.0084	281	0.0006	373	0.0000
7	-0.0000	99	0.0010	191	0.0085	283	0.0005	375	0.0001
9	-0.0001	101	0.0009	193	0.0084	285	0.0005	377	-0.0000
11	-0.0000	103	0.0012	195	0.0082	287	0.0004	379	0.0000
13	0.0000	105	0.0013	197	0.0082	289	0.0005	381	0.0000
15	-0.0000	107	0.0017	199	0.0077	291	0.0005	383	-0.0000
17	-0.0000	109	0.0016	201	0.0073	293	0.0004	385	0.0001
19	0.0001	111	0.0020	203	0.0070	295	0.0005	387	0.0000
21	-0.0001	113	0.0021	205	0.0067	297	0.0004	389	0.0000
23	0.0001	115	0.0026	207	0.0063	299	0.0002	391	0.0001
25	-0.0000	117	0.0025	209	0.0062	301	0.0004	393	-0.0000
27	0.0000	119	0.0028	211	0.0059	303	0.0004	395	-0.0001
29	-0.0001	121	0.0033	213	0.0055	305	0.0003	397	0.0001
31	0.0001	123	0.0036	215	0.0055	307	0.0002	399	-0.0000
33	0.0001	125	0.0042	217	0.0052	309	0.0002	401	-0.0000
35	-0.0001	127	0.0046	219	0.0049	311	0.0003	403	-0.0001
37	0.0001	129	0.0052	221	0.0046	313	0.0002	405	0.0000
39	-0.0000	131	0.0054	223	0.0048	315	0.0002	407	0.0000
41	0.0000	133	0.0060	225	0.0043	317	0.0002	409	-0.0001
43	0.0001	135	0.0063	227	0.0042	319	0.0002	411	0.0000
45	0.0000	137	0.0066	229	0.0038	321	0.0002	413	-0.0001
47	0.0000	139	0.0073	231	0.0032	323	0.0001	415	-0.0001
49	0.0000	141	0.0076	233	0.0033	325	0.0001	417	-0.0001
51	-0.0000	143	0.0083	235	0.0029	327	0.0002	419	0.0001
53	0.0001	145	0.0088	237	0.0028	329	0.0001	421	0.0000
55	-0.0000	147	0.0090	239	0.0027	331	0.0002	423	0.0001
57	-0.0000	149	0.0093	241	0.0026	333	0.0002	425	-0.0000
59	0.0001	151	0.0106	243	0.0025	335	0.0001	427	0.0000
61	0.0000	153	0.0094	245	0.0022	337	0.0001	429	-0.0000
63	0.0002	155	0.0100	247	0.0020	339	0.0002	431	0.0000
65	0.0002	157	0.0104	249	0.0022	341	0.0000	433	0.0000
67	0.0002	159	0.0106	251	0.0018	343	0.0001	435	0.0000
69	0.0001	161	0.0105	253	0.0015	345	0.0002	437	0.0001
71	0.0002	163	0.0108	255	0.0017	347	0.0000	439	-0.0000
73	0.0002	165	0.0107	257	0.0016	349	0.0001	441	-0.0000
75	0.0001	167	0.0106	259	0.0014	351	0.0001	443	-0.0000
77	0.0001	169	0.0107	261	0.0014	353	0.0000	445	-0.0001
79	0.0002	171	0.0108	263	0.0012	355	0.0000	447	-0.0001
81	0.0002	173	0.0105	265	0.0011	357	0.0001	449	0.0000
83	0.0003	175	0.0107	267	0.0011	359	0.0001	451	0.0000
85	0.0003	177	0.0096	269	0.0010	361	0.0000	453	-0.0001
87	0.0003	179	0.0100	271	0.0007	363	0.0000	455	-0.0000
89	0.0005	181	0.0098	273	0.0007	365	0.0000		

B. PILOT COLUMN RTD STUDY

B.5	TRACER: +38-75 micron Gangue Material						
Time (sec)	E(t)	Time (sec)	E(t)	Time (sec)	E(t)	Time (sec)	E(t)
0	-0.0001	91	0.0109	183	0.0010	275	0.0003
1	0.0001	93	0.0117	185	0.0010	277	0.0002
3	0.0000	95	0.0127	187	0.0010	279	0.0002
5	-0.0001	97	0.0144	189	0.0010	281	0.0001
7	-0.0000	99	0.0133	191	0.0011	283	0.0002
9	-0.0002	101	0.0146	193	0.0011	285	0.0002
11	0.0000	103	0.0158	195	0.0009	287	0.0002
13	0.0001	105	0.0166	197	0.0006	289	-0.0002
15	0.0000	107	0.0170	199	0.0007	291	-0.0001
17	0.0000	109	0.0161	201	0.0009	293	0.0001
19	0.0001	111	0.0158	203	0.0005	295	0.0002
21	-0.0000	113	0.0143	205	0.0004	297	0.0004
23	-0.0002	115	0.0154	207	0.0005	299	0.0001
25	0.0000	117	0.0160	209	0.0005	301	0.0000
27	-0.0000	119	0.0148	211	0.0005	303	0.0002
29	-0.0000	121	0.0140	213	0.0006	305	0.0003
31	0.0001	123	0.0133	215	0.0005	307	0.0001
33	-0.0001	125	0.0129	217	0.0005	309	-0.0002
35	0.0002	127	0.0126	219	0.0005	311	0.0002
37	0.0001	129	0.0118	221	0.0004	313	0.0001
39	0.0001	131	0.0108	223	0.0004	315	0.0001
41	0.0002	133	0.0102	225	0.0007	317	-0.0001
43	0.0001	135	0.0095	227	0.0006	319	-0.0001
45	0.0002	137	0.0093	229	0.0003	321	-0.0001
47	0.0003	139	0.0087	231	0.0003	323	0.0001
49	0.0002	141	0.0073	233	0.0003	325	0.0000
51	-0.0000	143	0.0074	235	0.0002	327	-0.0001
53	0.0004	145	0.0065	237	0.0003	329	-0.0002
55	0.0002	147	0.0058	239	0.0003	331	0.0001
57	0.0006	149	0.0051	241	0.0002	333	-0.0000
59	0.0002	151	0.0045	243	0.0001	335	-0.0002
61	0.0004	153	0.0045	245	0.0004	337	-0.0001
63	0.0008	155	0.0042	247	0.0003	339	0.0000
65	0.0007	157	0.0039	249	0.0000	341	0.0001
67	0.0018	159	0.0036	251	0.0002	343	-0.0001
69	0.0014	161	0.0036	253	0.0000	345	-0.0001
71	0.0022	163	0.0034	255	-0.0001	347	-0.0002
73	0.0027	165	0.0030	257	0.0001	349	-0.0000
75	0.0034	167	0.0028	259	0.0001	351	0.0001
77	0.0042	169	0.0029	261	-0.0000		
79	0.0060	171	0.0024	263	0.0004		
81	0.0065	173	0.0021	265	0.0002		
83	0.0066	175	0.0020	267	0.0001		
85	0.0070	177	0.0018	269	0.0003		
87	0.0091	179	0.0013	271	0.0002		
89	0.0103	181	0.0015	273	0.0006		

B. PILOT COLUMN RTD STUDY

B.6	TRACER: +75-106 micron Gangue Material						
Time (sec)	E(t)	Time (sec)	E(t)	Time (sec)	E(t)	Time (sec)	E(t)
0	0.0000	91	0.0192	183	0.0005	275	0.0001
1	0.0001	93	0.0178	185	0.0006	277	0.0004
3	-0.0002	95	0.0179	187	0.0003	279	0.0002
5	0.0001	97	0.0187	189	0.0006	281	-0.0000
7	-0.0004	99	0.0178	191	0.0006	283	-0.0000
9	0.0000	101	0.0154	193	0.0006	285	-0.0003
11	-0.0001	103	0.0142	195	0.0007	287	-0.0002
13	-0.0000	105	0.0121	197	0.0004	289	0.0002
15	0.0002	107	0.0127	199	0.0002	291	0.0001
17	-0.0002	109	0.0102	201	0.0007	293	0.0002
19	0.0001	111	0.0088	203	0.0004	295	-0.0005
21	0.0001	113	0.0099	205	0.0004	297	0.0002
23	0.0003	115	0.0073	207	0.0002	299	0.0000
25	-0.0000	117	0.0069	209	0.0003	301	0.0001
27	-0.0000	119	0.0054	211	-0.0001	303	0.0002
29	0.0001	121	0.0053	213	0.0005	305	-0.0000
31	0.0001	123	0.0048	215	0.0004	307	-0.0002
33	-0.0000	125	0.0041	217	0.0001	309	0.0000
35	-0.0000	127	0.0036	219	0.0004	311	-0.0002
37	0.0000	129	0.0029	221	-0.0001		
39	0.0001	131	0.0031	223	0.0003		
41	0.0002	133	0.0026	225	-0.0000		
43	0.0003	135	0.0024	227	0.0003		
45	0.0004	137	0.0021	229	0.0003		
47	0.0006	139	0.0020	231	-0.0000		
49	0.0011	141	0.0017	233	0.0007		
51	0.0009	143	0.0019	235	0.0003		
53	0.0003	145	0.0019	237	0.0002		
55	0.0012	147	0.0014	239	-0.0002		
57	0.0024	149	0.0011	241	0.0001		
59	0.0040	151	0.0016	243	0.0004		
61	0.0048	153	0.0012	245	0.0003		
63	0.0050	155	0.0013	247	-0.0001		
65	0.0079	157	0.0012	249	0.0003		
67	0.0095	159	0.0008	251	0.0001		
69	0.0118	161	0.0012	253	-0.0000		
71	0.0113	163	0.0012	255	0.0005		
73	0.0154	165	0.0012	257	0.0005		
75	0.0163	167	0.0007	259	-0.0001		
77	0.0191	169	0.0007	261	0.0003		
79	0.0227	171	0.0007	263	0.0000		
81	0.0196	173	0.0008	265	0.0002		
83	0.0202	175	0.0005	267	0.0001		
85	0.0215	177	0.0003	269	-0.0001		
87	0.0206	179	0.0002	271	0.0002		
89	0.0199	181	0.0010	273	0.0002		

B. PILOT COLUMN RTD STUDY

B.7	TRACER: +106-150 micron Gangue Material						
Time (sec)	E(t)	Time (sec)	E(t)	Time (sec)	E(t)	Time (sec)	E(t)
0	-0.0003	91	0.0124	183	0.0012	275	0.0004
1	0.0001	93	0.0123	185	0.0007	277	0.0002
3	0.0001	95	0.0108	187	0.0010	279	0.0003
5	-0.0001	97	0.0087	189	0.0005	281	0.0004
7	-0.0000	99	0.0106	191	0.0007	283	0.0001
9	0.0001	101	0.0091	193	0.0006	285	0.0001
11	0.0000	103	0.0095	195	0.0004	287	0.0001
13	0.0000	105	0.0100	197	0.0005	289	0.0000
15	0.0000	107	0.0080	199	0.0005	291	0.0000
17	0.0000	109	0.0071	201	0.0005	293	0.0002
19	-0.0001	111	0.0058	203	0.0005	295	0.0002
21	0.0002	113	0.0058	205	0.0005	297	0.0001
23	0.0001	115	0.0059	207	0.0008	299	0.0002
25	0.0003	117	0.0061	209	0.0005	301	0.0001
27	0.0001	119	0.0056	211	0.0004	303	-0.0002
29	0.0001	121	0.0056	213	0.0006	305	0.0003
31	0.0001	123	0.0048	215	0.0003	307	0.0002
33	-0.0000	125	0.0039	217	0.0008	309	0.0000
35	0.0001	127	0.0038	219	0.0006	311	0.0001
37	0.0003	129	0.0040	221	0.0002	313	0.0001
39	0.0000	131	0.0036	223	0.0005	315	-0.0001
41	0.0008	133	0.0028	225	0.0001	317	0.0000
43	0.0011	135	0.0020	227	0.0003	319	-0.0002
45	0.0013	137	0.0020	229	0.0006	321	-0.0000
47	0.0020	139	0.0021	231	0.0004	323	-0.0004
49	0.0019	141	0.0019	233	0.0003	325	-0.0002
51	0.0034	143	0.0020	235	0.0001	327	-0.0002
53	0.0058	145	0.0026	237	0.0005	329	-0.0002
55	0.0072	147	0.0017	239	0.0004	331	-0.0001
57	0.0088	149	0.0021	241	0.0003	333	-0.0002
59	0.0105	151	0.0023	243	0.0002	335	0.0000
61	0.0151	153	0.0018	245	0.0004	337	0.0002
63	0.0141	155	0.0009	247	0.0002	339	0.0001
65	0.0214	157	0.0015	249	0.0005	341	0.0002
67	0.0163	159	0.0011	251	0.0001	343	0.0003
69	0.0196	161	0.0012	253	0.0004	345	-0.0002
71	0.0167	163	0.0010	255	-0.0000	347	0.0002
73	0.0195	165	0.0011	257	0.0000	349	0.0001
75	0.0199	167	0.0009	259	0.0003	351	0.0001
77	0.0215	169	0.0015	261	0.0005	353	-0.0002
79	0.0159	171	0.0006	263	0.0001	355	0.0002
81	0.0150	173	0.0010	265	0.0002	357	-0.0000
83	0.0122	175	0.0008	267	0.0002	359	-0.0002
85	0.0122	177	0.0012	269	0.0002	361	-0.0003
87	0.0138	179	0.0007	271	0.0001	363	0.0001
89	0.0113	181	0.0009	273	0.0002		

C. PRESIDENT STEYN INDUSTRIAL COLUMN RTD STUDY

C.1	TRACER: Gangue Material								
Time (min)	E(t)	Time (min)	E(t)	Time (min)	E(t)	Time (min)	E(t)	Time (min)	E(t)
20.00	0.0136	24.00	0.0103	28.00	0.0034	32.00	0.0042	36.00	0.0034
20.08	0.0146	24.08	0.0072	28.08	0.0052	32.08	0.0047	36.08	0.0024
20.17	0.0123	24.17	0.0065	28.17	0.0047	32.17	0.0032	36.17	0.0021
20.25	0.0136	24.25	0.0106	28.25	0.0062	32.25	0.0014	36.25	0.0027
20.33	0.0123	24.33	0.0083	28.33	0.0072	32.33	0.0052	36.33	0.0052
20.42	0.0136	24.42	0.0075	28.42	0.0055	32.42	0.0032	36.42	0.0032
20.50	0.0129	24.50	0.0090	28.50	0.0042	32.50	0.0027	36.50	0.0014
20.58	0.0129	24.58	0.0088	28.58	0.0057	32.58	0.0014	36.58	0.0044
20.67	0.0131	24.67	0.0083	28.67	0.0034	32.67	0.0029	36.67	0.0029
20.75	0.0134	24.75	0.0065	28.75	0.0052	32.75	0.0034	36.75	0.0019
20.83	0.0131	24.83	0.0093	28.83	0.0055	32.83	0.0042	36.83	0.0014
20.92	0.0144	24.92	0.0080	28.92	0.0067	32.92	0.0014	36.92	0.0029
21.00	0.0116	25.00	0.0067	29.00	0.0078	33.00	0.0047	37.00	0.0014
21.08	0.0095	25.08	0.0108	29.08	0.0060	33.08	0.0055	37.08	0.0037
21.17	0.0126	25.17	0.0062	29.17	0.0042	33.17	0.0027	37.17	0.0009
21.25	0.0116	25.25	0.0047	29.25	0.0042	33.25	0.0032	37.25	0.0027
21.33	0.0118	25.33	0.0101	29.33	0.0080	33.33	0.0032	37.33	0.0029
21.42	0.0129	25.42	0.0055	29.42	0.0065	33.42	0.0052	37.42	-0.0012
21.50	0.0116	25.50	0.0072	29.50	0.0047	33.50	0.0049	37.50	0.0021
21.58	0.0108	25.58	0.0080	29.58	0.0044	33.58	0.0044	37.58	0.0016
21.67	0.0106	25.67	0.0072	29.67	0.0060	33.67	0.0032	37.67	0.0014
21.75	0.0129	25.75	0.0049	29.75	0.0049	33.75	0.0065	37.75	0.0027
21.83	0.0113	25.83	0.0098	29.83	0.0037	33.83	0.0024	37.83	0.0021
21.92	0.0098	25.92	0.0078	29.92	0.0065	33.92	0.0060	37.92	0.0009
22.00	0.0116	26.00	0.0080	30.00	0.0037	34.00	0.0034	38.00	0.0029
22.08	0.0108	26.08	0.0065	30.08	0.0065	34.08	0.0032	38.08	0.0037
22.17	0.0116	26.17	0.0057	30.17	0.0049	34.17	0.0027	38.17	0.0021
22.25	0.0111	26.25	0.0067	30.25	0.0037	34.25	0.0021	38.25	0.0016
22.33	0.0098	26.33	0.0065	30.33	0.0032	34.33	0.0055	38.33	0.0011
22.42	0.0111	26.42	0.0072	30.42	0.0037	34.42	0.0047	38.42	0.0016
22.50	0.0129	26.50	0.0085	30.50	0.0037	34.50	0.0029	38.50	0.0014
22.58	0.0095	26.58	0.0106	30.58	0.0062	34.58	0.0042	38.58	0.0011
22.67	0.0118	26.67	0.0083	30.67	0.0029	34.67	0.0024	38.67	0.0019
22.75	0.0088	26.75	0.0075	30.75	0.0055	34.75	0.0014	38.75	0.0037
22.83	0.0101	26.83	0.0044	30.83	0.0037	34.83	0.0027	38.83	0.0032
22.92	0.0098	26.92	0.0080	30.92	0.0047	34.92	-0.0007		
23.00	0.0085	27.00	0.0060	31.00	0.0065	35.00	0.0034		
23.08	0.0111	27.08	0.0090	31.08	0.0044	35.08	0.0024		
23.17	0.0103	27.17	0.0065	31.17	0.0049	35.17	0.0034		
23.25	0.0108	27.25	0.0029	31.25	0.0039	35.25	0.0034		
23.33	0.0083	27.33	0.0057	31.33	0.0032	35.33	0.0027		
23.42	0.0090	27.42	0.0055	31.42	0.0019	35.42	0.0021		
23.50	0.0093	27.50	0.0052	31.50	0.0032	35.50	0.0001		
23.58	0.0118	27.58	0.0070	31.58	0.0044	35.58	-0.0004		
23.67	0.0078	27.67	0.0088	31.67	0.0037	35.67	0.0019		
23.75	0.0106	27.75	0.0067	31.75	0.0055	35.75	0.0032		
23.83	0.0078	27.83	0.0070	31.83	0.0027	35.83	0.0021		
23.92	0.0090	27.92	0.0072	31.92	0.0034	35.92	0.0014		

C. PRESIDENT STEYN INDUSTRIAL COLUMN RTD STUDY

C.1	TRACER: Gangue Material								
Time (min)	E(t)	Time (min)	E(t)	Time (min)	E(t)	Time (min)	E(t)	Time (min)	E(t)
0.00	0.0000	4.00	0.0935	8.00	0.0519	12.00	0.0325	16.00	0.0210
0.08	0.0006	4.08	0.0901	8.08	0.0542	12.08	0.0330	16.08	0.0218
0.17	0.0001	4.17	0.0868	8.17	0.0519	12.17	0.0330	16.17	0.0203
0.25	-0.0007	4.25	0.0912	8.25	0.0547	12.25	0.0338	16.25	0.0185
0.33	-0.0007	4.33	0.0868	8.33	0.0514	12.33	0.0348	16.33	0.0185
0.42	-0.0004	4.42	0.0840	8.42	0.0506	12.42	0.0310	16.42	0.0192
0.50	-0.0002	4.50	0.0845	8.50	0.0519	12.50	0.0348	16.50	0.0203
0.58	-0.0007	4.58	0.0774	8.58	0.0491	12.58	0.0310	16.58	0.0200
0.67	-0.0017	4.67	0.0835	8.67	0.0493	12.67	0.0289	16.67	0.0195
0.75	0.0011	4.75	0.0886	8.75	0.0488	12.75	0.0274	16.75	0.0185
0.83	0.0027	4.83	0.0909	8.83	0.0488	12.83	0.0338	16.83	0.0200
0.92	0.0049	4.92	0.0787	8.92	0.0437	12.92	0.0297	16.92	0.0182
1.00	0.0118	5.00	0.0848	9.00	0.0506	13.00	0.0292	17.00	0.0210
1.08	0.0164	5.08	0.0822	9.08	0.0481	13.08	0.0292	17.08	0.0185
1.17	0.0228	5.17	0.0799	9.17	0.0470	13.17	0.0284	17.17	0.0192
1.25	0.0348	5.25	0.0776	9.25	0.0458	13.25	0.0297	17.25	0.0180
1.33	0.0440	5.33	0.0787	9.33	0.0437	13.33	0.0261	17.33	0.0172
1.42	0.0549	5.42	0.0766	9.42	0.0414	13.42	0.0297	17.42	0.0192
1.50	0.0616	5.50	0.0799	9.50	0.0424	13.50	0.0284	17.50	0.0177
1.58	0.0713	5.58	0.0805	9.58	0.0442	13.58	0.0292	17.58	0.0208
1.67	0.0756	5.67	0.0738	9.67	0.0453	13.67	0.0264	17.67	0.0180
1.75	0.0820	5.75	0.0710	9.75	0.0435	13.75	0.0287	17.75	0.0174
1.83	0.0891	5.83	0.0736	9.83	0.0468	13.83	0.0271	17.83	0.0169
1.92	0.0945	5.92	0.0776	9.92	0.0414	13.92	0.0269	17.92	0.0185
2.00	0.0973	6.00	0.0662	10.00	0.0483	14.00	0.0289	18.00	0.0177
2.08	0.1009	6.08	0.0629	10.08	0.0419	14.08	0.0284	18.08	0.0154
2.17	0.0993	6.17	0.0690	10.17	0.0409	14.17	0.0251	18.17	0.0157
2.25	0.1060	6.25	0.0644	10.25	0.0407	14.25	0.0248	18.25	0.0164
2.33	0.1052	6.33	0.0680	10.33	0.0404	14.33	0.0243	18.33	0.0154
2.42	0.1021	6.42	0.0634	10.42	0.0396	14.42	0.0248	18.42	0.0164
2.50	0.1072	6.50	0.0606	10.50	0.0371	14.50	0.0246	18.50	0.0154
2.58	0.1072	6.58	0.0616	10.58	0.0381	14.58	0.0228	18.58	0.0152
2.67	0.1080	6.67	0.0626	10.67	0.0394	14.67	0.0256	18.67	0.0162
2.75	0.1080	6.75	0.0588	10.75	0.0404	14.75	0.0269	18.75	0.0136
2.83	0.1093	6.83	0.0585	10.83	0.0386	14.83	0.0264	18.83	0.0141
2.92	0.1095	6.92	0.0567	10.92	0.0366	14.92	0.0264	18.92	0.0131
3.00	0.1083	7.00	0.0595	11.00	0.0371	15.00	0.0254	19.00	0.0141
3.08	0.1024	7.08	0.0547	11.08	0.0350	15.08	0.0236	19.08	0.0139
3.17	0.1037	7.17	0.0570	11.17	0.0373	15.17	0.0231	19.17	0.0134
3.25	0.0996	7.25	0.0565	11.25	0.0348	15.25	0.0233	19.25	0.0116
3.33	0.0993	7.33	0.0562	11.33	0.0356	15.33	0.0218	19.33	0.0136
3.42	0.0927	7.42	0.0600	11.42	0.0389	15.42	0.0228	19.42	0.0169
3.50	0.0968	7.50	0.0562	11.50	0.0384	15.50	0.0190	19.50	0.0152
3.58	0.0947	7.58	0.0526	11.58	0.0322	15.58	0.0238	19.58	0.0141
3.67	0.0945	7.67	0.0542	11.67	0.0338	15.67	0.0231	19.67	0.0131
3.75	0.0884	7.75	0.0524	11.75	0.0317	15.75	0.0225	19.75	0.0139
3.83	0.0935	7.83	0.0555	11.83	0.0345	15.83	0.0208	19.83	0.0139
3.92	0.0955	7.92	0.0493	11.92	0.0338	15.92	0.0225	19.92	0.0134

C. PRESIDENT STEYN INDUSTRIAL COLUMN RTD STUDY

C.2	TRACER: Gangue Material								
Time (min)	E(t)	Time (min)	E(t)	Time (min)	E(t)	Time (min)	E(t)	Time (min)	E(t)
0.00	-0.0018	4.00	0.0887	8.00	0.0566	12.00	0.0325	16.00	0.0243
0.08	-0.0002	4.08	0.0923	8.08	0.0564	12.08	0.0346	16.08	0.0223
0.17	-0.0007	4.17	0.0884	8.17	0.0566	12.17	0.0334	16.17	0.0205
0.25	-0.0009	4.25	0.0880	8.25	0.0535	12.25	0.0346	16.25	0.0196
0.33	-0.0007	4.33	0.0902	8.33	0.0530	12.33	0.0328	16.33	0.0223
0.42	-0.0006	4.42	0.0839	8.42	0.0555	12.42	0.0321	16.42	0.0218
0.50	0.0003	4.50	0.0873	8.50	0.0541	12.50	0.0334	16.50	0.0203
0.58	0.0002	4.58	0.0868	8.58	0.0519	12.58	0.0321	16.58	0.0198
0.67	0.0007	4.67	0.0848	8.67	0.0544	12.67	0.0318	16.67	0.0223
0.75	-0.0002	4.75	0.0818	8.75	0.0489	12.75	0.0316	16.75	0.0187
0.83	0.0018	4.83	0.0816	8.83	0.0521	12.83	0.0310	16.83	0.0202
0.92	0.0037	4.92	0.0853	8.92	0.0489	12.92	0.0309	16.92	0.0177
1.00	0.0087	5.00	0.0803	9.00	0.0466	13.00	0.0284	17.00	0.0196
1.08	0.0144	5.08	0.0807	9.08	0.0468	13.08	0.0268	17.08	0.0177
1.17	0.0223	5.17	0.0835	9.17	0.0464	13.17	0.0305	17.17	0.0191
1.25	0.0268	5.25	0.0773	9.25	0.0546	13.25	0.0296	17.25	0.0191
1.33	0.0375	5.33	0.0752	9.33	0.0471	13.33	0.0259	17.33	0.0191
1.42	0.0469	5.42	0.0737	9.42	0.0459	13.42	0.0278	17.42	0.0175
1.50	0.0623	5.50	0.0787	9.50	0.0460	13.50	0.0260	17.50	0.0189
1.58	0.0669	5.58	0.0752	9.58	0.0453	13.58	0.0280	17.58	0.0159
1.67	0.0762	5.67	0.0764	9.67	0.0439	13.67	0.0280	17.67	0.0173
1.75	0.0784	5.75	0.0746	9.75	0.0427	13.75	0.0269	17.75	0.0175
1.83	0.0859	5.83	0.0760	9.83	0.0439	13.83	0.0266	17.83	0.0164
1.92	0.0943	5.92	0.0750	9.92	0.0435	13.92	0.0260	17.92	0.0153
2.00	0.0952	6.00	0.0721	10.00	0.0410	14.00	0.0262	18.00	0.0196
2.08	0.1034	6.08	0.0710	10.08	0.0412	14.08	0.0280	18.08	0.0175
2.17	0.1039	6.17	0.0680	10.17	0.0409	14.17	0.0262	18.17	0.0175
2.25	0.1094	6.25	0.0700	10.25	0.0387	14.25	0.0262	18.25	0.0153
2.33	0.1103	6.33	0.0677	10.33	0.0380	14.33	0.0253	18.33	0.0162
2.42	0.1118	6.42	0.0657	10.42	0.0402	14.42	0.0250	18.42	0.0171
2.50	0.1087	6.50	0.0673	10.50	0.0375	14.50	0.0235	18.50	0.0152
2.58	0.1094	6.58	0.0635	10.58	0.0359	14.58	0.0262	18.58	0.0155
2.67	0.1078	6.67	0.0669	10.67	0.0369	14.67	0.0275	18.67	0.0182
2.75	0.1053	6.75	0.0655	10.75	0.0410	14.75	0.0244	18.75	0.0155
2.83	0.1105	6.83	0.0650	10.83	0.0362	14.83	0.0248	18.83	0.0157
2.92	0.1093	6.92	0.0623	10.92	0.0371	14.92	0.0241	18.92	0.0148
3.00	0.1050	7.00	0.0641	11.00	0.0396	15.00	0.0264	19.00	0.0166
3.08	0.1039	7.08	0.0610	11.08	0.0377	15.08	0.0235	19.08	0.0137
3.17	0.1057	7.17	0.0594	11.17	0.0343	15.17	0.0239	19.17	0.0191
3.25	0.0996	7.25	0.0619	11.25	0.0377	15.25	0.0225	19.25	0.0161
3.33	0.1010	7.33	0.0609	11.33	0.0350	15.33	0.0243	19.33	0.0162
3.42	0.1007	7.42	0.0537	11.42	0.0341	15.42	0.0230	19.42	0.0159
3.50	0.0955	7.50	0.0596	11.50	0.0337	15.50	0.0257	19.50	0.0137
3.58	0.0957	7.58	0.0566	11.58	0.0325	15.58	0.0227	19.58	0.0134
3.67	0.0943	7.67	0.0552	11.67	0.0321	15.67	0.0223	19.67	0.0141
3.75	0.0932	7.75	0.0546	11.75	0.0341	15.75	0.0244	19.75	0.0137
3.83	0.0980	7.83	0.0591	11.83	0.0369	15.83	0.0225	19.83	0.0148
3.92	0.0934	7.92	0.0528	11.92	0.0319	15.92	0.0214	19.92	0.0130

C. PRESIDENT STEYN INDUSTRIAL COLUMN RTD STUDY

C.2	TRACER: Gangue Material								
Time (min)	E(t)	Time (min)	E(t)	Time (min)	E(t)	Time (min)	E(t)	Time (min)	E(t)
20.00	0.0118	24.00	0.0084	28.00	0.0057	32.00	0.0036	36.00	0.0021
20.08	0.0155	24.08	0.0071	28.08	0.0043	32.08	0.0019	36.08	0.0012
20.17	0.0144	24.17	0.0086	28.17	0.0062	32.17	0.0039	36.17	0.0014
20.25	0.0116	24.25	0.0077	28.25	0.0044	32.25	0.0034	36.25	0.0016
20.33	0.0132	24.33	0.0069	28.33	0.0059	32.33	0.0036	36.33	0.0032
20.42	0.0130	24.42	0.0089	28.42	0.0053	32.42	0.0037	36.42	0.0039
20.50	0.0128	24.50	0.0091	28.50	0.0059	32.50	0.0036	36.50	0.0037
20.58	0.0139	24.58	0.0084	28.58	0.0048	32.58	0.0030	36.58	0.0041
20.67	0.0119	24.67	0.0071	28.67	0.0041	32.67	0.0037	36.67	0.0018
20.75	0.0127	24.75	0.0077	28.75	0.0041	32.75	0.0043	36.75	0.0025
20.83	0.0109	24.83	0.0066	28.83	0.0036	32.83	0.0034	36.83	0.0025
20.92	0.0125	24.92	0.0077	28.92	0.0043	32.92	0.0018	36.92	0.0014
21.00	0.0100	25.00	0.0077	29.00	0.0041	33.00	0.0030	37.00	-0.0004
21.08	0.0123	25.08	0.0064	29.08	0.0061	33.08	0.0030	37.08	-0.0025
21.17	0.0125	25.17	0.0084	29.17	0.0036	33.17	0.0039	37.17	-0.0009
21.25	0.0118	25.25	0.0080	29.25	0.0048	33.25	0.0036	37.25	-0.0025
21.33	0.0144	25.33	0.0078	29.33	0.0050	33.33	0.0025	37.33	-0.0027
21.42	0.0136	25.42	0.0073	29.42	0.0059	33.42	0.0044	37.42	-0.0006
21.50	0.0125	25.50	0.0102	29.50	0.0032	33.50	0.0041	37.50	-0.0011
21.58	0.0116	25.58	0.0068	29.58	0.0030	33.58	0.0034	37.58	0.0011
21.67	0.0109	25.67	0.0057	29.67	0.0057	33.67	0.0032	37.67	0.0027
21.75	0.0112	25.75	0.0066	29.75	0.0028	33.75	0.0028	37.75	0.0014
21.83	0.0125	25.83	0.0084	29.83	0.0037	33.83	0.0034	37.83	0.0011
21.92	0.0100	25.92	0.0077	29.92	0.0032	33.92	0.0028		
22.00	0.0094	26.00	0.0062	30.00	0.0032	34.00	0.0036		
22.08	0.0111	26.08	0.0061	30.08	0.0037	34.08	0.0023		
22.17	0.0096	26.17	0.0053	30.17	0.0027	34.17	0.0034		
22.25	0.0109	26.25	0.0043	30.25	0.0044	34.25	0.0030		
22.33	0.0077	26.33	0.0055	30.33	0.0041	34.33	0.0036		
22.42	0.0107	26.42	0.0077	30.42	0.0016	34.42	0.0023		
22.50	0.0094	26.50	0.0053	30.50	0.0050	34.50	0.0023		
22.58	0.0093	26.58	0.0087	30.58	0.0044	34.58	0.0021		
22.67	0.0091	26.67	0.0062	30.67	0.0023	34.67	0.0011		
22.75	0.0086	26.75	0.0059	30.75	0.0080	34.75	0.0028		
22.83	0.0107	26.83	0.0052	30.83	0.0052	34.83	0.0007		
22.92	0.0096	26.92	0.0064	30.92	0.0061	34.92	0.0036		
23.00	0.0084	27.00	0.0068	31.00	0.0036	35.00	0.0036		
23.08	0.0075	27.08	0.0053	31.08	0.0046	35.08	0.0036		
23.17	0.0094	27.17	0.0061	31.17	0.0048	35.17	0.0009		
23.25	0.0093	27.25	0.0062	31.25	0.0027	35.25	0.0003		
23.33	0.0071	27.33	0.0061	31.33	0.0046	35.33	0.0028		
23.42	0.0052	27.42	0.0080	31.42	0.0028	35.42	0.0023		
23.50	0.0044	27.50	0.0062	31.50	0.0039	35.50	0.0036		
23.58	0.0068	27.58	0.0057	31.58	0.0023	35.58	0.0041		
23.67	0.0057	27.67	0.0055	31.67	0.0016	35.67	0.0021		
23.75	0.0066	27.75	0.0073	31.75	0.0055	35.75	0.0027		
23.83	0.0075	27.83	0.0064	31.83	0.0050	35.83	0.0009		
23.92	0.0091	27.92	0.0068	31.92	0.0034	35.92	0.0036		

C. PRESIDENT STEYN INDUSTRIAL COLUMN RTD STUDY

C.3	TRACER: Liquid								
Time (min)	E(t)	Time (min)	E(t)	Time (min)	E(t)	Time (min)	E(t)	Time (min)	E(t)
0.00	0.0000	4.00	0.1021	8.00	0.0624	12.00	0.0388	16.00	0.0240
0.08	0.0000	4.08	0.1008	8.08	0.0610	12.08	0.0386	16.08	0.0236
0.17	0.0000	4.17	0.0991	8.17	0.0618	12.17	0.0384	16.17	0.0236
0.25	0.0000	4.25	0.0988	8.25	0.0606	12.25	0.0371	16.25	0.0237
0.33	0.0000	4.33	0.0960	8.33	0.0594	12.33	0.0371	16.33	0.0231
0.42	0.0000	4.42	0.0955	8.42	0.0596	12.42	0.0369	16.42	0.0233
0.50	0.0000	4.50	0.0949	8.50	0.0589	12.50	0.0361	16.50	0.0226
0.58	0.0000	4.58	0.0925	8.58	0.0572	12.58	0.0358	16.58	0.0221
0.67	0.0000	4.67	0.0910	8.67	0.0585	12.67	0.0355	16.67	0.0222
0.75	0.0000	4.75	0.0913	8.75	0.0559	12.75	0.0356	16.75	0.0220
0.83	0.0000	4.83	0.0915	8.83	0.0564	12.83	0.0349	16.83	0.0213
0.92	0.0000	4.92	0.0876	8.92	0.0562	12.92	0.0353	16.92	0.0206
1.00	0.0001	5.00	0.0869	9.00	0.0554	13.00	0.0344	17.00	0.0209
1.08	0.0004	5.08	0.0870	9.08	0.0542	13.08	0.0341	17.08	0.0204
1.17	0.0012	5.17	0.0863	9.17	0.0558	13.17	0.0338	17.17	0.0208
1.25	0.0017	5.25	0.0857	9.25	0.0538	13.25	0.0332	17.25	0.0201
1.33	0.0042	5.33	0.0849	9.33	0.0538	13.33	0.0323	17.33	0.0204
1.42	0.0119	5.42	0.0844	9.42	0.0530	13.42	0.0333	17.42	0.0200
1.50	0.0247	5.50	0.0837	9.50	0.0517	13.50	0.0327	17.50	0.0203
1.58	0.0375	5.58	0.0822	9.58	0.0517	13.58	0.0315	17.58	0.0197
1.67	0.0506	5.67	0.0808	9.67	0.0513	13.67	0.0311	17.67	0.0195
1.75	0.0631	5.75	0.0817	9.75	0.0500	13.75	0.0315	17.75	0.0199
1.83	0.0700	5.83	0.0796	9.83	0.0500	13.83	0.0311	17.83	0.0190
1.92	0.0776	5.92	0.0788	9.92	0.0486	13.92	0.0308	17.92	0.0189
2.00	0.0857	6.00	0.0786	10.00	0.0493	14.00	0.0303	18.00	0.0190
2.08	0.0928	6.08	0.0773	10.08	0.0480	14.08	0.0315	18.08	0.0183
2.17	0.0945	6.17	0.0760	10.17	0.0483	14.17	0.0294	18.17	0.0184
2.25	0.0974	6.25	0.0759	10.25	0.0478	14.25	0.0298	18.25	0.0184
2.33	0.1024	6.33	0.0756	10.33	0.0463	14.33	0.0298	18.33	0.0183
2.42	0.1040	6.42	0.0737	10.42	0.0470	14.42	0.0300	18.42	0.0180
2.50	0.1045	6.50	0.0748	10.50	0.0453	14.50	0.0285	18.50	0.0179
2.58	0.1062	6.58	0.0730	10.58	0.0457	14.58	0.0277	18.58	0.0175
2.67	0.1053	6.67	0.0712	10.67	0.0448	14.67	0.0277	18.67	0.0178
2.75	0.1064	6.75	0.0728	10.75	0.0444	14.75	0.0277	18.75	0.0174
2.83	0.1066	6.83	0.0718	10.83	0.0439	14.83	0.0272	18.83	0.0171
2.92	0.1056	6.92	0.0704	10.92	0.0431	14.92	0.0273	18.92	0.0171
3.00	0.1040	7.00	0.0687	11.00	0.0432	15.00	0.0269	19.00	0.0170
3.08	0.1045	7.08	0.0686	11.08	0.0432	15.08	0.0272	19.08	0.0169
3.17	0.1062	7.17	0.0684	11.17	0.0422	15.17	0.0268	19.17	0.0162
3.25	0.1053	7.25	0.0681	11.25	0.0427	15.25	0.0269	19.25	0.0159
3.33	0.1064	7.33	0.0665	11.33	0.0417	15.33	0.0259	19.33	0.0167
3.42	0.1066	7.42	0.0665	11.42	0.0422	15.42	0.0254	19.42	0.0161
3.50	0.1056	7.50	0.0663	11.50	0.0417	15.50	0.0248	19.50	0.0157
3.58	0.1042	7.58	0.0649	11.58	0.0412	15.58	0.0248	19.58	0.0155
3.67	0.1039	7.67	0.0642	11.67	0.0402	15.67	0.0251	19.67	0.0151
3.75	0.1033	7.75	0.0639	11.75	0.0405	15.75	0.0248	19.75	0.0152
3.83	0.1030	7.83	0.0633	11.83	0.0397	15.83	0.0243	19.83	0.0151
3.92	0.1033	7.92	0.0613	11.92	0.0388	15.92	0.0244	19.92	0.0146

C. PRESIDENT STEYN INDUSTRIAL COLUMN RTD STUDY

C.3	TRACER: Liquid										
Time (min)	E(t)	Time (min)	E(t)	Time (min)	E(t)	Time (min)	E(t)	Time (min)	E(t)	Time (min)	E(t)
20.00	0.0147	24.00	0.0093	28.00	0.0049	32.00	0.0032	36.00	0.0019	40.00	0.0009
20.08	0.0143	24.08	0.0088	28.08	0.0058	32.08	0.0028	36.08	0.0018	40.08	0.0009
20.17	0.0144	24.17	0.0088	28.17	0.0050	32.17	0.0031	36.17	0.0018	40.17	0.0010
20.25	0.0146	24.25	0.0085	28.25	0.0051	32.25	0.0033	36.25	0.0016	40.25	0.0005
20.33	0.0141	24.33	0.0087	28.33	0.0050	32.33	0.0030	36.33	0.0018	40.33	0.0010
20.42	0.0141	24.42	0.0086	28.42	0.0052	32.42	0.0029	36.42	0.0014	40.42	0.0010
20.50	0.0140	24.50	0.0083	28.50	0.0048	32.50	0.0030	36.50	0.0017	40.50	0.0007
20.58	0.0139	24.58	0.0086	28.58	0.0050	32.58	0.0027	36.58	0.0021	40.58	0.0007
20.67	0.0132	24.67	0.0083	28.67	0.0049	32.67	0.0029	36.67	0.0012	40.67	0.0004
20.75	0.0137	24.75	0.0082	28.75	0.0048	32.75	0.0027	36.75	0.0019	40.75	0.0005
20.83	0.0135	24.83	0.0078	28.83	0.0045	32.83	0.0028	36.83	0.0014	40.83	0.0009
20.92	0.0126	24.92	0.0075	28.92	0.0046	32.92	0.0026	36.92	0.0012	40.92	0.0008
21.00	0.0129	25.00	0.0076	29.00	0.0046	33.00	0.0030	37.00	0.0016	41.00	0.0009
21.08	0.0128	25.08	0.0079	29.08	0.0048	33.08	0.0026	37.08	0.0014	41.08	0.0011
21.17	0.0128	25.17	0.0075	29.17	0.0045	33.17	0.0025	37.17	0.0015	41.17	0.0004
21.25	0.0125	25.25	0.0077	29.25	0.0048	33.25	0.0028	37.25	0.0017	41.25	0.0009
21.33	0.0125	25.33	0.0074	29.33	0.0047	33.33	0.0024	37.33	0.0016	41.33	0.0008
21.42	0.0118	25.42	0.0075	29.42	0.0044	33.42	0.0024	37.42	0.0014	41.42	0.0010
21.50	0.0119	25.50	0.0076	29.50	0.0042	33.50	0.0027	37.50	0.0014	41.50	0.0008
21.58	0.0116	25.58	0.0074	29.58	0.0041	33.58	0.0025	37.58	0.0010	41.58	0.0009
21.67	0.0119	25.67	0.0075	29.67	0.0042	33.67	0.0025	37.67	0.0015	41.67	0.0007
21.75	0.0117	25.75	0.0073	29.75	0.0046	33.75	0.0022	37.75	0.0014	41.75	0.0008
21.83	0.0115	25.83	0.0072	29.83	0.0042	33.83	0.0024	37.83	0.0014	41.83	0.0007
21.92	0.0112	25.92	0.0073	29.92	0.0048	33.92	0.0021	37.92	0.0015	41.92	0.0006
22.00	0.0117	26.00	0.0074	30.00	0.0039	34.00	0.0026	38.00	0.0014	42.00	0.0006
22.08	0.0114	26.08	0.0069	30.08	0.0041	34.08	0.0026	38.08	0.0013	42.08	0.0006
22.17	0.0111	26.17	0.0068	30.17	0.0041	34.17	0.0022	38.17	0.0011	42.17	0.0007
22.25	0.0114	26.25	0.0066	30.25	0.0040	34.25	0.0022	38.25	0.0013	42.25	0.0005
22.33	0.0110	26.33	0.0068	30.33	0.0040	34.33	0.0022	38.33	0.0011	42.33	0.0008
22.42	0.0104	26.42	0.0062	30.42	0.0040	34.42	0.0021	38.42	0.0011	42.42	0.0005
22.50	0.0107	26.50	0.0064	30.50	0.0037	34.50	0.0023	38.50	0.0010	42.50	0.0007
22.58	0.0110	26.58	0.0065	30.58	0.0037	34.58	0.0022	38.58	0.0013	42.58	0.0004
22.67	0.0105	26.67	0.0069	30.67	0.0037	34.67	0.0019	38.67	0.0010	42.67	0.0003
22.75	0.0106	26.75	0.0063	30.75	0.0039	34.75	0.0022	38.75	0.0013	42.75	0.0003
22.83	0.0103	26.83	0.0065	30.83	0.0036	34.83	0.0021	38.83	0.0009	42.83	0.0006
22.92	0.0107	26.92	0.0064	30.92	0.0035	34.92	0.0023	38.92	0.0010	42.92	0.0006
23.00	0.0102	27.00	0.0063	31.00	0.0036	35.00	0.0020	39.00	0.0011	43.00	0.0005
23.08	0.0097	27.08	0.0062	31.08	0.0033	35.08	0.0023	39.08	0.0010	43.08	0.0005
23.17	0.0104	27.17	0.0060	31.17	0.0035	35.17	0.0021	39.17	0.0007	43.17	0.0005
23.25	0.0100	27.25	0.0058	31.25	0.0036	35.25	0.0019	39.25	0.0009	43.25	0.0003
23.33	0.0096	27.33	0.0060	31.33	0.0035	35.33	0.0020	39.33	0.0010	43.33	0.0004
23.42	0.0095	27.42	0.0061	31.42	0.0033	35.42	0.0017	39.42	0.0013	43.42	0.0005
23.50	0.0092	27.50	0.0058	31.50	0.0032	35.50	0.0021	39.50	0.0008	43.50	0.0004
23.58	0.0091	27.58	0.0057	31.58	0.0032	35.58	0.0018	39.58	0.0008	43.58	0.0003
23.67	0.0095	27.67	0.0059	31.67	0.0037	35.67	0.0020	39.67	0.0005	43.67	0.0006
23.75	0.0095	27.75	0.0055	31.75	0.0030	35.75	0.0018	39.75	0.0010	43.75	0.0005
23.83	0.0093	27.83	0.0055	31.83	0.0031	35.83	0.0017	39.83	0.0011	43.83	0.0004
23.92	0.0096	27.92	0.0055	31.92	0.0031	35.92	0.0018	39.92	0.0009	43.92	0.0005

C. PRESIDENT STEYN INDUSTRIAL COLUMN RTD STUDY

C.4	TRACER: Feed Material								
Time (min)	E(t)	Time (min)	E(t)	Time (min)	E(t)	Time (min)	E(t)	Time (min)	E(t)
0.00	-0.0004	4.00	0.0972	8.00	0.0611	12.00	0.0331	16.00	0.0211
0.08	-0.0002	4.08	0.0960	8.08	0.0575	12.08	0.0335	16.08	0.0184
0.17	-0.0015	4.17	0.0944	8.17	0.0576	12.17	0.0333	16.17	0.0204
0.25	0.0001	4.25	0.0955	8.25	0.0600	12.25	0.0338	16.25	0.0209
0.33	-0.0006	4.33	0.0881	8.33	0.0576	12.33	0.0362	16.33	0.0197
0.42	-0.0011	4.42	0.0881	8.42	0.0562	12.42	0.0336	16.42	0.0190
0.50	-0.0009	4.50	0.0852	8.50	0.0535	12.50	0.0324	16.50	0.0213
0.58	0.0005	4.58	0.0861	8.58	0.0496	12.58	0.0317	16.58	0.0206
0.67	-0.0004	4.67	0.0899	8.67	0.0508	12.67	0.0310	16.67	0.0211
0.75	0.0005	4.75	0.0879	8.75	0.0551	12.75	0.0299	16.75	0.0202
0.83	0.0007	4.83	0.0840	8.83	0.0512	12.83	0.0315	16.83	0.0200
0.92	0.0039	4.92	0.0838	8.92	0.0517	12.92	0.0319	16.92	0.0177
1.00	0.0075	5.00	0.0838	9.00	0.0492	13.00	0.0338	17.00	0.0198
1.08	0.0152	5.08	0.0843	9.08	0.0512	13.08	0.0302	17.08	0.0186
1.17	0.0188	5.17	0.0824	9.17	0.0528	13.17	0.0310	17.17	0.0177
1.25	0.0225	5.25	0.0802	9.25	0.0471	13.25	0.0310	17.25	0.0175
1.33	0.0265	5.33	0.0888	9.33	0.0478	13.33	0.0311	17.33	0.0181
1.42	0.0387	5.42	0.0784	9.42	0.0476	13.42	0.0304	17.42	0.0191
1.50	0.0491	5.50	0.0802	9.50	0.0550	13.50	0.0254	17.50	0.0157
1.58	0.0568	5.58	0.0729	9.58	0.0514	13.58	0.0297	17.58	0.0182
1.67	0.0630	5.67	0.0791	9.67	0.0485	13.67	0.0302	17.67	0.0193
1.75	0.0741	5.75	0.0761	9.75	0.0439	13.75	0.0290	17.75	0.0177
1.83	0.0781	5.83	0.0766	9.83	0.0465	13.83	0.0283	17.83	0.0181
1.92	0.0854	5.92	0.0752	9.92	0.0440	13.92	0.0277	17.92	0.0161
2.00	0.0913	6.00	0.0731	10.00	0.0421	14.00	0.0267	18.00	0.0182
2.08	0.0999	6.08	0.0731	10.08	0.0444	14.08	0.0263	18.08	0.0152
2.17	0.0962	6.17	0.0722	10.17	0.0464	14.17	0.0245	18.17	0.0170
2.25	0.1017	6.25	0.0738	10.25	0.0437	14.25	0.0249	18.25	0.0188
2.33	0.1032	6.33	0.0709	10.33	0.0422	14.33	0.0254	18.33	0.0164
2.42	0.0999	6.42	0.0702	10.42	0.0424	14.42	0.0258	18.42	0.0152
2.50	0.1080	6.50	0.0693	10.50	0.0417	14.50	0.0252	18.50	0.0143
2.58	0.1110	6.58	0.0688	10.58	0.0424	14.58	0.0263	18.58	0.0152
2.67	0.1144	6.67	0.0671	10.67	0.0413	14.67	0.0272	18.67	0.0134
2.75	0.1123	6.75	0.0662	10.75	0.0424	14.75	0.0240	18.75	0.0159
2.83	0.1091	6.83	0.0671	10.83	0.0424	14.83	0.0249	18.83	0.0157
2.92	0.1114	6.92	0.0662	10.92	0.0421	14.92	0.0259	18.92	0.0154
3.00	0.1103	7.00	0.0646	11.00	0.0428	15.00	0.0213	19.00	0.0139
3.08	0.1098	7.08	0.0664	11.08	0.0401	15.08	0.0240	19.08	0.0145
3.17	0.1094	7.17	0.0646	11.17	0.0403	15.17	0.0241	19.17	0.0134
3.25	0.1076	7.25	0.0605	11.25	0.0387	15.25	0.0216	19.25	0.0143
3.33	0.1032	7.33	0.0637	11.33	0.0369	15.33	0.0231	19.33	0.0130
3.42	0.1033	7.42	0.0625	11.42	0.0353	15.42	0.0256	19.42	0.0127
3.50	0.1008	7.50	0.0596	11.50	0.0363	15.50	0.0209	19.50	0.0127
3.58	0.0998	7.58	0.0614	11.58	0.0370	15.58	0.0206	19.58	0.0141
3.67	0.0985	7.67	0.0628	11.67	0.0365	15.67	0.0215	19.67	0.0130
3.75	0.1001	7.75	0.0594	11.75	0.0349	15.75	0.0216	19.75	0.0148
3.83	0.0987	7.83	0.0580	11.83	0.0331	15.83	0.0225	19.83	0.0121
3.92	0.0974	7.92	0.0619	11.92	0.0335	15.92	0.0234	19.92	0.0123

C. PRESIDENT STEYN INDUSTRIAL COLUMN RTD STUDY

C.4	TRACER: Feed Material								
Time (min)	E(t)	Time (min)	E(t)	Time (min)	E(t)	Time (min)	E(t)	Time (min)	E(t)
20.00	0.0145	24.00	0.0052	28.00	0.0059	32.00	0.0007	36.00	0.0016
20.08	0.0136	24.08	0.0064	28.08	0.0035	32.08	0.0030	36.08	0.0005
20.17	0.0130	24.17	0.0073	28.17	0.0041	32.17	0.0021	36.17	0.0016
20.25	0.0129	24.25	0.0050	28.25	0.0046	32.25	0.0025	36.25	0.0009
20.33	0.0121	24.33	0.0066	28.33	0.0043	32.33	0.0026	36.33	0.0019
20.42	0.0130	24.42	0.0068	28.42	0.0046	32.42	0.0012	36.42	0.0012
20.50	0.0112	24.50	0.0055	28.50	0.0048	32.50	0.0018	36.50	0.0012
20.58	0.0098	24.58	0.0073	28.58	0.0043	32.58	0.0025	36.58	0.0009
20.67	0.0134	24.67	0.0064	28.67	0.0052	32.67	0.0014	36.67	0.0012
20.75	0.0095	24.75	0.0082	28.75	0.0030	32.75	0.0009	36.75	0.0012
20.83	0.0123	24.83	0.0095	28.83	0.0028	32.83	0.0021	36.83	0.0019
20.92	0.0116	24.92	0.0073	28.92	0.0055	32.92	0.0032	36.92	0.0003
21.00	0.0109	25.00	0.0053	29.00	0.0034	33.00	0.0010	37.00	0.0018
21.08	0.0109	25.08	0.0057	29.08	0.0037	33.08	0.0019	37.08	-0.0002
21.17	0.0093	25.17	0.0069	29.17	0.0026	33.17	0.0025	37.17	0.0019
21.25	0.0098	25.25	0.0112	29.25	0.0035	33.25	0.0018	37.25	0.0012
21.33	0.0123	25.33	0.0057	29.33	0.0032	33.33	0.0012	37.33	-0.0006
21.42	0.0116	25.42	0.0059	29.42	0.0019	33.42	0.0010	37.42	-0.0017
21.50	0.0105	25.50	0.0066	29.50	0.0053	33.50	0.0010	37.50	-0.0002
21.58	0.0098	25.58	0.0053	29.58	0.0030	33.58	0.0026	37.58	0.0019
21.67	0.0100	25.67	0.0071	29.67	0.0023	33.67	0.0025	37.67	0.0012
21.75	0.0096	25.75	0.0064	29.75	0.0032	33.75	0.0014	37.75	-0.0002
21.83	0.0100	25.83	0.0071	29.83	0.0034	33.83	0.0005	37.83	0.0019
21.92	0.0107	25.92	0.0059	29.92	0.0032	33.92	0.0019	37.92	0.0012
22.00	0.0093	26.00	0.0052	30.00	0.0061	34.00	0.0019	38.00	-0.0006
22.08	0.0096	26.08	0.0050	30.08	0.0034	34.08	0.0010	38.08	-0.0017
22.17	0.0096	26.17	0.0061	30.17	0.0019	34.17	0.0016	38.17	-0.0000
22.25	0.0091	26.25	0.0055	30.25	0.0025	34.25	0.0010		
22.33	0.0107	26.33	0.0046	30.33	0.0035	34.33	0.0019		
22.42	0.0082	26.42	0.0066	30.42	0.0025	34.42	0.0025		
22.50	0.0091	26.50	0.0041	30.50	0.0039	34.50	0.0018		
22.58	0.0077	26.58	0.0057	30.58	0.0039	34.58	0.0012		
22.67	0.0078	26.67	0.0066	30.67	0.0046	34.67	0.0010		
22.75	0.0080	26.75	0.0059	30.75	0.0016	34.75	0.0010		
22.83	0.0069	26.83	0.0050	30.83	0.0026	34.83	0.0026		
22.92	0.0087	26.92	0.0035	30.92	0.0014	34.92	0.0025		
23.00	0.0100	27.00	0.0064	31.00	0.0009	35.00	0.0014		
23.08	0.0087	27.08	0.0034	31.08	0.0034	35.08	0.0019		
23.17	0.0073	27.17	0.0039	31.17	0.0019	35.17	0.0019		
23.25	0.0075	27.25	0.0053	31.25	0.0048	35.25	0.0001		
23.33	0.0095	27.33	0.0043	31.33	0.0032	35.33	0.0012		
23.42	0.0086	27.42	0.0037	31.42	0.0025	35.42	0.0012		
23.50	0.0075	27.50	0.0035	31.50	0.0019	35.50	0.0009		
23.58	0.0073	27.58	0.0034	31.58	0.0018	35.58	0.0014		
23.67	0.0084	27.67	0.0030	31.67	0.0037	35.67	0.0016		
23.75	0.0098	27.75	0.0016	31.75	0.0023	35.75	0.0014		
23.83	0.0068	27.83	0.0039	31.83	0.0018	35.83	0.0007		
23.92	0.0082	27.92	0.0048	31.92	0.0034	35.92	0.0007		

C. PRESIDENT STEYN INDUSTRIAL COLUMN RTD STUDY

C.5	TRACER: -38 micron Gangue Material								
Time (min)	E(t)	Time (min)	E(t)	Time (min)	E(t)	Time (min)	E(t)	Time (min)	E(t)
0.00	0.0001	4.00	0.0876	8.00	0.0548	12.00	0.0368	16.00	0.0227
0.08	-0.0006	4.08	0.0849	8.08	0.0535	12.08	0.0367	16.08	0.0236
0.17	-0.0016	4.17	0.0844	8.17	0.0525	12.17	0.0361	16.17	0.0219
0.25	-0.0003	4.25	0.0852	8.25	0.0536	12.25	0.0333	16.25	0.0236
0.33	-0.0001	4.33	0.0818	8.33	0.0528	12.33	0.0329	16.33	0.0236
0.42	0.0009	4.42	0.0820	8.42	0.0535	12.42	0.0340	16.42	0.0218
0.50	0.0012	4.50	0.0793	8.50	0.0521	12.50	0.0333	16.50	0.0224
0.58	0.0007	4.58	0.0795	8.58	0.0520	12.58	0.0341	16.58	0.0209
0.67	0.0009	4.67	0.0791	8.67	0.0507	12.67	0.0318	16.67	0.0208
0.75	-0.0001	4.75	0.0775	8.75	0.0511	12.75	0.0328	16.75	0.0212
0.83	0.0015	4.83	0.0788	8.83	0.0488	12.83	0.0316	16.83	0.0204
0.92	0.0022	4.92	0.0756	8.92	0.0503	12.92	0.0314	16.92	0.0211
1.00	0.0027	5.00	0.0758	9.00	0.0503	13.00	0.0329	17.00	0.0195
1.08	0.0063	5.08	0.0770	9.08	0.0491	13.08	0.0310	17.08	0.0199
1.17	0.0108	5.17	0.0755	9.17	0.0469	13.17	0.0306	17.17	0.0196
1.25	0.0171	5.25	0.0762	9.25	0.0468	13.25	0.0308	17.25	0.0197
1.33	0.0250	5.33	0.0749	9.33	0.0462	13.33	0.0308	17.33	0.0206
1.42	0.0290	5.42	0.0735	9.42	0.0458	13.42	0.0299	17.42	0.0190
1.50	0.0370	5.50	0.0729	9.50	0.0465	13.50	0.0289	17.50	0.0192
1.58	0.0472	5.58	0.0728	9.58	0.0475	13.58	0.0292	17.58	0.0180
1.67	0.0529	5.67	0.0698	9.67	0.0486	13.67	0.0290	17.67	0.0208
1.75	0.0653	5.75	0.0698	9.75	0.0447	13.75	0.0289	17.75	0.0191
1.83	0.0685	5.83	0.0705	9.83	0.0459	13.83	0.0267	17.83	0.0182
1.92	0.0739	5.92	0.0683	9.92	0.0457	13.92	0.0281	17.92	0.0173
2.00	0.0808	6.00	0.0683	10.00	0.0450	14.00	0.0279	18.00	0.0183
2.08	0.0850	6.08	0.0668	10.08	0.0464	14.08	0.0274	18.08	0.0184
2.17	0.0909	6.17	0.0657	10.17	0.0442	14.17	0.0289	18.17	0.0180
2.25	0.0941	6.25	0.0686	10.25	0.0434	14.25	0.0260	18.25	0.0192
2.33	0.0940	6.33	0.0651	10.33	0.0420	14.33	0.0254	18.33	0.0171
2.42	0.0989	6.42	0.0638	10.42	0.0445	14.42	0.0275	18.42	0.0175
2.50	0.0957	6.50	0.0627	10.50	0.0419	14.50	0.0275	18.50	0.0178
2.58	0.1016	6.58	0.0647	10.58	0.0404	14.58	0.0267	18.58	0.0182
2.67	0.1030	6.67	0.0645	10.67	0.0429	14.67	0.0267	18.67	0.0179
2.75	0.0995	6.75	0.0642	10.75	0.0400	14.75	0.0257	18.75	0.0167
2.83	0.1008	6.83	0.0633	10.83	0.0403	14.83	0.0251	18.83	0.0173
2.92	0.0996	6.92	0.0622	10.92	0.0394	14.92	0.0243	18.92	0.0169
3.00	0.0991	7.00	0.0612	11.00	0.0413	15.00	0.0245	19.00	0.0172
3.08	0.0980	7.08	0.0608	11.08	0.0380	15.08	0.0219	19.08	0.0180
3.17	0.0966	7.17	0.0585	11.17	0.0390	15.17	0.0256	19.17	0.0173
3.25	0.0938	7.25	0.0577	11.25	0.0367	15.25	0.0248	19.25	0.0178
3.33	0.0953	7.33	0.0581	11.33	0.0384	15.33	0.0260	19.33	0.0164
3.42	0.0973	7.42	0.0579	11.42	0.0374	15.42	0.0224	19.42	0.0175
3.50	0.0926	7.50	0.0554	11.50	0.0362	15.50	0.0256	19.50	0.0156
3.58	0.0922	7.58	0.0581	11.58	0.0373	15.58	0.0248	19.58	0.0162
3.67	0.0922	7.67	0.0575	11.67	0.0359	15.67	0.0245	19.67	0.0159
3.75	0.0888	7.75	0.0543	11.75	0.0362	15.75	0.0237	19.75	0.0139
3.83	0.0854	7.83	0.0543	11.83	0.0387	15.83	0.0243	19.83	0.0152
3.92	0.0895	7.92	0.0544	11.92	0.0368	15.92	0.0227	19.92	0.0160

C. PRESIDENT STEYN INDUSTRIAL COLUMN RTD STUDY

C.5	TRACER: -38 micron Gangue Material										
Time (min)	E(t)	Time (min)	E(t)	Time (min)	E(t)	Time (min)	E(t)	Time (min)	E(t)	Time (min)	E(t)
20.00	0.0150	24.00	0.0093	28.00	0.0061	32.00	0.0046	36.00	0.0022	40.00	0.0016
20.08	0.0153	24.08	0.0086	28.08	0.0053	32.08	0.0038	36.08	0.0023	40.08	0.0021
20.17	0.0140	24.17	0.0098	28.17	0.0063	32.17	0.0032	36.17	0.0020	40.17	0.0022
20.25	0.0147	24.25	0.0087	28.25	0.0048	32.25	0.0041	36.25	0.0026	40.25	0.0022
20.33	0.0157	24.33	0.0091	28.33	0.0061	32.33	0.0042	36.33	0.0023	40.33	0.0019
20.42	0.0144	24.42	0.0087	28.42	0.0063	32.42	0.0029	36.42	0.0032	40.42	0.0021
20.50	0.0141	24.50	0.0085	28.50	0.0078	32.50	0.0033	36.50	0.0015	40.50	0.0021
20.58	0.0136	24.58	0.0088	28.58	0.0051	32.58	0.0033	36.58	0.0032	40.58	0.0013
20.67	0.0130	24.67	0.0102	28.67	0.0058	32.67	0.0035	36.67	0.0028	40.67	0.0019
20.75	0.0136	24.75	0.0089	28.75	0.0049	32.75	0.0042	36.75	0.0013	40.75	0.0015
20.83	0.0146	24.83	0.0087	28.83	0.0052	32.83	0.0030	36.83	0.0012	40.83	0.0015
20.92	0.0126	24.92	0.0084	28.92	0.0061	32.92	0.0033	36.92	0.0015	40.92	0.0026
21.00	0.0147	25.00	0.0093	29.00	0.0056	33.00	0.0040	37.00	0.0025	41.00	0.0015
21.08	0.0131	25.08	0.0084	29.08	0.0058	33.08	0.0036	37.08	0.0026	41.08	0.0022
21.17	0.0124	25.17	0.0091	29.17	0.0053	33.17	0.0034	37.17	0.0021	41.17	0.0015
21.25	0.0118	25.25	0.0104	29.25	0.0065	33.25	0.0041	37.25	0.0020	41.25	0.0021
21.33	0.0136	25.33	0.0084	29.33	0.0048	33.33	0.0025	37.33	0.0029	41.33	0.0016
21.42	0.0120	25.42	0.0088	29.42	0.0043	33.42	0.0047	37.42	0.0029	41.42	0.0022
21.50	0.0120	25.50	0.0092	29.50	0.0059	33.50	0.0032	37.50	0.0033	41.50	0.0019
21.58	0.0133	25.58	0.0084	29.58	0.0054	33.58	0.0026	37.58	0.0023	41.58	0.0017
21.67	0.0120	25.67	0.0074	29.67	0.0061	33.67	0.0027	37.67	0.0021	41.67	0.0020
21.75	0.0128	25.75	0.0081	29.75	0.0043	33.75	0.0040	37.75	0.0017	41.75	0.0021
21.83	0.0118	25.83	0.0080	29.83	0.0046	33.83	0.0032	37.83	0.0012	41.83	0.0014
21.92	0.0124	25.92	0.0072	29.92	0.0062	33.92	0.0032	37.92	0.0020	41.92	0.0015
22.00	0.0118	26.00	0.0076	30.00	0.0056	34.00	0.0028	38.00	0.0019	42.00	0.0001
22.08	0.0118	26.08	0.0071	30.08	0.0052	34.08	0.0029	38.08	0.0028	42.08	0.0021
22.17	0.0115	26.17	0.0089	30.17	0.0048	34.17	0.0040	38.17	0.0014	42.17	0.0009
22.25	0.0124	26.25	0.0092	30.25	0.0059	34.25	0.0033	38.25	0.0019	42.25	0.0004
22.33	0.0120	26.33	0.0084	30.33	0.0046	34.33	0.0030	38.33	0.0017	42.33	0.0008
22.42	0.0104	26.42	0.0068	30.42	0.0045	34.42	0.0041	38.42	0.0015	42.42	0.0012
22.50	0.0121	26.50	0.0081	30.50	0.0043	34.50	0.0036	38.50	0.0016	42.50	0.0015
22.58	0.0108	26.58	0.0068	30.58	0.0054	34.58	0.0036	38.58	0.0021	42.58	0.0017
22.67	0.0110	26.67	0.0068	30.67	0.0052	34.67	0.0038	38.67	0.0009	42.67	0.0013
22.75	0.0106	26.75	0.0065	30.75	0.0042	34.75	0.0030	38.75	0.0016	42.75	0.0023
22.83	0.0118	26.83	0.0071	30.83	0.0048	34.83	0.0030	38.83	0.0027	42.83	0.0025
22.92	0.0106	26.92	0.0082	30.92	0.0038	34.92	0.0028	38.92	0.0009	42.92	0.0014
23.00	0.0102	27.00	0.0061	31.00	0.0048	35.00	0.0021	39.00	0.0036	43.00	0.0019
23.08	0.0107	27.08	0.0074	31.08	0.0041	35.08	0.0028	39.08	0.0017	43.08	0.0010
23.17	0.0094	27.17	0.0061	31.17	0.0047	35.17	0.0019	39.17	0.0014	43.17	0.0003
23.25	0.0115	27.25	0.0069	31.25	0.0038	35.25	0.0021	39.25	0.0025	43.25	0.0014
23.33	0.0108	27.33	0.0081	31.33	0.0054	35.33	0.0023	39.33	0.0020	43.33	0.0014
23.42	0.0105	27.42	0.0074	31.42	0.0055	35.42	0.0032	39.42	0.0026	43.42	0.0006
23.50	0.0118	27.50	0.0073	31.50	0.0054	35.50	0.0034	39.50	0.0008	43.50	0.0009
23.58	0.0106	27.58	0.0066	31.58	0.0052	35.58	0.0019	39.58	0.0014	43.58	0.0023
23.67	0.0099	27.67	0.0078	31.67	0.0056	35.67	0.0026	39.67	0.0022	43.67	0.0004
23.75	0.0102	27.75	0.0072	31.75	0.0048	35.75	0.0028	39.75	0.0015	43.75	0.0010
23.83	0.0111	27.83	0.0055	31.83	0.0042	35.83	0.0033	39.83	0.0010	43.83	0.0016
23.92	0.0092	27.92	0.0042	31.92	0.0038	35.92	0.0035	39.92	0.0015		

C. PRESIDENT STEYN INDUSTRIAL COLUMN RTD STUDY

C.6	TRACER: +38-75 micron Gangue Material								
Time (min)	E(t)	Time (min)	E(t)	Time (min)	E(t)	Time (min)	E(t)	Time (min)	E(t)
0.00	0.0005	4.00	0.1005	8.00	0.0578	12.00	0.0333	16.00	0.0240
0.08	0.0005	4.08	0.0968	8.08	0.0594	12.08	0.0341	16.08	0.0192
0.17	-0.0011	4.17	0.0938	8.17	0.0565	12.17	0.0336	16.17	0.0189
0.25	0.0008	4.25	0.0949	8.25	0.0544	12.25	0.0322	16.25	0.0192
0.33	0.0005	4.33	0.0954	8.33	0.0528	12.33	0.0328	16.33	0.0184
0.42	0.0013	4.42	0.0906	8.42	0.0520	12.42	0.0336	16.42	0.0205
0.50	-0.0019	4.50	0.0914	8.50	0.0530	12.50	0.0328	16.50	0.0202
0.58	-0.0006	4.58	0.0874	8.58	0.0562	12.58	0.0349	16.58	0.0184
0.67	0.0016	4.67	0.0882	8.67	0.0557	12.67	0.0333	16.67	0.0200
0.75	-0.0008	4.75	0.0834	8.75	0.0504	12.75	0.0296	16.75	0.0197
0.83	-0.0008	4.83	0.0848	8.83	0.0522	12.83	0.0317	16.83	0.0165
0.92	0.0008	4.92	0.0869	8.92	0.0488	12.92	0.0288	16.92	0.0181
1.00	0.0018	5.00	0.0845	9.00	0.0504	13.00	0.0290	17.00	0.0173
1.08	0.0069	5.08	0.0842	9.08	0.0520	13.08	0.0301	17.08	0.0181
1.17	0.0154	5.17	0.0821	9.17	0.0485	13.17	0.0306	17.17	0.0184
1.25	0.0226	5.25	0.0826	9.25	0.0506	13.25	0.0317	17.25	0.0189
1.33	0.0322	5.33	0.0786	9.33	0.0490	13.33	0.0296	17.33	0.0197
1.42	0.0365	5.42	0.0792	9.42	0.0501	13.42	0.0290	17.42	0.0160
1.50	0.0530	5.50	0.0794	9.50	0.0418	13.50	0.0304	17.50	0.0176
1.58	0.0600	5.58	0.0752	9.58	0.0442	13.58	0.0258	17.58	0.0184
1.67	0.0704	5.67	0.0773	9.67	0.0477	13.67	0.0277	17.67	0.0146
1.75	0.0784	5.75	0.0738	9.75	0.0472	13.75	0.0290	17.75	0.0162
1.83	0.0901	5.83	0.0736	9.83	0.0485	13.83	0.0309	17.83	0.0162
1.92	0.0925	5.92	0.0741	9.92	0.0426	13.92	0.0280	17.92	0.0181
2.00	0.0992	6.00	0.0741	10.00	0.0458	14.00	0.0280	18.00	0.0130
2.08	0.1056	6.08	0.0712	10.08	0.0442	14.08	0.0298	18.08	0.0130
2.17	0.1072	6.17	0.0738	10.17	0.0440	14.17	0.0280	18.17	0.0181
2.25	0.1125	6.25	0.0680	10.25	0.0402	14.25	0.0269	18.25	0.0144
2.33	0.1157	6.33	0.0706	10.33	0.0456	14.33	0.0250	18.33	0.0168
2.42	0.1101	6.42	0.0688	10.42	0.0397	14.42	0.0226	18.42	0.0170
2.50	0.1184	6.50	0.0680	10.50	0.0408	14.50	0.0253	18.50	0.0128
2.58	0.1184	6.58	0.0658	10.58	0.0429	14.58	0.0256	18.58	0.0160
2.67	0.1195	6.67	0.0653	10.67	0.0400	14.67	0.0221	18.67	0.0136
2.75	0.1123	6.75	0.0669	10.75	0.0424	14.75	0.0213	18.75	0.0152
2.83	0.1115	6.83	0.0656	10.83	0.0426	14.83	0.0213	18.83	0.0149
2.92	0.1035	6.92	0.0666	10.92	0.0440	14.92	0.0226	18.92	0.0138
3.00	0.1104	7.00	0.0664	11.00	0.0402	15.00	0.0245	19.00	0.0136
3.08	0.1075	7.08	0.0666	11.08	0.0389	15.08	0.0245	19.08	0.0136
3.17	0.1136	7.17	0.0658	11.17	0.0434	15.17	0.0240	19.17	0.0144
3.25	0.1093	7.25	0.0642	11.25	0.0400	15.25	0.0245	19.25	0.0154
3.33	0.1059	7.33	0.0621	11.33	0.0394	15.33	0.0224	19.33	0.0120
3.42	0.1080	7.42	0.0600	11.42	0.0370	15.42	0.0229	19.42	0.0090
3.50	0.1032	7.50	0.0581	11.50	0.0378	15.50	0.0253	19.50	0.0144
3.58	0.1037	7.58	0.0632	11.58	0.0365	15.58	0.0202	19.58	0.0130
3.67	0.0970	7.67	0.0589	11.67	0.0384	15.67	0.0216	19.67	0.0133
3.75	0.0973	7.75	0.0584	11.75	0.0354	15.75	0.0216	19.75	0.0125
3.83	0.0962	7.83	0.0573	11.83	0.0408	15.83	0.0205	19.83	0.0114
3.92	0.0962	7.92	0.0608	11.92	0.0336	15.92	0.0194	19.92	0.0128

C. PRESIDENT STEYN INDUSTRIAL COLUMN RTD STUDY

C.6	TRACER: +38-75 micron Gangue Material						
Time (min)	E(t)	Time (min)	E(t)	Time (min)	E(t)	Time (min)	E(t)
20.00	0.0146	24.00	0.0064	28.00	0.0021	32.00	0.0010
20.08	0.0130	24.08	0.0072	28.08	0.0045	32.08	0.0016
20.17	0.0120	24.17	0.0058	28.17	0.0024	32.17	0.0026
20.25	0.0093	24.25	0.0053	28.25	0.0056	32.25	0.0018
20.33	0.0114	24.33	0.0082	28.33	0.0040	32.33	0.0018
20.42	0.0128	24.42	0.0058	28.42	0.0026	32.42	0.0045
20.50	0.0117	24.50	0.0053	28.50	0.0034	32.50	0.0024
20.58	0.0133	24.58	0.0072	28.58	0.0032	32.58	0.0037
20.67	0.0112	24.67	0.0069	28.67	0.0034	32.67	0.0032
20.75	0.0128	24.75	0.0082	28.75	0.0042	32.75	0.0026
20.83	0.0128	24.83	0.0042	28.83	0.0032	32.83	0.0018
20.92	0.0109	24.92	0.0058	28.92	0.0045	32.92	0.0040
21.00	0.0101	25.00	0.0088	29.00	0.0018	33.00	0.0005
21.08	0.0128	25.08	0.0056	29.08	0.0034	33.08	0.0008
21.17	0.0114	25.17	0.0045	29.17	0.0016	33.17	0.0002
21.25	0.0114	25.25	0.0064	29.25	0.0037	33.25	0.0034
21.33	0.0098	25.33	0.0069	29.33	0.0026	33.33	0.0018
21.42	0.0085	25.42	0.0056	29.42	0.0013	33.42	0.0026
21.50	0.0117	25.50	0.0064	29.50	0.0053	33.50	0.0026
21.58	0.0112	25.58	0.0066	29.58	0.0066	33.58	0.0016
21.67	0.0096	25.67	0.0056	29.67	0.0018	33.67	0.0029
21.75	0.0090	25.75	0.0037	29.75	0.0021	33.75	0.0026
21.83	0.0114	25.83	0.0053	29.83	0.0048	33.83	0.0034
21.92	0.0061	25.92	0.0040	29.92	0.0034	33.92	0.0005
22.00	0.0098	26.00	0.0066	30.00	0.0037	34.00	0.0013
22.08	0.0082	26.08	0.0053	30.08	0.0042	34.08	0.0010
22.17	0.0096	26.17	0.0037	30.17	0.0026	34.17	0.0016
22.25	0.0069	26.25	0.0064	30.25	0.0029	34.25	0.0029
22.33	0.0128	26.33	0.0066	30.33	0.0034	34.33	0.0002
22.42	0.0088	26.42	0.0040	30.42	0.0026	34.42	0.0013
22.50	0.0082	26.50	0.0045	30.50	0.0050	34.50	-0.0000
22.58	0.0104	26.58	0.0045	30.58	0.0029	34.58	-0.0008
22.67	0.0082	26.67	0.0053	30.67	0.0032	34.67	0.0002
22.75	0.0104	26.75	0.0066	30.75	0.0034	34.75	0.0021
22.83	0.0106	26.83	0.0026	30.83	0.0050	34.83	0.0018
22.92	0.0109	26.92	0.0064	30.92	0.0024	34.92	0.0040
23.00	0.0066	27.00	0.0050	31.00	0.0010	35.00	0.0024
23.08	0.0096	27.08	0.0034	31.08	0.0010	35.08	0.0024
23.17	0.0098	27.17	0.0058	31.17	0.0008	35.17	-0.0016
23.25	0.0088	27.25	0.0050	31.25	-0.0000	35.25	-0.0000
23.33	0.0080	27.33	0.0072	31.33	0.0024	35.33	0.0008
23.42	0.0085	27.42	0.0032	31.42	0.0040	35.42	0.0002
23.50	0.0077	27.50	0.0034	31.50	0.0032	35.50	0.0010
23.58	0.0088	27.58	0.0024	31.58	0.0032	35.58	0.0029
23.67	0.0077	27.67	0.0037	31.67	0.0016	35.67	0.0018
23.75	0.0048	27.75	0.0058	31.75	0.0013	35.75	0.0016
23.83	0.0082	27.83	0.0037	31.83	0.0042	35.83	-0.0008
23.92	0.0061	27.92	0.0034	31.92	0.0037		

C. PRESIDENT STEYN INDUSTRIAL COLUMN RTD STUDY

C.7	TRACER: +75-106 micron Gangue Material								
Time (min)	E(t)	Time (min)	E(t)	Time (min)	E(t)	Time (min)	E(t)	Time (min)	E(t)
0.00	0.0016	4.00	0.0991	8.00	0.0567	12.00	0.0368	16.00	0.0187
0.08	-0.0011	4.08	0.0943	8.08	0.0536	12.08	0.0358	16.08	0.0232
0.17	0.0003	4.17	0.0905	8.17	0.0556	12.17	0.0310	16.17	0.0204
0.25	-0.0015	4.25	0.0950	8.25	0.0543	12.25	0.0331	16.25	0.0191
0.33	-0.0025	4.33	0.0932	8.33	0.0570	12.33	0.0338	16.33	0.0160
0.42	0.0009	4.42	0.0919	8.42	0.0570	12.42	0.0283	16.42	0.0218
0.50	-0.0011	4.50	0.0878	8.50	0.0587	12.50	0.0276	16.50	0.0143
0.58	0.0013	4.58	0.0826	8.58	0.0491	12.58	0.0310	16.58	0.0211
0.67	-0.0018	4.67	0.0871	8.67	0.0529	12.67	0.0310	16.67	0.0167
0.75	0.0013	4.75	0.0864	8.75	0.0502	12.75	0.0303	16.75	0.0170
0.83	0.0026	4.83	0.0854	8.83	0.0485	12.83	0.0256	16.83	0.0170
0.92	0.0044	4.92	0.0888	8.92	0.0546	12.92	0.0269	16.92	0.0180
1.00	0.0109	5.00	0.0830	9.00	0.0485	13.00	0.0259	17.00	0.0184
1.08	0.0215	5.08	0.0878	9.08	0.0509	13.08	0.0290	17.08	0.0211
1.17	0.0218	5.17	0.0868	9.17	0.0491	13.17	0.0297	17.17	0.0146
1.25	0.0300	5.25	0.0840	9.25	0.0491	13.25	0.0276	17.25	0.0184
1.33	0.0433	5.33	0.0809	9.33	0.0461	13.33	0.0290	17.33	0.0170
1.42	0.0529	5.42	0.0758	9.42	0.0512	13.42	0.0290	17.42	0.0170
1.50	0.0608	5.50	0.0779	9.50	0.0481	13.50	0.0286	17.50	0.0153
1.58	0.0673	5.58	0.0779	9.58	0.0478	13.58	0.0266	17.58	0.0160
1.67	0.0820	5.67	0.0721	9.67	0.0461	13.67	0.0256	17.67	0.0180
1.75	0.0885	5.75	0.0779	9.75	0.0420	13.75	0.0303	17.75	0.0153
1.83	0.0939	5.83	0.0741	9.83	0.0481	13.83	0.0290	17.83	0.0153
1.92	0.1049	5.92	0.0806	9.92	0.0379	13.92	0.0276	17.92	0.0163
2.00	0.1097	6.00	0.0724	10.00	0.0447	14.00	0.0259	18.00	0.0170
2.08	0.1131	6.08	0.0762	10.08	0.0437	14.08	0.0211	18.08	0.0167
2.17	0.1138	6.17	0.0734	10.17	0.0420	14.17	0.0232	18.17	0.0132
2.25	0.1179	6.25	0.0700	10.25	0.0468	14.25	0.0262	18.25	0.0156
2.33	0.1203	6.33	0.0721	10.33	0.0399	14.33	0.0242	18.33	0.0153
2.42	0.1213	6.42	0.0707	10.42	0.0430	14.42	0.0225	18.42	0.0146
2.50	0.1209	6.50	0.0700	10.50	0.0420	14.50	0.0242	18.50	0.0139
2.58	0.1192	6.58	0.0700	10.58	0.0447	14.58	0.0283	18.58	0.0153
2.67	0.1144	6.67	0.0656	10.67	0.0372	14.67	0.0266	18.67	0.0126
2.75	0.1144	6.75	0.0690	10.75	0.0396	14.75	0.0218	18.75	0.0184
2.83	0.1185	6.83	0.0676	10.83	0.0447	14.83	0.0201	18.83	0.0143
2.92	0.1134	6.92	0.0700	10.92	0.0379	14.92	0.0208	18.92	0.0153
3.00	0.1127	7.00	0.0659	11.00	0.0413	15.00	0.0235	19.00	0.0139
3.08	0.1121	7.08	0.0645	11.08	0.0403	15.08	0.0228	19.08	0.0129
3.17	0.1069	7.17	0.0652	11.17	0.0358	15.17	0.0235	19.17	0.0129
3.25	0.1127	7.25	0.0580	11.25	0.0368	15.25	0.0225	19.25	0.0091
3.33	0.1100	7.33	0.0669	11.33	0.0365	15.33	0.0204	19.33	0.0129
3.42	0.1059	7.42	0.0628	11.42	0.0341	15.42	0.0228	19.42	0.0132
3.50	0.1028	7.50	0.0560	11.50	0.0420	15.50	0.0218	19.50	0.0098
3.58	0.1066	7.58	0.0635	11.58	0.0334	15.58	0.0204	19.58	0.0126
3.67	0.1056	7.67	0.0604	11.67	0.0372	15.67	0.0197	19.67	0.0119
3.75	0.0974	7.75	0.0597	11.75	0.0368	15.75	0.0208	19.75	0.0136
3.83	0.1008	7.83	0.0591	11.83	0.0362	15.83	0.0232	19.83	0.0119
3.92	0.0909	7.92	0.0532	11.92	0.0382	15.92	0.0191	19.92	0.0119

C. PRESIDENT STEYN INDUSTRIAL COLUMN RTD STUDY

C.7	TRACER: +75-106 micron Gangue Material						
Time (min)	E(t)	Time (min)	E(t)	Time (min)	E(t)	Time (min)	E(t)
20.00	0.0109	24.00	0.0061	28.00	0.0040	32.00	0.0020
20.08	0.0132	24.08	0.0071	28.08	0.0030	32.08	-0.0001
20.17	0.0098	24.17	0.0067	28.17	0.0040	32.17	0.0030
20.25	0.0085	24.25	0.0054	28.25	0.0033	32.25	-0.0004
20.33	0.0126	24.33	0.0064	28.33	0.0057	32.33	-0.0018
20.42	0.0122	24.42	0.0026	28.42	0.0026	32.42	0.0040
20.50	0.0109	24.50	0.0044	28.50	0.0040	32.50	-0.0008
20.58	0.0088	24.58	0.0081	28.58	0.0030	32.58	0.0016
20.67	0.0105	24.67	0.0098	28.67	-0.0011	32.67	0.0061
20.75	0.0119	24.75	0.0085	28.75	0.0044	32.75	0.0026
20.83	0.0081	24.83	0.0064	28.83	0.0030	32.83	0.0030
20.92	0.0102	24.92	0.0061	28.92	0.0064	32.92	0.0009
21.00	0.0105	25.00	0.0078	29.00	0.0044	33.00	0.0006
21.08	0.0119	25.08	0.0054	29.08	0.0050	33.08	0.0003
21.17	0.0112	25.17	0.0040	29.17	0.0047	33.17	0.0033
21.25	0.0085	25.25	0.0067	29.25	0.0023	33.25	0.0047
21.33	0.0122	25.33	0.0085	29.33	0.0064	33.33	0.0023
21.42	0.0067	25.42	0.0064	29.42	0.0020	33.42	0.0023
21.50	0.0109	25.50	0.0071	29.50	0.0023	33.50	0.0020
21.58	0.0085	25.58	0.0047	29.58	0.0047	33.58	0.0047
21.67	0.0078	25.67	0.0067	29.67	0.0016	33.67	0.0030
21.75	0.0112	25.75	0.0071	29.75	0.0030	33.75	0.0023
21.83	0.0081	25.83	0.0016	29.83	0.0064	33.83	0.0016
21.92	0.0091	25.92	0.0061	29.92	0.0003	33.92	0.0013
22.00	0.0109	26.00	0.0061	30.00	0.0064	34.00	-0.0001
22.08	0.0040	26.08	0.0057	30.08	0.0023	34.08	0.0006
22.17	0.0098	26.17	0.0026	30.17	0.0026	34.17	-0.0056
22.25	0.0078	26.25	0.0047	30.25	0.0054	34.25	0.0020
22.33	0.0057	26.33	0.0085	30.33	-0.0008	34.33	0.0013
22.42	0.0098	26.42	0.0057	30.42	-0.0001	34.42	0.0013
22.50	0.0081	26.50	0.0057	30.50	0.0023	34.50	0.0033
22.58	0.0067	26.58	0.0078	30.58	0.0033	34.58	-0.0001
22.67	0.0095	26.67	0.0013	30.67	0.0030	34.67	0.0009
22.75	0.0085	26.75	0.0040	30.75	0.0033	34.75	0.0040
22.83	0.0102	26.83	0.0047	30.83	0.0033	34.83	0.0047
22.92	0.0067	26.92	0.0033	30.92	0.0023	34.92	-0.0021
23.00	0.0078	27.00	0.0023	31.00	0.0030	35.00	-0.0028
23.08	0.0057	27.08	0.0047	31.08	0.0006	35.08	-0.0056
23.17	0.0085	27.17	0.0033	31.17	0.0020	35.17	-0.0021
23.25	0.0050	27.25	0.0037	31.25	0.0026	35.25	0.0009
23.33	0.0026	27.33	0.0067	31.33	0.0040	35.33	0.0006
23.42	0.0102	27.42	0.0030	31.42	0.0026	35.42	-0.0080
23.50	0.0040	27.50	0.0016	31.50	0.0003	35.50	-0.0035
23.58	0.0037	27.58	0.0050	31.58	0.0064	35.58	-0.0025
23.67	0.0057	27.67	0.0020	31.67	-0.0008		
23.75	0.0050	27.75	0.0078	31.75	0.0050		
23.83	0.0064	27.83	0.0026	31.83	0.0033		
23.92	0.0081	27.92	0.0040	31.92	0.0023		

DISPUTADA INDUSTRIAL COLUMN RTD STUDY
(Yianatos and Bergh, 1990)

TRACER: Liquid				TRACER: Gangue Material			
Time (min)	E(t)	Time (min)	E(t)	Time (min)	E(t)	Time (min)	E(t)
0	0.0000	46	0.0021	0	0.0000	46	0.0038
1	0.0066	47	0.0020	1	0.0030	47	0.0036
2	0.0511	48	0.0018	2	0.0322	48	0.0034
3	0.0765	49	0.0017	3	0.0467	49	0.0032
4	0.0798	50	0.0016	4	0.0522	50	0.0030
5	0.0782	51	0.0015	5	0.0530	51	0.0028
6	0.0650	52	0.0014	6	0.0479	52	0.0027
7	0.0575	53	0.0012	7	0.0494	53	0.0025
8	0.0515	54	0.0011	8	0.0465	54	0.0023
9	0.0451	55	0.0010	9	0.0447	55	0.0021
10	0.0431	56	0.0009	10	0.0401	56	0.0020
11	0.0397	57	0.0009	11	0.0379	57	0.0019
12	0.0365	58	0.0008	12	0.0357	58	0.0018
13	0.0332	59	0.0007	13	0.0336	59	0.0017
14	0.0301	60	0.0006	14	0.0316	60	0.0015
15	0.0268	61	0.0005	15	0.0296	61	0.0014
16	0.0236	62	0.0004	16	0.0276	62	0.0013
17	0.0216	63	0.0003	17	0.0258	63	0.0012
18	0.0195	64	0.0002	18	0.0239	64	0.0010
19	0.0175	65	0.0001	19	0.0222	65	0.0009
20	0.0163	66	0.0000	20	0.0208	66	0.0008
21	0.0150	67	0.0000	21	0.0194	67	0.0006
22	0.0137	68	0.0000	22	0.0180	68	0.0005
23	0.0125	69	0.0000	23	0.0171	69	0.0004
24	0.0115	70	0.0000	24	0.0161	70	0.0003
25	0.0103			25	0.0150		
26	0.0095			26	0.0141		
27	0.0087			27	0.0132		
28	0.0082			28	0.0120		
29	0.0075			29	0.0116		
30	0.0068			30	0.0111		
31	0.0062			31	0.0105		
32	0.0057			32	0.0098		
33	0.0053			33	0.0092		
34	0.0048			34	0.0085		
35	0.0046			35	0.0078		
36	0.0042			36	0.0071		
37	0.0039			37	0.0065		
38	0.0035			38	0.0064		
39	0.0031			39	0.0063		
40	0.0029			40	0.0061		
41	0.0027			41	0.0056		
42	0.0026			42	0.0051		
43	0.0025			43	0.0046		
44	0.0023			44	0.0041		
45	0.0022			45	0.0039		

DISPUTADA INDUSTRIAL COLUMN RTD STUDY
(Yianatos and Bergh, 1990)

TRACE -38 micron Gangue Material				TRACE +38-75 micron Gangue Material				TRACE +38-75 micron Gangue Material			
Time (min)	E(t)	Time (min)	E(t)	Time (min)	E(t)	Time (min)	E(t)	Time (min)	E(t)	Time (min)	E(t)
0.00	0.00000	46.00	0.00316	0.00	0.00000	46.00	0.00170	0.00	0.00000	46.00	0.00028
1.00	0.00423	47.00	0.00293	1.00	0.02420	47.00	0.00156	1.00	0.01107	47.00	0.00021
2.00	0.03815	48.00	0.00277	2.00	0.04882	48.00	0.00147	2.00	0.09036	48.00	0.00021
3.00	0.05658	49.00	0.00250	3.00	0.06733	49.00	0.00138	3.00	0.11305	49.00	0.00014
4.00	0.06197	50.00	0.00223	4.00	0.07527	50.00	0.00124	4.00	0.10329	50.00	0.00007
5.00	0.05928	51.00	0.00216	5.00	0.07082	51.00	0.00115	5.00	0.10177	51.00	0.00000
6.00	0.05570	52.00	0.00208	6.00	0.06517	52.00	0.00101	6.00	0.07564	52.00	0.00000
7.00	0.05200	53.00	0.00192	7.00	0.05897	53.00	0.00092	7.00	0.06608	53.00	0.00000
8.00	0.04839	54.00	0.00185	8.00	0.05220	54.00	0.00083	8.00	0.05591	54.00	0.00000
9.00	0.04507	55.00	0.00173	9.00	0.04758	55.00	0.00073	9.00	0.04896	55.00	0.00000
10.00	0.04157	56.00	0.00162	10.00	0.04285	56.00	0.00073	10.00	0.04167	56.00	0.00000
11.00	0.03869	57.00	0.00154	11.00	0.03996	57.00	0.00060	11.00	0.03803	57.00	0.00000
12.00	0.03580	58.00	0.00139	12.00	0.03656	58.00	0.00055	12.00	0.03411	58.00	0.00000
13.00	0.03283	59.00	0.00131	13.00	0.03348	59.00	0.00046	13.00	0.03012	59.00	0.00000
14.00	0.03064	60.00	0.00123	14.00	0.03022	60.00	0.00046	14.00	0.02606	60.00	0.00000
15.00	0.02848	61.00	0.00115	15.00	0.02728	61.00	0.00037	15.00	0.02228	61.00	0.00000
16.00	0.02656	62.00	0.00104	16.00	0.02434	62.00	0.00028	16.00	0.01815	62.00	0.00000
17.00	0.02502	63.00	0.00092	17.00	0.02255	63.00	0.00023	17.00	0.01616	63.00	0.00000
18.00	0.02337	64.00	0.00077	18.00	0.02085	64.00	0.00014	18.00	0.01444	64.00	0.00000
19.00	0.02175	65.00	0.00065	19.00	0.01929	65.00	0.00000	19.00	0.01258	65.00	0.00000
20.00	0.02029	66.00	0.00058	20.00	0.01759	66.00	0.00000	20.00	0.01100	66.00	0.00000
21.00	0.01886	67.00	0.00046	21.00	0.01589	67.00	0.00000	21.00	0.00928	67.00	0.00000
22.00	0.01732	68.00	0.00038	22.00	0.01414	68.00	0.00000	22.00	0.00756	68.00	0.00000
23.00	0.01597	69.00	0.00027	23.00	0.01295	69.00	0.00000	23.00	0.00667	69.00	0.00000
24.00	0.01443	70.00	0.00000	24.00	0.01171	70.00	0.00000	24.00	0.00591	70.00	0.00000
25.00	0.01313			25.00	0.01042			25.00	0.00509		
26.00	0.01228			26.00	0.00969			26.00	0.00454		
27.00	0.01147			27.00	0.00891			27.00	0.00388		
28.00	0.01078			28.00	0.00808			28.00	0.00323		
29.00	0.01016			29.00	0.00744			29.00	0.00302		
30.00	0.00935			30.00	0.00666			30.00	0.00261		
31.00	0.00874			31.00	0.00611			31.00	0.00234		
32.00	0.00812			32.00	0.00551			32.00	0.00206		
33.00	0.00751			33.00	0.00496			33.00	0.00179		
34.00	0.00674			34.00	0.00432			34.00	0.00151		
35.00	0.00635			35.00	0.00413			35.00	0.00123		
36.00	0.00593			36.00	0.00377			36.00	0.00123		
37.00	0.00558			37.00	0.00358			37.00	0.00117		
38.00	0.00531			38.00	0.00340			38.00	0.00110		
39.00	0.00500			39.00	0.00317			39.00	0.00096		
40.00	0.00466			40.00	0.00285			40.00	0.00089		
41.00	0.00443			41.00	0.00271			41.00	0.00076		
42.00	0.00412			42.00	0.00248			42.00	0.00055		
43.00	0.00385			43.00	0.00220			43.00	0.00041		
44.00	0.00354			44.00	0.00197			44.00	0.00028		
45.00	0.00335			45.00	0.00184			45.00	0.00028		

APPENDIX 2

KINETICS TESTWORK DATA

D. Determination of Flotation Kinetics by Varying Column Length and Feed Rate

E. Determination of Flotation Kinetics using a Chalcopyrite Tracer

F. Determination of Flotation Kinetics using Pyrite Tracers (Pilot Column)

G. Determination of Flotation Kinetics using Pyrite Tracers (President Steyn Industrial Column)

D. DETERMINATION OF FLOTATION KINETICS BY VARYING COLUMN LENGTH AND FEED RATE

D.1	AIR RATE: 0.81 cm/s					
Mean Residence Time (min)	Sulphur Recovery (%) 1	2	3	Average Sulphur Recovery	Standard Deviation (%)	Average Conc. Grade (%S)
0.0	0.0	0.0	0.0	0.0	0.0	0.0
0.8	26.1	34.2	27.1	29.1	4.4	41.1
1.0	30.2	35.4	34.5	33.4	2.6	40.2
1.6	47.5	41.0	44.3	44.3	3.0	37.6
2.1	50.3	49.0	57.2	52.2	4.4	37.3
2.9	55.1	50.3	51.0	52.1	2.6	36.8
3.8	53.6	60.1	55.8	56.5	3.6	36.2

D.2	AIR RATE: 1.69 cm/s					
Mean Residence Time (min)	Sulphur Recovery (%) 1	2	3	Average Sulphur Recovery	Standard Deviation (%)	Average Conc. Grade (%S)
0.00	0.0	0.0	0.0	0.0	0.0	0
0.79	62.2	52.4	60.1	58.2	5.3	38.3
1.00	64.3	68.3	63.7	65.4	2.6	36.7
1.57	77.5	79.9	79.1	78.8	1.2	35.2
2.01	78.1	80.1	79.7	79.3	1.0	34.3
2.88	80.2	79.2	78.6	79.3	1.0	32.4
3.71	75.8	80.2	79.3	78.4	2.6	31.5

D.3	AIR RATE: 2.53 cm/s					
Mean Residence Time (min)	Sulphur Recovery (%) 1	2	3	Average Sulphur Recovery	Standard Deviation (%)	Average Conc. Grade (%S)
0.00	0.0	0.0	0.0	0.0	0.0	0.0
0.82	55.5	58.5	49.0	54.3	5.1	36.3
1.10	59.0	66.3	64.5	63.3	3.8	36.0
1.38	76.1	72.0	72.6	73.6	2.3	32.1
1.68	74.3	75.8	77.5	75.9	2.0	31.8
1.68	76.5	75.4	78.6	76.8	1.5	30.8
2.04	75.2	77.8	75.2	76.1	1.2	29.0
2.53	76.7	80.4	79.4	78.8	2.1	28.9
3.07	80.2	76.2	77.6	78.0	2.1	27.0
3.54	82.1	78.1	80.5	80.2	2.1	28.1

E. DETERMINATION OF THE FLOTATION KINETICS USING A CHALCOPYRITE TRACER

E.1	60cm Froth Frother Concentration:		50ppm
Time (sec)	Incremental Mass Copper (g)	Cumulative Mass Copper (g)	Cumulative Copper Recovery (%)
0	0.000	0.000	0.0
8	0.046	0.046	2.0
15	0.226	0.272	11.5
20	0.155	0.427	18.1
25	0.127	0.554	23.5
30	0.095	0.649	27.5
35	0.127	0.776	32.9
40	0.099	0.875	37.1
45	0.062	0.937	39.7
50	0.056	0.993	42.1
55	0.046	1.039	44.0
60	0.042	1.081	45.8
65	0.017	1.098	46.5
70	0.032	1.130	47.9
75	0.020	1.150	48.7
80	0.051	1.201	50.9
85	0.053	1.254	53.1
90	0.063	1.317	55.8
95	0.033	1.350	57.2
100	0.030	1.380	58.5
105	0.021	1.401	59.4
110	0.024	1.425	60.4
115	0.021	1.446	61.3
120	0.009	1.455	61.7
Mass of Cu Injected		2.360	

E.6	10cm Froth Frother Concentration:		50ppm
Time (sec)	Incremental Mass Copper (g)	Cumulative Mass Copper (g)	Cumulative Copper Recovery (%)
0	0.000	0.000	0.0
5	0.033	0.033	1.6
10	0.278	0.311	14.8
15	0.290	0.601	28.6
20	0.174	0.775	36.9
25	0.141	0.916	43.6
30	0.103	1.019	48.5
35	0.091	1.110	52.9
40	0.070	1.180	56.2
45	0.053	1.233	58.7
50	0.049	1.282	61.1
55	0.042	1.324	63.1
60	0.042	1.366	65.1
65	0.032	1.398	66.6
70	0.030	1.428	68.0
75	0.021	1.449	69.0
80	0.025	1.474	70.2
85	0.023	1.497	71.3
90	0.014	1.511	72.0
95	0.015	1.526	72.7
100	0.014	1.540	73.4
105	0.013	1.553	74.0
110	0.011	1.564	74.5
115	0.013	1.577	75.1
120	0.010	1.587	75.6
Mass of Cu Injected		2.099	

E. DETERMINATION OF FLOTATION KINETICS USING CHALCOPYRITE TRACERS

E.2	10cm Froth Frother Concentration: 4ppm		
Time (sec)	Incremental Mass Copper (g)	Cumulative Mass Copper (g)	Cumulative Copper Recovery (%)
0	0.000	0.000	0.0
5	0.043	0.043	1.3
10	0.079	0.122	3.8
15	0.243	0.365	11.3
20	0.353	0.718	22.3
25	0.279	0.997	30.9
30	0.229	1.226	38.1
35	0.179	1.405	43.6
40	0.117	1.522	47.2
45	0.088	1.610	50.0
50	0.074	1.684	52.3
55	0.071	1.755	54.5
60	0.050	1.805	56.0
65	0.058	1.863	57.8
70	0.036	1.899	58.9
75	0.033	1.932	60.0
80	0.033	1.965	61.0
85	0.028	1.993	61.9
90	0.027	2.020	62.7
95	0.020	2.040	63.3
100	0.024	2.064	64.1
105	0.020	2.084	64.7
110	0.023	2.107	65.4
115	0.020	2.127	66.0
265	0.067	2.372	73.6
445	0.082	2.454	76.2
Total Cu Injected (g)		3.221	

E.3	10cm Froth Frother Concentration: 10ppm		
Time (sec)	Incremental Mass Copper (g)	Cumulative Mass Copper (g)	Cumulative Copper Recovery (%)
0	0.000	0.000	0.00
5	0.067	0.067	2.08
10	0.159	0.226	7.01
15	0.379	0.605	18.78
20	0.329	0.934	28.99
25	0.274	1.208	37.49
30	0.203	1.411	43.79
35	0.171	1.582	49.10
40	0.123	1.705	52.92
45	0.106	1.811	56.21
50	0.086	1.897	58.88
55	0.080	1.977	61.36
60	0.053	2.030	63.00
65	0.040	2.070	64.25
70	0.048	2.118	65.74
75	0.036	2.154	66.85
80	0.034	2.188	67.91
85	0.032	2.220	68.90
90	0.036	2.256	70.02
95	0.028	2.284	70.89
100	0.024	2.308	71.63
105	0.028	2.336	72.50
110	0.020	2.356	73.12
140	0.123	2.479	76.94
170	0.071	2.550	79.14
200	0.051	2.601	80.73
260	0.074	2.675	83.02
363	0.069	2.744	85.16
Total Cu Injected (g)		3.222	

E. DETERMINATION OF FLOTATION KINETICS USING CHALCOPYRITE TRACERS

E.4	10cm Froth Frother Concentration: 20ppm			E.5	10cm Froth Frother Concentration: 50ppm		
Time (sec)	Incremental Mass Copper (g)	Cumulative Mass Copper (g)	Cumulative Copper Recovery (%)	Time (sec)	Incremental Mass Copper (g)	Cumulative Mass Copper (g)	Cumulative Copper Recovery (%)
0	0.000	0.000	0.0	0	0.000	0.000	0.0
5	0.024	0.024	0.6	5	0.033	0.033	1.6
10	0.114	0.138	3.7	10	0.278	0.311	14.8
15	0.598	0.736	19.9	15	0.290	0.601	28.6
20	0.483	1.219	32.9	20	0.174	0.775	36.9
25	0.355	1.574	42.5	25	0.141	0.916	43.6
30	0.195	1.769	47.8	30	0.103	1.019	48.5
35	0.205	1.974	53.4	35	0.091	1.110	52.9
40	0.111	2.085	56.4	40	0.070	1.180	56.2
45	0.119	2.204	59.6	45	0.053	1.233	58.7
50	0.085	2.289	61.9	50	0.049	1.282	61.0
55	0.108	2.397	64.8	55	0.042	1.324	63.0
60	0.086	2.483	67.1	60	0.042	1.366	65.0
65	0.063	2.546	68.8	65	0.032	1.398	66.6
70	0.049	2.595	70.1	70	0.030	1.428	68.0
75	0.043	2.638	71.3	75	0.021	1.449	69.0
80	0.043	2.681	72.5	80	0.025	1.474	70.2
85	0.036	2.717	73.4	85	0.023	1.497	71.3
90	0.028	2.745	74.2	90	0.014	1.511	72.0
95	0.031	2.775	75.0	95	0.015	1.526	72.7
100	0.025	2.800	75.7	100	0.014	1.540	73.3
105	0.021	2.822	76.3	105	0.013	1.553	74.0
110	0.016	2.837	76.7	110	0.011	1.564	74.5
115	0.021	2.858	77.2	115	0.013	1.577	75.1
145	0.100	2.958	79.9	145	0.051	1.628	77.5
175	0.072	3.030	81.9	175	0.065	1.693	80.6
205	0.052	3.082	83.3	205	0.039	1.732	82.5
265	0.072	3.154	85.2	260	0.055	1.787	85.1
445	0.086	3.240	87.6	363	0.043	1.830	87.1
Total Cu Injected (g)		3.700		Total Cu Injected (g)		2.100	

F. DETERMINATION OF FLOTATION KINETICS USING PYRITE TRACERS
(Pilot Column)

F.1	GAS RATE: 2.00 cm/s										
Time (sec)	Cumulative Pyrite Recovery (%)	Time (sec)	Cumulative Pyrite Recovery (%)	Time (sec)	Cumulative Pyrite Recovery (%)	Time (sec)	Cumulative Pyrite Recovery (%)	Time (sec)	Cumulative Pyrite Recovery (%)	Time (sec)	Cumulative Pyrite Recovery (%)
0	0.03	88	58.26	176	65.65	264	68.47	352	69.33	440	69.75
2	4.72	90	58.57	178	65.76	266	68.50	354	69.34	442	69.70
4	9.43	92	58.87	180	65.84	268	68.50	356	69.37	444	69.74
6	13.28	94	59.15	182	65.95	270	68.52	358	69.38	446	69.72
8	16.47	96	59.38	184	66.01	272	68.56	360	69.38	448	69.72
10	19.25	98	59.63	186	66.09	274	68.60	362	69.39	450	69.73
12	21.61	100	59.87	188	66.18	276	68.63	364	69.39	452	69.76
14	23.63	102	60.10	190	66.22	278	68.66	366	69.41	454	69.87
16	25.46	104	60.35	192	66.28	280	68.67	368	69.45	456	69.87
18	27.12	106	60.58	194	66.36	282	68.67	370	69.45	458	69.87
20	28.81	108	60.79	196	66.45	284	68.70	372	69.52	460	69.87
22	30.50	110	61.00	198	66.54	286	68.71	374	69.54		
24	32.21	112	61.21	200	66.60	288	68.75	376	69.59		
26	33.82	114	61.40	202	66.67	290	68.78	378	69.59		
28	35.33	116	61.59	204	66.74	292	68.83	380	69.59		
30	36.80	118	61.77	206	66.80	294	68.83	382	69.60		
32	38.13	120	61.96	208	66.89	296	68.85	384	69.58		
34	39.35	122	62.17	210	66.94	298	68.86	386	69.60		
36	40.39	124	62.34	212	67.02	300	68.93	388	69.59		
38	41.33	126	62.50	214	67.12	302	68.94	390	69.58		
40	42.46	128	62.65	216	67.21	304	68.97	392	69.66		
42	43.40	130	62.83	218	67.31	306	69.03	394	69.81		
44	44.32	132	62.98	220	67.37	308	69.03	396	69.79		
46	45.18	134	63.18	222	67.45	310	69.04	398	69.74		
48	45.91	136	63.33	224	67.50	312	69.08	400	69.73		
50	46.76	138	63.50	226	67.57	314	69.07	402	69.73		
52	47.84	140	63.62	228	67.60	316	69.08	404	69.71		
54	48.61	142	63.75	230	67.65	318	69.08	406	69.70		
56	49.40	144	63.90	232	67.71	320	69.10	408	69.71		
58	50.16	146	64.05	234	67.76	322	69.14	410	69.70		
60	50.97	148	64.23	236	67.81	324	69.16	412	69.69		
62	51.73	150	64.36	238	67.86	326	69.14	414	69.69		
64	52.33	152	64.49	240	67.91	328	69.20	416	69.67		
66	52.91	154	64.59	242	67.96	330	69.20	418	69.67		
68	53.51	156	64.73	244	67.97	332	69.20	420	69.67		
70	54.04	158	64.84	246	67.99	334	69.18	422	69.66		
72	54.52	160	64.92	248	68.27	336	69.21	424	69.65		
74	55.13	162	65.05	250	68.30	338	69.21	426	69.67		
76	55.60	164	65.13	252	68.33	340	69.18	428	69.66		
78	56.09	166	65.22	254	68.31	342	69.19	430	69.64		
80	56.61	168	65.30	256	68.38	344	69.20	432	69.66		
82	57.17	170	65.36	258	68.38	346	69.19	434	69.66		
84	57.55	172	65.48	260	68.41	348	69.28	436	69.66		
86	57.91	174	65.54	262	68.43	350	69.29	438	69.67		

F. DETERMINATION OF FLOTATION KINETICS USING PYRITE TRACERS
(Pilot Column)

F.2	GAS RATE: 2.24 cm/s								
Time (sec)	Cumulative Pyrite Recovery (%)	Time (sec)	Cumulative Pyrite Recovery (%)	Time (sec)	Cumulative Pyrite Recovery (%)	Time (sec)	Cumulative Pyrite Recovery (%)	Time (sec)	Cumulative Pyrite Recovery (%)
0	0.30	88	59.63	176	70.34	264	72.47	352	73.20
2	0.91	90	60.02	178	70.45	266	72.45	354	73.22
4	3.67	92	60.45	180	70.54	268	72.43	356	73.17
6	7.74	94	61.03	182	70.60	270	72.47	358	73.16
8	11.43	96	61.62	184	70.73	272	72.47	360	73.19
10	14.52	98	61.98	186	70.82	274	72.49	362	73.17
12	17.25	100	62.38	188	70.91	276	72.51	364	73.19
14	19.76	102	62.76	190	70.97	278	72.54	366	73.18
16	21.94	104	63.14	192	71.06	280	72.55	368	73.15
18	23.91	106	63.47	194	71.15	282	72.58	370	73.18
20	25.82	108	63.89	196	71.24	284	72.58	372	73.16
22	27.65	110	64.17	198	71.30	286	72.61	374	73.16
24	29.37	112	64.49	200	71.39	288	72.64	376	73.17
26	31.14	114	64.86	202	71.43	290	72.79	378	73.16
28	32.96	116	65.17	204	71.48	292	72.81	380	73.18
30	34.45	118	65.44	206	71.57	294	72.81	382	73.17
32	35.95	120	65.71	208	71.65	296	72.85	384	73.15
34	37.28	122	65.90	210	71.66	298	72.86	386	73.17
36	38.68	124	66.20	212	71.74	300	72.88	388	73.12
38	39.97	126	66.44	214	71.82	302	72.87	390	73.15
40	41.27	128	66.66	216	71.84	304	72.90	392	73.24
42	42.80	130	66.90	218	71.91	306	72.92	394	73.23
44	43.91	132	67.15	220	71.98	308	72.93	396	73.20
46	44.98	134	67.36	222	72.03	310	72.95	398	73.17
48	46.12	136	67.55	224	72.02	312	72.98		
50	47.09	138	67.77	226	72.06	314	73.00		
52	47.97	140	67.93	228	72.11	316	73.03		
54	48.89	142	68.10	230	72.10	318	73.00		
56	49.86	144	68.25	232	72.13	320	73.01		
58	50.56	146	68.42	234	72.17	322	73.02		
60	51.43	148	68.62	236	72.20	324	73.03		
62	52.11	150	68.79	238	72.23	326	73.03		
64	52.81	152	68.95	240	72.26	328	73.08		
66	53.51	154	69.03	242	72.24	330	73.07		
68	54.18	156	69.22	244	72.27	332	73.09		
70	54.78	158	69.38	246	72.26	334	73.10		
72	55.57	160	69.50	248	72.25	336	73.12		
74	56.08	162	69.55	250	72.30	338	73.16		
76	56.62	164	69.67	252	72.34	340	73.17		
78	57.17	166	69.84	254	72.35	342	73.23		
80	57.70	168	69.95	256	72.38	344	73.20		
82	58.14	170	70.05	258	72.37	346	73.18		
84	58.66	172	70.17	260	72.39	348	73.18		
86	59.09	174	70.29	262	72.45	350	73.16		

F. DETERMINATION OF FLOTATION KINETICS USING PYRITE TRACERS
(Pilot Column)

F.3	GAS RATE: 2.42 cm/s										
Time (sec)	Cumulative Pyrite Recovery (%)	Time (sec)	Cumulative Pyrite Recovery (%)	Time (sec)	Cumulative Pyrite Recovery (%)	Time (sec)	Cumulative Pyrite Recovery (%)	Time (sec)	Cumulative Pyrite Recovery (%)	Time (sec)	Cumulative Pyrite Recovery (%)
0	0.19	88	59.21	176	67.72	264	72.18	352	74.99	440	75.04
2	0.46	90	59.45	178	67.81	266	72.27	354	75.02	442	75.02
4	3.99	92	59.71	180	67.90	268	72.34	356	75.04	444	75.04
6	8.51	94	59.95	182	67.98	270	72.43	358	75.06	446	75.04
8	12.29	96	60.18	184	68.11	272	72.48	360	75.08	448	75.04
10	15.48	98	60.48	186	68.26	274	72.56	362	75.09	450	75.01
12	18.60	100	60.69	188	68.39	276	72.66	364	75.10	452	75.03
14	21.29	102	60.90	190	68.46	278	72.78	366	75.12	454	75.02
16	23.90	104	61.15	192	68.51	280	72.88	368	75.11	456	75.01
18	26.59	106	61.43	194	68.53	282	72.99	370	75.13	458	74.99
20	29.24	108	61.67	196	68.66	284	73.14	372	75.15	460	74.99
22	31.59	110	61.86	198	68.80	286	73.20	374	75.16	462	75.00
24	34.16	112	62.14	200	68.89	288	73.31	376	75.18	464	75.01
26	36.43	114	62.34	202	69.02	290	73.36	378	75.17	466	74.98
28	38.14	116	62.58	204	69.18	292	73.42	380	75.17	468	74.97
30	39.95	118	62.82	206	69.30	294	73.54	382	75.15	470	74.98
32	41.70	120	63.01	208	69.41	296	73.62	384	75.16	472	74.99
34	42.98	122	63.21	210	69.50	298	73.71	386	75.18	474	75.00
36	44.33	124	63.47	212	69.58	300	73.77	388	75.15	476	74.99
38	45.38	126	63.63	214	69.66	302	73.81	390	75.13	478	75.00
40	46.46	128	63.80	216	69.82	304	73.86	392	75.12	480	74.99
42	47.36	130	63.96	218	69.95	306	73.93	394	75.11	482	75.02
44	48.25	132	64.15	220	70.07	308	73.99	396	75.09	484	75.02
46	49.19	134	64.26	222	70.21	310	74.02	398	75.07		
48	50.01	136	64.45	224	70.31	312	74.07	400	75.07		
50	50.69	138	64.60	226	70.41	314	74.14	402	75.08		
52	51.36	140	64.76	228	70.53	316	74.20	404	75.07		
54	51.97	142	64.88	230	70.66	318	74.25	406	75.06		
56	52.57	144	65.04	232	70.75	320	74.31	408	75.06		
58	53.13	146	65.17	234	70.89	322	74.37	410	75.05		
60	53.71	148	65.33	236	70.99	324	74.45	412	75.06		
62	54.32	150	65.50	238	71.11	326	74.48	414	75.07		
64	54.83	152	65.64	240	71.16	328	74.52	416	75.09		
66	55.25	154	65.78	242	71.25	330	74.58	418	75.08		
68	55.67	156	65.90	244	71.35	332	74.62	420	75.08		
70	56.05	158	66.08	246	71.43	334	74.68	422	75.08		
72	56.43	160	66.21	248	71.54	336	74.76	424	75.08		
74	56.84	162	66.42	250	71.59	338	74.80	426	75.07		
76	57.28	164	66.65	252	71.67	340	74.86	428	75.07		
78	57.66	166	66.84	254	71.81	342	74.90	430	75.04		
80	58.01	168	67.31	256	71.89	344	74.92	432	75.04		
82	58.37	170	67.43	258	71.97	346	74.98	434	75.05		
84	58.64	172	67.51	260	72.03	348	74.99	436	75.04		
86	58.93	174	67.63	262	72.09	350	75.00	438	75.04		

F. DETERMINATION OF FLOTATION KINETICS USING PYRITE TRACERS
(Pilot Column)

F.4	GAS RATE: 2.67 cm/s										
Time (sec)	Cumulative Pyrite Recovery (%)	Time (sec)	Cumulative Pyrite Recovery (%)	Time (sec)	Cumulative Pyrite Recovery (%)	Time (sec)	Cumulative Pyrite Recovery (%)	Time (sec)	Cumulative Pyrite Recovery (%)	Time (sec)	Cumulative Pyrite Recovery (%)
0	0.01	88	65.71	176	74.29	264	76.63	352	77.71	440	78.02
2	5.43	90	66.00	178	74.39	266	76.70	354	77.72	442	78.05
4	10.19	92	66.29	180	74.49	268	76.78	356	77.73	444	78.03
6	14.12	94	66.64	182	74.55	270	76.75	358	77.76	446	77.98
8	17.66	96	66.94	184	74.66	272	76.77	360	77.81	448	77.98
10	20.91	98	67.30	186	74.72	274	76.85	362	77.77	450	77.97
12	23.96	100	67.50	188	74.79	276	76.89	364	77.82	452	77.97
14	26.74	102	67.75	190	74.94	278	76.91	366	77.84	454	77.95
16	30.02	104	67.99	192	74.97	280	76.94	368	77.86	456	77.97
18	32.80	106	68.28	194	75.03	282	76.96	370	77.89	458	77.95
20	35.24	108	68.51	196	75.09	284	77.00	372	77.87	460	77.93
22	37.62	110	68.74	198	75.14	286	77.04	374	77.88	462	77.93
24	39.52	112	68.96	200	75.20	288	77.07	376	77.96	464	77.91
26	41.42	114	69.19	202	75.29	290	77.11	378	77.99	466	77.88
28	43.12	116	69.43	204	75.36	292	77.14	380	77.97	468	77.88
30	45.04	118	69.66	206	75.43	294	77.17	382	78.00	470	77.93
32	46.55	120	69.85	208	75.52	296	77.18	384	78.02	472	77.94
34	47.76	122	70.01	210	75.58	298	77.20	386	78.03	474	77.94
36	48.89	124	70.26	212	75.65	300	77.24	388	78.04	476	77.93
38	49.99	126	70.42	214	75.77	302	77.24	390	78.15	478	77.93
40	51.00	128	70.59	216	75.77	304	77.26	392	78.17	480	77.92
42	51.94	130	70.79	218	75.82	306	77.21	394	78.18	482	77.87
44	53.28	132	71.05	220	75.86	308	77.25	396	78.21	484	77.85
46	54.22	134	71.23	222	75.91	310	77.29	398	78.17	486	77.86
48	55.06	136	71.37	224	76.01	312	77.29	400	78.17	488	77.86
50	56.01	138	71.50	226	76.01	314	77.32	402	78.14	490	77.81
52	56.75	140	71.67	228	76.01	316	77.32	404	78.16	492	77.80
54	57.63	142	71.85	230	75.99	318	77.32	406	78.10	494	77.79
56	58.27	144	72.01	232	76.04	320	77.37	408	78.07	496	77.76
58	58.86	146	72.17	234	76.07	322	77.32	410	78.12	498	77.76
60	59.40	148	72.34	236	76.11	324	77.40	412	78.10	500	77.74
62	59.98	150	72.49	238	76.17	326	77.46	414	78.16	502	77.80
64	60.51	152	72.72	240	76.20	328	77.49	416	78.18	504	77.87
66	60.97	154	72.93	242	76.19	330	77.55	418	78.18	506	77.92
68	61.45	156	73.07	244	76.22	332	77.59	420	78.18	508	77.96
70	61.99	158	73.19	246	76.29	334	77.62	422	78.20	510	77.95
72	62.46	160	73.33	248	76.33	336	77.62	424	78.17	512	77.90
74	62.90	162	73.49	250	76.37	338	77.61	426	78.16	514	77.85
76	63.34	164	73.62	252	76.40	340	77.64	428	78.15	516	77.83
78	63.76	166	73.76	254	76.40	342	77.66	430	78.14	518	77.84
80	64.16	168	73.85	256	76.44	344	77.67	432	78.11	520	77.88
82	64.50	170	73.96	258	76.51	346	77.69	434	78.10	522	77.84
84	64.94	172	74.06	260	76.55	348	77.68	436	78.09	524	77.92
86	65.36	174	74.20	262	76.59	350	77.74	438	78.03	526	77.86

F. DETERMINATION OF FLOTATION KINETICS USING PYRITE TRACERS
(Pilot Column)

F.5	GAS RATE: 2.86 cm/s								
Time (sec)	Cumulative Pyrite Recovery (%)	Time (sec)	Cumulative Pyrite Recovery (%)	Time (sec)	Cumulative Pyrite Recovery (%)	Time (sec)	Cumulative Pyrite Recovery (%)	Time (sec)	Cumulative Pyrite Recovery (%)
0	0.68	88	66.18	176	74.66	264	77.81	352	78.65
2	6.26	90	66.44	178	74.71	266	77.83	354	78.62
4	11.03	92	66.74	180	74.83	268	77.81	356	78.66
6	14.89	94	67.10	182	74.94	270	77.83	358	78.66
8	18.50	96	67.41	184	74.99	272	77.87	360	78.72
10	21.86	98	67.73	186	75.26	274	77.92	362	78.71
12	25.06	100	68.02	188	75.38	276	77.94	364	78.75
14	28.19	102	68.34	190	75.44	278	77.96	366	78.67
16	31.02	104	68.85	192	75.49	280	78.02	368	78.67
18	33.52	106	69.13	194	75.53	282	78.09	370	78.70
20	35.89	108	69.37	196	75.61	284	78.13	372	78.73
22	38.10	110	69.64	198	75.70	286	78.13	374	78.75
24	40.28	112	69.82	200	75.81	288	78.10	376	78.75
26	42.05	114	70.05	202	75.95	290	78.13	378	78.73
28	43.79	116	70.21	204	76.02	292	78.15	380	78.74
30	45.29	118	70.43	206	76.12	294	78.24	382	78.76
32	46.62	120	70.62	208	76.20	296	78.25	384	78.76
34	47.81	122	70.84	210	76.29	298	78.32	386	78.75
36	49.03	124	71.06	212	76.36	300	78.41	388	78.77
38	50.14	126	71.29	214	76.47	302	78.43	390	78.73
40	51.33	128	71.42	216	76.58	304	78.52	392	78.70
42	52.31	130	71.63	218	76.59	306	78.61	394	78.72
44	53.21	132	71.87	220	76.69	308	78.62	396	78.71
46	54.14	134	72.07	222	76.79	310	78.60	398	78.71
48	55.14	136	72.27	224	76.81	312	78.64	400	78.73
50	55.90	138	72.38	226	76.86	314	78.60	402	78.70
52	56.76	140	72.52	228	76.88	316	78.70	404	78.69
54	57.55	142	72.70	230	76.97	318	78.70	406	78.68
56	58.30	144	72.89	232	77.09	320	78.67	408	78.70
58	58.84	146	73.02	234	77.12	322	78.67	410	78.74
60	59.54	148	73.11	236	77.16	324	78.70	412	78.80
62	60.17	150	73.27	238	77.21	326	78.68	414	78.84
64	60.87	152	73.41	240	77.27	328	78.71	416	78.86
66	61.33	154	73.65	242	77.33	330	78.76	418	78.88
68	61.81	156	73.73	244	77.38	332	78.78	420	78.94
70	62.34	158	73.91	246	77.55	334	78.80		
72	62.85	160	74.01	248	77.61	336	78.75		
74	63.48	162	74.09	250	77.65	338	78.71		
76	63.94	164	74.20	252	77.70	340	78.64		
78	64.32	166	74.25	254	77.71	342	78.60		
80	64.73	168	74.34	256	77.71	344	78.61		
82	65.09	170	74.42	258	77.74	346	78.59		
84	65.53	172	74.50	260	77.76	348	78.65		
86	65.88	174	74.55	262	77.79	350	78.61		

F. DETERMINATION OF FLOTATION KINETICS USING PYRITE TRACERS
(Pilot Column)

F.6	Frother Concentration:			4ppm								
Time (sec)	Cumulative Pyrite Recovery (%)	Time (sec)	Cumulative Pyrite Recovery (%)	Time (sec)	Cumulative Pyrite Recovery (%)	Time (sec)	Cumulative Pyrite Recovery (%)	Time (sec)	Cumulative Pyrite Recovery (%)	Time (sec)	Cumulative Pyrite Recovery (%)
0	0.21	88	44.21	176	55.93	264	59.61	352	61.45	440	62.24
2	3.23	90	44.68	178	56.11	266	59.63	354	61.47	442	62.26
4	6.71	92	45.07	180	56.25	268	59.81	356	61.50	444	62.25
6	9.51	94	45.42	182	56.38	270	59.89	358	61.52	446	62.27
8	11.92	96	45.82	184	56.56	272	59.93	360	61.50	448	62.25
10	14.05	98	46.25	186	56.68	274	59.93	362	61.47	450	62.23
12	15.86	100	46.59	188	56.80	276	59.95	364	61.50	452	62.24
14	17.46	102	46.92	190	56.99	278	59.98	366	61.50	454	62.25
16	18.88	104	47.25	192	57.14	280	60.01	368	61.52	456	62.24
18	20.17	106	47.53	194	57.25	282	60.05	370	61.50	458	62.23
20	21.39	108	47.81	196	57.35	284	60.09	372	61.53	460	62.26
22	22.50	110	48.09	198	57.43	286	60.12	374	61.53	462	62.23
24	23.52	112	48.37	200	57.55	288	60.16	376	61.51	464	62.25
26	24.51	114	48.70	202	57.64	290	60.20	378	61.49	466	62.25
28	25.42	116	49.05	204	57.75	292	60.20	380	61.53	468	62.23
30	26.18	118	49.36	206	57.83	294	60.23	382	61.54	470	62.25
32	27.00	120	49.69	208	57.90	296	60.25	384	61.52	472	62.26
34	27.85	122	49.95	210	58.01	298	60.31	386	61.51	474	62.26
36	28.60	124	50.28	212	58.10	300	60.33	388	61.48	476	62.28
38	29.33	126	50.55	214	58.13	302	60.34	390	61.51	478	62.30
40	30.03	128	50.87	216	58.16	304	60.38	392	61.55	480	62.32
42	30.74	130	51.11	218	58.26	306	60.44	394	61.59	482	62.30
44	31.49	132	51.42	220	58.36	308	60.48	396	61.77	484	62.34
46	32.18	134	51.64	222	58.44	310	60.56	398	61.78	486	62.34
48	32.85	136	51.87	224	58.48	312	60.54	400	61.81	488	62.39
50	33.45	138	52.12	226	58.55	314	60.54	402	61.86	490	62.36
52	34.13	140	52.39	228	58.61	316	60.54	404	61.92	492	62.43
54	34.81	142	52.62	230	58.67	318	60.62	406	61.94	494	62.47
56	35.48	144	52.91	232	58.73	320	60.66	408	61.93	496	62.45
58	36.15	146	53.11	234	58.81	322	60.69	410	61.97	498	62.51
60	36.78	148	53.25	236	58.85	324	60.78	412	61.98	500	62.51
62	37.32	150	53.50	238	58.88	326	60.84	414	62.02	502	62.50
64	38.09	152	53.75	240	58.96	328	60.93	416	62.03	504	62.51
66	38.60	154	53.91	242	58.99	330	61.00	418	62.10	506	62.50
68	39.11	156	54.11	244	59.03	332	61.08	420	62.11	508	62.51
70	39.75	158	54.29	246	59.12	334	61.11	422	62.11	510	62.48
72	40.32	160	54.54	248	59.18	336	61.13	424	62.10	512	62.47
74	40.83	162	54.89	250	59.24	338	61.16	426	62.09	514	62.51
76	41.30	164	55.13	252	59.30	340	61.21	428	62.09	516	62.48
78	41.90	166	55.30	254	59.36	342	61.22	430	62.11	518	62.46
80	42.38	168	55.45	256	59.45	344	61.27	432	62.13	520	62.41
82	42.84	170	55.56	258	59.47	346	61.32	434	62.16	522	62.37
84	43.32	172	55.71	260	59.54	348	61.36	436	62.23	524	62.36
86	43.82	174	55.83	262	59.56	350	61.43	438	62.22	526	62.39

F. DETERMINATION OF FLOTATION KINETICS USING PYRITE TRACERS
(Pilot Column)

F.7	Frother Concentration:			7ppm								
Time (sec)	Cumulative Pyrite Recovery (%)	Time (sec)	Cumulative Pyrite Recovery (%)	Time (sec)	Cumulative Pyrite Recovery (%)	Time (sec)	Cumulative Pyrite Recovery (%)	Time (sec)	Cumulative Pyrite Recovery (%)	Time (sec)	Cumulative Pyrite Recovery (%)
0	0.18	88	42.14	176	55.03	264	62.56	352	66.87	440	68.77
2	2.42	90	42.53	178	55.20	266	62.68	354	66.92	442	68.78
4	5.60	92	42.95	180	55.38	268	62.82	356	66.99	444	68.87
6	8.31	94	43.49	182	55.69	270	62.95	358	67.06	446	68.87
8	10.60	96	43.99	184	55.87	272	63.07	360	67.10	448	68.91
10	12.56	98	44.45	186	56.00	274	63.18	362	67.19	450	68.93
12	14.25	100	44.92	188	56.17	276	63.34	364	67.26	452	68.94
14	15.71	102	45.32	190	56.41	278	63.45	366	67.33	454	68.96
16	17.04	104	45.72	192	56.57	280	63.59	368	67.40	456	68.97
18	18.32	106	46.17	194	56.77	282	63.75	370	67.48	458	68.97
20	19.47	108	46.56	196	57.00	284	63.86	372	67.60	460	69.01
22	20.55	110	46.89	198	57.16	286	63.97	374	67.62	462	69.02
24	21.56	112	47.34	200	57.32	288	64.04	376	67.69	464	69.05
26	22.46	114	47.68	202	57.53	290	64.18	378	67.75	466	69.02
28	23.35	116	47.98	204	57.70	292	64.29	380	67.77	468	69.02
30	24.12	118	48.29	206	57.91	294	64.41	382	67.83	470	69.02
32	24.90	120	48.65	208	58.10	296	64.49	384	67.87	472	69.03
34	25.69	122	48.90	210	58.30	298	64.61	386	67.90	474	69.02
36	26.38	124	49.18	212	58.45	300	64.71	388	67.95	476	69.05
38	27.09	126	49.45	214	58.72	302	64.92	390	67.97	478	69.07
40	27.77	128	49.70	216	58.94	304	65.01	392	68.01	480	69.04
42	28.46	130	49.97	218	59.12	306	65.08	394	68.04	482	69.05
44	29.10	132	50.23	220	59.28	308	65.18	396	68.09	484	69.05
46	29.73	134	50.48	222	59.59	310	65.26	398	68.09	486	69.05
48	30.41	136	50.76	224	59.77	312	65.34	400	68.15	488	69.07
50	31.03	138	50.96	226	59.96	314	65.41	402	68.19	490	69.07
52	31.69	140	51.18	228	60.18	316	65.53	404	68.23	492	69.06
54	32.32	142	51.42	230	60.36	318	65.60	406	68.27	494	69.05
56	32.89	144	51.70	232	60.52	320	65.67	408	68.31	496	69.05
58	33.62	146	51.92	234	60.67	322	65.79	410	68.35	498	69.03
60	34.20	148	52.14	236	60.81	324	65.88	412	68.36	500	69.01
62	34.85	150	52.36	238	60.95	326	65.95	414	68.40	502	69.02
64	35.48	152	52.60	240	61.09	328	66.03	416	68.43	504	68.99
66	36.25	154	52.83	242	61.21	330	66.07	418	68.55	506	68.99
68	36.92	156	53.03	244	61.33	332	66.16	420	68.54	508	69.00
70	37.55	158	53.23	246	61.44	334	66.24	422	68.56	510	69.01
72	38.10	160	53.46	248	61.58	336	66.33	424	68.61	512	69.02
74	38.83	162	53.66	250	61.72	338	66.39	426	68.64		
76	39.38	164	53.84	252	61.83	340	66.48	428	68.67		
78	39.85	166	54.08	254	61.97	342	66.55	430	68.68		
80	40.31	168	54.26	256	62.09	344	66.60	432	68.73		
82	40.80	170	54.46	258	62.19	346	66.68	434	68.75		
84	41.20	172	54.65	260	62.32	348	66.73	436	68.75		
86	41.69	174	54.85	262	62.45	350	66.80	438	68.75		

F. DETERMINATION OF FLOTATION KINETICS USING PYRITE TRACERS
(Pilot Column)

F.8	Frother Concentration: 10ppm											
Time (sec)	Cumulative Pyrite Recovery (%)	Time (sec)	Cumulative Pyrite Recovery (%)	Time (sec)	Cumulative Pyrite Recovery (%)	Time (sec)	Cumulative Pyrite Recovery (%)	Time (sec)	Cumulative Pyrite Recovery (%)	Time (sec)	Cumulative Pyrite Recovery (%)
0	0.01	88	40.58	176	54.21	264	62.60	352	67.78	440	72.12
2	1.87	90	41.03	178	54.43	266	62.74	354	67.89	442	72.15
4	4.76	92	41.48	180	54.67	268	62.89	356	67.97	444	72.18
6	7.21	94	41.95	182	54.86	270	63.02	358	68.09	446	72.22
8	9.32	96	42.38	184	55.11	272	63.19	360	68.17	448	72.25
10	11.09	98	42.81	186	55.30	274	63.32	362	68.29	450	72.27
12	12.71	100	43.24	188	55.52	276	63.47	364	68.41	452	72.31
14	14.10	102	43.62	190	55.72	278	63.60	366	68.50	454	72.35
16	15.33	104	44.03	192	55.94	280	63.72	368	68.59	456	72.39
18	16.41	106	44.46	194	56.12	282	63.86	370	68.82	458	72.44
20	17.42	108	44.86	196	56.35	284	64.01	372	68.95	460	72.48
22	18.39	110	45.20	198	56.56	286	64.16	374	69.05	462	72.53
24	19.30	112	45.53	200	56.78	288	64.28	376	69.15	464	72.55
26	20.14	114	45.85	202	56.98	290	64.40	378	69.38	466	72.60
28	21.04	116	46.23	204	57.17	292	64.55	380	69.59	468	72.63
30	21.89	118	46.55	206	57.39	294	64.68	382	69.68	470	72.65
32	22.72	120	46.86	208	57.56	296	64.82	384	69.79	472	72.68
34	23.54	122	47.21	210	57.77	298	64.92	386	69.88	474	72.72
36	24.36	124	47.56	212	57.99	300	65.00	388	69.99	476	72.78
38	25.13	126	47.87	214	58.19	302	65.26	390	70.11	478	72.81
40	25.80	128	48.16	216	58.37	304	65.36	392	70.19	480	72.84
42	26.51	130	48.44	218	58.60	306	65.47	394	70.29	482	72.88
44	27.25	132	48.76	220	58.78	308	65.58	396	70.39	484	72.91
46	27.94	134	49.03	222	59.00	310	65.67	398	70.46	486	72.93
48	28.72	136	49.28	224	59.22	312	65.80	400	70.59	488	72.94
50	29.47	138	49.58	226	59.41	314	65.91	402	70.66	490	72.94
52	30.11	140	49.87	228	59.58	316	65.98	404	70.77	492	73.01
54	30.79	142	50.16	230	59.73	318	66.08	406	70.82	494	73.02
56	31.39	144	50.39	232	59.88	320	66.19	408	70.90	496	73.01
58	32.23	146	50.62	234	60.09	322	66.29	410	70.98	498	73.02
60	32.85	148	50.88	236	60.25	324	66.38	412	71.13	500	73.00
62	33.52	150	51.11	238	60.44	326	66.49	414	71.20	502	73.02
64	34.29	152	51.37	240	60.61	328	66.57	416	71.24	504	73.02
66	34.86	154	51.64	242	60.92	330	66.71	418	71.31	506	73.09
68	35.46	156	51.86	244	61.17	332	66.79	420	71.37	508	73.08
70	35.99	158	52.08	246	61.33	334	66.87	422	71.48	510	73.06
72	36.55	160	52.33	248	61.49	336	66.96	424	71.57	512	73.07
74	37.11	162	52.58	250	61.64	338	67.05	426	71.59	514	73.10
76	37.67	164	52.80	252	61.78	340	67.14	428	71.66	516	73.09
78	38.21	166	53.03	254	61.93	342	67.25	430	71.71	518	73.09
80	38.73	168	53.27	256	62.08	344	67.35	432	71.75	520	73.18
82	39.18	170	53.50	258	62.21	346	67.45	434	71.92	522	73.20
84	39.60	172	53.74	260	62.35	348	67.57	436	71.99	524	73.12
86	40.09	174	53.98	262	62.46	350	67.66	438	72.09	526	73.09

F. DETERMINATION OF FLOTATION KINETICS USING PYRITE TRACERS
(Pilot Column)

F.9	Frother Concentration: 40ppm											
Time (sec)	Cumulative Pyrite Recovery (%)	Time (sec)	Cumulative Pyrite Recovery (%)	Time (sec)	Cumulative Pyrite Recovery (%)	Time (sec)	Cumulative Pyrite Recovery (%)	Time (sec)	Cumulative Pyrite Recovery (%)	Time (sec)	Cumulative Pyrite Recovery (%)
0	0.04	88	64.96	176	70.84	264	72.81	352	73.34	440	73.02
2	4.89	90	65.21	178	70.88	266	72.84	354	73.35	442	73.00
4	9.89	92	65.53	180	70.92	268	72.85	356	73.35	444	73.02
6	14.02	94	65.72	182	70.96	270	72.94	358	73.35	446	73.01
8	17.64	96	65.97	184	71.05	272	72.91	360	73.35	448	73.04
10	20.88	98	66.13	186	71.05	274	72.94	362	73.36	450	73.03
12	23.94	100	66.47	188	71.17	276	72.95	364	73.33	452	73.02
14	27.34	102	66.70	190	71.17	278	72.95	366	73.35	454	72.98
16	30.96	104	66.88	192	71.22	280	72.98	368	73.34	456	72.93
18	33.97	106	67.05	194	71.30	282	73.01	370	73.33	458	72.91
20	36.62	108	67.23	196	71.38	284	73.01	372	73.30	460	72.85
22	38.95	110	67.37	198	71.49	286	73.00	374	73.30	462	72.83
24	41.27	112	67.55	200	71.56	288	73.07	376	73.26	464	72.84
26	43.12	114	67.76	202	71.56	290	73.06	378	73.28	466	72.89
28	44.82	116	67.89	204	71.58	292	73.03	380	73.27	468	72.90
30	46.66	118	68.01	206	71.60	294	73.08	382	73.24	470	72.89
32	48.19	120	68.27	208	71.69	296	73.08	384	73.20	472	72.85
34	49.54	122	68.35	210	71.72	298	73.08	386	73.24	474	72.86
36	50.70	124	68.47	212	71.77	300	73.08	388	73.20	476	72.84
38	51.69	126	68.59	214	71.75	302	73.10	390	73.19	478	72.84
40	52.88	128	68.79	216	71.76	304	73.17	392	73.19	480	72.83
42	53.81	130	68.91	218	71.83	306	73.17	394	73.20	482	72.85
44	54.61	132	69.02	220	71.88	308	73.22	396	73.19	484	72.88
46	55.41	134	69.15	222	71.93	310	73.23	398	73.17	486	72.89
48	56.11	136	69.27	224	71.94	312	73.25	400	73.16	488	72.89
50	56.75	138	69.42	226	71.98	314	73.29	402	73.14	490	72.88
52	57.44	140	69.51	228	72.03	316	73.33	404	73.12	492	72.92
54	58.07	142	69.55	230	72.10	318	73.33	406	73.11	494	72.90
56	58.68	144	69.67	232	72.13	320	73.30	408	73.11	496	72.91
58	59.20	146	69.80	234	72.15	322	73.32	410	73.14	498	72.92
60	59.72	148	69.86	236	72.34	324	73.39	412	73.25	500	72.91
62	60.26	150	69.96	238	72.46	326	73.39	414	73.28		
64	60.73	152	70.05	240	72.48	328	73.42	416	73.26		
66	61.25	154	70.13	242	72.50	330	73.42	418	73.23		
68	61.64	156	70.22	244	72.50	332	73.40	420	73.19		
70	62.06	158	70.29	246	72.56	334	73.41	422	73.20		
72	62.41	160	70.33	248	72.58	336	73.41	424	73.19		
74	62.84	162	70.39	250	72.59	338	73.41	426	73.17		
76	63.23	164	70.46	252	72.65	340	73.40	428	73.18		
78	63.51	166	70.53	254	72.68	342	73.36	430	73.17		
80	63.78	168	70.60	256	72.70	344	73.39	432	73.08		
82	64.09	170	70.70	258	72.74	346	73.40	434	73.02		
84	64.36	172	70.78	260	72.73	348	73.36	436	73.01		
86	64.63	174	70.81	262	72.78	350	73.37	438	73.00		

F. DETERMINATION OF FLOTATION KINETICS USING PYRITE TRACERS
(Pilot Column)

F.10	Particle Size:		19.0 micron									
Time (sec)	Cumulative Pyrite Recovery (%)	Time (sec)	Cumulative Pyrite Recovery (%)	Time (sec)	Cumulative Pyrite Recovery (%)	Time (sec)	Cumulative Pyrite Recovery (%)	Time (sec)	Cumulative Pyrite Recovery (%)	Time (sec)	Cumulative Pyrite Recovery (%)
0	0.35	88	20.17	176	26.05	264	27.62	352	28.25	440	28.60
2	0.86	90	20.39	178	26.13	266	27.63	354	28.26	442	28.61
4	1.30	92	20.59	180	26.18	268	27.65	356	28.27	444	28.61
6	1.74	94	20.80	182	26.23	270	27.67	358	28.29	446	28.63
8	2.49	96	20.99	184	26.28	272	27.70	360	28.31	448	28.63
10	3.33	98	21.19	186	26.33	274	27.70	362	28.32	450	28.64
12	4.17	100	21.36	188	26.37	276	27.72	364	28.33	452	28.64
14	4.96	102	21.54	190	26.41	278	27.74	366	28.35	454	28.65
16	5.71	104	21.74	192	26.45	280	27.76	368	28.35	456	28.66
18	6.44	106	21.94	194	26.49	282	27.77	370	28.35	458	28.67
20	7.13	108	22.14	196	26.54	284	27.80	372	28.36	460	28.67
22	7.74	110	22.33	198	26.58	286	27.81	374	28.36	462	28.68
24	8.36	112	22.53	200	26.63	288	27.84	376	28.37	464	28.68
26	8.97	114	22.72	202	26.66	290	27.84	378	28.38	466	28.68
28	9.60	116	22.92	204	26.71	292	27.86	380	28.38	468	28.70
30	10.19	118	23.10	206	26.75	294	27.86	382	28.40	470	28.71
32	10.74	120	23.26	208	26.79	296	27.88	384	28.40	472	28.71
34	11.33	122	23.45	210	26.83	298	27.89	386	28.41	474	28.71
36	11.87	124	23.61	212	26.88	300	27.91	388	28.43	476	28.70
38	12.35	126	23.76	214	26.91	302	27.93	390	28.44	478	28.71
40	12.86	128	23.92	216	26.95	304	27.94	392	28.44	480	28.71
42	13.29	130	24.10	218	26.98	306	27.96	394	28.44	482	28.71
44	13.73	132	24.24	220	27.01	308	27.98	396	28.44	484	28.71
46	14.19	134	24.40	222	27.04	310	27.98	398	28.45	486	28.71
48	14.58	136	24.55	224	27.06	312	27.99	400	28.47	488	28.72
50	14.93	138	24.75	226	27.08	314	28.00	402	28.49	490	28.72
52	15.28	140	24.84	228	27.11	316	28.01	404	28.50	492	28.72
54	15.65	142	24.92	230	27.13	318	28.02	406	28.51	494	28.73
56	15.98	144	25.00	232	27.16	320	28.04	408	28.51	496	28.74
58	16.28	146	25.06	234	27.18	322	28.06	410	28.51	498	28.73
60	16.59	148	25.14	236	27.21	324	28.07	412	28.52	500	28.73
62	16.92	150	25.18	238	27.24	326	28.08	414	28.53	502	28.74
64	17.20	152	25.25	240	27.25	328	28.09	416	28.53	504	28.76
66	17.49	154	25.34	242	27.28	330	28.09	418	28.53	506	28.77
68	17.77	156	25.41	244	27.31	332	28.11	420	28.54	508	28.77
70	18.02	158	25.49	246	27.34	334	28.14	422	28.56	510	28.75
72	18.29	160	25.57	248	27.37	336	28.16	424	28.57	512	28.76
74	18.55	162	25.62	250	27.40	338	28.17	426	28.56	514	28.76
76	18.78	164	25.67	252	27.43	340	28.17	428	28.56	516	28.77
78	19.02	166	25.74	254	27.46	342	28.18	430	28.57	518	28.77
80	19.26	168	25.81	256	27.48	344	28.19	432	28.57	520	28.78
82	19.48	170	25.88	258	27.52	346	28.21	434	28.58	522	28.79
84	19.74	172	25.94	260	27.55	348	28.22	436	28.59	524	28.80
86	19.96	174	25.99	262	27.59	350	28.23	438	28.59	526	28.79

F. DETERMINATION OF FLOTATION KINETICS USING PYRITE TRACERS
(Pilot Column)

F.11	Particle Size:		90.5 micron		
Time (sec)	Cumulative Pyrite Recovery (%)	Time (sec)	Cumulative Pyrite Recovery (%)	Time (sec)	Cumulative Pyrite Recovery (%)
0	0.72	88	64.88	176	72.43
2	1.74	90	65.25	178	72.42
4	8.83	92	65.59	180	72.56
6	15.09	94	65.86	182	72.63
8	19.93	96	66.24	184	72.58
10	23.76	98	66.60	186	72.68
12	27.12	100	66.93	188	72.76
14	29.86	102	67.14	190	72.85
16	32.43	104	67.35	192	72.88
18	35.40	106	67.64	194	72.92
20	37.60	108	67.85	196	72.97
22	39.44	110	68.08	198	72.97
24	41.20	112	68.32	200	72.94
26	42.78	114	68.55	202	72.99
28	44.32	116	68.74	204	72.97
30	45.84	118	68.99	206	73.05
32	47.29	120	69.19	208	72.98
34	48.60	122	69.40	210	73.02
36	49.63	124	69.57	212	73.08
38	50.60	126	69.81	214	73.08
40	51.52	128	69.96	216	73.18
42	52.33	130	70.09	218	73.18
44	53.21	132	70.19	220	73.08
46	53.97	134	70.31	222	73.13
48	54.79	136	70.47	224	73.18
50	55.42	138	70.60	226	73.28
52	56.00	140	70.69	228	73.29
54	56.77	142	70.77	230	73.29
56	57.42	144	70.91	232	73.27
58	58.16	146	71.06	234	73.25
60	58.83	148	71.14	236	73.29
62	59.38	150	71.25	238	73.26
64	59.93	152	71.33	240	73.28
66	60.44	154	71.44	242	73.28
68	61.00	156	71.49	244	73.21
70	61.45	158	71.61	246	73.10
72	61.83	160	71.70	248	73.01
74	62.33	162	71.85	250	72.98
76	62.69	164	71.99		
78	63.09	166	72.04		
80	63.48	168	72.09		
82	63.79	170	72.15		
84	64.14	172	72.20		
86	64.48	174	72.31		

F. DETERMINATION OF FLOTATION KINETICS USING PYRITE TRACERS
(Pilot Column)

F.12	Particle Size:		128.0 micron				
Time (sec)	Cumulative Pyrite Recovery (%)	Time (sec)	Cumulative Pyrite Recovery (%)	Time (sec)	Cumulative Pyrite Recovery (%)	Time (sec)	Cumulative Pyrite Recovery (%)
0	0.29	88	41.22	176	49.42	264	50.28
2	0.99	90	41.63	178	49.41	266	50.28
4	3.65	92	42.06	180	49.38	268	50.32
6	5.79	94	42.43	182	49.33	270	50.35
8	7.70	96	42.87	184	49.31	272	50.45
10	9.43	98	43.36	186	49.25	274	50.43
12	11.02	100	43.70	188	49.15	276	50.41
14	12.52	102	44.09	190	49.10	278	50.39
16	14.10	104	44.38	192	49.14	280	50.35
18	15.53	106	44.64	194	49.21	282	50.42
20	16.72	108	44.87	196	49.30	284	50.38
22	17.80	110	45.17	198	49.22	286	50.43
24	18.90	112	45.53	200	49.25	288	50.41
26	19.93	114	45.79	202	49.25	290	50.28
28	20.87	116	45.97	204	49.33	292	50.30
30	22.02	118	46.18	206	49.61	294	50.33
32	23.07	120	46.39	208	49.68	296	50.23
34	23.98	122	46.61	210	49.58	298	50.25
36	24.95	124	46.71	212	49.50		
38	25.94	126	46.91	214	49.63		
40	26.70	128	47.12	216	49.66		
42	27.49	130	47.24	218	49.75		
44	28.24	132	47.36	220	49.75		
46	28.99	134	47.66	222	49.79		
48	29.76	136	47.81	224	49.98		
50	30.44	138	47.90	226	49.97		
52	31.10	140	48.00	228	49.88		
54	31.82	142	48.08	230	49.96		
56	32.48	144	48.15	232	50.03		
58	33.02	146	48.34	234	50.04		
60	33.78	148	48.43	236	50.02		
62	34.33	150	48.44	238	49.99		
64	34.99	152	48.60	240	50.07		
66	35.56	154	48.72	242	50.04		
68	36.20	156	48.80	244	50.04		
70	36.77	158	48.94	246	50.04		
72	37.29	160	49.01	248	50.18		
74	37.95	162	49.00	250	50.12		
76	38.46	164	48.99	252	50.20		
78	38.98	166	49.08	254	50.29		
80	39.47	168	49.22	256	50.25		
82	39.84	170	49.27	258	50.35		
84	40.26	172	49.37	260	50.34		
86	40.69	174	49.37	262	50.32		

F. DETERMINATION OF FLOTATION KINETICS USING PYRITE TRACERS
(Pilot Column)

F.13	Particle Size:		181.0 micron				
Time (sec)	Cumulative Pyrite Recovery (%)	Time (sec)	Cumulative Pyrite Recovery (%)	Time (sec)	Cumulative Pyrite Recovery (%)	Time (sec)	Cumulative Pyrite Recovery (%)
0	0.37	88	32.71	176	34.87	264	35.72
2	2.91	90	32.94	178	34.88	266	35.49
4	7.62	92	33.20	180	34.94	268	35.59
6	10.69	94	33.38	182	34.93	270	35.57
8	12.68	96	33.42	184	34.98	272	35.62
10	14.14	98	33.51	186	34.99	274	35.61
12	15.42	100	33.60	188	35.00	276	35.65
14	16.28	102	33.68	190	35.02	278	35.66
16	17.10	104	33.78	192	35.15	280	35.61
18	17.90	106	33.87	194	35.25	282	35.64
20	18.52	108	33.87	196	35.32	284	35.55
22	19.93	110	33.87	198	35.41	286	35.57
24	20.47	112	33.90	200	35.52	288	35.54
26	21.12	114	34.04	202	35.66	290	35.52
28	21.80	116	34.14	204	35.76	292	35.52
30	22.46	118	34.27	206	35.79	294	35.60
32	22.92	120	34.19	208	35.71	296	35.50
34	23.60	122	34.14	210	35.69	298	35.55
36	24.34	124	34.14	212	35.72		
38	24.92	126	34.23	214	35.64		
40	25.60	128	34.26	216	35.64		
42	26.24	130	34.37	218	35.65		
44	26.82	132	34.24	220	35.69		
46	27.37	134	34.23	222	35.67		
48	27.84	136	34.35	224	35.59		
50	28.35	138	34.50	226	35.62		
52	28.69	140	34.51	228	35.67		
54	29.03	142	34.59	230	35.63		
56	29.26	144	34.66	232	35.55		
58	29.55	146	34.74	234	35.57		
60	29.68	148	34.69	236	35.57		
62	30.01	150	34.73	238	35.45		
64	30.27	152	34.81	240	35.46		
66	30.49	154	34.80	242	35.42		
68	30.73	156	34.90	244	35.42		
70	30.96	158	34.86	246	35.58		
72	31.11	160	34.71	248	35.69		
74	31.27	162	34.68	250	35.77		
76	31.47	164	34.68	252	35.76		
78	31.72	166	34.67	254	35.66		
80	31.88	168	34.63	256	35.55		
82	32.16	170	34.69	258	35.62		
84	32.34	172	34.83	260	35.58		
86	32.49	174	34.87	262	35.73		

G. DETERMINATION OF FLOTATION KINETICS USING PYRITE TRACERS
(President Steyn Industrial Column)

G.1	TRACER: -38 micron								
Time (min)	Cumulative Pyrite Recovered (%)	Time (min)	Cumulative Pyrite Recovered (%)	Time (min)	Cumulative Pyrite Recovered (%)	Time (min)	Cumulative Pyrite Recovered (%)	Time (min)	Cumulative Pyrite Recovered (%)
0.00	0.01	3.75	4.89	7.50	7.61	11.25	9.25	15.00	10.19
0.08	0.08	3.83	4.98	7.58	7.64	11.33	9.27	15.08	10.21
0.17	0.17	3.92	5.05	7.67	7.69	11.42	9.30	15.17	10.23
0.25	0.28	4.00	5.13	7.75	7.73	11.50	9.32	15.25	10.25
0.33	0.40	4.08	5.21	7.83	7.77	11.58	9.35	15.33	10.27
0.42	0.54	4.17	5.27	7.92	7.82	11.67	9.37	15.42	10.29
0.50	0.72	4.25	5.36	8.00	7.87	11.75	9.39	15.50	10.32
0.58	0.92	4.33	5.42	8.08	7.90	11.83	9.42	15.58	10.33
0.67	1.12	4.42	5.49	8.17	7.94	11.92	9.44	15.67	10.34
0.75	1.33	4.50	5.56	8.25	7.98	12.00	9.46	15.75	10.35
0.83	1.50	4.58	5.63	8.33	8.03	12.08	9.49	15.83	10.37
0.92	1.69	4.67	5.69	8.42	8.07	12.17	9.51	15.92	10.38
1.00	1.84	4.75	5.76	8.50	8.11	12.25	9.54	16.00	10.39
1.08	1.99	4.83	5.83	8.58	8.16	12.33	9.57	16.08	10.40
1.17	2.12	4.92	5.90	8.67	8.19	12.42	9.59	16.17	10.42
1.25	2.24	5.00	5.95	8.75	8.24	12.50	9.62	16.25	10.44
1.33	2.36	5.08	6.02	8.83	8.28	12.58	9.64	16.33	10.46
1.42	2.47	5.17	6.09	8.92	8.31	12.67	9.66	16.42	10.47
1.50	2.57	5.25	6.15	9.00	8.35	12.75	9.69	16.50	10.49
1.58	2.66	5.33	6.21	9.08	8.39	12.83	9.71	16.58	10.49
1.67	2.77	5.42	6.27	9.17	8.43	12.92	9.73	16.67	10.50
1.75	2.86	5.50	6.33	9.25	8.47	13.00	9.74	16.75	10.50
1.83	2.97	5.58	6.38	9.33	8.51	13.08	9.76	16.83	10.51
1.92	3.06	5.67	6.44	9.42	8.55	13.17	9.77	16.92	10.52
2.00	3.15	5.75	6.49	9.50	8.59	13.25	9.80	17.00	10.54
2.08	3.24	5.83	6.56	9.58	8.62	13.33	9.82	17.08	10.55
2.17	3.33	5.92	6.62	9.67	8.66	13.42	9.84	17.17	10.56
2.25	3.42	6.00	6.67	9.75	8.70	13.50	9.86	17.25	10.56
2.33	3.51	6.08	6.74	9.83	8.73	13.58	9.87	17.33	10.58
2.42	3.59	6.17	6.80	9.92	8.77	13.67	9.90	17.42	10.59
2.50	3.68	6.25	6.86	10.00	8.80	13.75	9.92	17.50	10.61
2.58	3.76	6.33	6.90	10.08	8.84	13.83	9.94	17.58	10.62
2.67	3.84	6.42	6.95	10.17	8.87	13.92	9.97	17.67	10.62
2.75	3.93	6.50	7.01	10.25	8.90	14.00	9.99	17.75	10.64
2.83	4.00	6.58	7.06	10.33	8.92	14.08	10.01	17.83	10.64
2.92	4.08	6.67	7.11	10.42	8.96	14.17	10.04	17.92	10.65
3.00	4.16	6.75	7.15	10.50	8.99	14.25	10.05	18.00	10.65
3.08	4.24	6.83	7.20	10.58	9.02	14.33	10.06	18.08	10.66
3.17	4.32	6.92	7.25	10.67	9.06	14.42	10.07	18.17	10.68
3.25	4.41	7.00	7.30	10.75	9.08	14.50	10.10	18.25	10.69
3.33	4.49	7.08	7.35	10.83	9.11	14.58	10.11	18.33	10.71
3.42	4.58	7.17	7.41	10.92	9.14	14.67	10.13	18.42	10.71
3.50	4.66	7.25	7.46	11.00	9.17	14.75	10.14	18.50	10.72
3.58	4.73	7.33	7.51	11.08	9.20	14.83	10.16	18.58	10.72
3.67	4.82	7.42	7.56	11.17	9.22	14.92	10.18	18.67	10.73

G. DETERMINATION OF FLOTATION KINETICS USING PYRITE TRACER
(President Steyn Industrial Column)

G.1	TRACER:	-38 micron			
Time (min)	Cumulative Pyrite Recovered (%)	Time (min)	Cumulative Pyrite Recovered (%)	Time (min)	Cumulative Pyrite Recovered (%)
18.75	10.74	22.50	10.97	26.25	11.02
18.83	10.75	22.58	10.97	26.33	11.01
18.92	10.75	22.67	10.97	26.42	11.01
19.00	10.76	22.75	10.98	26.50	11.01
19.08	10.77	22.83	10.98	26.58	11.01
19.17	10.77	22.92	10.97	26.67	11.01
19.25	10.78	23.00	10.98	26.75	11.02
19.33	10.79	23.08	10.98	26.83	11.01
19.42	10.80	23.17	10.98	26.92	11.02
19.50	10.81	23.25	10.98	27.00	11.02
19.58	10.81	23.33	10.98	27.08	11.02
19.67	10.81	23.42	10.99	27.17	11.02
19.75	10.82	23.50	10.98	27.25	11.02
19.83	10.83	23.58	10.98	27.33	11.01
19.92	10.84	23.67	10.99	27.42	11.01
20.00	10.85	23.75	10.99		
20.08	10.85	23.83	11.00		
20.17	10.87	23.92	11.00		
20.25	10.88	24.00	11.00		
20.33	10.88	24.08	11.00		
20.42	10.88	24.17	11.00		
20.50	10.88	24.25	11.01		
20.58	10.89	24.33	11.01		
20.67	10.88	24.42	11.01		
20.75	10.89	24.50	11.01		
20.83	10.90	24.58	11.01		
20.92	10.90	24.67	11.01		
21.00	10.91	24.75	11.01		
21.08	10.91	24.83	11.01		
21.17	10.92	24.92	11.01		
21.25	10.93	25.00	11.01		
21.33	10.94	25.08	11.02		
21.42	10.94	25.17	11.02		
21.50	10.95	25.25	11.02		
21.58	10.96	25.33	11.01		
21.67	10.95	25.42	11.01		
21.75	10.95	25.50	11.01		
21.83	10.96	25.58	11.01		
21.92	10.96	25.67	11.00		
22.00	10.96	25.75	11.01		
22.08	10.97	25.83	11.01		
22.17	10.97	25.92	11.01		
22.25	10.97	26.00	11.01		
22.33	10.97	26.08	11.01		
22.42	10.97	26.17	11.01		

G. DETERMINATION OF FLOTATION KINETICS USING PYRITE TRACERS
(President Steyn Industrial Column)

G.2	TRACER:	+38-75 micron							
Time (min)	Cumulative Pyrite Recovered (%)	Time (min)	Cumulative Pyrite Recovered (%)	Time (min)	Cumulative Pyrite Recovered (%)	Time (min)	Cumulative Pyrite Recovered (%)	Time (min)	Cumulative Pyrite Recovered (%)
0.00	0.01	3.75	27.79	7.50	39.93	11.25	45.30	15.00	47.67
0.08	0.05	3.83	28.19	7.58	40.11	11.33	45.37	15.08	47.69
0.17	0.13	3.92	28.59	7.67	40.27	11.42	45.45	15.17	47.71
0.25	0.24	4.00	28.99	7.75	40.45	11.50	45.53	15.25	47.74
0.33	0.40	4.08	29.35	7.83	40.61	11.58	45.60	15.33	47.77
0.42	0.55	4.17	29.72	7.92	40.76	11.67	45.66	15.42	47.80
0.50	1.30	4.25	30.10	8.00	40.91	11.75	45.73	15.50	47.83
0.58	2.49	4.33	30.45	8.08	41.05	11.83	45.81	15.58	47.85
0.67	3.79	4.42	30.81	8.17	41.20	11.92	45.88	15.67	47.88
0.75	4.94	4.50	31.12	8.25	41.36	12.00	45.94	15.75	47.90
0.83	6.02	4.58	31.44	8.33	41.50	12.08	46.00	15.83	47.93
0.92	7.06	4.67	31.77	8.42	41.65	12.17	46.08	15.92	47.97
1.00	8.51	4.75	32.11	8.50	41.79	12.25	46.15	16.00	48.01
1.08	9.35	4.83	32.43	8.58	41.92	12.33	46.21	16.08	48.04
1.17	10.30	4.92	32.71	8.67	42.05	12.42	46.27	16.17	48.07
1.25	11.11	5.00	33.00	8.75	42.19	12.50	46.33	16.25	48.09
1.33	11.82	5.08	33.30	8.83	42.33	12.58	46.39	16.33	48.13
1.42	12.38	5.17	33.59	8.92	42.48	12.67	46.46	16.42	48.14
1.50	12.87	5.25	33.88	9.00	42.59	12.75	46.50	16.50	48.17
1.58	13.58	5.33	34.17	9.08	42.72	12.83	46.56	16.58	48.19
1.67	14.94	5.42	34.46	9.17	42.85	12.92	46.63	16.67	48.20
1.75	16.25	5.50	34.73	9.25	42.98	13.00	46.67		
1.83	16.84	5.58	35.00	9.33	43.09	13.08	46.73		
1.92	17.31	5.67	35.25	9.42	43.20	13.17	46.79		
2.00	17.70	5.75	35.51	9.50	43.34	13.25	46.85		
2.08	18.38	5.83	35.75	9.58	43.47	13.33	46.89		
2.17	18.83	5.92	35.99	9.67	43.57	13.42	46.93		
2.25	19.26	6.00	36.22	9.75	43.68	13.50	46.97		
2.33	19.62	6.08	36.43	9.83	43.79	13.58	47.02		
2.42	20.00	6.17	36.66	9.92	43.87	13.67	47.08		
2.50	20.37	6.25	36.91	10.00	43.98	13.75	47.11		
2.58	20.89	6.33	37.14	10.08	44.07	13.83	47.14		
2.67	21.44	6.42	37.38	10.17	44.17	13.92	47.18		
2.75	21.91	6.50	37.60	10.25	44.26	14.00	47.22		
2.83	22.51	6.58	37.84	10.33	44.35	14.08	47.27		
2.92	23.08	6.67	38.05	10.42	44.43	14.17	47.30		
3.00	23.60	6.75	38.26	10.50	44.51	14.25	47.33		
3.08	24.16	6.83	38.46	10.58	44.60	14.33	47.37		
3.17	24.66	6.92	38.64	10.67	44.71	14.42	47.42		
3.25	25.15	7.00	38.83	10.75	44.81	14.50	47.46		
3.33	25.61	7.08	39.03	10.83	44.89	14.58	47.48		
3.42	26.04	7.17	39.22	10.92	44.98	14.67	47.51		
3.50	26.51	7.25	39.40	11.00	45.07	14.75	47.56		
3.58	26.96	7.33	39.58	11.08	45.15	14.83	47.60		
3.67	27.36	7.42	39.77	11.17	45.21	14.92	47.63		

G. DETERMINATION OF FLOTATION KINETICS USING PYRITE TRACERS
(President Steyn Industrial Column)

G.3	TRACER:	+38-75 micron							
Time (min)	Cumulative Pyrite Recovered (%)	Time (min)	Cumulative Pyrite Recovered (%)	Time (min)	Cumulative Pyrite Recovered (%)	Time (min)	Cumulative Pyrite Recovered (%)	Time (min)	Cumulative Pyrite Recovered (%)
0.00	0.01	3.75	25.86	7.50	39.37	11.25	45.64	15.00	48.31
0.08	0.05	3.83	26.28	7.58	39.56	11.33	45.73	15.08	48.34
0.17	0.14	3.92	26.70	7.67	39.74	11.42	45.83	15.17	48.38
0.25	0.26	4.00	27.09	7.75	39.93	11.50	45.91	15.25	48.41
0.33	0.44	4.08	27.49	7.83	40.11	11.58	45.99	15.33	48.44
0.42	0.63	4.17	27.90	7.92	40.31	11.67	46.07	15.42	48.47
0.50	0.88	4.25	28.31	8.00	40.49	11.75	46.15	15.50	48.52
0.58	1.35	4.33	28.72	8.08	40.67	11.83	46.24	15.58	48.55
0.67	2.07	4.42	29.11	8.17	40.85	11.92	46.32	15.67	48.58
0.75	2.98	4.50	29.47	8.25	41.02	12.00	46.39	15.75	48.61
0.83	4.05	4.58	29.83	8.33	41.18	12.08	46.46	15.83	48.64
0.92	5.17	4.67	30.19	8.42	41.35	12.17	46.52	15.92	48.67
1.00	6.29	4.75	30.56	8.50	41.51	12.25	46.58	16.00	48.70
1.08	7.37	4.83	30.89	8.58	41.69	12.33	46.66		
1.17	8.37	4.92	31.22	8.67	41.87	12.42	46.72		
1.25	9.38	5.00	31.55	8.75	42.04	12.50	46.79		
1.33	10.36	5.08	31.86	8.83	42.20	12.58	46.86		
1.42	11.28	5.17	32.16	8.92	42.35	12.67	46.92		
1.50	12.16	5.25	32.47	9.00	42.50	12.75	46.99		
1.58	12.96	5.33	32.79	9.08	42.66	12.83	47.05		
1.67	13.67	5.42	33.12	9.17	42.80	12.92	47.11		
1.75	14.31	5.50	33.43	9.25	42.92	13.00	47.17		
1.83	14.92	5.58	33.74	9.33	43.07	13.08	47.23		
1.92	15.48	5.67	34.04	9.42	43.21	13.17	47.29		
2.00	16.02	5.75	34.34	9.50	43.34	13.25	47.35		
2.08	16.55	5.83	34.62	9.58	43.48	13.33	47.41		
2.17	17.04	5.92	34.90	9.67	43.61	13.42	47.47		
2.25	17.54	6.00	35.17	9.75	43.73	13.50	47.52		
2.33	18.01	6.08	35.43	9.83	43.85	13.58	47.57		
2.42	18.48	6.17	35.69	9.92	43.97	13.67	47.61		
2.50	18.96	6.25	35.95	10.00	44.09	13.75	47.67		
2.58	19.45	6.33	36.21	10.08	44.22	13.83	47.71		
2.67	19.93	6.42	36.47	10.17	44.33	13.92	47.76		
2.75	20.42	6.50	36.71	10.25	44.44	14.00	47.80		
2.83	20.89	6.58	36.95	10.33	44.56	14.08	47.85		
2.92	21.38	6.67	37.20	10.42	44.67	14.17	47.89		
3.00	21.86	6.75	37.43	10.50	44.78	14.25	47.94		
3.08	22.34	6.83	37.67	10.58	44.88	14.33	47.99		
3.17	22.81	6.92	37.92	10.67	44.98	14.42	48.04		
3.25	23.26	7.00	38.15	10.75	45.09	14.50	48.08		
3.33	23.72	7.08	38.37	10.83	45.18	14.58	48.13		
3.42	24.16	7.17	38.58	10.92	45.27	14.67	48.17		
3.50	24.59	7.25	38.78	11.00	45.37	14.75	48.21		
3.58	25.01	7.33	38.98	11.08	45.47	14.83	48.25		
3.67	25.44	7.42	39.18	11.17	45.56	14.92	48.29		

G. DETERMINATION OF FLOTATION KINETICS USING PYRITE TRACERS
(President Steyn Industrial Column)

G.4	TRACER:	+75-106 micron							
Time (min)	Cumulative Pyrite Recovered (%)	Time (min)	Cumulative Pyrite Recovered (%)	Time (min)	Cumulative Pyrite Recovered (%)	Time (min)	Cumulative Pyrite Recovered (%)	Time (min)	Cumulative Pyrite Recovered (%)
0.00	0.01	3.75	20.62	7.50	33.22	11.25	39.04	15.00	42.62
0.08	0.10	3.83	20.94	7.58	33.37	11.33	39.14	15.08	42.70
0.17	0.25	3.92	21.24	7.67	33.52	11.42	39.24	15.17	42.76
0.25	0.46	4.00	21.65	7.75	33.69	11.50	39.34	15.25	42.83
0.33	0.72	4.08	21.94	7.83	33.85	11.58	39.43	15.33	42.89
0.42	1.13	4.17	22.23	7.92	34.04	11.67	39.51	15.42	42.95
0.50	1.75	4.25	22.54	8.00	34.21	11.75	39.63	15.50	43.01
0.58	2.52	4.33	22.99	8.08	34.36	11.83	39.73	15.58	43.06
0.67	3.36	4.42	23.35	8.17	34.53	11.92	39.83	15.67	43.12
0.75	4.19	4.50	23.77	8.25	34.69	12.00	39.93	15.75	43.18
0.83	4.93	4.58	24.06	8.33	34.82	12.08	40.01	15.83	43.24
0.92	5.61	4.67	24.43	8.42	34.95	12.17	40.11	15.92	43.31
1.00	6.32	4.75	24.75	8.50	35.08	12.25	40.19	16.00	43.36
1.08	7.22	4.83	25.05	8.58	35.21	12.33	40.27	16.08	43.41
1.17	7.78	4.92	25.42	8.67	35.36	12.42	40.36	16.17	43.47
1.25	8.23	5.00	25.82	8.75	35.49	12.50	40.46	16.25	43.53
1.33	8.63	5.08	26.18	8.83	35.62	12.58	40.55	16.33	43.59
1.42	9.01	5.17	26.47	8.92	35.74	12.67	40.63	16.42	43.64
1.50	9.37	5.25	26.83	9.00	35.89	12.75	40.72	16.50	43.69
1.58	9.92	5.33	27.13	9.08	36.01	12.83	40.80	16.58	43.75
1.67	10.44	5.42	27.38	9.17	36.14	12.92	40.88	16.67	43.80
1.75	10.80	5.50	27.64	9.25	36.26	13.00	40.97	16.75	43.84
1.83	11.12	5.58	27.88	9.33	36.39	13.08	41.05	16.83	43.89
1.92	11.65	5.67	28.19	9.42	36.52	13.17	41.13	16.92	43.94
2.00	12.02	5.75	28.58	9.50	36.65	13.25	41.20	17.00	43.98
2.08	12.60	5.83	28.83	9.58	36.79	13.33	41.26	17.08	44.03
2.17	12.97	5.92	29.07	9.67	36.92	13.42	41.33	17.17	44.06
2.25	13.56	6.00	29.29	9.75	37.04	13.50	41.40	17.25	44.13
2.33	13.94	6.08	29.50	9.83	37.16	13.58	41.47	17.33	44.18
2.42	14.28	6.17	29.78	9.92	37.30	13.67	41.53	17.42	44.22
2.50	14.59	6.25	30.05	10.00	37.43	13.75	41.60	17.50	44.25
2.58	14.96	6.33	30.25	10.08	37.55	13.83	41.69	17.58	44.29
2.67	15.52	6.42	30.52	10.17	37.66	13.92	41.75	17.67	44.33
2.75	15.96	6.50	30.76	10.25	37.76	14.00	41.82	17.75	44.37
2.83	16.31	6.58	31.03	10.33	37.87	14.08	41.90	17.83	44.41
2.92	16.72	6.67	31.23	10.42	37.99	14.17	41.97	17.92	44.47
3.00	17.11	6.75	31.42	10.50	38.10	14.25	42.04	18.00	44.50
3.08	17.57	6.83	31.59	10.58	38.21	14.33	42.11	18.08	44.54
3.17	17.98	6.92	31.83	10.67	38.33	14.42	42.16	18.17	44.58
3.25	18.34	7.00	32.11	10.75	38.43	14.50	42.24	18.25	44.62
3.33	18.86	7.08	32.33	10.83	38.53	14.58	42.31	18.33	44.66
3.42	19.35	7.17	32.51	10.92	38.64	14.67	42.36	18.42	44.69
3.50	19.67	7.25	32.69	11.00	38.75	14.75	42.42	18.50	44.73
3.58	19.97	7.33	32.86	11.08	38.85	14.83	42.48	18.58	44.76
3.67	20.27	7.42	33.04	11.17	38.94	14.92	42.56	18.67	44.81

G. DETERMINATION OF FLOTATION KINETICS USING PYRITE TRACERS
(President Steyn Industrial Column)

G.4	TRACER:	+75-106 micron							
Time (min)	Cumulative Pyrite Recovered (%)	Time (min)	Cumulative Pyrite Recovered (%)	Time (min)	Cumulative Pyrite Recovered (%)	Time (min)	Cumulative Pyrite Recovered (%)	Time (min)	Cumulative Pyrite Recovered (%)
18.75	44.86	22.50	46.39	26.25	47.18	30.00	47.56	33.75	47.88
18.83	44.91	22.58	46.42	26.33	47.20	30.08	47.57	33.83	47.88
18.92	44.97	22.67	46.45	26.42	47.20	30.17	47.57	33.92	47.88
19.00	45.03	22.75	46.47	26.50	47.20	30.25	47.59	34.00	47.89
19.08	45.05	22.83	46.49	26.58	47.20	30.33	47.60	34.08	47.89
19.17	45.07	22.92	46.50	26.67	47.22	30.42	47.59	34.17	47.89
19.25	45.11	23.00	46.52	26.75	47.22	30.50	47.61	34.25	47.88
19.33	45.15	23.08	46.54	26.83	47.22	30.58	47.61	34.33	47.90
19.42	45.18	23.17	46.58	26.92	47.22	30.67	47.62	34.42	47.89
19.50	45.21	23.25	46.60	27.00	47.23	30.75	47.63	34.50	47.89
19.58	45.23	23.33	46.62	27.08	47.25	30.83	47.63	34.58	47.89
19.67	45.27	23.42	46.64	27.17	47.26	30.92	47.64	34.67	47.90
19.75	45.30	23.50	46.65	27.25	47.26	31.00	47.64	34.75	47.91
19.83	45.34	23.58	46.67	27.33	47.27	31.08	47.64	34.83	47.93
19.92	45.38	23.67	46.69	27.42	47.27	31.17	47.64	34.92	47.94
20.00	45.41	23.75	46.72	27.50	47.28	31.25	47.64	35.00	47.95
20.08	45.45	23.83	46.74	27.58	47.29	31.33	47.67	35.08	47.97
20.17	45.50	23.92	46.76	27.67	47.29	31.42	47.68	35.17	47.96
20.25	45.54	24.00	46.77	27.75	47.31	31.50	47.68	35.25	47.97
20.33	45.58	24.08	46.79	27.83	47.32	31.58	47.70	35.33	47.97
20.42	45.60	24.17	46.81	27.92	47.32	31.67	47.71	35.42	47.97
20.50	45.63	24.25	46.81	28.00	47.33	31.75	47.72	35.50	47.98
20.58	45.66	24.33	46.83	28.08	47.32	31.83	47.72	35.58	47.97
20.67	45.69	24.42	46.85	28.17	47.32	31.92	47.72	35.67	47.98
20.75	45.73	24.50	46.87	28.25	47.33	32.00	47.72	35.75	47.98
20.83	45.78	24.58	46.88	28.33	47.34	32.08	47.72	35.83	47.98
20.92	45.81	24.67	46.90	28.42	47.35	32.17	47.72	35.92	47.98
21.00	45.85	24.75	46.94	28.50	47.35	32.25	47.73	36.00	48.00
21.08	45.89	24.83	46.95	28.58	47.36	32.33	47.75	36.08	48.01
21.17	45.90	24.92	46.96	28.67	47.38	32.42	47.76	36.17	48.02
21.25	45.94	25.00	46.97	28.75	47.38	32.50	47.77	36.25	48.02
21.33	45.97	25.08	46.98	28.83	47.40	32.58	47.78	36.33	48.02
21.42	45.98	25.17	47.00	28.92	47.40	32.67	47.79	36.42	48.04
21.50	46.01	25.25	47.01	29.00	47.41	32.75	47.79	36.50	48.03
21.58	46.04	25.33	47.03	29.08	47.42	32.83	47.80	36.58	48.05
21.67	46.07	25.42	47.05	29.17	47.42	32.92	47.81	36.67	48.05
21.75	46.11	25.50	47.06	29.25	47.42	33.00	47.82	36.75	48.05
21.83	46.14	25.58	47.08	29.33	47.44	33.08	47.82	36.83	48.05
21.92	46.18	25.67	47.09	29.42	47.45	33.17	47.83	36.92	48.05
22.00	46.20	25.75	47.11	29.50	47.47	33.25	47.82	37.00	48.05
22.08	46.24	25.83	47.12	29.58	47.48	33.33	47.83	37.08	48.05
22.17	46.26	25.92	47.14	29.67	47.50	33.42	47.84	37.17	48.03
22.25	46.29	26.00	47.14	29.75	47.52	33.50	47.86	37.25	48.04
22.33	46.33	26.08	47.16	29.83	47.53	33.58	47.87	37.33	48.05
22.42	46.36	26.17	47.17	29.92	47.55	33.67	47.88	37.42	48.05

APPENDIX 3

PARTICLE COLLECTION MODEL SAMPLE CALCULATION

PARTICLE COLLECTION MODEL

COLLISION EFFICIENCY

Terminal bubble rise velocity
Bubble Reynolds Number

Ub:	18.72	cm/s	
Ub:	18.71	cm/s	Eqn.(1.45)
Reb:	312.62		Eqn.(1.44b)
Ub:	18.71	cm/s	Eqn.(1.45)

NB: Ut must be iteratively determined

Stokes Number (Sk)

Sk: 0.165552 Eqn.(1.44a)

Low Particle Inetria (Sk = 0)

Interceptional collision

Eci: 0.0085 Eqn.(1.48)

gravitational collision

thetac: 35.760 Eqn.(1.50)

Ecg: 0.009972 Eqn.(1.49)

Eco = Ecg + Eci

Eco: 0.018507 Eqn.(1.47)

Intermediate Particle Inertia (Sk > 0.1)

Ec: 0.0285 Eqn.(1.51)

ATTACHMENT EFFICIENCY

Particle tangential sliding velocity

dp/db = 0.030874

For dp/db < 0.03

theta	Vtheta	Average Vtheta	
12	2.581	4.499	
48	6.977		
84	3.938		Eqn.(1.55)

For dp/db > 0.03

theta	Vtheta	Average Vtheta	
12	2.579	4.495	
48	6.972		
84	3.936		Eqn.(1.56)

Maximum Angle of Contact

Thetam: 65.59 Eqn.(1.53)

PARAMETERS

feed % solids:	15	%
gas rate, jg:	2.240	cm/s
gravity, g:	980.0	cm/s2
bubble size, db:	0.183	cm
slurry density, psl:	1.200	g/cm3
gas density, pb:	0.017	g/cm3
slurry viscosity, musl:	0.013	g/cm.s **
particle density, pp:	5.000	g/cm3
liquid density, pl:	1.000	g/cm3
particle size, dp:	0.006	cm
particle size, dp:	56.5	micron
Stokes Equation		
Eqn.(1.46)		
particle velocity, up:	0.529	cm/s
dim.up viz. up/Ub, up*:	0.028	dimen.

** musl = mu(water) + 1.4E10-5(feed%sol) ^ 2
Alford (1990)

theta	surface vorticity	
12	6.11	Eqn.(1.54)
48	16.28	Eqn.(1.54)
84	8.44	Eqn.(1.54)

Reb:	312.62	Eqn.(1.44b)
a:	-1.31E-01	)
b:	5.66E-01	)See
c:	-3.52E-03	)Appendix 4
d:	-2.38E-05	)

Attachment Efficiency

dp/db > 0.03			dp/db < 0.03			
* ti:	0.0215	s	* ti:	0.0215	s	* Iteratively determined induction time
Eqn.(1.59)						
Theta':	6.88		Theta':	6.84		
Eqn.(1.60)						
Ea:	0.0421		Ea:	0.0415		

COLLECTION EFFICIENCY

Ek = Ec Ea Ed Eqn.(1.42)
Ed = 1

dp/db > 0.03		dp/db < 0.03	
Ek:	0.0012	Ek:	0.0012

COLLECTION ZONE RATE CONSTANT

k = 1.5*Ek*vg/db Eqn.(1.41)

jg:	2.24	cm/s
db:	0.183	cm

dp/db = 0.031

dp/db > 0.03			dp/db < 0.03		
k:	0.02	s^-1	k:	0.02	s^-1
	1.32	min^-1		1.31	min^-1

Experimental k: 1.31 min^-1

Ec:	0.029		Ec:	0.029	
Ea:	0.042		Ea:	0.042	
Ek:	0.0012		Ek:	0.0012	
Reb:	312.617		Reb:	312.617	
Ut:	18.711	cm/s	Ut:	18.711	cm/s
ti:	0.0215	sec	ti:	0.0215	sec

APPENDIX 4

NUMERICAL SOLUTIONS OF SURFACE VORTICITY

NUMERICAL SOLUTIONS OF SURFACE VORTICITY

(After Dobby and Finch, 1987)

$$\xi = a + b\,\theta + c\,\theta^2 + d\,\theta^3$$

where

$$a = -0.01082 - 7.273\times10^{-4}\,Re_b + 1.735\times10^{-6}\,Re_b^2 - 2.046\times10^{-9}\,Re_b^3$$

$$b = +0.0745 + 3.013\times10^{-3}\,Re_b - 7.402\times10^{-6}\,Re_b^2 + 8.931\times10^{-9}\,Re_b^3$$

$$c = -4.276\times10^{-4} - 1.977\times10^{-5}\,Re_b + 5.194\times10^{-8}\,Re_b^2 - 6.520\times10^{-11}\,Re_b^3$$

$$d = -1.103\times10^{-6} - 1.032\times10_{-7}\,Re_b + 1.397\times10_{-10}\,Re_b^2 - 1.334\times10^{-13}\,Re_b^3$$

for $20 < Re_b < 400$.